Dissertation

submitted to the

Combined Faculties for the Natural Sciences and for Mathematics

of the Ruperto-Carola University of Heidelberg, Germany

for the degree of

Doctor of Natural Sciences

presented by

Diplom-Biologe - .Robert André Knieß

born in: Groß-Gerau

Oral-examination: .....

Analysis of replicative aging in Saccharomyces cerevisiae using fluorescence activated cell sorting

Referees: Prof. Dr. Matthias P.Mayer

Prof. Dr. Victor Sourjik

Mit bestem Dank an Matthias Mayer für die vielen hilfreichen Diskussionen, für die Unterstützung und Ermutigungen, für die Anregungen und Ideen und das gelegentliche Philosophieren.

Vielen Dank auch an Matthias Seedorf für die zeitweilige Bereitstellung eines Laborplatzes während der Umbauphase unseres Stockwerks.

Ich danke ebenfalls Frau Minh Nguyen für die gute Zusammenarbeit bei den Hsp90 Projekten.

Und ganz besonderen Dank an meine Eltern für die logistische Unterstützung und Motivation während der gesamten Laborzeit.

Table of contents

Part B – Establishment of a flow cytometry based aging-assay

Part C – Redox homeostasis in old yeast cells

Abstract

1 Summary of the thesis

Aging cells show a number of characteristic phenotypes usually summarized by the generic term: senescence. Amongst them there is accumulation of damaged proteins or DNA, changes in metabolism and a reduced replicative capacity.
The lifespan of actively dividing cells is limited by replicative senescence whereas stationary cells age in a chronological way. Single-celled organisms like yeast are potentially immortal as offspring continuously rejuvenate. Pedigree-analysis, however, demonstrates that this is not the case for both product cells originating from a cell division. This becomes clearly visible when the organism divides asymmetrically. For that reason bakers yeast *Saccharomyces cerevisiae* has long since become an important organism for aging research. The unfavorable relative abundance of old cells in an exponentially growing culture and the separation from the rejuvenated young cells however, makes it difficult to study this model system on a molecular level.

The molecular chaperone Hsp90 and its regulators play a central role in stress-resistance and adaptation and are thought to be involved in the aging process as well. The initial aim of this work was therefore the development of a system to monitor and quantify age-associated changes with fluorescent reporters. To attain single-cell resolution at high-throughput, measurement by flow-cytometry was the method of choice. For that reason it was necessary to modify the established Hsp90 reporter-systems and to eliminate many sources of error. By that I could show a progressive decline in the heat-shock response and loss of the Hsp90 dependent pheromone response in old yeast cells.
In addition, the newly designed reporter systems were used in young cells for functional studies of Hsp90 mutants.

During the establishment of the method, I had the opportunity to test the recently optimized redox-sensitive roGFP2-systems and the pH sensitive pHluorin reporter in old cells. As the results were promising and unexpected, the redox homeostasis in old cells became the main focus of my project. I could successfully monitor changes in the cytosolic glutathione equilibrium, hydrogen-peroxide abundance and pH in replicatively aged yeast cells. Surprisingly, the glutathione reporter was progressively more reduced in aging cells during fermentative growth whereas hydrogen-peroxide levels seem to rise at the same time. Simultaneously, the redox-pools became more resistant to oxidant treatment and the pH in old cells decreased. The reducing phenotype turned out to be dependent on the glutareductase Glr1. Using *in vivo* acidification measurements I could demonstrate that Glr1 is pH dependently regulated and could reproduce the glutathione-reduction phenotype in young yeast cells by lowering the cytosolic pH. Furthermore, similar pH changes occurred in a model system for telomere-induced senescence, but no distinct changes in the redox reporters could be seen, suggesting that redox homeostasis is differentially regulated in this context.

Yeast cells grown under respiratory conditions have a lower cytosolic pH and a more reduced glutathione-pool, consistent with the Glr1 activation. During aging, oxidation of both the glutathione and peroxide-pools increased in this case. Unfortunately, pH measurements in old respiring cells could not be performed due to instrument problems.

Interestingly, respiring cells have an extended replicative lifespan even when Glr1 is deleted and the cells are vastly oxidized. In fermenting cells Glr1 knockout also leads to a strong oxidation without affecting the replicative lifespan. This leads to the conclusion that homeostasis of the glutathione-pool is not limiting replicative lifespan in yeast.

Given that the cytosolic pH is actively maintained by H^+-ATPases, I speculate that the age-associated acidification may be the result of impaired ATP production.

2 Zusammenfassung der Arbeit

Alternde Zellen zeigen charakteristische Phänotypen, die unter dem Begriff Seneszenz zusammengefasst werden. Dazu zählen verminderte Teilungsfähigkeit, Anhäufung von DNA- und Proteinschäden und Veränderungen im Stoffwechsel.
Aktiv teilende Zellen sind von einer replikativen Seneszenz betroffen, während die Lebensspanne von stationären Zellen zeitlich begrenzt ist. Einzellige Organismen wie Hefezellen sind potentiell unsterblich, da sich die Nachkommen kontinuierlich regenerieren. Stammbaumanalysen zeigen jedoch, dass dies nicht auf alle Einzelzellen zutrifft. Dies lässt sich besonders gut an Organismen studieren, die sich asymmetrisch teilen. Daher ist die Bäckerhefe (*Saccharomyces cerevisiae)* seit langem ein bedeutender Modellorganismus in der Alterungsforschung. Die Schwierigkeit bei der Erforschung dieses Modellsystems liegt an dem verschwindend geringen Anteil an gealterten Zellen in einer exponentiell wachsenden Kultur und der Abtrennung der regenerierten, jungen Zellen.

Ziel dieser Arbeit war die Etablierung eines Systems, welches ermöglicht, altersbedingte Veränderungen in Einzelzellen mittels fluoreszierender Reporterkonstrukte nachzuweisen und zu quantifizieren. Um Einzelzellauflösung bei hohem Durchsatz zu erhalten, wurde daher die Technik der Fluoreszenz basierten Durchfuss-cytometrie (FACS) eingesetzt. Der Forschungsschwerpunkt lag dabei zunächst auf der Aktivität des molekularen Chaperons Hsp90 und dessen Regulatoren, die im Kontext der Stress-Adaption der Zelle beim Altern eine Schlüsselrolle spielen könnten. Zu diesem Zweck war es nötig, die bisher gängigen Reporterkonstrukte den Anforderungen anzupassen und Fehlerquellen zu eliminieren. Dadurch konnte ich zeigen, dass die Hitzeschockantwort in alten Zellen schwächer wird und dass die Hsp90 abhängige Pheromon-Antwort in Hefezellen im Alter ausbleibt.
Darüber hinaus wurde das entwickelte Messverfahren auch zur Untersuchung von Hsp90-Mutanten in jungen Zellen eingesetzt.

Während der Etablierungsphase der Methode bot sich die Möglichkeit das kürzlich optimierte Redox-sensitive roGFP2-system und den pH-sensitiven pHluorin Reporter in alten Zellen zu messen. Da die Ergebnisse vielversprechend und teilweise unerwartet ausfielen, verschob sich der Schwerpunkt der Arbeit auf die Messung des Redox-Haushaltes in alternden Hefezellen.
Ich konnte dabei eine gesteigerte H_2O_2 Produktion in alten Zellen unter fermentativen Wachstumsbedingungen nachweisen, während sich der Glutathion-Puffer in die reduzierte Form verschob und das Cytosol ansäuerte. Gleichzeitig wurden die Glutathion- und Peroxid-Puffer resistenter gegenüber der Zugabe von H_2O_2 und Diamide.
Es stellte sich heraus, dass die Reduktion des Glutathion-Puffers von der Glutareduktase Glr1 abhing. Durch artifizielle Ansäuerung des Cytosols junger Zellen mittels eines Protonophors konnte

ich eine pH-abhängige Aktivitätssteigerung von Glr1 nachweisen und somit den Phänotyp der alten Zellen nachstellen. Darüber hinaus konnte ich in einem Modellsystem für Telomer-induzierte Seneszenz eine ähnliche Ansäuerung feststellen, allerdings ohne offensichtliche Veränderungen der Redox-Reporter, was auf prinzipielle Unterschiede in der Redox-Homöostase in diesem Kontext hinweist.

Hefezellen die durch die Wahl der Kohlenstoffquelle zum Atmen gezwungen werden, besitzen schon zu Beginn einen niedrigeren pH und ein stärker reduziertes Redox-System. Unter diesen Bedingungen zeigen sowohl der Glutathion- als auch der Peroxid-Reporter eine fortschreitende Oxidation während der Alterung an. Unglücklicherweise konnte wegen einem Gerätedefekt der pH in diesem Fall noch nicht in alten Zellen gemessen werden.

Interessanterweise haben atmende Zellen eine deutlich erhöhte replikative Lebensspanne, selbst wenn Glr1 ausgeschaltet und das Cytosol stark oxidiert ist. In Zellen die Gärung betreiben führt das Ausschalten von Glr1 ebenfalls zu einer drastischen Oxidation was aber keinerlei Auswirkung auf die Lebensspanne hat. Dies legt nahe, dass der Zustand des Glutathion-Puffers keine Alterungsbegrenzung für Hefezellen darstellt.

Die Tatsache, dass der pH-Wert des Cytosols aktiv durch H^+-ATPasen erhalten werden muss, lässt mich spekulieren, dass die Ansäuerung von alten Zellen auf eine mangelnde ATP-Produktion zurückzuführen ist.

Part A – Measuring Hsp90-dependent Pathways with a Fluorescent Reporter-Plasmid-System in *Saccharomyces cerevisiae*

1 Introduction

1.1 The Hsp90 chaperone-system

Before beginning their work, proteins have to go a long and troublesome way. After synthesis on the ribosomes they have to fold into an active state and to be processed. Often their maturation is assisted by other proteins called chaperones. In most cases the final protein is able to fulfill its work, but there are still a large number of proteins which rely on the action of chaperones even in their native state. The 90 kDa heat shock protein (Hsp90) is a prominent representative of these "protein companions". It is involved in a plethora of processes and is known to interact with over two hundred substrate proteins, also called clients (*http://www.picard.ch/downloads/Hsp90interactors.pdf*) (Picard, 2002); (Stankiewicz and Mayer, 2012). The homodimeric molecular chaperone Hsp90 is highly conserved throughout evolution. In bacteria it is called HtpG (high temperature protein G); however, its functional role there is still under debate. There are also homologs found in plastids (HSP90C-family), mitochondria (TRAP family and the endoplasmatic reticulum (Hsp90B family – in humans called Grp94). For eukaryotes cytosolic Hsp90 is an essential protein and belongs to the HSP90A family, which is most thoroughly studied (Taipale et al., 2010). In humans there are two isoforms called Hsp90α and Hsp90β, in yeast they are termed Hsp82 and Hsc82.
In a yeast cell, Hsc82 is constitutively expressed and contributes about 100 000 molecules (Ghaemmaghami et al., 2003). The Hsp82 gene has a basal expression of about 500 000 molecules and is still inducible by heat-stress. The mammalian Hsp90s are also regulated by heat-stress. Whereas the Hsp90α isoform is highly inducible and upregulated in some cancer cells, Hsp90β makes up the main pool of Hsp90 under non-stressed conditions but can also be induced by heat-shock elements in the first intron under long-term stress-conditions (Sreedhar et al., 2004).

The protein can be divided in three functional parts. The C-terminal domain is required for dimerization and possesses a characteristic MEEVD motif for interaction with proteins containing a tetratricopeptide repeat (TPR) domain. The middle domain is thought to be the interface for client protein interaction. The N-terminal domain contains an ATP binding site which regulates N-terminal dimerization and structural rearrangements. It is connected to the middle domain via an unstructured and variable linker. The action of Hsp90 is driven by a cycle of ATP binding and hydrolysis (Li and Buchner, 2012), leading to conformational changes of the dimer [Fig.A1a]. Client proteins therefore become dependent on the speed of this ATPase-cycle which itself is strongly regulated by other proteins - called cochaperones (Taipale et al., 2010). The regulation could either be stimulating in the case of the cochaperones Aha1 and Cpr6 or inhibiting (Hop/Sti1, Cdc37, p23). Hop/Sti1 acts also as a scaffold, which couples the Hsp90 and the Hsp40/Hsp70-system [Fig.A1a]. Another coupling is the interaction between Hsp70, Hsp90 and the ubiquitin-ligase CHIP, linking Hsp90 to the protein degradation machinery.

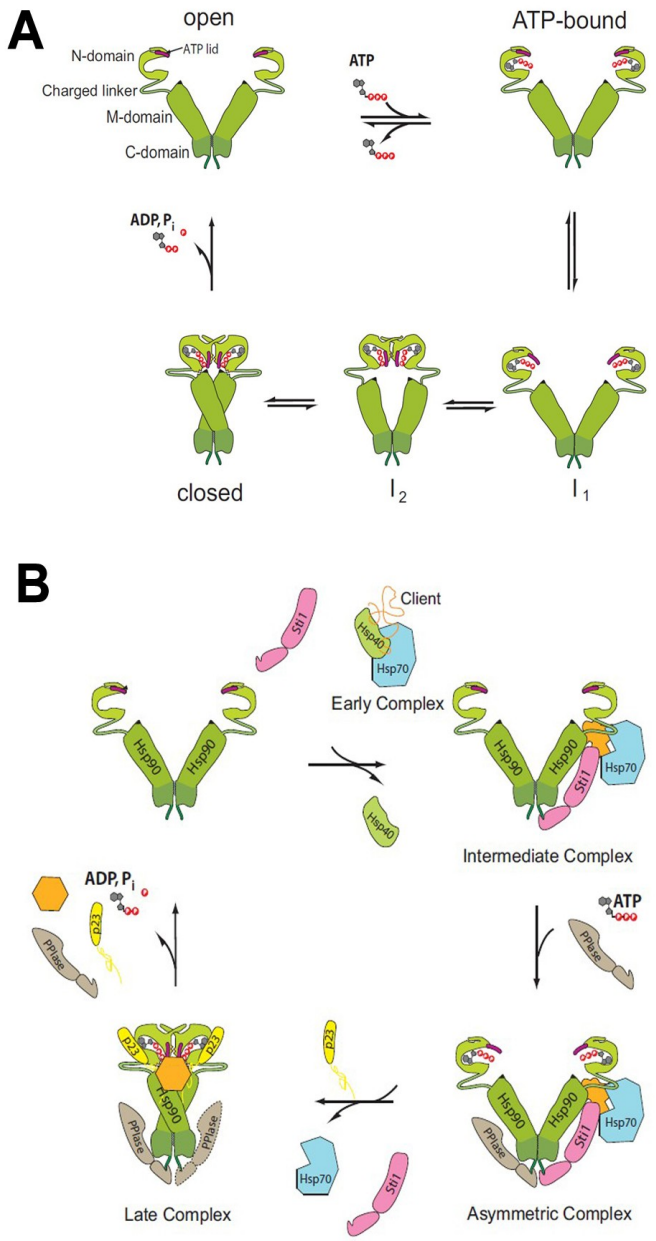

Fig.A1
Hsp90 chaperone cycle (adapted from Li and Buchner, 2012)
a.) Conformational changes of Hsp90 are driven by the binding and hydrolysis of ATP.
b.) Model of client (steroid hormone receptor) delivery by the Hsp70/40-system and chaperoning by the Hsp90-system. The Sti1 co-chaperone serves as an adaptor molecule to couple both systems. Other co-chaperones like PPIases and p23 are needed to drive Hsp90 to the "closed' conformation where ATP can be hydrolyzed. In a last step the co-chaperones and the client are released.

Hsp90 does not seem to play a general role in *de novo* protein folding, but binds instead to a defined range of clients in their native or near native conformation. The detailed mechanism of how Hsp90 recognizes its clients remains unknown. Some clients are bound directly, whereas others are delivered by cochaperones. It is thought that exposed hydrophobic patches like the ligand binding cleft of hormone receptors (Pratt et al., 2008) are one of the signals for interaction.

The Hsp90 clients can be divided into two distinct, functionally homogeneous groups and a third rather heterogeneous group. The first group comprises transcription-factors like p53 and steroid receptors. In the second group there are kinases such as the proto-oncoproteins c-Src, b-Raf, Bcl/Abl and PKB/Akt1. The third group includes proteins like Telomerase, Sir2, the potassium channel Kir6.2, the chloride channel CFTR, the proteasome, the Tau-protein and proteins involved in viral replication like SV40-LTA or reverse transcriptase. Therefore Hsp90 has a broad spectrum of activities, which affect for example cell survival, cytoskeletal rearrangements, cell-cycle control, chromatin remodeling, transcription, stress response, autophagy, and apoptosis. The amazing number of regulatory functions and specific interactions makes Hsp90 a very prominent protein to study. Considering that Hsp90 clients are key components of many signal transduction pathways, it is tempting to hypothesize that Hsp90 is a global coordinator of different pathways, linking them to environmental changes.

The high expression level of Hsp90 - about 3% in unstressed cells and more than 5% in stressed and cancer cells - illustrates the universal functions of this protein. This raises the question on how client specificity and subtle regulations can be achieved.
Hsp90 is heavily regulated by post-translational modifications (Wandinger et al., 2006) such as S-nitrosylation (Martínez-Ruiz et al., 2005), phosphorylation (by Casein kinase II, Akt – Sch9 in yeast) or acetylation (deacetylation by HDAC6) (Scroggins et al., 2007). Over 100 post-translational modifications of human Hsp90 are meanwhile annotated (www.phosphosite.org) and it is thought that they determine the subset of clients to interact with. This also makes clear that there is not only one species of Hsp90 in a cell and one cannot measure a global activity of this protein just by measuring its abundance.

1.2 Objective

The aim of this part of the thesis was the development of a robust fluorescent reporter system to quantify specific Hsp90 activities in yeast cells on a single-cell level by using flow cytometry. The reporters then should serve as a universal tool to analyze Hsp90 dependent pathways in the context of co-chaperone regulation, mutant analysis, complementation studies and aging in *Saccharomyces cerevisiae*.

2 Hsp90 reporters

One of the largest groups of Hsp90 clients are transcription-factors and kinases. Some of the kinases are involved in signal transduction and also lead to the regulation of genes. The strategy to address Hsp90 activity *in vivo* was therefore the creation of a reporter system which uses Hsp90 regulated promoter-elements and a detectable enzyme as readout. By monitoring different pathways a comprehensive view of Hsp90 activity should be given.

2.1 The Hsp90 clients

2.1.1 Pheromone response (Ste11)

Natural yeast isolates grow in a heterothallic life-cycle. Normally they propagate as diploid cells with mitotic divisions. Under certain conditions they undergo meiosis and form four haploid spores of two opposing mating types termed **a** and α (or MAT**a** and MATα), which can also propagate by mitotic divisions under rich nutrient supply. Cells secrete a mating-type specific pheromone-factor - a short peptide of 12 to 13 amino-acids. MAT**a** cells produce the **a**-factor, which is posttranslationally farnesylated, and MATα cells secrete the α-factor. Specific receptors for the factors are expressed on cells of the opposite mating-type.
When the nitrogen sources are low, a mating competent state is induced stimulating the fusion of cells of opposite mating types. This leads to a chemotactic outgrowth of the cells and formation of the characteristic pear-shaped Shmoo phenotype. Wild-type yeast is able to switch the mating type using the so-called homothallic endonuclease. Common laboratory strains are deleted for the gene encoding this nuclease to prevent mating-type switching and spontaneous transition to the dipoid state. This is possible because the sequences defining the mating type are encoded elsewhere in the genome at silenced loci and only one of those genes is copied into an active separate locus. In that way a haploid culture of a single mating-type can be maintained. For practical reasons the pheromone response is mostly studied in MAT**a** cells which respond to α-factor. The signal transduction of the pheromone pathway is well known (Bardwell, 2005). It starts with the activation of a G-protein coupled pheromone receptor and signal amplification by a MAP-kinase cascade. The MAP-kinase-kinase Ste11 (a homolog of the mammalian Raf-kinase) is dependent on the chaperoning by Hsp90.
Finally, the cascade leads to the activation of the transcription factor Ste12 and its binding to pheromone response-elements (PRE) on DNA, inducing transcription of a defined set of genes. In a MAT**a**/α (diploid) cell, genes of both mating-type loci are expressed and lead to an inactivation of the pathway.

2.1.2 Heat-shock response (Hsf1)

Heat shock factors (HSFs) are transcriptions factors at the center of the heat shock response. They are involved in stress-adaptation, development and apoptosis but also in aging and tumor genesis (Åkerfelt et al., 2010).
The model says that under unstressed conditions HSF1 is in complex with Hsp90 and kept inactive. In metazoans, HSF1 is monomeric when bound by Hsp90 whereas yeast Hsf1 seems to be already trimerized and located to DNA in a repressed state. By increased amounts of unfolded proteins, Hsp90 is titrated away from HSF, which is subsequently activated in a trimerized form and promotes transcription of heat shock genes by interacting with the heat-shock response element (HSE) and recruiting co-activators. Like the heat-shock proteins, HSF has many sites to be post-translationally modified. Hyper-phosphorylation and sumoylation is associated with active transcription whereas acetylation in the DNA-binding domain attenuates the activity.

2.1.3 Heme-response (Hap1)

The zink-finger transcription factor Hap1 is a sensor for heme molecules and is needed for the growth under anaerobic conditions. In yeast Hap1 associates with Hsp82, Ssa1, Ydj1 and Sro1 (Zhang and Hach, 1999); (Mense and Zhang, 2006). The chaperones are thought to keep Hap1 in a competent state for heme binding but also to enable it to act as a gene repressor (including its

own gene) in the absence of heme (Hon et al., 2005) . In the presence of oxygen heme synthesis is upregulated in the mitochondria. By increasing heme levels Hap1 gets activated presumably by complex disassembly and binds DNA with high affinity. This promotes transcription of cytochrome c (Cyc1, Cyc2, Cyt1), catalase (Ctt1), Yhb1 and the anoxic gene repressor Rox1. By acting on the Hap1 complex, Hsp90 seems to play the role of a co-activator for the expression of Hap-Response-Element (HapRE) controlled genes, whereas Ssa1 rather acts as repressor of Hap1 (Lan et al., 2004).

Unfortunately, the most frequently used lab strain BY4741 harbors a Ty1 transposon insertion in the Hap1 transcription factor (Gaisne et al., 1999).

2.1.4 Glucocorticoid response (Glucocorticoid receptor)

Glucocorticoids are steroid hormones regulating glucose metabolism, stress and immunological responses in mammalian cells. Glucocorticoid receptors (GRs) belong to the family of nuclear receptors, which are transcription factors and can directly activate genes when hormones are bound. The GRs are well studied and their maturation and activation is largely dependent on the activity of molecular chaperones. The current model (reviewed by (Grad and Picard, 2007)) states that GR is pre-folded by Hsp70/Hsp40 and transferred by Hop1 to Hsp90/p23, which makes the receptor competent for hormone binding (Kirschke et al., 2014). This is also the minimal requirement for GR activation. After hormone binding the receptor translocates to the nucleus and binds to the glucocorticoid response elements (GRE). The transport can be further modulated by immunophilins (FKBP51/52).
Yeast cells do not contain steroid-hormone receptors. However, it was shown that glucocorticoid receptors can be activated in yeast in a Hsp82-dependent manner (Picard et al., 1990). To utilize this Hsp90 reporter a gene encoding the glucocorticoid receptor as well as the response-element containing reporter construct must be introduced into the cells. Since GR is an unknown protein to yeast, it should be independent of endogenous regulations and feedback-loops and is likely to be an unbiased system to address Hsp90's activity.

2.2 The reporter readout

The original set of reporters was received from Kevin Morano (Morano and Thiele, 1999) and contained the minimal CYC1-promoter and a specific response-element driving the expression of β-Galactosidase (β-Gal). The expression can be quantified by adding ortho-nitrophenyl-β-galactopyranosid (ONPG), the substrate of β-Gal, which is converted into a colored compound after cell lysis.
This kind of quantification has several disadvantages. Yeast has a rigid cell-wall, which makes it robust and hard to break. For β-Gal the method of choice is disrupting the cells with glass beads either through vigorous vortexing or by using a bead-beater. However, the procedure heats up the sample, requires large amounts of cells and needs to be carefully normalized to the number of lysed cells or the total protein which leads to high inaccuracy.
Especially when considering aging experiments, all these factors make the reporters unfeasible to use.

Much more sensitive and easy to handle is the use of a luciferase. A specific substrate is added, which is used by the luciferase to produce light. Here, the cells can just be permeabilized by detergents or the substrate itself is membrane permeable. The problem of normalization can be

solved when using two different luciferases, such as firefly luciferase for the reporter and renilla luciferase for a constitutive signal. Both luciferases use different substrates and can be measured subsequently by using different buffer conditions. Initial experiments with the reporters worked well but also revealed some major drawbacks. First, reagents for dual luciferase assays are offered by companies and are very expensive. Self-made systems usually have a much lower sensitivity. Secondly, especially when dealing with heat-shocks, luciferase itself becomes a problem, as luciferase - at least firefly luciferase – is prone to aggregation and heat-denaturation and for that reason often utilized for refolding assays. Third, dead cells may lyse and release luciferase into the medium. The signal would then not be proportional to the living cells anymore. Another problem can arise when a whole culture is quantified. If a small subpopulation with high reporter expression is present it would not be distinguishable from a moderate expressing homogenous culture. Conversely, dead or non-expressing cells would mimic a lower expression of the whole culture.

The best way to account for individual differences is to go down to the single-cell level. For this reason we wanted to use the fluorescence of GFP as readout. Previous attempts with conventional GFP gave unsatisfactory results; therefore we obtained a yeast-optimized superfolder-GFP (sfGFP), which was a kind gift from Michael Knop (ZMBH, University of Heidelberg). In order to yield a strong signal, the sfGFP-gene was cloned as a tetra-repeat into the reporters - now referred to as “sf4x”.
For the quantification of the sfGFP reporters we decided to use a flow-cytometer (see below).

3 Characterizing Hsp90-Reporters and yeast cells on the flow-cytometer

3.1 Basic principle of flow-cytometers

The principle of a flow-cytometer is simple. Cells are lined up by liquid flow and rapidly pass a laser beam. The fluorescent light, perpendicular to the beam and flow, is separated into spectral bands by different sets of filters and detected by photomultiplier tubes. The instrument can be equipped with several lasers and filter sets to allow measurements of different fluorescent probes. Many thousand events per second can be detected and recorded in that way. In addition to the fluorescent light also the scattering of the laser-beam in forward and sideward direction is detected. The forward-scattering (FSC) relates to the size of the cells whereas the sideward-scatter (SSC) is a measure of granularity of the cells. These terms come from the mainly medical application of flow-cytometers where blood cells are analyzed. For yeast cells, which are much smaller than mammalian cells and have a different architecture, these parameters are less well defined.
As a cell enters the laser-beam the signal increases until the cell is fully illuminated and decreases when it leaves the beam. The time-scaled factor of the signal duration is called the signal-*width* (W-parameter) the peak-fluorescence is called the signal-height (H-parameter). The quantified and scaled total signal, the area of the signal-curve, is called the *area* (A-parameter). To account for the total GFP-content of the cell, always the A-parameter was used in this work.
Flow-cytometers are available as analyzers, which only record the events, but there are also FACS-systems, which are built to sort selected cells. For this work I was using the sorter FACS-Aria (BD-Biosystems), which breaks the liquid flow into positively or negatively charged

droplets after measuring. The drops carrying the cells can then be sorted in the electrical field of a capacitor.

3.2 Measurement of centromeric reporters

For this part of my work I used the yeast strain BY4741 with reporter constructs initially based on centromeric plasmids derived from pRS416. The culture was grown and measured directly from selective SC(-Ura)-medium. As reporter fluorescence was analyzed on the cytometer, it became obvious that some cells show a rather weak GFP-signal [Fig.A2a,b]. To test whether those cells are still alive or have already died, cells with high-GFP and low-GFP-signal of two different strain backgrounds were sorted and spotted onto agar-plates. In [Fig.A2c] it can be seen that both populations grew fine on rich-medium (YPD). However, on medium selecting for the reporter-plasmid, only high-GFP-cells were able to grow. This means, in a logarithmic culture of BY4741 about 20% of the cells will lose the centromeric reporter-plasmids and have to be excluded from analysis.

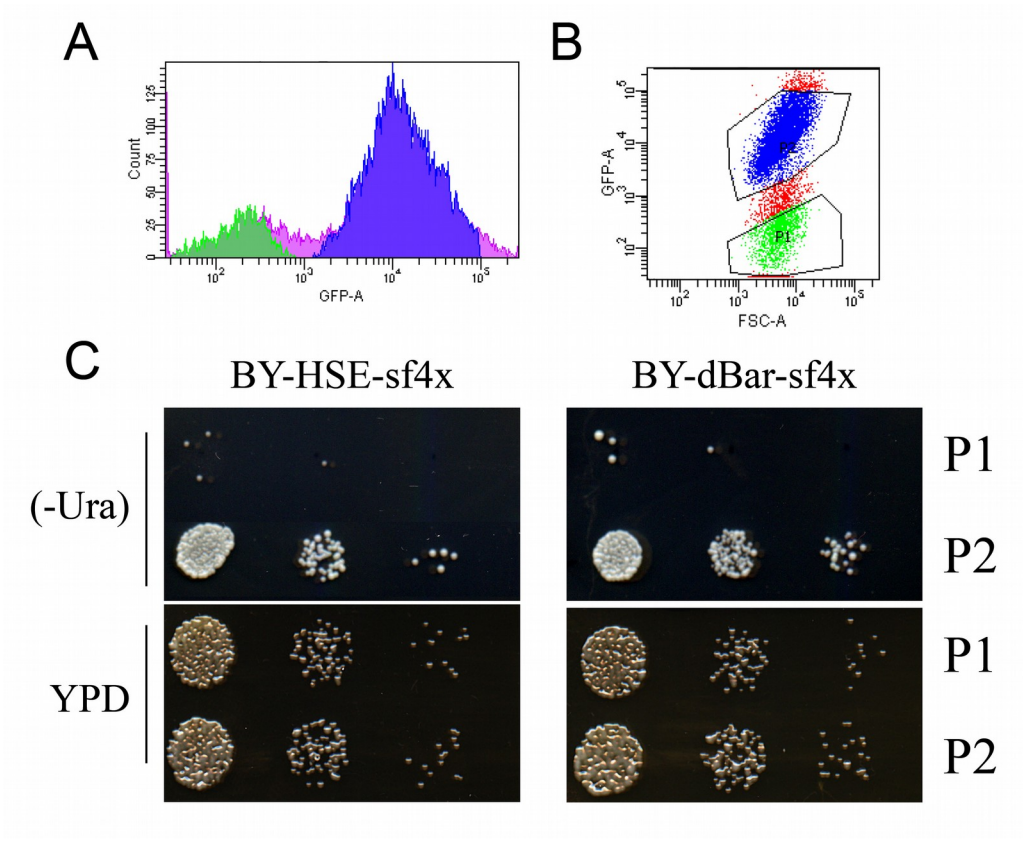

Fig.A2
pRS416 based vectors are readily lost during cell culture. The pRS416-HSE1-sfGFP4x reporter was transformed in BY4741 and grown in SC(-Ura) medium. Populations were analyzed by their GFP content.
a.) GFP intensity measured by flow-cytometry. Populations are artificial colored based on the gatings in b.)
b.) Sorting gates for low-GFP (P1) and high-GFP (P2) populations. GFP-intensity (area-parameter) is plotted against the forward-scatter FSC (area-parameter).
c.) Sorted cells of the populations P1 and P2 from two different strain backgrounds (wt and Δbar1) were spotted either on SC(-Ura) or YPD plates.

3.3 Integration of reporters

In order to achieve a stable expression of the reporters I changed the plasmid-backbone to the integrative pRS303-vector. Compared to cells carrying the centromeric reporter [Fig.A3], cells with the integrated HSE1-reporter showed a homogenous population with a high GFP-signal. However, after heat-shock some low-GFP-cells appeared. To test for viability, cells with different brightness [Fig.A4a] were separated by FACS and spotted on agar-plates [Fig.A4b]. Cells with low GFP-signal did not grow on both YPD or SC(-His) whereas cells with a stronger GFP-signal did. This clearly indicates that the GFP-signal with the integrated reporters can be used as a vital-marker. Loss of GFP-fluorescence could be due to growth in synthetic medium which has a pH of 3.92. GFP-fluorescence is quenched at low pH and leakiness of a cell could lead to pH equilibration with the medium or loss of GFP-molecules.
In conclusion, integration of the reporters gives a stable expression of GFP and cells with low fluorescence can be considered dead.

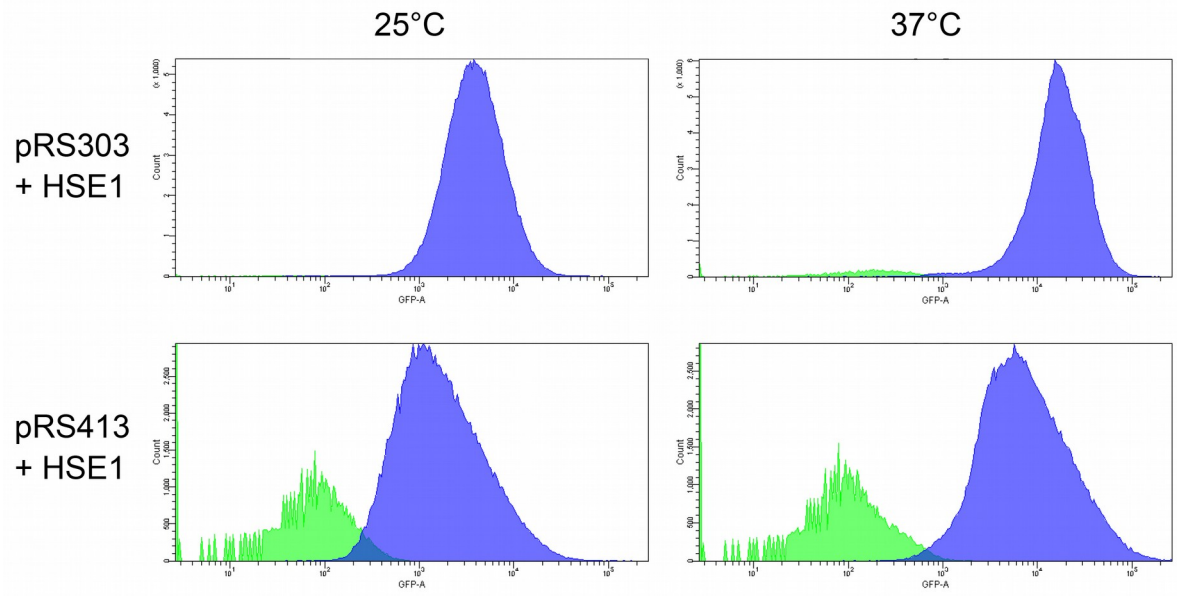

Fig.A3
Expression of fluorescent reporters from integrative vectors is more stable then from centromeric vectors. The HSE1 reporter was expressed in BY4741 from either pRS303 or pRS413. Fluorescence at 25°C or after 1h at 37°C was measured by flow-cytometry. Cells lacking GFP expression are colored in green and GFP expressing cells are colored in blue. Selection of the population was based on a GFP-A/FSC-A plot similar to [Fig.A2] (not shown).

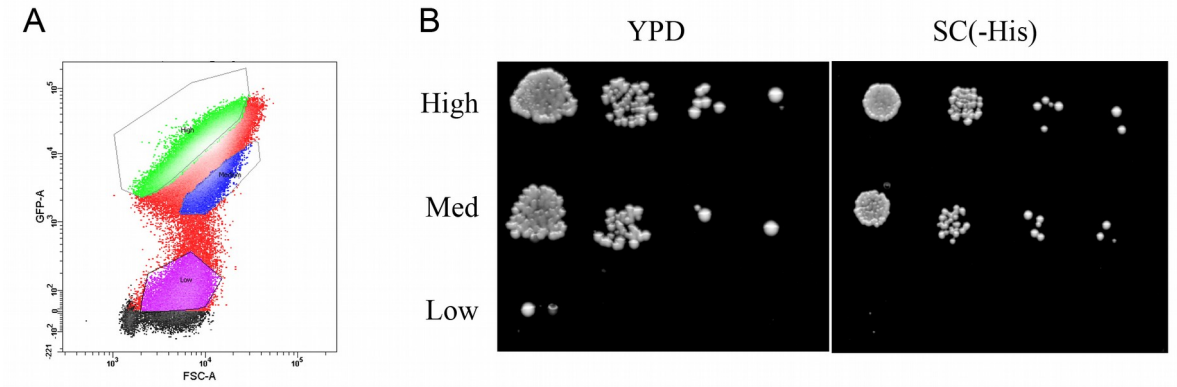

Fig.A4
Characterization of GFP expression from the pRS303-HSE1-sfGFP4x reporter in BY4741.
a.) Cells possessing high, medium or low GFP content were sorted by FACS
b.) Spot-test of the sorted cells on YPD plate (left) and SC(-His) plate (right)

3.4 Single-cells

Flow cytometry is an event-based method. The events could consist of a single cell but also of aggregates, bacteria or debris. As most of the smaller particles are excluded from the measurement by a cutoff in the forward-scatter it leaves the problem to distinguish between single-cells and aggregates. One can assume that aggregates are much bigger and therefore have a higher forward-scatter. Indeed, there is a strong correlation between FSC and GFP-fluorescence [Fig.A4a], but no clear separation in different size-species can be seen. As mentioned above, a signal can be detected in width, height and area. The signal-width of an event seems to be a reasonable measure for the diameter of a particle. The best separation of

populations could be seen in the SSC-W parameter and a bit less clearer in the FSC-W [Fig.A5a,b]. To see what species the populations consist of, sorting was performed and analyzed by light microscopy. It turned out that cells with low SSC-W are mostly single or with a small bud whereas less single cells were found in the high SSC-W fractions [Fig.A5c]. The results however must be treated with caution because sorting and spotting on the microscope slide can cause shear-stress to aggregates and may tear them apart, so they may be underrepresented in the data.

Because aggregates consist of many cells that may or may not disassemble at different conditions, it is desirable to measure only single-cells from the culture. In an undisturbed logarithmic culture the single-cells are quite rare, so it is recommended to increase their fraction. For that purpose I made use of the power of sound waves from a sonicator-bath to separate the cells. Sonication efficiently increased the single-cell-population [Fig.A6a,b]. Although one should take care not to sonicate too much as long exposure will eventually disrupt some cells. One will need a little experience to know when to stop sonication to minimize the destructive effect. Initial experiments were done with 15 seconds but 5 seconds are already sufficient, depending also on the position of the sample in the bath.

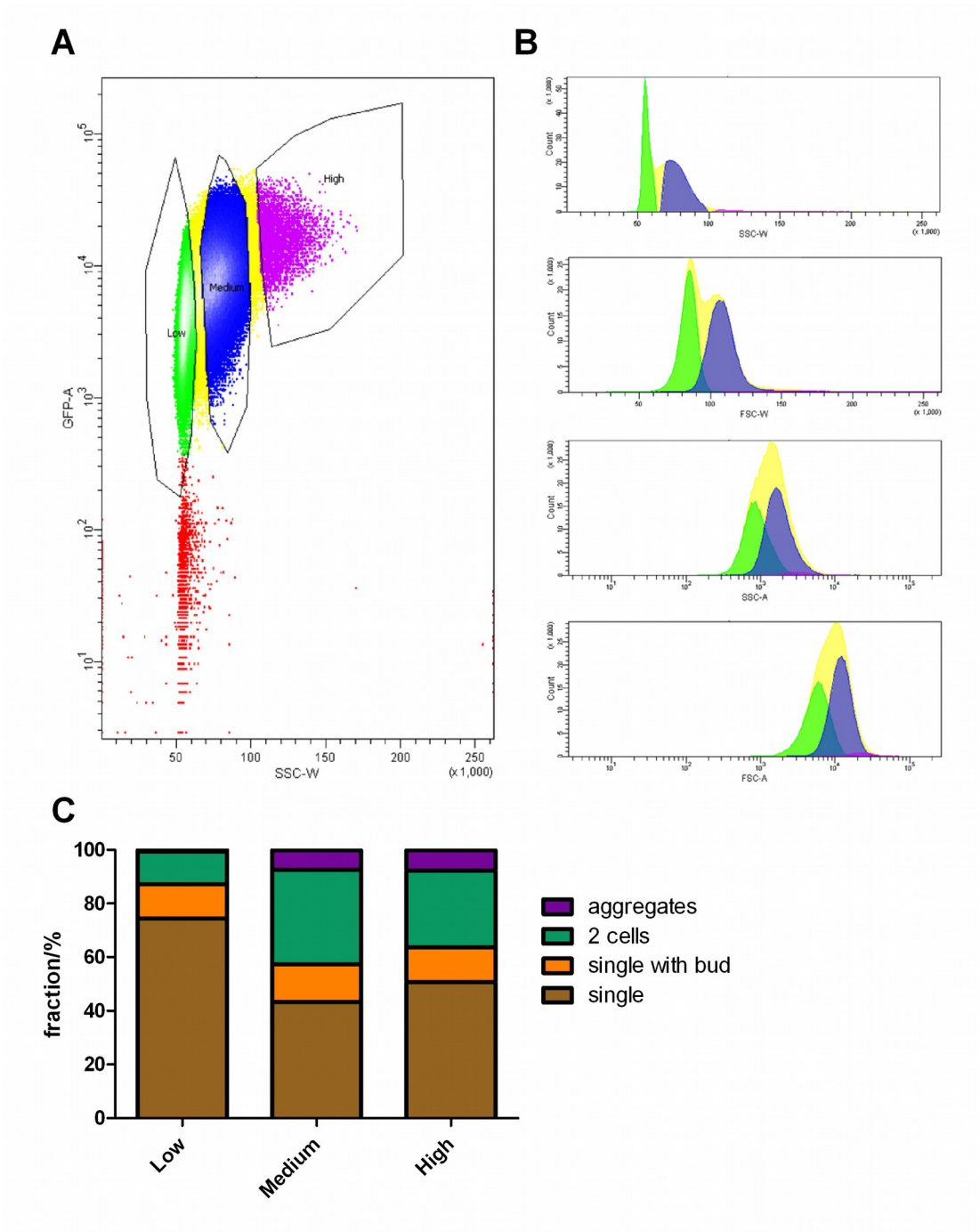

Fig.A5
Characterization of the scatter parameters of BY4741 expressing the HSE1-sfGFP4x reporter.
a.) GFP expressing cells were selected in the side-scatter (width parameter) at low, medium and high scattering. The selected populations were differentially colored.
b.) Based on the gatings from a.), cells are shown at different scatterings. From top: side-scatter (width parameter), forward-scatter (width parameter), side-scatter (area parameter), forward-scatter (area parameter)
c.) Microscopic analysis of the three populations defined in a.)

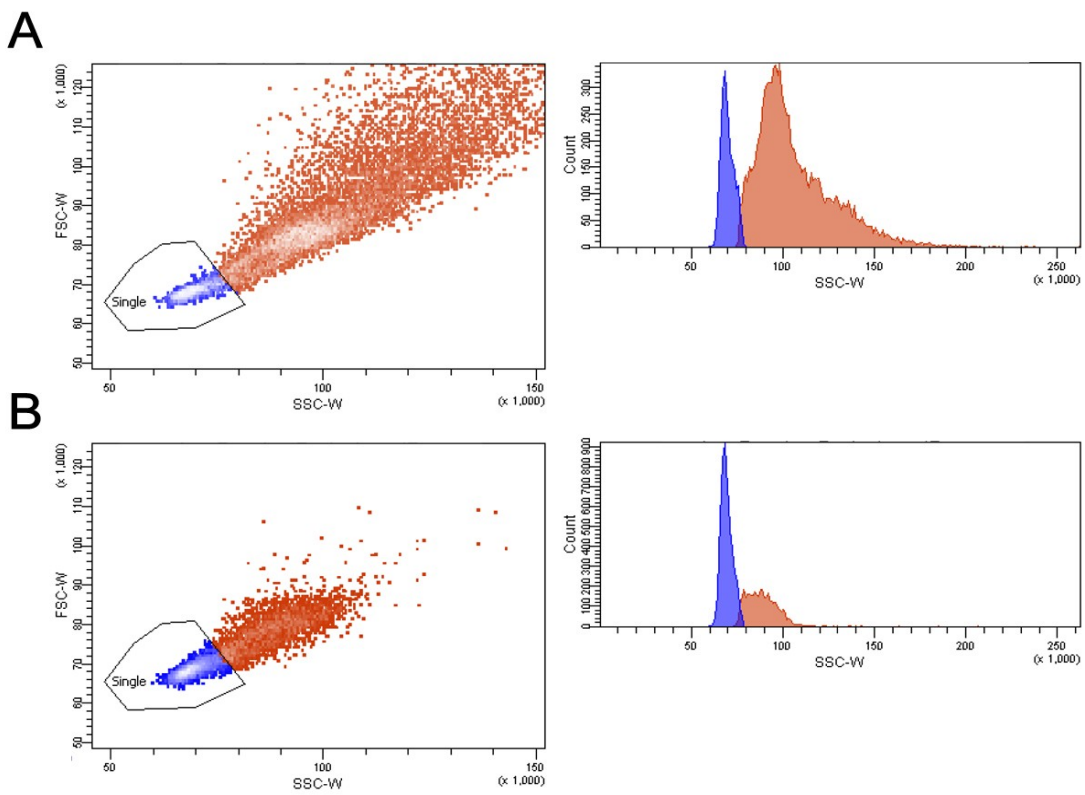

Fig.A6
Influence of sonication on the population of single cells. The population was defined in the FSC-W/SSC-W representation (left). The SSC-W histogram of the population is shown on the right.
a.) Logarithmic culture of WΣ measured directly. Fraction of single cells is 18%.
b.) Logarithmic culture of WΣ sonicated before measurement. Fraction of single cells is 62%.

3.5 Induction kinetics – a first trial

Having now a standardized population of single cells, first quantitative measurements could be taken. The induction kinetic of the HSE1-reporter was measured over 150 minutes with five overnight cultures at different densities to see a possible dependency of the heat shock response on cell density or growth phase [Fig.A7b]. In parallel to each 37°C time-point an uninduced sample of the 25°C overnight culture was recorded [Fig.A7a]. The ratio of GFP-expression at 37°C/25°C gives the induction [Fig.A7c].
Induction worked well at all different densities. However, the very low densities seemed to respond slightly stronger. It also becomes evident that basal activity increased slightly during the experiment which could be due to altered conditions when cells were transferred from erlenmayer flasks to eppendorf tubes on a thermomixer which may have a deviating temperature setting compared to the shaker.

The final goal of the reporters is to make them suitable for aging studies (*see Part B*). In these cases data acquisition times of 30 minutes could happen. Especially when the induction of a reporter is not saturated, the reporter will still change during recording. To overcome this problem I used the translational inhibitor cycloheximide to block protein synthesis at a certain

time-point. The pheromone response was induced in BY4741 by stimulation with the alpha-mating factor and monitored with the PRE-reporter. After 2h of induction, cycloheximide at 15µg/ml or just ethanol was added, and further time-points were taken [Fig.A8]. Addition of cycloheximide successfully blocked GFP-production and the fluorescence stayed constant whereas the mock treated cells proceeded with induction. This treatment therefore will make a snapshot of the current reporter state and would allow long integration times.

The original glucocorticoid-reporter was barely inducible at all. It contained the minimal Cyc1-Promoter with an undefined about 400nt upstream-fragment. I decided to redesign the response-element and remove the additional sequence. According to (Nordeen et al., 1990), a sequence optimal for induction was chosen and cloned as a tetra-repeat in front of the mini-CYC1-promoter. The capital letters indicate the consensus binding sequence:
(gttagttGGTACAtgaTGTTCTcccaagttagttGGTACAtgaTGTTCTcccaagttagttGGTACAtgaTGTTCTcccaagttagttGGTACAtgaTGTTCTccca).
The new construct was cloned together with the mammalian glucocorticoid receptor (rGR) into the pRS403 integrative vector and integrated into BY4741. Induced by 10 µM Desoxycorticosterone (DOC) the reporter now showd a strong induction [Fig.A9]. Unfortunately, a fraction of cells showed only weak induction and this fraction increased when the strain was reused days or weeks later (data not shown).

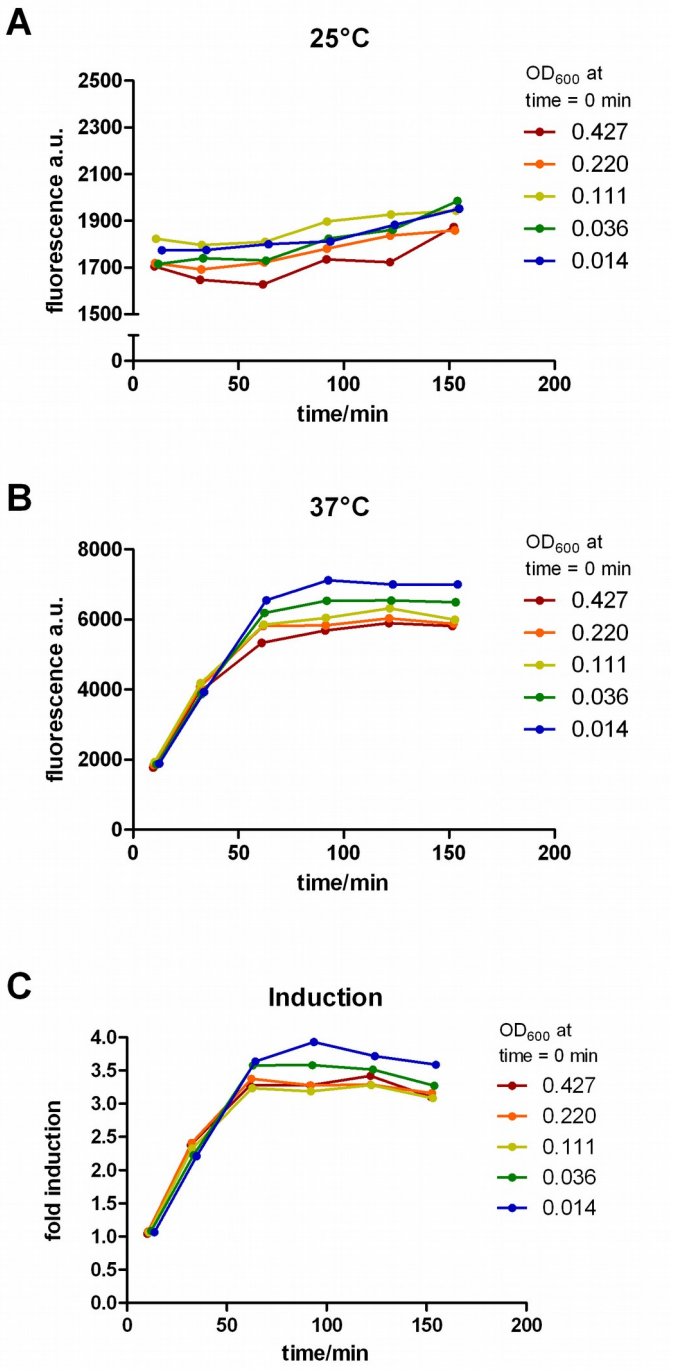

Fig.A7
Heat induction of the HSE1-sfGFP4x reporter in BY4741 at different optical densities. Population averaged GFP intensities are shown. Optical densities (OD_{600}) of the cultures at the beginning of the heat-shock are differentially colored.
a.) Basal reporter fluorescence at 25°C followed over time.
b.) Reporter fluorescence during heat-shock at 37°C
c.) Reporter induction calculated as fluorescence at 37°C/25°C

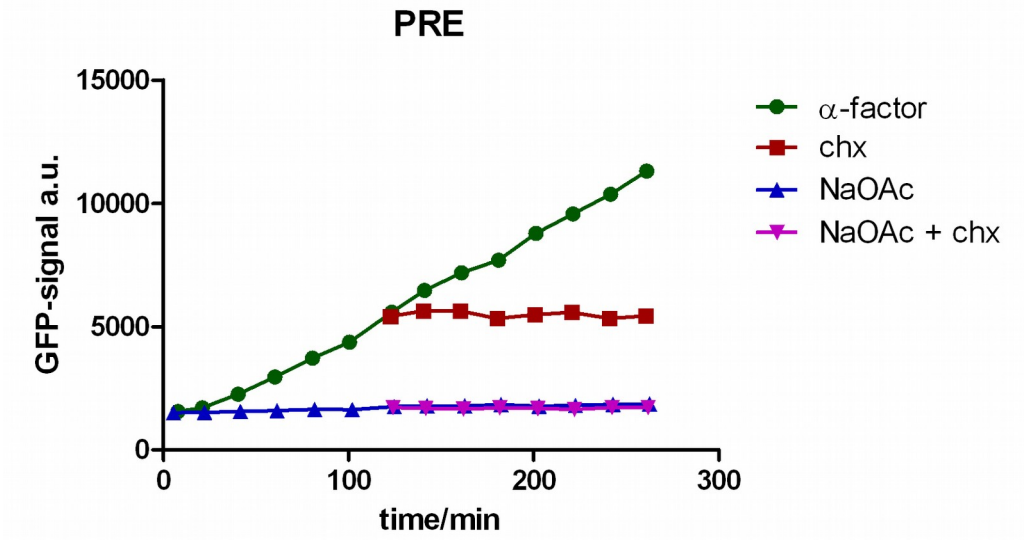

Fig.A8
Induction-kinetic of the pheromone reporter (PRE-sfGFP4x) in BY4741. Cells were either stimulated with 5.9 µM alpha-factor or mock-treated with sodium-acetate (NaOAc). After 120 minutes aliquots was taken and treated with cycloheximid (chx) to block translation.

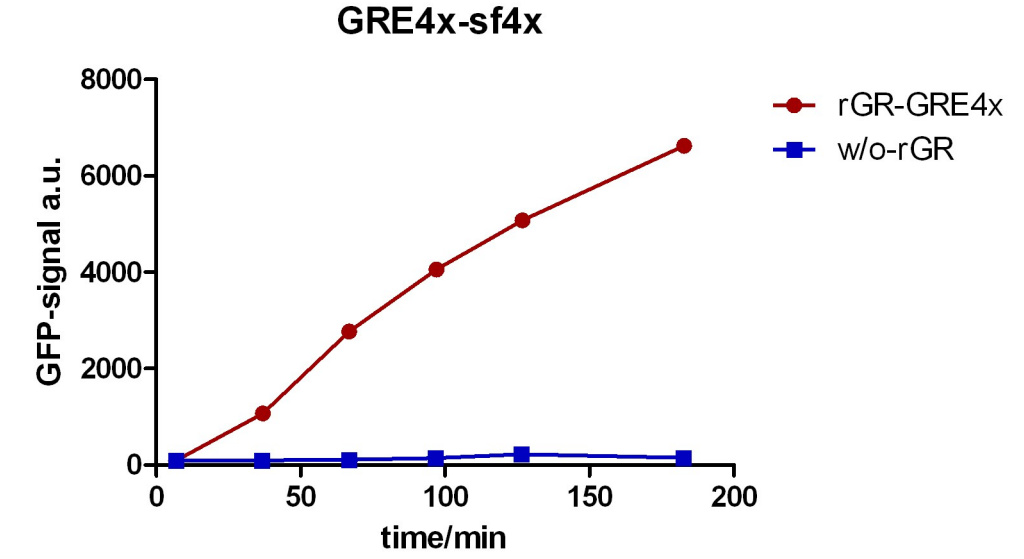

Fig.A9
Induction-kinetic of the glucocorticoid-reporter (GRE-sfGFP4x) in BY4741. Cells coexpressing (red) or lacking (blue) rat glucocorticoid receptor (rGR) were induced with 10 µM desoxycorticosterone.

3.6 Problems with the integrated reporters

It was generally observed that brightness of all reporters declined over the weeks. Furthermore, there was a strong clone-to-clone variation of expression. Normally, I screened the transformation plates under a binocular microscope capable to show GFP-fluorescence and picked colonies with bright basal expression.
The heterogeneity of the clones and the gradual decline led to the assumption that recombination events are responsible for this behavior.
When transforming yeast with integrative pRS-plasmids, the plasmid is cut in the selection marker and recombines with the disrupted endogenous allele to restore its function (Sikorski and Hieter, 1989). Once integrated, the target site for the plasmid is duplicated – one disrupted site and one restored. At high plasmid concentrations during transformation, integration could then happen several times. By picking the bright clones most likely cells with multiple integrations have been chosen. Because of the repeats this process is reversible and yeast could eventually loop out one or more of the integrations over time. The glucocorticoid-reporter was extremely prone to those events: The system is relatively large due to the additional glucocorticoid-receptor and it consists of two components. Looping out one copy would remove one reporter and one transcription factor thus resulting in large differences among the cells. Moreover this difference in stoichiometry would also change the rates of induction. For the other reporters with only the promoter driven GFP, this would not be the case.
Checking for the copy number with a genomic southern blot would be extremely time-consuming and the problem of recombination would not be solved. Picking always the dimmest clones would also not be an option for reporters with a very low basal activity and the signal should be clearly above autofluorescence to discriminate between living and dead cells.

Taken together, integrative reporters of the pRS-series have the benefit of not being lost upon cell-division and can give clones with very high expressions but are not suitable for quantitative measurements because of possible recombination or copy-number variation.

3.7 A reporter for the internal standard

Gene expression and translation in a cell can be regulated on many different levels. A GFP-reporter as readout for a transcription factor is an artificial system and may be influenced by any global processes. Beyond this, a dividing cell will also dilute proteins into daughter cells and a change in cell-cycle progression will most likely affect GFP-levels. To account for general influences on the reporters an internal standard is needed. In most cases a housekeeping gene is used as a reference. The expression should be strong and not be influenced by the carbon source supplied because some experiments also have to be done in glycerol or galactose medium. In addition, since I wanted to measure Hsp90-acticity, it should not be regulated directly by Hsp90 itself. As the reporters depend on translation I thought the promoter of the translation-elongation-factor1 (TEF1) would be a good candidate. To avoid recombination with the endogenous TEF1-locus, promoters and selection markers with the same functionality are often taken from related species. For my reporter I decided to take the TEF1-promoter from Ashbya gossypii from the yeast plasmid pAG25 (Goldstein and McCusker, 1999). This plasmid is used for gene knockouts in *S.cerevisiae* and the TEF1-promoter there is driving the expression of the NAT-resistance marker.
Next I had to choose a fluorescent protein to be detected in parallel to GFP. Multiple filter-sets and lasers allow flow-cytometers to detect different fluorescent proteins in one cell. Many

factors have to be considered when coexpression should work as a reliable internal standard. Firstly, the protein should be readily detectable in the instrument and spectral overlap to GFP should be small to allow separation of the signal. Secondly, the proteins should be monomeric to avoid binding to and avoid quenching of GFP. Thirdly, fluorescence resonance energy-transfer (FRET) should not play a role. Fourthly, the protein should be functional in yeast-cells. Fifthly, the maturation time should not be too long compared to superfolder-GFP, which can be detected already after five minutes. Sixthly, folding should be efficient at room-temperature and the fluorophor should still be active at 42°C heat-shock. Seventh, the protein should be as bright as possible because every GFP-measurement has to be normalized against it.
After screening the available fluorescent proteins, only two suitable candidates remained: mT-Sapphire and TagBFP. mT-Sapphire we obtained as kind gift from Oliver Griesbeck (see also (Zapata-Hommer and Griesbeck, 2003), and a yeast codon-optimized version of TagBFP we received from Michael Knop (ZMBH, University of Heidelberg) Both of these proteins were cloned as a tetra-repeat under the control of the TEF-promoter (P_{TEF}) in pRS304. For transformation of BY4741, an additional NAT-marker was also cloned into the plasmid. Because T-Sapphire was the first protein I obtained, it was used for most of the experiments. In addition, I also constructed a GFP-reporter for the Actin-promoter (ACT1/ YFL039C) to compare the expression of pRS305-(P_{Act}-sfGFP4x) with pRS304-(P_{TEF}-T-Sapphire4x) in the same cells.

Meanwhile the aging experiments, which were established in parallel, required the change from the strain BY4741 to the W303-derivative WΣ (*see Part B*). This strain has the advantage of not producing large amounts of petite cells and all selection markers could be used for integrative plasmids because they only harbor point mutations instead of deletions of the open reading frame. Both the P_{TEF}-T-Sapphire and P_{Act}-sfGFP were transformed into WΣ and tested for the stimuli which are applied normally for the Hsp90-reporters.
As expected the addition of desoxcorticosterone (DOC) did not change the activity of both P_{TEF} and P_{Act} significantly [Fig.A10a]. In contrast, induction of the mating-response results in a strong reporter signal of P_{Act} [Fig.A10b], which was expected, because it harbors a Ste12 binding-site (the main transcription factor of the mating-response – see introduction). A weaker induction could be seen for the P_{TEF} suggesting a general accumulation of proteins during α-factor induced G1-arrest. Under heat-shock conditions, P_{Act} driven fluorescence was first stimulated (compared to P_{TEF}) but after about 90 min no further increase could be observed [Fig.A10c]. P_{TEF} showed a constant signal first but then a decline in fluorescence after about 90 min. Noteworthy, the forward-scatter of the cells (which is an approximate measure of the cell-size and refractive index) was increased by heat-shock and pheromone treatment [Fig.A10d-f]. At least for the latter case this is expected because cells will grow into the large pear-shaped Shmoo-form when the mating-response is activated. The changes in forward-scatter are similar to the expression of the actin-reporter suggesting a correlation between cell-size and actin-content. The P_{TEF}-reporter seems to be less affected and therefore may better resemble the global protein regulation. For this reason the P_{TEF}-reporter was now used for signal normalization in this work.

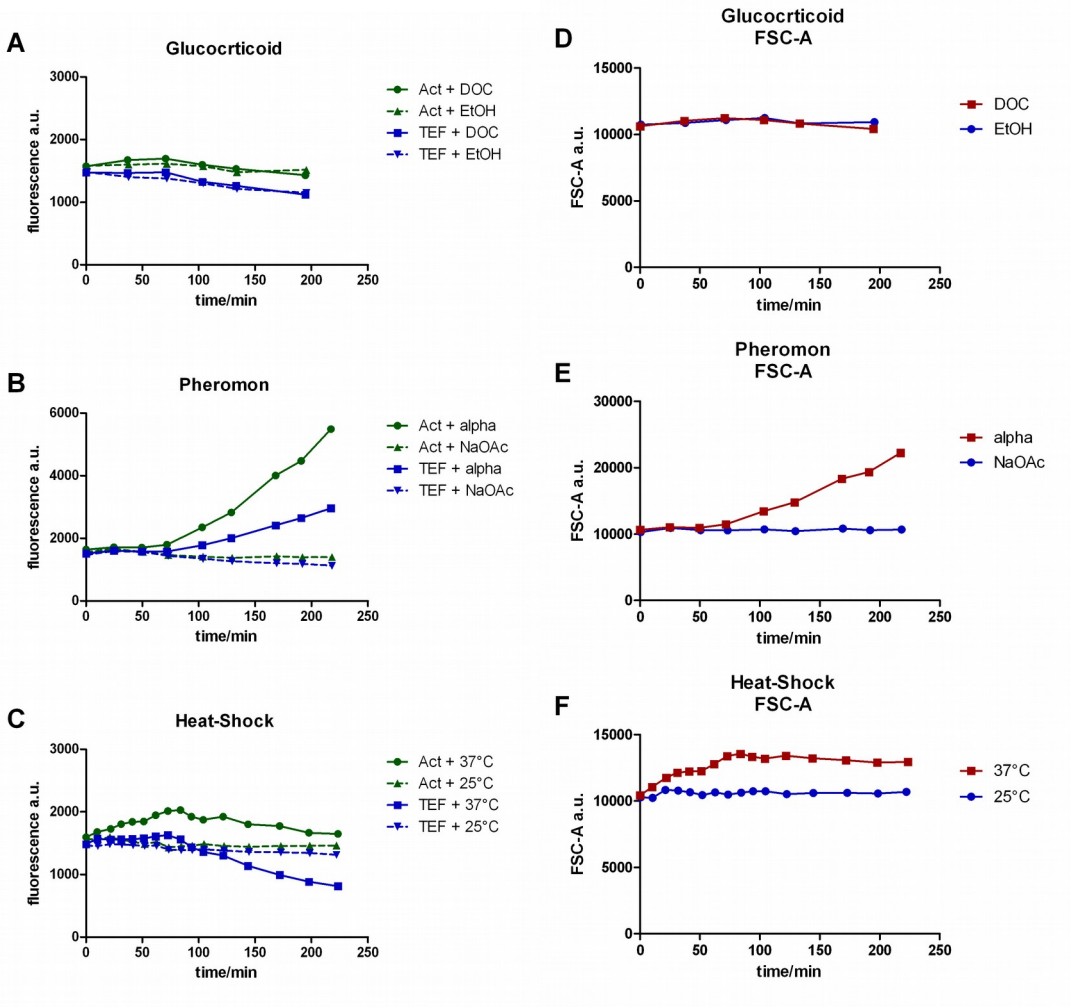

Fig.A10
Influence of stimuli on fluorescence levels of the constitutive promoters from the TEF1 gene (*Ashbya gossypii*) or the Act1 gene (*S.cerevisiae*) in WΣ. sfGFP4x was expressed from the Act1-promoter and T-Sapphire4x was expressed from the TEF1 promoter in the same cells.
a.) Measurement after mock treatment (dashed lines) or addition of 20 µM desoxycorticosterone (DOC) (solid lines).
b.) Measurement after mock treatment (dashed lines) or addition of 5.9 µM alpha factor (solid lines).
c.) Measurement at 25°C or heat-shock at 37°C (solid lines).
d.) Forward-scatter after DOC/mock treatment
e.) Forward-scatter after alpha-factor/mock treatment
f.) Forward-scatter after 37°C/25°C incubation

3.8 The normalized response of the Hsp90-reporters

WΣ was transformed with pRS304_P_{TEF}_T-Sapphire4x (or short: WΣ-TS4x) and then with the Hsp90-reporters. A gating for T-Sapphire expressing single cells was set and a compensation matrix (which was established later with the same instrument settings) was applied. No further gatings on the GFP-channel were used. HSE1-transformed cells were either heat-shocked or kept at 25°C and the response was measured. For the HSE1-reporter first an increase of the signal

could be observed and then after about 90 min fluorescence decreased [Fig.A11a]. However, a similar behavior could also be seen for the P_{TEF}-T-Sapphire signal [Fig.A11b]. In the ratio-plot [Fig.A11c] the decrease is exactly compensated. The induction calculated from the ratios saturates whereas the induction calculated only by the HSE1-reporter reaches a peak and then declines [Fig.A11d].

Similar measurements were done with the PRE-reporter [Fig.A12a-f]. As mentioned before, by the addition of alpha-factor, mat-**a** type cells are arrested in G1-phase of the cell-cycle, represented by the percentage of cells in the single-cell gating [Fig.A12e], and form the mating competent Shmoo-phenotype. Thereby the cell-volume increases, as indicated by the stronger forward-scattering [Fig.A12f], and this eventually leads to accumulation of fluorescent protein. Therefore, the uninduced and induced cells become dissimilar and it would lead to an overestimation of reporter induction when only the PRE-signal would be considered. In [Fig.A12d] this difference is clearly visible.

Because of the recombination problem, the GRE-reporter still gave unsatisfying results (data not shown).

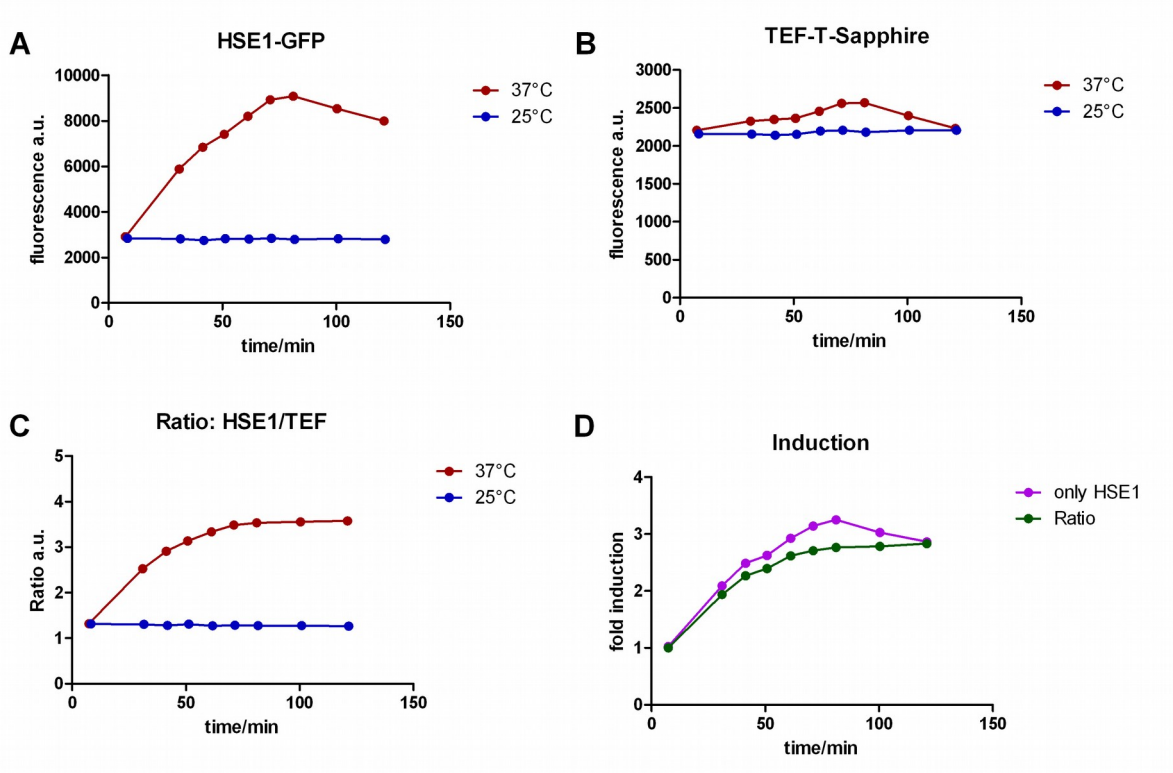

Fig.A11
Signal normalization to constitutive promoter. HSE1-sfGFP and TEF1-T-Sapphire4x were expressed together in WΣ and the kinetic was followed after incubation at 25°C and heat-shock at 37°C.
a.) HSE1-sfGFP4x signal
b.) TEF1-T-Sapphire4x signal
c.) Fluorescent ratio of HSE1-signal/TEF-signal
d.) Reporter induction calculated from the normalized signals from c.) (green) or directly form the GFP signals from a.) (magenta)

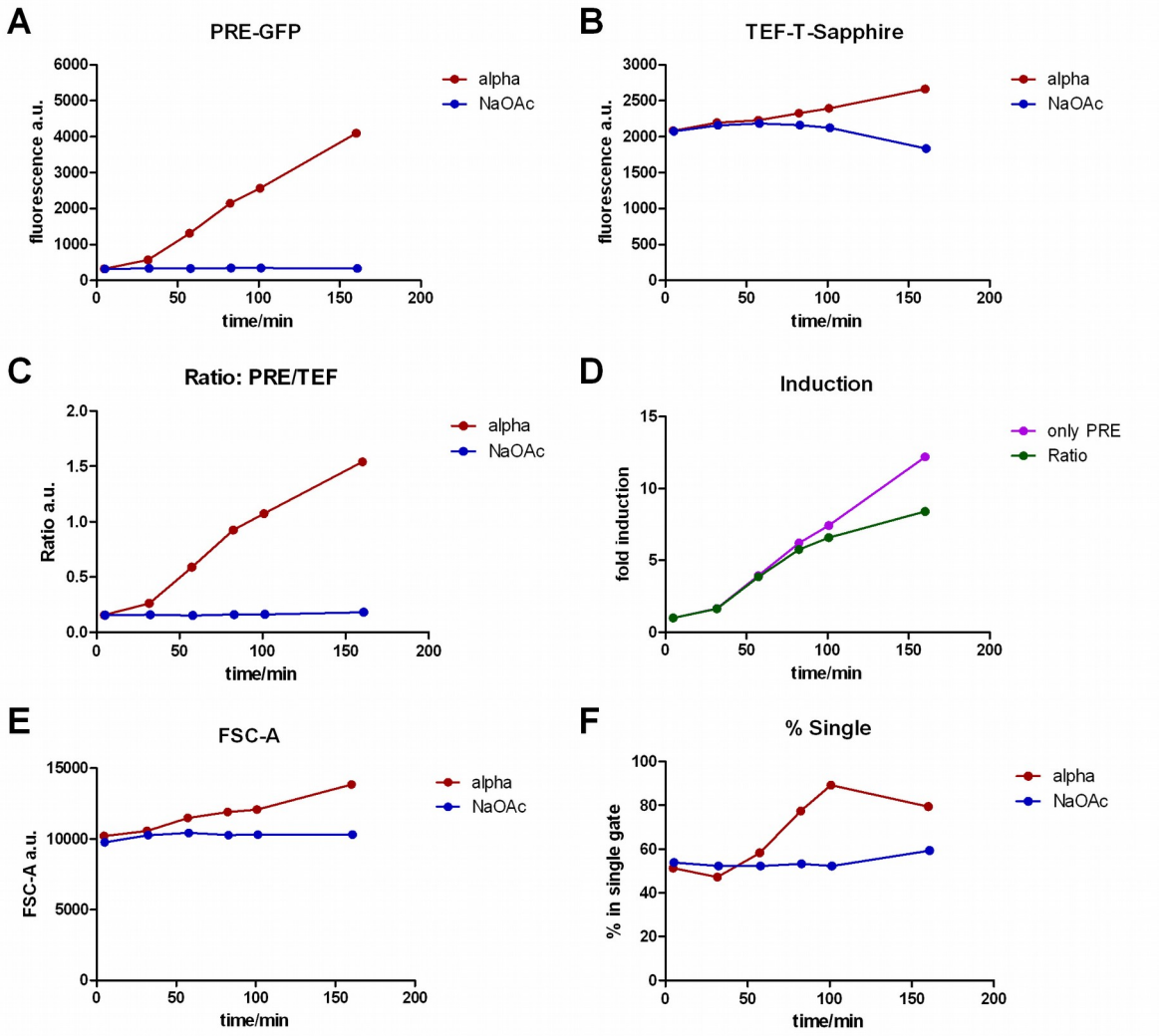

Fig.A12
Signal normalization of the pheromone reporter. PRE1-sfGFP and TEF1-T-Sapphire4x were expressed together in WΣ and the kinetic was followed after alpha-factor (5.9 µM) addition or mock treatment.
a.) PRE1-sfGFP4x signal
b.) TEF1-T-Sapphire4x signal
c.) Fluorescent ratio of PRE1-signal/TEF-signal
d.) Reporter induction calculated from the normalized signals from c.) (green) or directly form the GFP signals from a.) (magenta)
e.) Forward-scatter signal
f.) Fraction of cells in single-cell gate

3.9 Variation of the heat-shock-element

Although the HSE1-reporter yielded robust results, it remained unsatisfactory because of a low induction ratio as compared to literature values (Sorger et al., 1987); (Nieto-Sotelo et al.,

1990) and the other reporters. HSE1 contains four motifs for HSF1 binding so only one trimer is anticipated to bind at a time. We reasoned that increasing the number of HSF1-binding sites in the promoter could improve induction of the reporter. A second response-element based on the promoter of yeast Ssa4 was created and called HSE2. Interestingly, this promoter also contains four HSF1 binding sites but at imperfect spacing. We found that mutation of two bases in HSE2 can result in two different ideal binding motifs for two HSF1-trimers. The motif with a larger space between the binding sites we called HSE3 and the motif with all binding sites spaced similarly was termed HSE4 [Table_A1].

Table A 1 – Different heat-shock elements

```
HSE1 ACAGGGATCCTGTTTCTAGAAGCTTCTAGAACTAGAGTCGACC
HSE2 CTGCAGAAGTACATTCTAGAAGTTCCTAGAACCTTATGGAAGC
HSE3 CTGCAGAAGAACATTCTAGAAGTTCCTAGAACCTTCTGGAAGC
HSE4 CTGCAGAAGTACATTCTAGAAGTTCTAGAACCTTCTGGAAGC
```

All the elements were cloned as a GFP-reporter in the MetLR-His vector (*described below*). In addition, the complete HSE2-element was cloned as a tandem and tetra-repeat to see whether there is an additive effect of multiple HSF1-binding. The reporters were then integrated in the genome of WΣ also harboring the P_{TEF}-T-Sapphire reporter and tested under heat-shock conditions at 37°C [Fig.A13]. Surprisingly, the new HSE elements had a much lower basal fluorescence. Since the P_{TEF}-T-Sapphire signal changed after about 100 minutes, later time-points were excluded from the analysis of the induction [Fig.A14a]. Multiple copies of the HSE2 had no influence on the maximal induction of the heat-shock response [Fig.A14c], but a significantly lower basal activity [Fig.A14b]. HSE4 behaved as an intermediate between HSE1 and the rest of the elements. On the basis of the total amount of produced fluorophores after induction, the different constructs became quite similar [Fig.A14d]. On the basis of the induction level, multiplication of the response elements lead to a stronger activation of the system [Fig.A14e] but the low basal level would make this representation very prone to uncertainties in autofluorescence. Deducing from the architecture of the binding sites, one could conclude: cooperation of HSF1 trimers seems to lower basal activity, which argues for a repressive function of HSF1.
An explanation for the data from HSE1 and HSE4 could be that HSE1 can bind only one HSF1 trimer at a time whereas on HSE4 two trimers compete for binding at different positions because of steric hindrance. This could lead to a temporal cooperativity of the trimer-complexes and to an - on average - stronger repression of the promoter. In HSE2 and HSE3, two HSF1 trimers complexes may coexist on the DNA leading to full repression.

The drop in TEF-Signal after 100 minutes [Fig.A13b] can be explained by the assumption of a general attenuation of translation and subsequent dilution by cell division. This is supported by the fraction of single cells [Fig.A13f], which starts to increase again after 100 minutes. Interestingly, the forward-scatter signal [Fig.A13d] of the single cells increased during heat-shock and stayed constant after about 100 minutes. If one would interpret the forward-scatter as a measure for cell size, it would mean that yeast-cells at a higher temperature are bigger. This hypothesis remains to be verified by microscopic imaging.
During heat-shock dead cells accumulate in the culture, seen by the fraction of living cells [Fig.A13e]. Again after 100 minutes this trend was stopped indicating that most of the cells have adapted to the condition at this time. Also cell divisions appeared to be slightly faster after this

time [Fig.A13g] but this can also be misleading because the beginning of the growth curve is overlain by the accumulation of dead cells.

Taken together, having two or more HSF1 binding sites the heat-shock element lowers the basal activity of the system maybe through the repressing function of the HSF1-complex and makes it more sensitive to small changes. Since HSE2 is the wild-type sequence from the Ssa4-promoter and shows a stable signal after full induction, this construct was chosen for further experiments. Given the fact that the change in the normalized signal is dominated by the drop of the TEF-signal after 100 minutes (at least for HSE1 and HSE4), evaluation of the heat-shock response should be done between 60 and 90 minutes to circumvent interpretation issues arising from cell-division and adaptation.

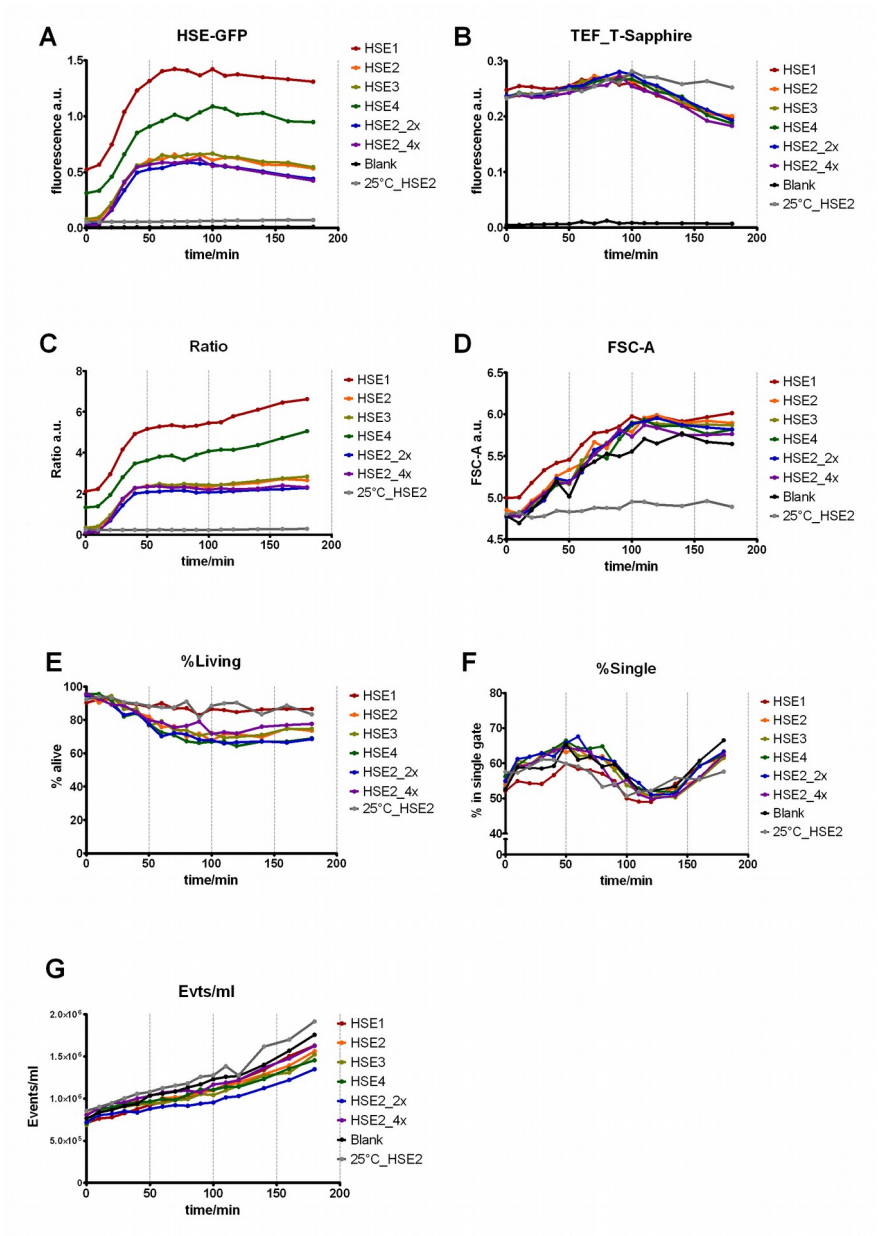

Fig.A13
Heat-shock reporters with different heat-shock elements (HSEs) and multiplications of HSEs. All HSE-sfGFP4x reporters were integrated in 2 copies with the MetLR-His vector in WΣ co-expressing TEF-T-Sapphire. Cells were shocked at 37°C except for one sample with the HSE2 reporter which was kept at 25°C. Blank cells did not harbor any reporter.
a.) HSE1-sfGFP4x signal
b.) TEF1-T-Sapphire4x signal
c.) Fluorescent ratio of HSE-signal/TEF-signal
d.) Forward-scatter signal
e.) Fraction of living cells defined by TEF-T-Sapphire expression
f.) Fraction of cells in single-cell gate
g.) Cell growth during the experiment calculated from the known sample flow-rate and recorded events in the flow-cytometer

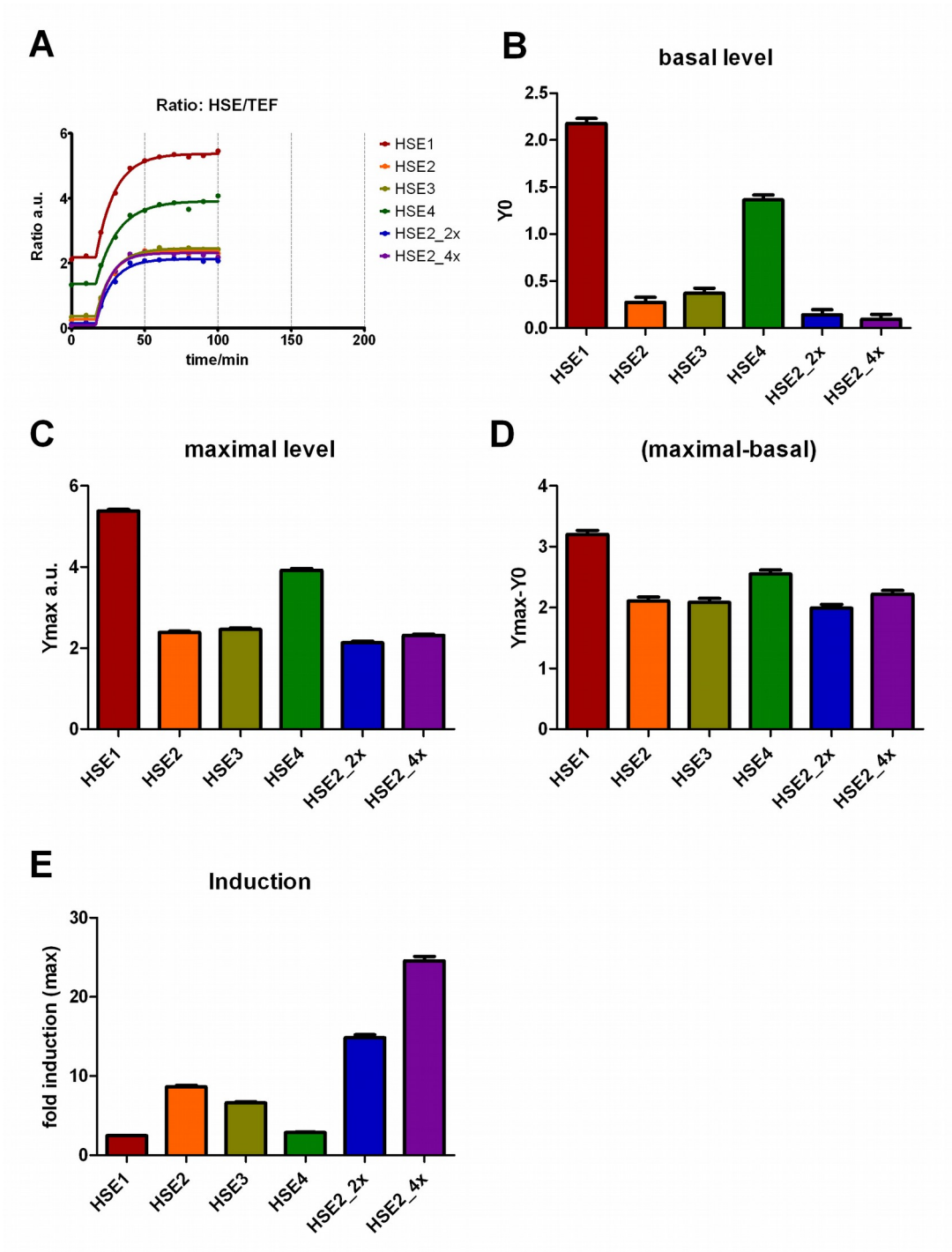

Fig.A14
One-phase association fittings with shared delay of the heat-shock response measured for the first 100 min of induction from [Fig.A13c].
a.) Data-points and fitted curves
b.) Basal reporter activity
c.) Maximal normalized reporter fluorescence
d.) Increase in fluorophore production during heat-shock (maximal induction – basal level)
e.) Induction level of the different heat-shock reporters

3.10 Recovery after Heat-shock

Upregulation of heat-shock genes is a fast process. To see if the maximal induction is triggered already by short heat-shock events, the culture expressing either the HSE1- or HSE2-reporter was shifted from 25°C to 37°C for 10, 30 or 60 min and then rapidly diluted in medium with 25°C. The further induction and the recovery-phase (or rather the dilution of GFP) was followed. As it can be seen in [Fig.A15a,b], short heat pulses can have a long aftereffect but do not lead to full induction. This may lead to thermotolerance by increasing the basal level of the chaperone and stress-adaptation systems, like Hsp104 (Lindquist and Kim, 1996). After full induction, no new GFP is synthesized and the signal decays.

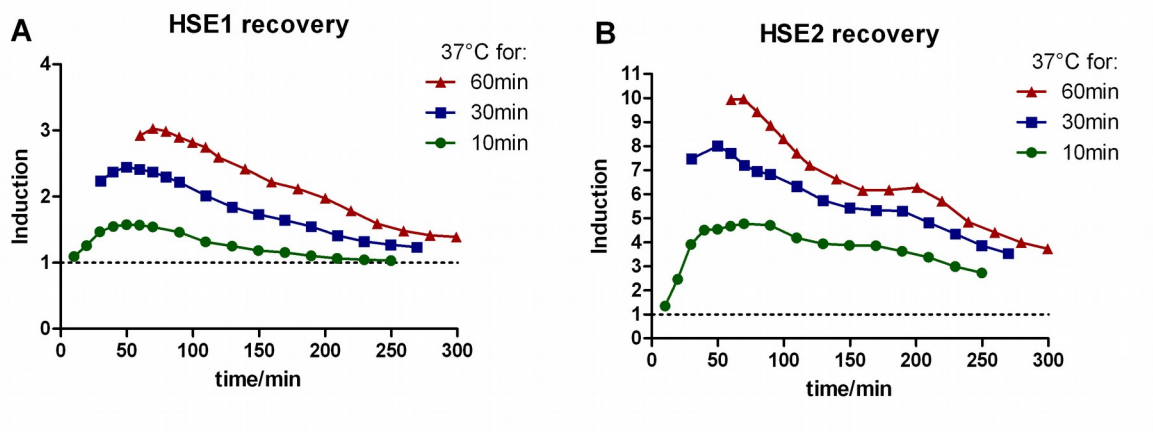

Fig.A15
Recovery after heat-shock. WΣ cells the respective heat-shock reporter were pre-cultured at 25°C, heat-shocked for the indicated times and then diluted back in 25°C medium. The progression of the reporter response was followed.
a.) Response of the HSE1 reporter
b.) Response of the HSE2 reporter

4 Redesign of the Hsp90-reporter

4.1 The plasmid backbone

Considering the problems with integrative pRS-plasmids caused by recombination and the fact that complex nature of the reporters hampers the subcloning to other selection markers or the linearization, I decided to redesign the architecture from scratch. The objective should be a system, where all elements are accessible by restriction sites to exchange them in a cassette-like manner. The system should only integrate in one copy at a defined locus which can be tested for afterwards.
Basis of the new design was the classical pBluescript II SK+ (pBSSK). An artificial multiple cloning site was introduced between the ApoI and BssHII sites of pBSSK and all the components were assembled sequentially. The cloning strategy for the MetLR-His-construct is depicted in [Fig.A16a], a plasmid map example is given in [Fig.A17]. The left (MetL) and right (MetR) regions are homologous sequences that target the reporter to the desired locus (in this case the Met17 locus - YLR303W) and used to create a knockout of the respective gene. Choosing a different selection marker (in this case the His5 gene from *S. pombe*) than the target

gene makes it possible to test for correct integration by replica-plating, at least if the yeast was prototroph for the knocked-out gene. Several elements were developed and are depicted in [Fig.A18]. Selection markers were taken from plasmids of the Euroscarf-deletion-plasmid-collection (Gueldener et al., 2002) and interfering restriction sites were removed. Linearization of the construct can be achieved by digestion with DraIII or NruI. Furthermore the system is designed to duplicate the reporter part as an inverted repeat in the plasmid. Later recombination in yeast would only lead to an inversion of the insert but not to a loop-out. Because of the versatile combinations I preferred the precise terminology "LokusLR-Marker_(ResponseElement-Fluorescentprotein)copys". For the duplicated Heat-shock-reporter1 with the tetrarepeat of superfolder-GFP for example "MetLR-His_(HSE1-sf4x)2x".

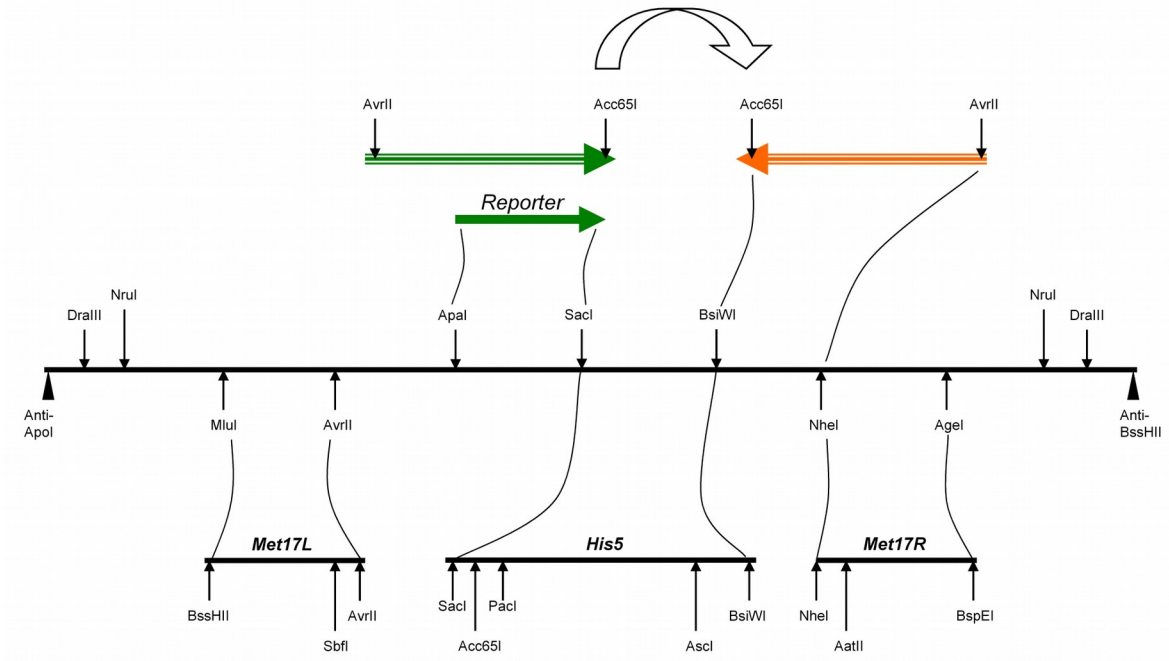

Fig.A16
Cloning strategy of the single integrative vectors. The central fragment is an artificial multiple cloning site which was ligated into the ApoI/BssHII sites of pBluescript II SK+. In this example, Met17L and Met17R are homologous sequences to the left and right part of the yeast gene coding for Met17. His5 is the histidine selection marker originating from *S.pombe*. The layout is designed in a way that a reporter sequence can be duplicated by using compatible restriction sites (striped green and orange arrows). The final construct can be linearized by digestion with either DraIII or NruI for transformation of yeast cells.

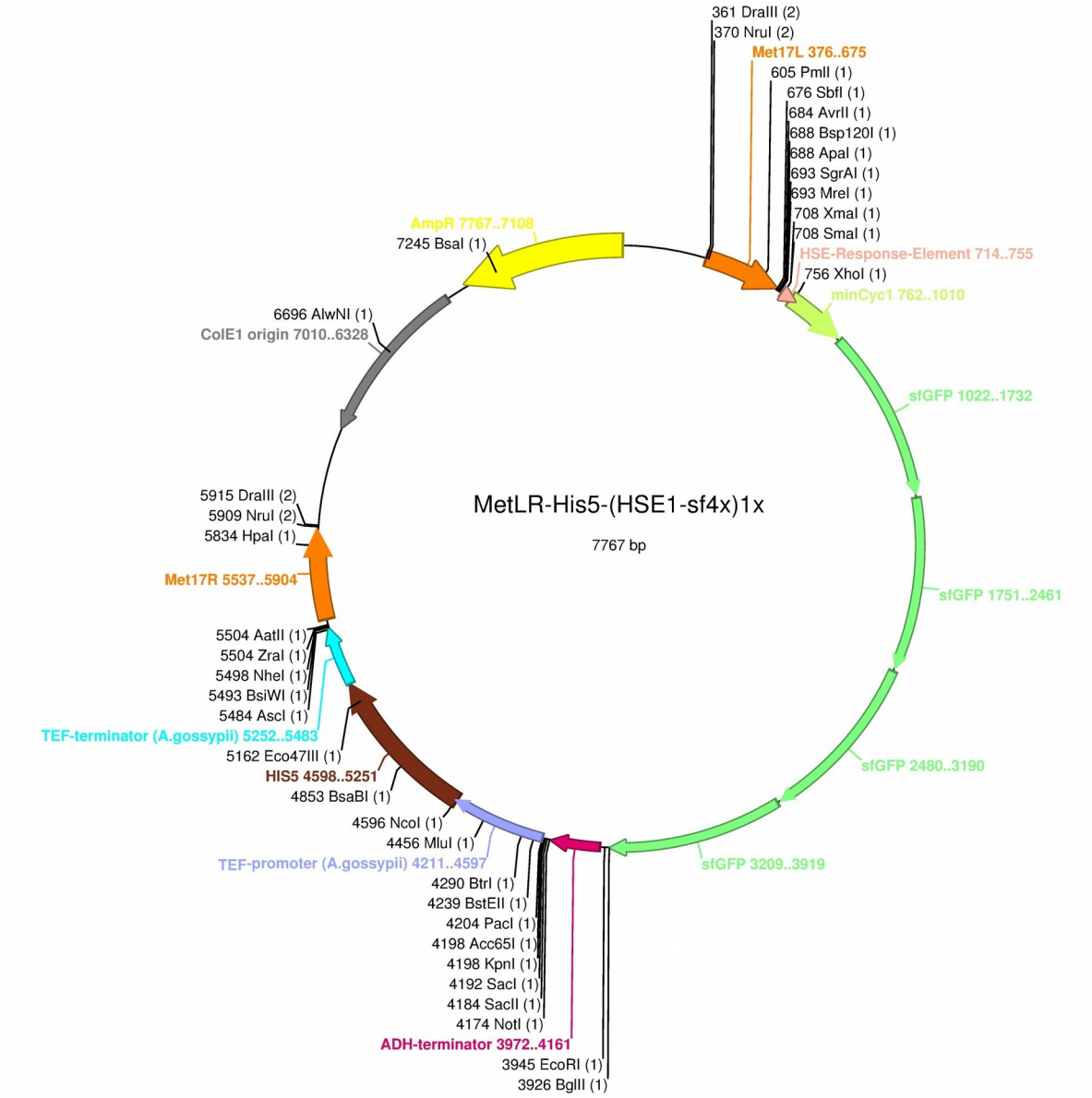

Fig.A17
Plasmid map of the final HSE1-sfGFP4x reporter (not yet duplicated). Unique restriction sites and DraIII/NruI sites are shown.

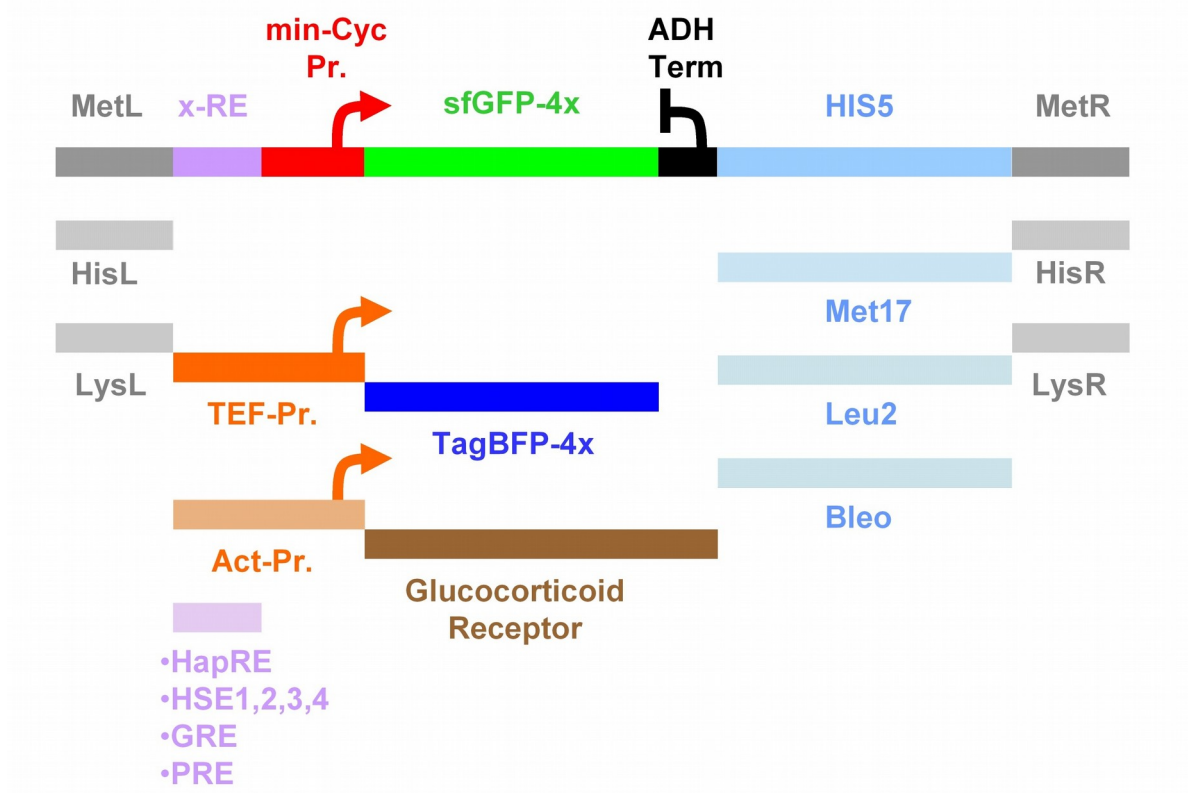

Fig.A18
Currently available reporter-elements. Every element was designed to have unique restriction sites for cloning in most of the combinations. MetL/R refers to the *S.cerevisiae* Met17 locus; LysLR refers to the *S.cerevisiae* Lys2 locus; HisL/R refers to the *S.cerevisiae* His3 locus; His5 refers to the *S.pombe* His5 selection marker; Met17 refers to the *S.cerevisiae* gene; Leu2 refers to the *K.lactis* Leu2 selection marker; Bleo refers to the Bleomycin/Zeocin® selection marker; x-RE is a placeholder for different response-elements (HapRE, HSE, GRE, PRE – see text); min-Cyc Pr. is the minimal cytochome c promoter; TEF-Pr. is the TEF1 promoter from *A.gossypii*; Act-Pr. is the Act1-promoter from *S.cerevisiae*; ADH Term, is the Adh1-terminator of *S.cerevisiae*; sfGFP-4x and TagBFP-4x are tandem-replications of the fluorescent proteins; and the glucocorticoid receptor is the intron-free gene from *R.norvegicus*.

4.2 Indicator for duplication

To make screening for reporter duplication easier, an additional feature was added to the backbone of some constructs. The original alpha-complementation-fragment of β-Galactosidase from the pBluescript-vector had been deleted together with the F1 origin by the addition of the multiple cloning site. The idea now was to add back the β-Gal fragment in two parts. The first part is the LacZ-promoter and the first five amino acids, which was placed upstream of the reporter facing outward and terminating in the left homologous region of the backbone. The second part was placed near the right homologous sequence and contained the rest of the alpha-complementation fragment and the F1-origin. If the duplication step is successful, the first part is placed in frame to the second part and the full alpha-complementation fragment is produced and can be detected in *E. coli* by blue-white screening. In this case the blue color of a colony indicates the duplication.

5 Application of the Hsp90-Reporters

5.1 Tester-Strains for Hsp90

For eukaryotic organisms, Hsp90 is an essential protein. Consequently a knockout strain would not be viable, which makes genetic studies more complicated. Yeast expresses two isoforms of Hsp90 called Hsp82 and Hsc82, each of which can support viability, if expressed alone from a single gene copy. As both isoforms share most of the known clients, an introduced mutant cannot be accessed in this background. To accomplish this, a double-knockout of hsp82 and hsc82 has to be made in the presence of a rescue plasmid. The mutant is then introduced with a second plasmid and the rescue plasmid is subsequently discarded.

5.1.1 WΣ-background

A double-deletion strain of WΣ was constructed (genotype: Δhsp82::NatMX, Δhsc82::HphNT, pRS416-hsp82). In the next step, the pRS304-P_{TEF}-T-Sapphire4x reporter was integrated and after that the Hsp90-reporters in the MetLR-His-(Reporter-sf4x)2x layout.
This configuration was used to measure mutants of the charged linker in Hsp82 and S365 phosphorylation mutants of human Hsp90β (*see below*).

5.1.2 DP533-background

Although human Hsp90β can complement the double knockout in yeast, human Hsp90α fails to support growth in the BY4741 or the WΣ-background. A strain that is reported to be viable under these conditions comes from the lab of Didier Picard (Wider et al., 2009) and had the stock number DP533. Its genotype was given as: Mat a, Δhsc82::KanMx4, Δhsp82::KanMx4, Δpdr5::loxP-LEU2-loxP, trp1-289, leu2-3,112, his3-Δ200, ura3-52, ade2-101oc, lys2-801am/2µ-HSC82-URA3[YEplac195].
However human Hsp90α (hHsp90α) could only complement, when expressed under the control of the very strong TDH3-promoter. Even two copies expressed under the natural Hsp82 promoter failed to grow [Fig.A19].
Because of the weak complementation a high percentage of dead cells accumulate in the culture. To minimize effects which are caused by the frequent plasmid loss of centromeric-plasmids I subcloned the P_{TDH3}-hHsp90α in my single-integrative vector backbone LysLR-Leu and used the duplication-feature.

To have a standard “platform” for hHsp90α-mutants, I decided to adapt the DP533 strain to the reporter system and the available selection markers. We received the DP533-strain as a mixture of cells forming red and white colonies on YPD-plates. Both white and red cells did not grow on medium lacking adenine, indicating that white colonies did not acquire a back-mutation of the ade2-101oc allele. Yeast cells harboring the Sup35-prions [PSI+] are able to suppress certain stop-codons and ADE2 mutations are often used as readout of this prion activity. To exclude [PSI+], red and white colonies were picked and streaked on YPB-plates containing 5 mM of guanidinium hydrochloride, which can cure cells from prions by inhibiting Hsp104 (Grimminger et al., 2004) and thus their propagation. White colonies did not revert to the red color, indicating that they do not harbor the Sup35-prion (data not shown). Since none of the reporters needs the ADE2-selection marker, a fragment of the ADE2-gene spanning codon 101 was transformed into cells originating from a red colony to create a new white strain. To check for integration of

mutants into the lysine-locus this gene needs to be functional. Luckily the strain was already able to grow on medium lacking lysine, contradicting the annotation, so no further actions had to be taken here. The DP533-strain had been deleted for the multidrug-resistance-transporter Pdr5 before. The selection marker used for this purpose was a LEU2-gene which is flanked by two loxP-sites. To get rid of that marker, the pSH62-plasmid (Gueldener et al., 2002) was transformed into the strain. This plasmid is selected by the HIS3-marker and contains the Cre-recombinase under control of the Gal1-promoter. After inducing the Cre-recombinase several colonies were checked for both loss of the LEU2-marker and the pSH62-plasmid. The final basis-strain was then transformed with pRS304-P_{TEF}-T-Sapphire4x and the MetLR-His_(Reporter-sf4x)2x. For the GRE-reporter in addition the HisLR-Bleo_(TEF-rGR)2x construct was integrated. In the last step, the duplicated hHsp90α-mutants in the LysLR-Leu-vector were introduced. Several colonies of this last transformation were picked and passaged over 5FOA to get rid of the Hsp82-rescue-plasmid. The bulk of surviving cells from each colony was then assayed for reporter activity.

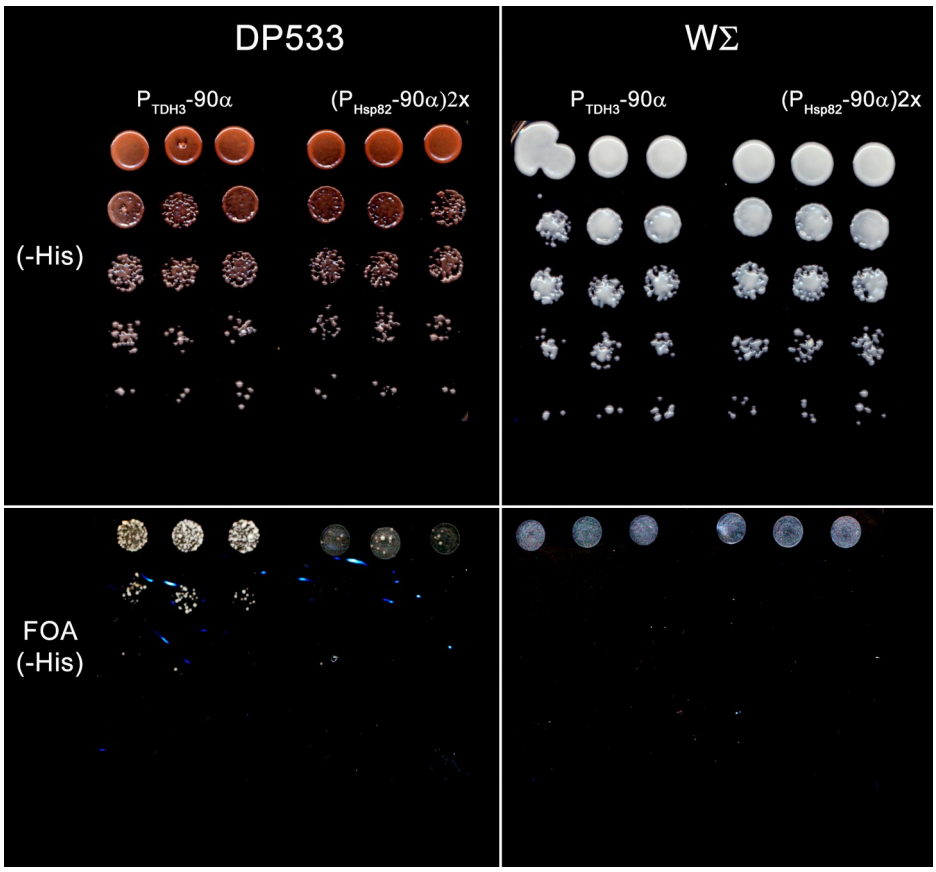

Fig.A19
Complementation of human Hsp90α in DP533 and WΣ. Both strains harbor a rescue plasmid with Ura3-marker containing yeast Hsp82. The hHsp90α-protein was expressed from the TDH3-promoter or twice from the yeast Hsp82 promoter in pRS413. Three independent clones were tested for complementation in a 10-fold dilution series without selective pressure (upper panels) or on 5-FOA containing plates to select for loss of the rescue plasmid (lower panels).

5.2 Mutants of the Hsp82-linker

All Hsp90 homologues possess a flexible linker region between the N-terminal and the middle domain (Tsutsumi, 2012). Depending on the organism this linker is of variable length and its function remained unclear. Several experiments indicated that the sequence of the linker is arbitrary but the length is important. The hypothesis was that upon client binding a rotation of the N-terminal domain is induced which was supported by cross-linking experiments and *in vitro* studies (*personal communication Matthias Mayer*). The *in vivo* reporter system was used to measure the effect of the linker-length on different Hsp82-clients. The strain background was WΣ Δhsp82::nat, Δhsc82::hygB complemented with the respective mutants. Five different constructs (see Table A2), expressed twice from the natural Hsp82- and Hsc82-promoter in a pRS415-vector, were tested for reporter activity. The L5-mutant has the same linker length than L2, but with an artificial GSSGSSG sequence inserted.

Table A 2 - Hsp82-linker variants used for in vivo activity measurements

Name	Mutant
L1 (wt)	hsp82-E57C
L2	hsp82Δ(211-259)-E57C
L3	hsp82Δ(211-263)-E57C
L4	hsp82Δ(211-266)-E57C
L5	hsp82Δ(211-266)-GSSGSSG-E57C

5.2.1 Hap response in the linker mutants

The expression of the HapRE-reporter was only mildly influenced by the different mutants [Fig.A20]. A small, but significant effect could be seen in the shortest L4-mutant. The insertion of the GSSGSSG in L5 restored the phenotype of the equivalent L2-mutant.

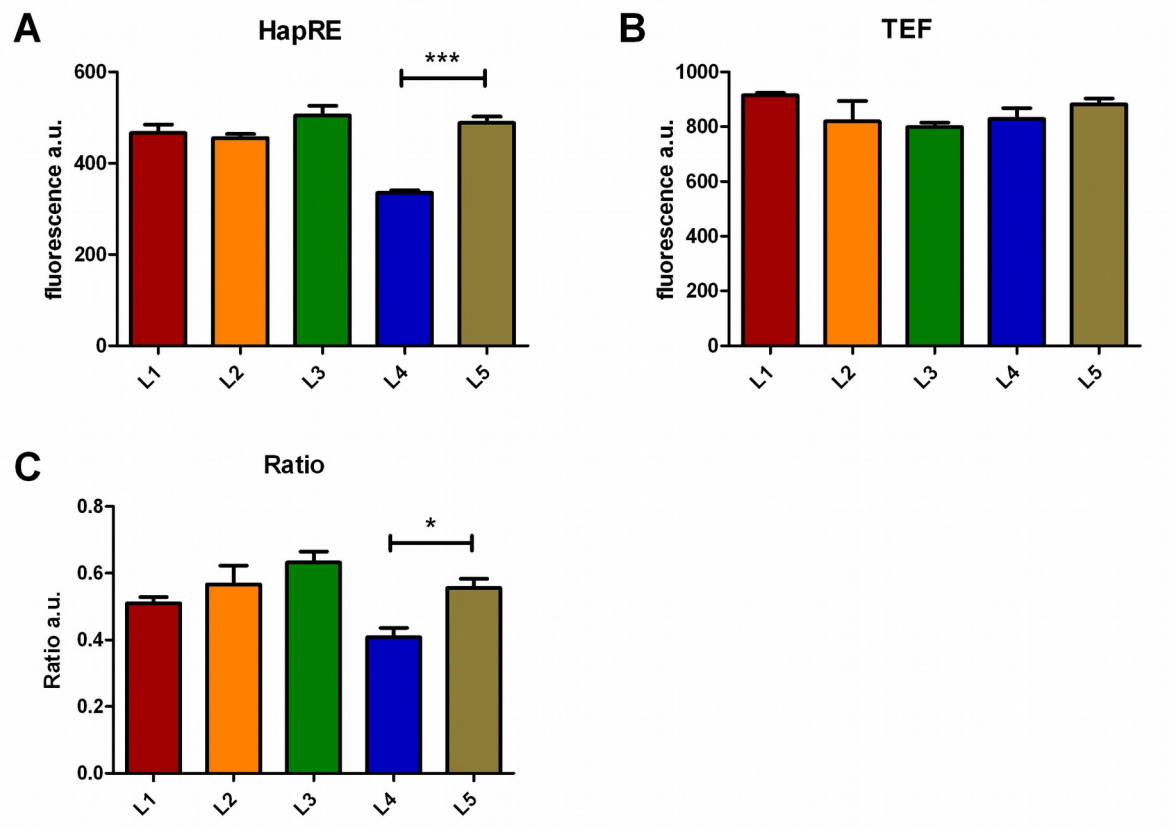

Fig.A20
Hap-reporter measurements in WΣ expressing different linker-mutants of Hsp82 (n=3).
a.) Signal of the Hap reporter (T-Test for L4 and L5: $P=5*10^{-4}$)
b.) Signal of the constitutive TEF1-reporter
c.) Signal of the Hap-response normalized to the TEF1-reporter (T-Test for L4 and L5: P=0.021)

5.2.2 Pheromone response in the linker mutants

A stronger influence by the mutants was observed with the pheromone reporter [Fig.A21]. Both basal and induced expression was largely decreased in the L4 background. Because of the lower basal activity in L4, the decrease in induction was less severe [Fig.A21d]. In L5 the signal strength was rescued.
This suggests that the Hsp90 dependent Ste11 MAPKK is less well chaperoned by the L4 mutant, which then acts as a bottleneck for signal transduction. Once activated, the kinase-cascade can amplify the signal and the induction becomes comparable.

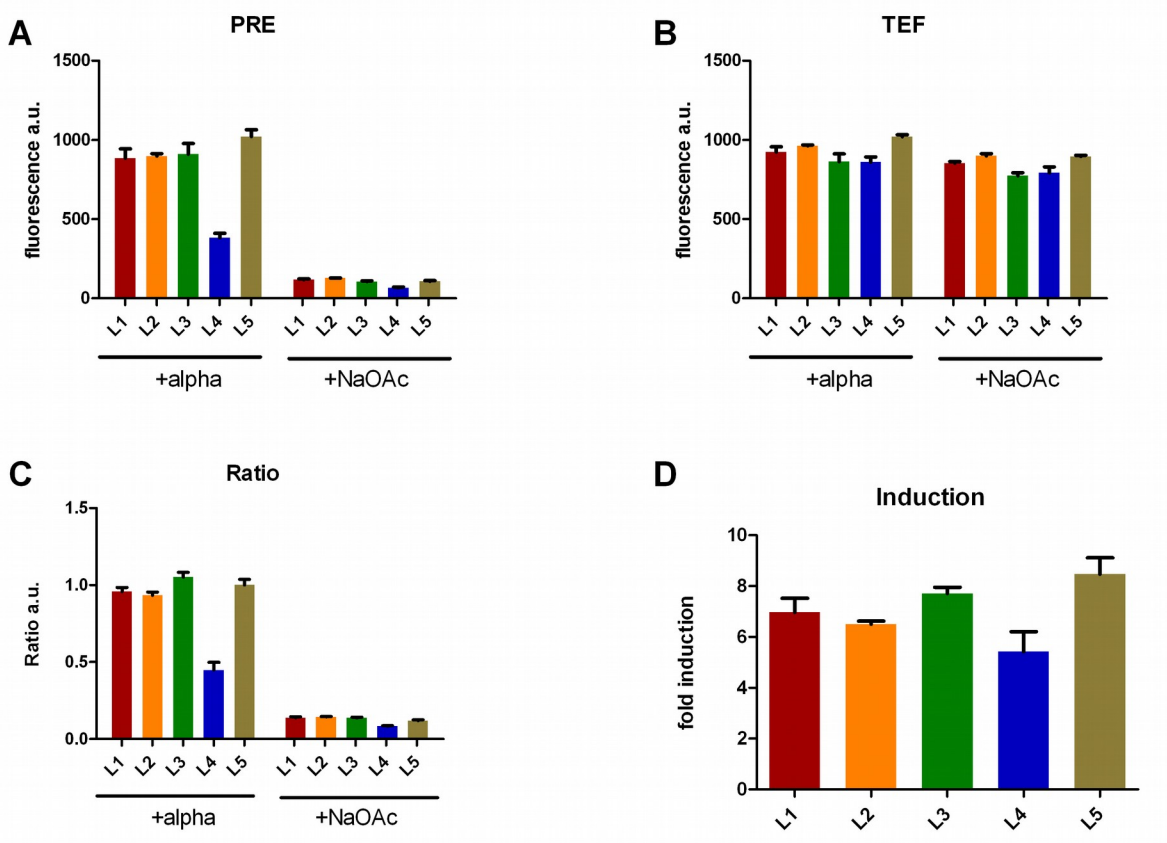

Fig.A21
Pheromone-reporter measurements in WΣ expressing different linker-mutants of Hsp82. Cells were either induced with 5.9 µM alpha-factor or mock–treated with NaOAc for 3h. Error-bars represent the standard error of the mean (n=3).
a.) Signal of the PRE-reporter
b.) Signal of the constitutive TEF1-reporter
c.) Signal of the PRE-response normalized to the TEF1-reporter
d.) Induction of the PRE-response, calculated from the normalized ratios.

5.2.3 Heat-shock response in the linker mutants

The effect on heat-shock response is less clear to interpret ([Fig.A22] and [Fig.A23]). Considering the normalized expression of the HSE1 and HSE2 reporters, it seems that the shorter linker mutants L3 and L4 have an impact on both the repression and the induction of Hsf1. Reporters at 25°C in the L3 and L4 background showed an increased basal activity suggesting a less efficient repression of the DNA bound Hsf1. At heat-shock however, induction of Hsf1 also seemed to be less efficient. The induction of the system decreased from L1 to L4 and was restored to L2 level by the L5-mutant. In addition the response was weaker at 42°C compared to 37°C.
To monitor the whole response, an induction-kinetic of L4 an L5 was recorded at both 37°C and 42°C [Fig.A24]. The absolute values obtained in this experiment were different from the previous experiment but the relative values were consistent [Fig.A23]. Both GFP expression and induction was higher at 42°C. This may reflect different growth conditions of the cultures at

different days (population doublings after stationary phase before the measurement or culturing in Erlenmeyer-flasks on a shaking incubator or in tubes on a rotator) so only a qualitative interpretation can be made. Considering only the relative values of the kinetic at 37°C, L4 is less inducible than L5 consistent with the previous result.

To interpret the HSE data of the linker-mutants, additional information is needed! Since Hsf1 in yeast is already bound to DNA, recruitment to the promoter should not be altered in the mutants. However the interchange rate or the dwell time of bound Hsf1 molecules could be different. Second, as the short linker-mutants may exhibit a weaker general chaperoning activity, they could be trapped in the chaperoning cycle in many cellular processes and therefore the "free" Hsp82 molecules could be reduced and limiting the repression of Hsf1. This can be checked by a simple experiment where the linker-mutants are over-expressed by a stronger promoter. Indeed the expression levels are critical as cells expressing the mutants only from the stress-inducible Hsp82 promoter, failed to induce a luciferase based HSE1 and GRE reporter (data not shown). Assuming that all linker-mutant backgrounds experience the same cytosolic conditions, the affinity to Hsf1 could still be different. The L4 mutant may be bound more tightly at heat-shock conditions and thus preventing full activation of Hsf1. The other possibility would be that the status of post-translational modifications on Hsf1 is altered by the linker-mutants. If for example the recruitment of kinases to Hsf1 is impaired, then hyperphosphorylation will be less efficient and the reporter will not be fully induced. If additionally the association with phosphatases is impaired, then the repression would be leaky and the basal level would go up.

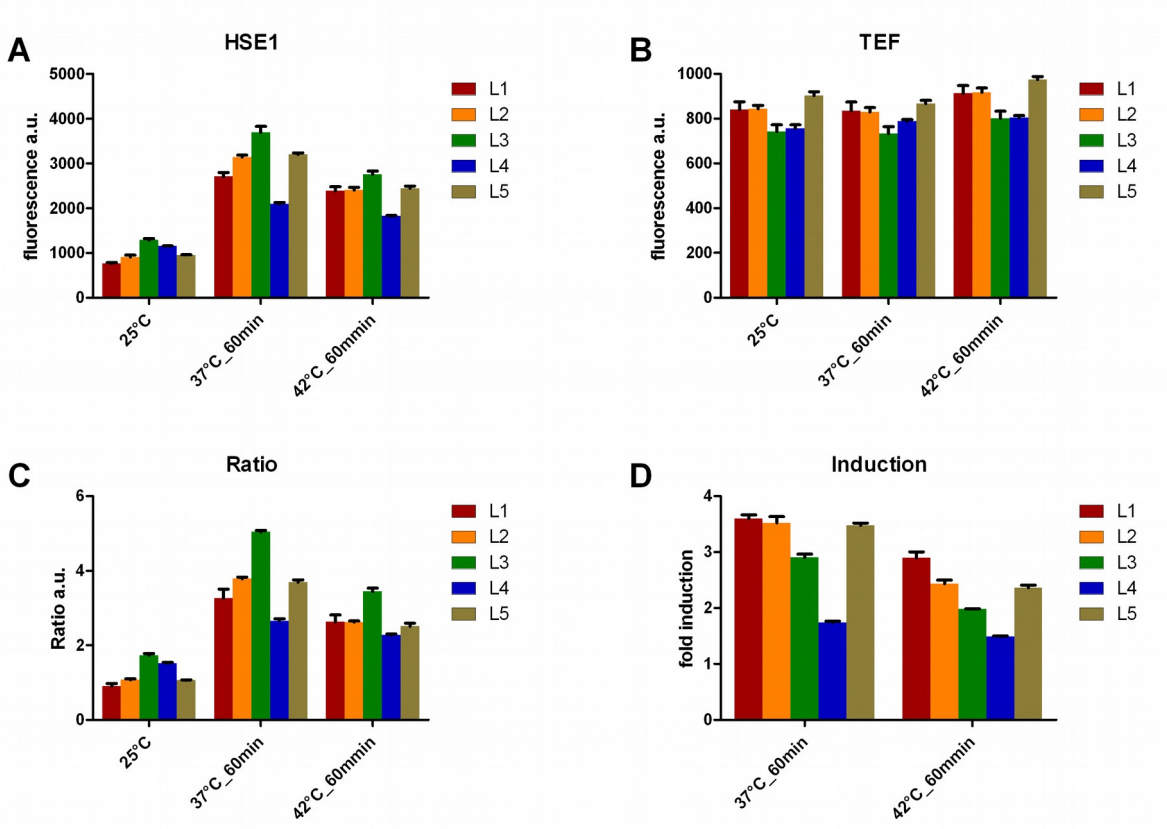

Fig.A22
Heat-shock-reporter measurements in WΣ expressing different linker-mutants of Hsp82. Cells were either kept at 25°C or heat-shocked for 1h at 37°C or 42°C. Error-bars represent the standard error of the mean (n=3).
a.) Signal of the HSE1-reporter
b.) Signal of the constitutive TEF1-reporter
c.) Signal of the HSE1-response normalized to the TEF1-reporter
d.) Induction of the HSE1-response, calculated from the normalized ratios.

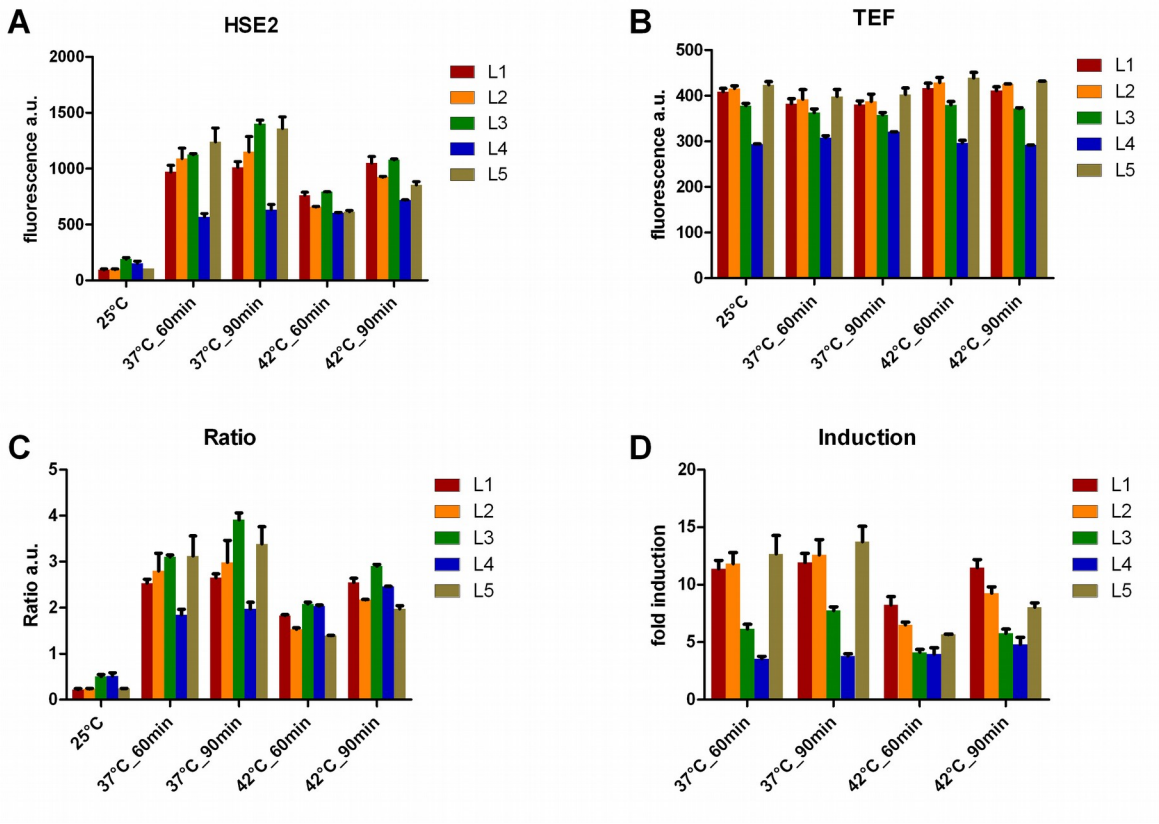

Fig.A23
Heat-shock-reporter measurements in WΣ expressing different linker-mutants of Hsp82. Cells were either kept at 25°C or heat-shocked for 1h at 37°C or 42°C. Error-bars represent the standard error of the mean (n=2).
a.) Signal of the HSE2-reporter
b.) Signal of the constitutive TEF1-reporter
c.) Signal of the HSE2-response normalized to the TEF1-reporter
d.) Induction of the HSE2-response, calculated from the normalized ratios.

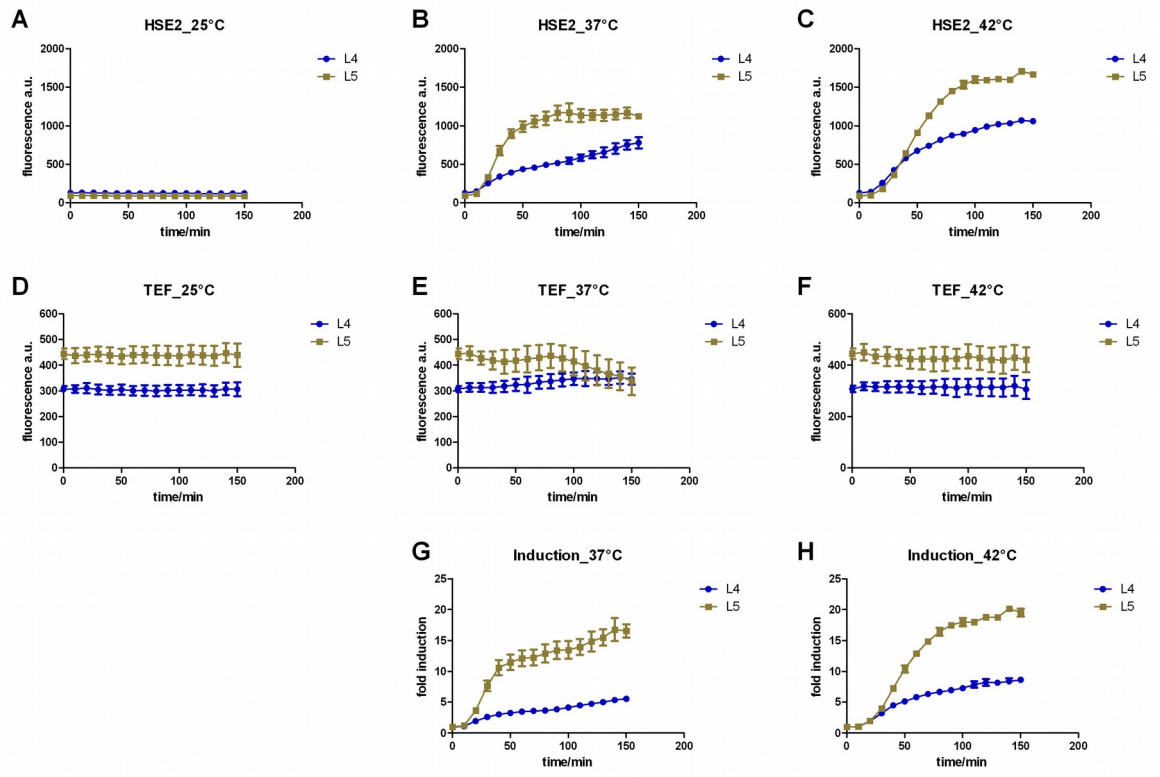

Fig.A24
Induction-kinetics of the HSE2-reporter in WΣ for the Hsp82 linker mutants L4 and L5. Cells were either kept at 25°C or heat-shocked for at 37°C or 42°C. Error-bars represent the standard error of the mean (n=2).
a-c.) Signal of the HSE2 reporter at 25°C, 37°C and 42°C
d-f.) Signal of the constitutive TEF1-reporter at 25°C, 37°C and 42°C
g-h.) Induction of the HSE2-response relative to the normalized signal at 25°C.

5.2.4 Glucocorticoid response in the linker mutants

The most prominent phenotype of the linker-mutants can be seen in the response of the glucocorticoid-receptor [Fig.A25a-d]. An induction kinetic was recorded [Fig.A26a,b] and a one-phase-association fit with delay was performed on the induction [Fig.A26d]. From L1 to L4 the maximal expression dramatically declined. Again, the restored linker-length in L5 gave the same results as the L2-mutant.

By looking at the data on the level of individual cells, a dichotomy in GRE-reporter expression can be observed which is correlated with the length of the linker [Fig.A27a]. The shorter the linker, the more cells are present in the weakly induced population. This dichotomy can also be seen in the pheromone response but only prominent in the shortest linker [Fig.A27b]. In the HapRE and HSE1-reporters the whole population shifts rather than forming distinctive subpopulations [Fig.A27c,d]. A general explanation for the GRE-reporter may be derived from the complementation of the mutants. Mutant proteins with short linkers complemented much weaker than the longer versions [Fig.A28] which could indicate that by chance, always some cells produce enough Hsp82 or have less misfolded proteins to maintain vital functions and thus

have the ability to induce the reporter. The shorter the linker, the more cells get overwhelmed by their physiological burden and would end-up in the poorly induced population. As the glucocorticoid-receptor has the strongest specific dependency on Hsp90, the GRE-reporter may be the most sensitive indicator for this kind of regulation.

5.2.5 Conclusion

In conclusion the flexible linker of Hsp82 seems to play an important role in the conformational changes during the chaperone cycle. The sequence however seems arbitrary as the L5-mutant resembles the phenotypes of the equally long L2-mutant.

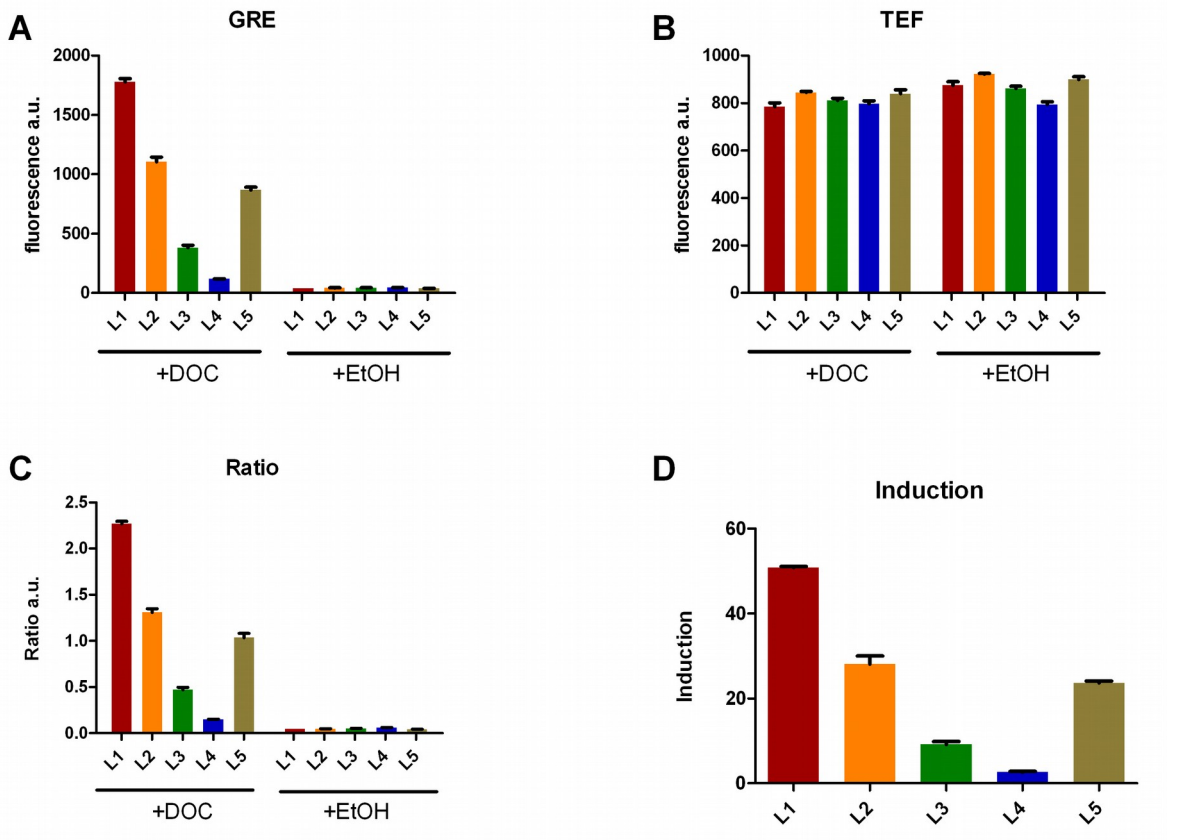

Fig.A25
Measurements of the glucocorticoid reporter in WΣ expressing different linker-mutants of Hsp82. Cells were either induced with 10 µM desoxycorticosterone or mock–treated with ethanol for 3h. Error-bars represent the standard error of the mean (n=3).
a.) Signal of the GRE-reporter
b.) Signal of the constitutive TEF1-reporter
c.) Signal of the GRE-response normalized to the TEF1-reporter
d.) Induction of the GRE-response, calculated from the normalized ratios.

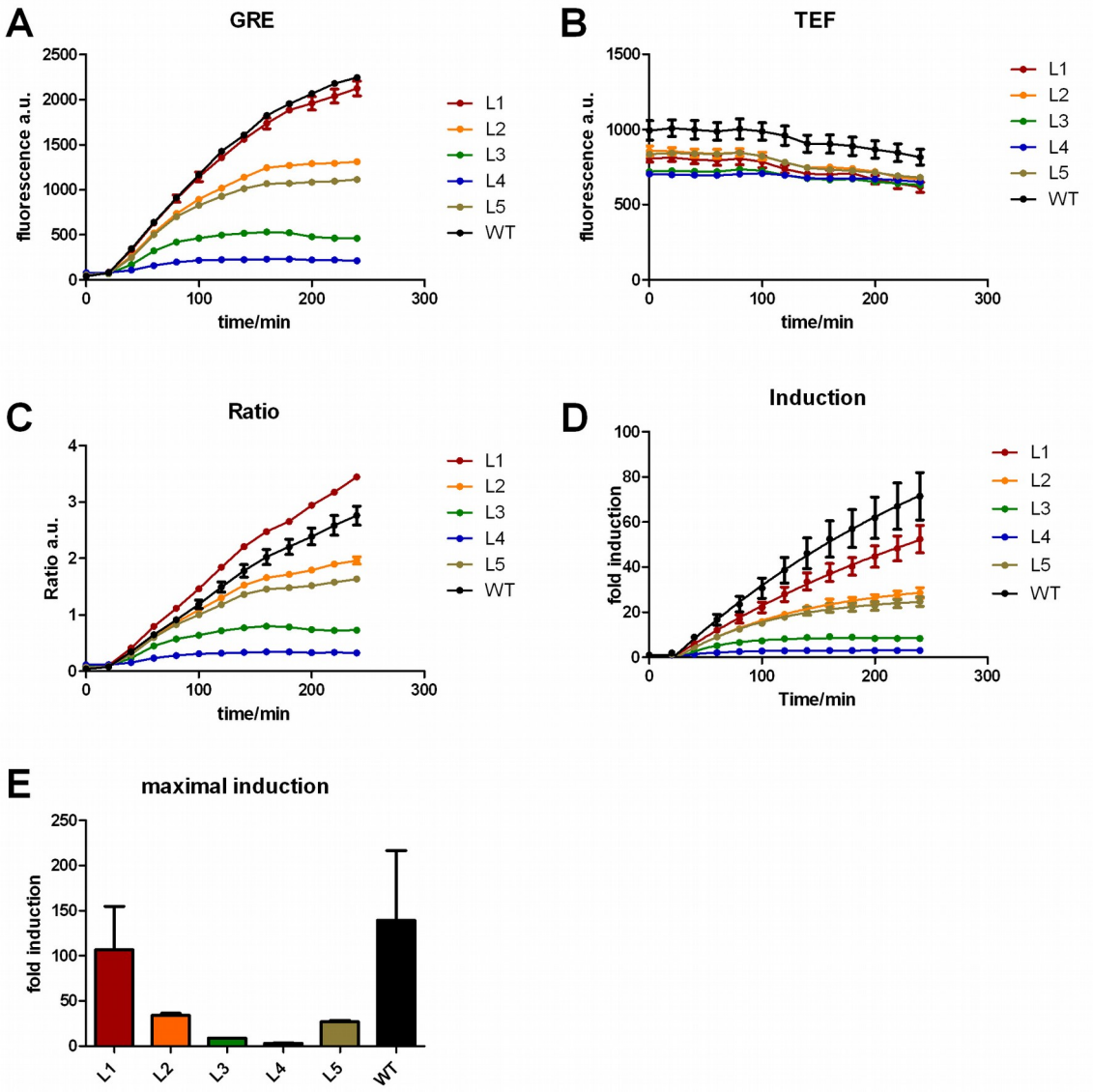

Fig.A26
Induction kinetics of the GRE-reporter reporter in WΣ for the Hsp82 linker mutants. Cells were induced with 20 µM DOC. Error-bars represent the standard error of the mean (n=2).
a.) Signal of the GRE-reporter
b.) Signal of the constitutive TEF1-reporter
c.) Signal of the GRE-response normalized to the TEF1-reporter
d.) Induction of the GRE-response, calculated from the normalized ratios. The data was fitted with a one phase association with delay.
e.) Maximal reporter induction derived from the fitting. Error-bars represent the standard error of the fitted parameter.

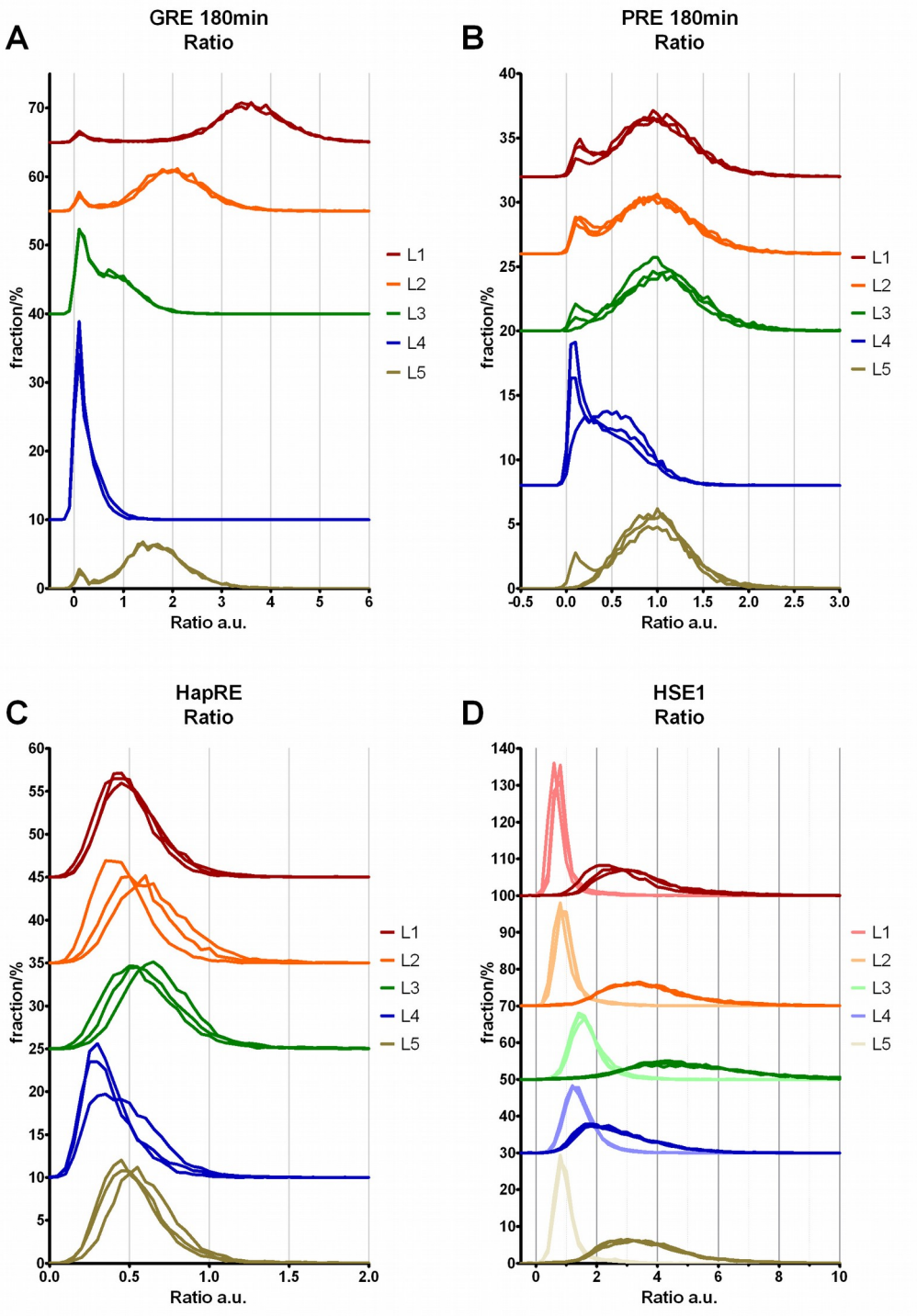

Fig.A27
Signal distribution of the Hsp90-reporter in WΣ expressing different linker mutants of Hsp82. The signals are normalized to the expression of the constitutive TEF-promoter on a single-cell level. The signal for three independent clones are shown.
a.) Signal of the GRE-reporter after 180 minutes induction.
b.) Signal of the PRE-reporter after 180 minutes induction.
c.) Signal of the HapRE-reporter.
d.) Signal of the HSE1-reporter at 25°C (light color) or after 1h heat-shock at 37°C (dark color).

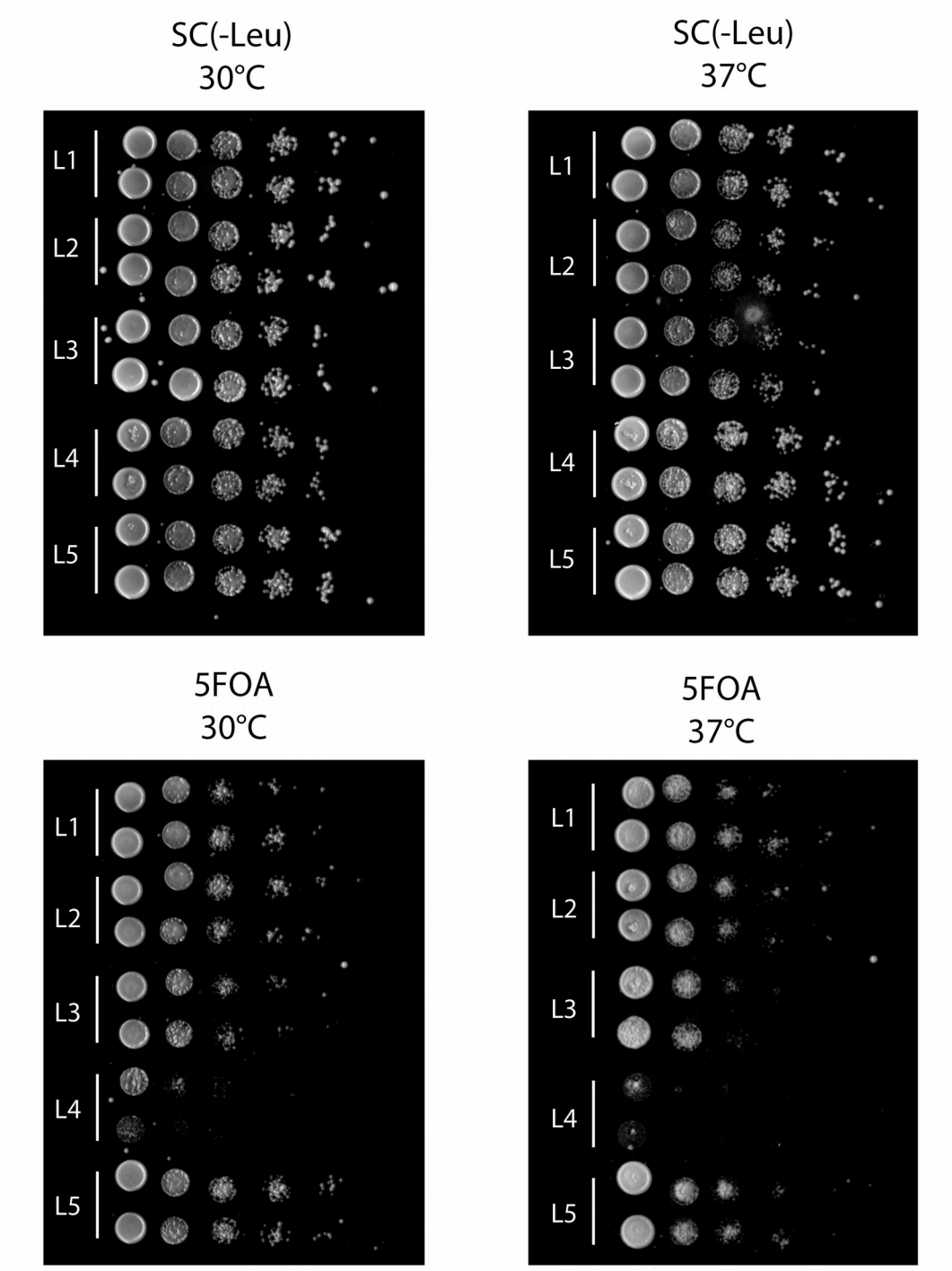

Fig.A28
Complementation of the Hsp82 linker-mutants in WΣ expressed from pRS415. All the strains harbored a rescue plasmid with Ura3-marker containing yeast Hsp82. Complementation was tested at 30°C (left) and 37°C (right) with two independent clones in a 10-fold dilution series without selective pressure (upper panels) or on 5-FOA containing plates to select for loss of the rescue plasmid (lower panels).

5.3 Mutants of the phosphorylation site S365 in human HSP90β

Phosphorylation is an important mechanism for Hsp90 to regulate substrate specificity and chaperoning activity. One project of our group focuses on the phosphorylation status of Hsp90 occurring in cancer cells. The previously unknown phosphorylation site S365 in human HSP90β (hHSP90β) was found in liver-cancer cell-lines by our group member Minh Nguyen (see her Thesis) and is meanwhile also annotated in the "Phosphosite" database (*www.phosphosite.org*). Interestingly, this site is not present in the hHSP90α-isoform. Different mutants were created [Table A3], introduced in the tandem yeast expression-vector and used for measuring reporter activity.

Table A 3 – List of Hsp90β mutants used in this study

Mutant	Detailes
wt	native hHSP90β
S365E	phospho-mimicking
S365A	non-phosphorylatable
S365N	residue found at the equivalent position in hHSP90α

5.3.1 Cell-size

It has to be mentioned here that complementation with human HSP90 is less efficient as compared to the natural gene in yeast, resulting in slower growth and abnormal cell-size [Fig.A29]. The cell size was quantified by outlining the cell-wall stained with Solophenylflavin. Assuming an ellipsoid cell-shape, the average volume was calculated from the semimajor and semiminor axis of a best-fit ellipse. The non-phosphorylatable S365A mutant was affected most, followed by the S365N mutant. HSP90β-wt and S365E exhibited the least severe phenotype with nearly the same cell-size but still about 3 times larger than the natural wild-type cell [Fig.A30a,b].

In the flow-cytometer, the single-cell population was not as clearly defined for the mutants as for the natural wild-type and only a small fraction of cells were associated with it. Together with the enlarged phenotype this points to a defect in cell-cycle progression. To check for the ploidy, cells were fixed with ethanol and DNA was stained with SYTOX-green™ (Invitrogen, Germany). The DNA-profiles showed that most of the HSP90β-expressing cells are in the G2/M-transition [Fig.A31].

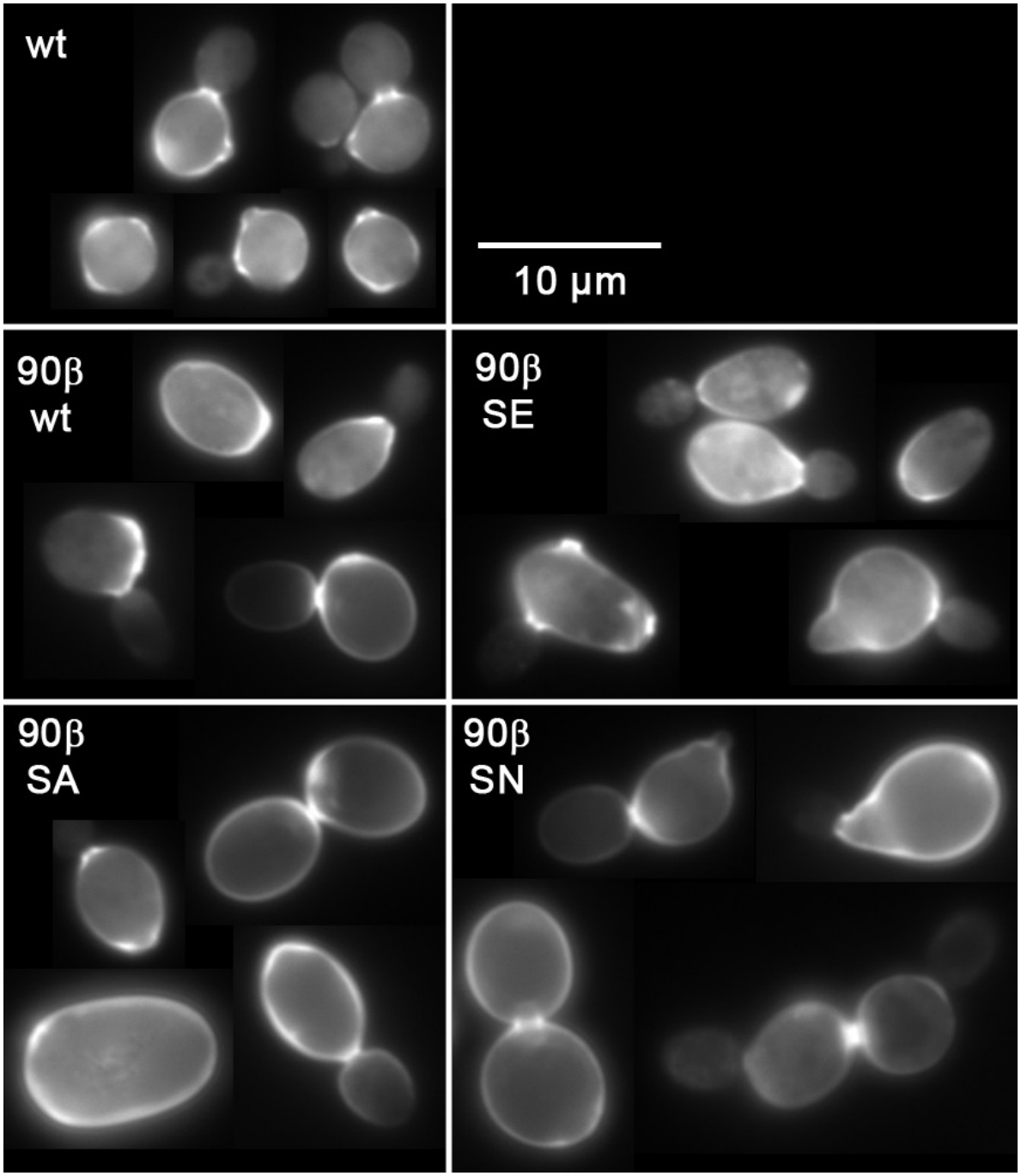

Fig.A29
Cell-size of WΣ-wt and human Hsp90β-S365 expressing mutants. The cell-wall was stained with solophenylflavin and cells were imaged at their maximal diameter. Representative images were taken from independent clones.

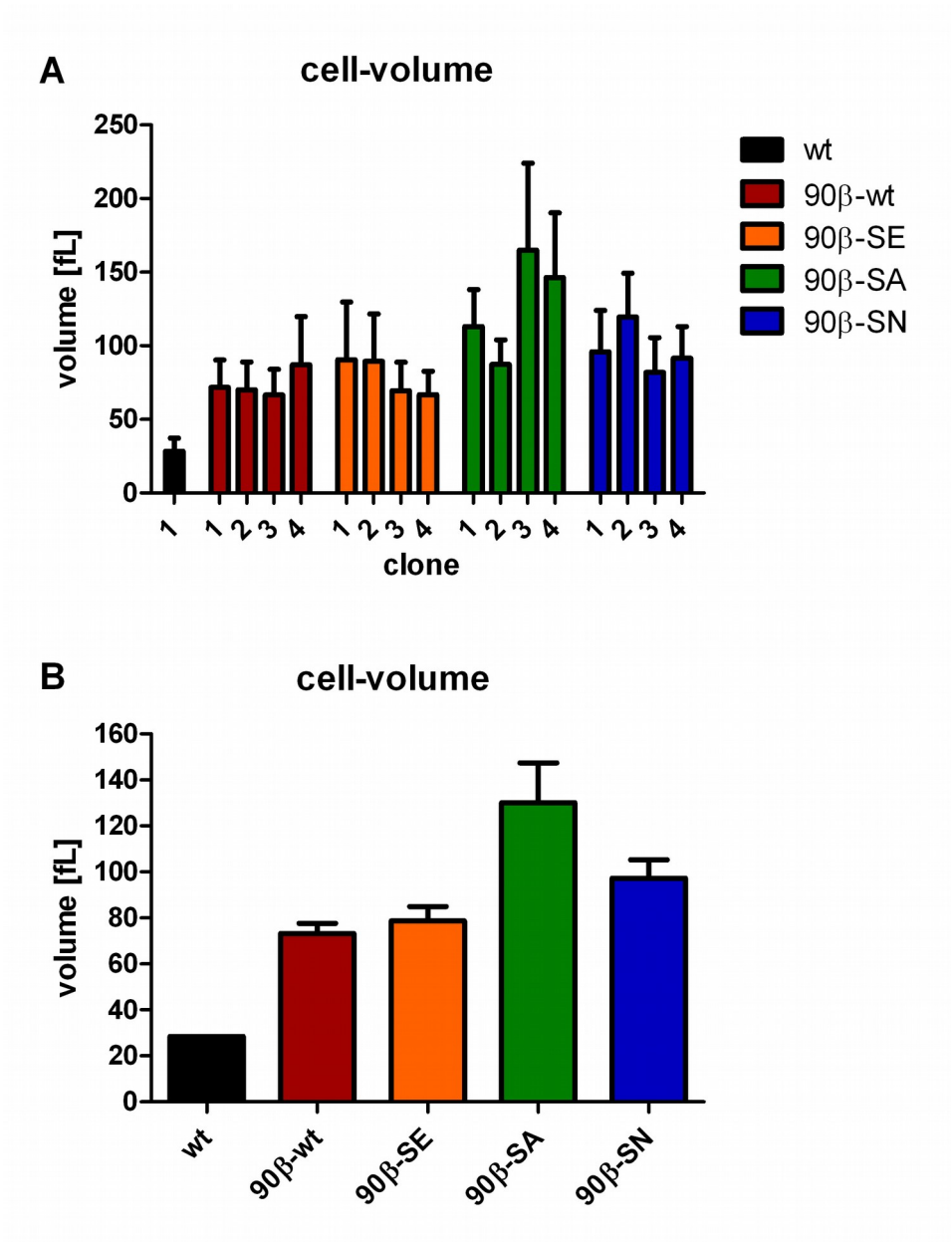

Fig.A30
Cell-volume quantification of WΣ-wt and human Hsp90β-S365 expressing mutants. For each Hsp90β-S365 mutant at least 17 cells of four independent clones were imaged. The outline of each cell was fitted with an ellipse in ImageJ and the semiminor and semimajor axis were used for the calculation of an ellipsoid from which the volume was determined.
a.) Average volume and standard deviation for each clone
b.) Averaged volume of all clones with standard error of the means from the average of each clone

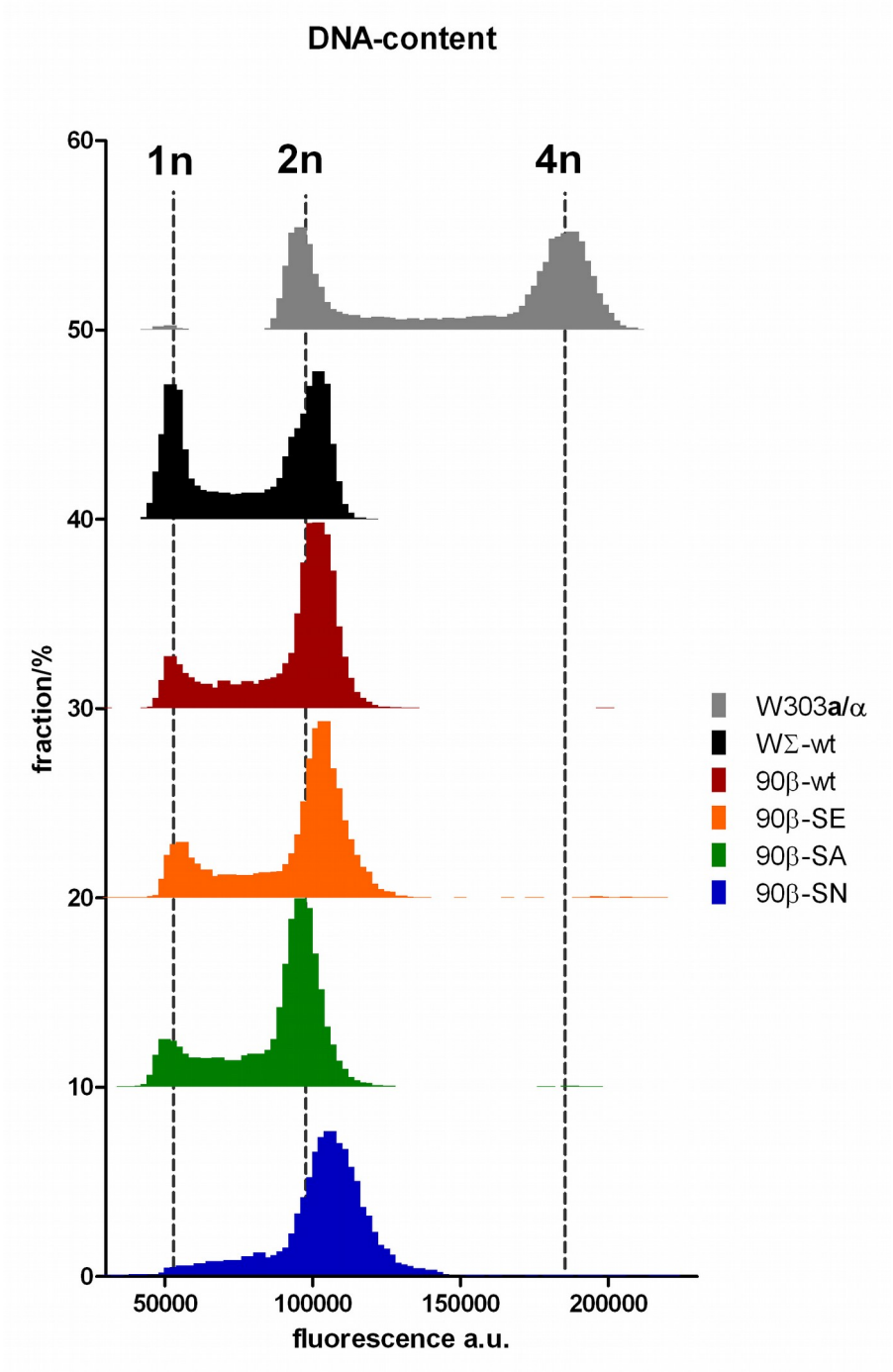

Fig.A31
Cell-cycle analysis of wild-type yeast and human Hsp90β-S365 expressing mutants. DNA content was quantified by SYTOX-green staining and flow-cytometric analysis. The diploid W303a/α and the haploid WΣ wild-type were chosen as controls.

5.3.2 Reporter measurements for S365-mutants

The reporter for the heme-response pathway did not show any significant differences between the hHSP90β mutants [Fig.A32].

In the pheromone pathway clear differences between the mutants can be seen [Fig.A33]. The inducibility of S365A and S365N was lower than in the wild-type and the S365E-mutant which had similar maximal inductions [Fig.A33g]. Compared to the endogenous yeast proteins [Fig.A12d], induction by wild-type-hHSP90β was rather low. Noteworthy, neither the fraction of single cells nor the forward-scatter was markedly increased by pheromone-treatment (compare with [Fig.A10e] and [Fig.A12]) which means that cell-cycle arrest in G1 and the formation of Shmoo is not induced.
There are two possibilities. Either hHSP90β has a low affinity for Ste11 and only few MAPKK molecules are chaperoned, or hHSP90 has a high affinity for Ste11 but keeps the molecule trapped in an inactive state. Since the difference in the hHSP90β-mutants is a putative regulatory phosphorylation, it is likely that the recruitment of co-chaperones is involved, arguing for the trapping hypothesis. On the other hand is hHSP90β not a yeast protein and therefore unlikely to have the same affinities for yeast clients as endogenous Hsc82. In the end it may be a combination of both effects.

The response of the glucocorticoid receptor showed a strong heterogeneity amongst the tested clones [Fig.A34a]. Unlike the pheromone response, the maximal induction for S365N was much higher than S365A and even higher than for the wild-type [Fig.A34b,c]. The S365E showed the strongest induction. Due to the high variability of the clones, the only conclusion to draw is that expression of S365A strongly impairs the chaperoning of glucocorticoid-receptor.

A more consistent result was obtained with the heat-shock reporter HSE1 [Fig.A35]. The left column shows the response to 37°C heat-shock and the right column the response to 42°C.
At 37°C the reporter was activated for all mutants to a similar level, seen by the increase of the HSE1-signal. At the same time, the TEF-signal was dramatically decreased starting already at 30 minutes after the heat-shock. No drop in TEF-signal was observed for the 42°C treated cells. The drop in TEF activity could also be seen in the natural wild-type (see [Fig.A10c], [Fig.A11b]and [Fig.A13b]) but at about 90 minutes after the heat-shock. An explanation for this behavior comes from the content of the single-cell gate. Coincident with the drop of the TEF-signal, the fraction of single cells increased. This means that general translation is paused at 37°C but the TEF-driven T-Sapphire still gets diluted by cell division. At 42°C the fraction of single-cells remains constant and also the TEF-signal is unchanged which means that cell/division is blocked.
Interestingly, despite starting with different basal HSE1 reporter-expression levels, the differences were mostly compensated by the TEF-signal as can be seen in the ratio-plot. Because of the bulk protein dilution by cell-division at 37°C while the HSE1-signal still increases, the effective concentration of HSE-regulated genes raises even stronger and thus providing better conditions to chaperone misfolded proteins. On the other hand, de-repression of the heat-shock promoter by hHSP90β seems to be less efficient at 42°C and no cell division takes place so the effective concentration of HSE-induced genes is lower. At 37°C the heat-shock response may still be adequate for surviving but at 42°C viability decreases [Fig.A35i,j]. Overall, the hHSP90β wild-type and the S365E-mutant behaved similar and S365N is comparable to S365A.

Taken together the data shows that HSP90β-S365E behaves mostly like wild-type whereas S365A and S365N show a more severe phenotype either because of interfering with the individual signaling pathways or by increased cellular stress levels and limiting amount of free chaperons. From the results one can conclude that phosphorylation at position S365 plays a regulatory role that may influence interaction with and chaperoning of specific client proteins.

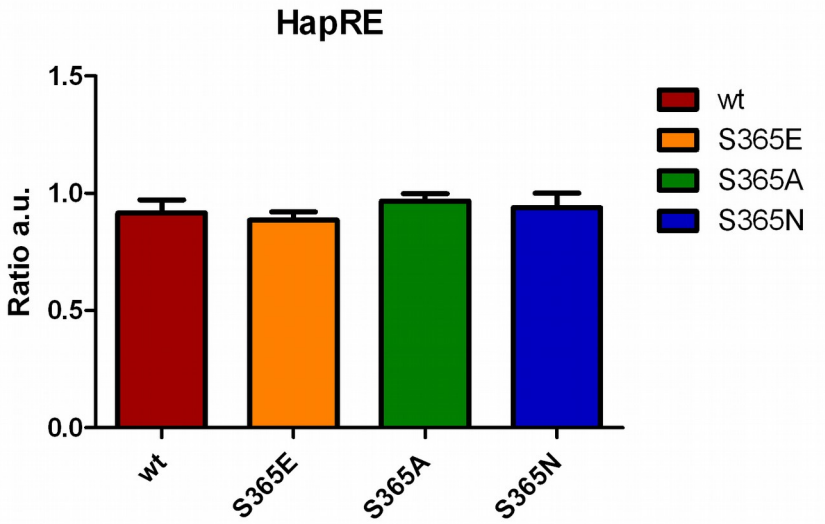

Fig.A32
Hap-reporter measurements in WΣ expressing different S365-mutants of human Hsp90β. The Signal of the Hap-response is normalized to the TEF1-reporter. Error bars represent the standard error of the means (n=4 for wt, S365E, S365A, and n=8 for S365N).

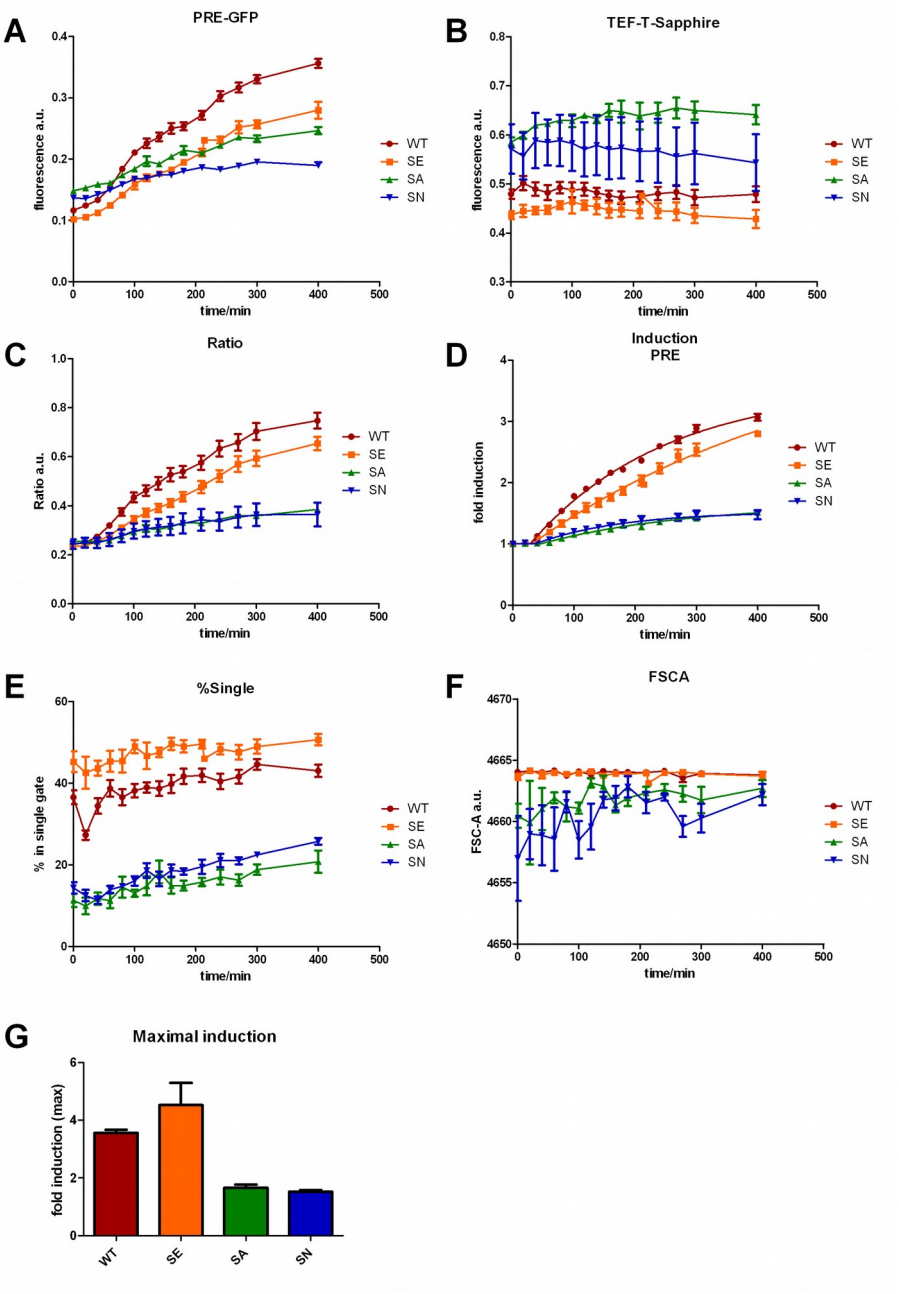

Fig.A33
Pheromone response kinetic in WΣ, expressing different S365-mutants of human Hsp90β. Error bars represent the standard error of the means (n=4). For induction, cells were treated with 5.9 µM alpha factor.
a.) Signal of the PRE-reporter
b.) Signal of the constitutive TEF1-reporter
c.) PRE-signal normalized to the TEF1 signal
d.) Normalized induction of the PRE-reporter. Data-points were fitted by a single exponential association with delay
e.) Fraction of cells in the single-cell gate
f.) Forward-scatter of single-cells
g.) Maximal induction of the PRE reporter determined by the fitting of the data. Error-bars represent the standard error of the fitted parameter.

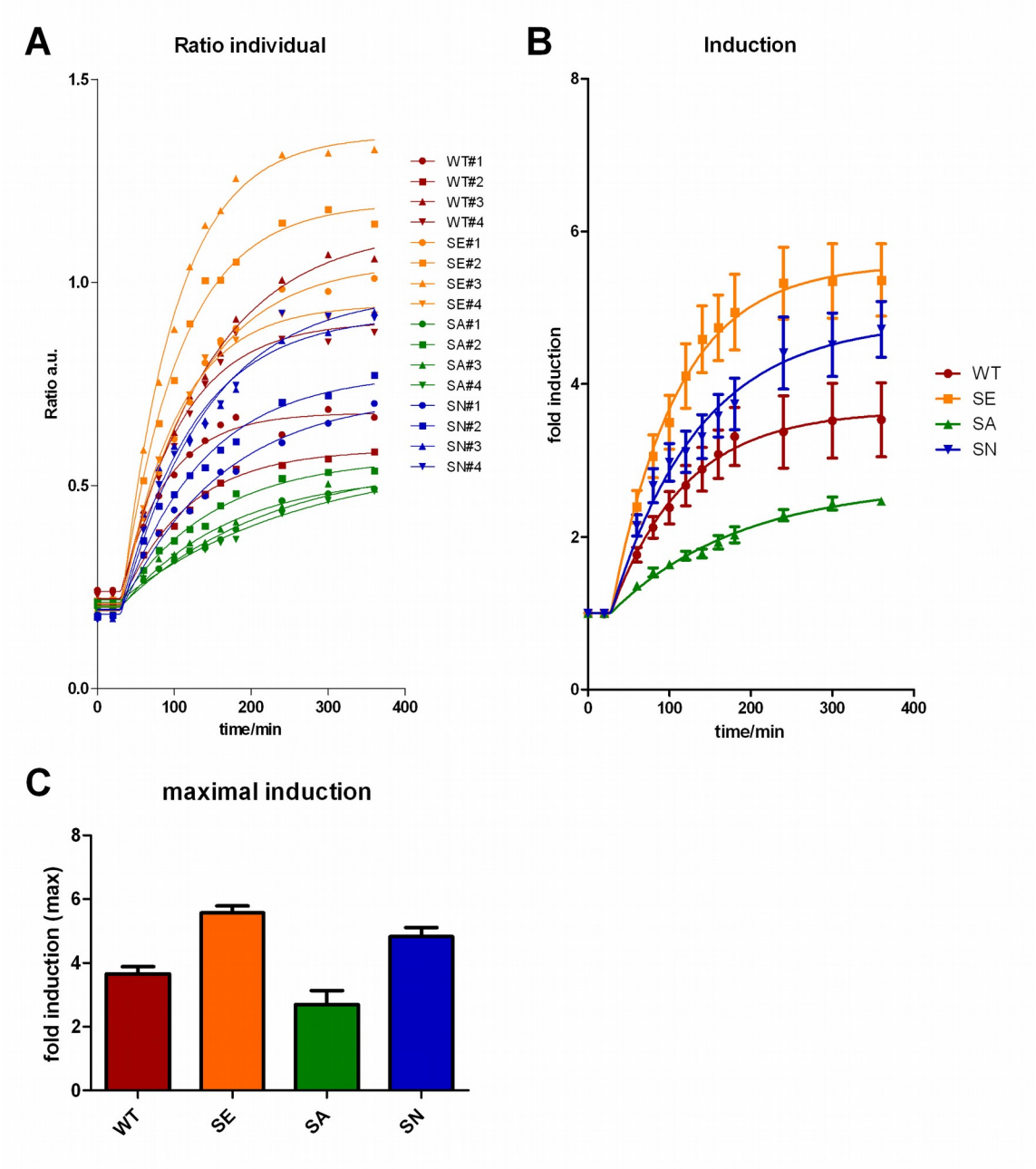

Fig.A34
Glucocorticoid response kinetic in WΣ, expressing different S365-mutants of human Hsp90β. Error bars represent the standard error of the means (n=4). For induction, cells were treated with 20 µM DOC.
a.) GRE-signal normalized to the TEF1 signal. Data-points were fitted by a single exponential association with a globally shared delay.
b.) Normalized induction of the GRE-reporter. Data-points were fitted by a single exponential association with a globally shared delay.
c.) Maximal induction of the GRE reporter determined by the fitting of the data. Error-bars represent the standard error of the mean of the fitted parameter.

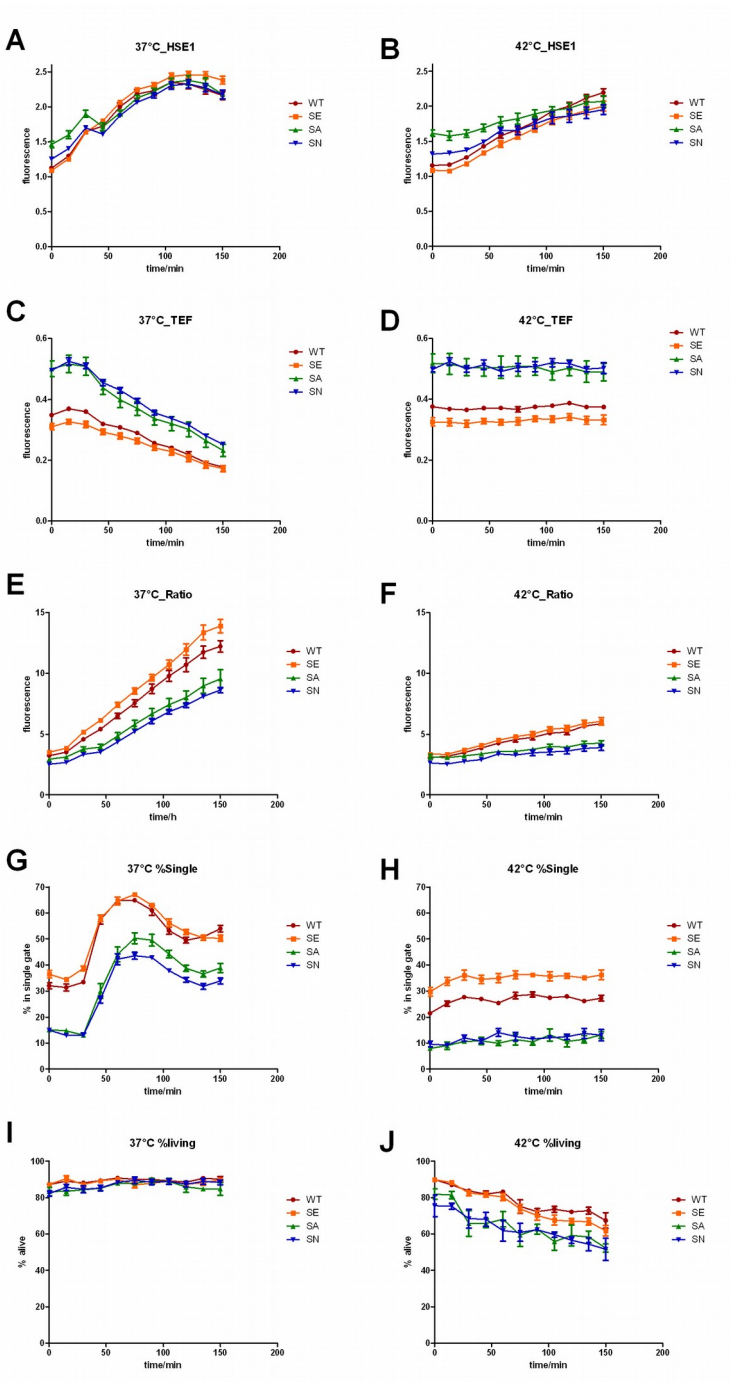

Fig.A35
Induction kinetic of the HSE1 reporter in WΣ, expressing different S365-mutants of human Hsp90β. Error bars represent the standard error of the means (n=4). Cells were either heat-shocked at 37°C (left) or 42°C (right).
a-b.) Signal of the HSE1-reporter
c-d.) Signal of the constitutive TEF1-reporter
e-f.) Normalized induction of the HSE1-reporter.
g-h.) Fraction of cells in the single-cell gate
i-j.) Forward-scatter of single-cells

Part B – Establishment of a flow cytometry based aging-assay

1 Introduction

1.1 Hsp90 in aging cells

During the aging process, vital functions get less and less efficient and misregulation takes place, making cells prone to degeneration and cancerous development. Interestingly, many Hsp90 clients are oncoproteins, hence these cells become even more dependent on Hsp90 activity.
On the one hand, there is a decline in the heat shock response during the aging process (Calderwood et al., 2009), resulting in misfolded proteins and aggregate formation. On the other hand many cancerous cells are hypersensitive to Hsp90 depletion (Whitesell and Lindquist, 2009).
It is hypothesized that the protective and coordinating influence of the chaperon systems breaks down in old cells, leading to a phenotype called senescence. By up-regulating Hsp90 cancer cells may overcome these effects and might be able to stabilize oncogenic mutant proteins.

The baker's yeast is a suitable model organism to study the aging process. As a unicellular eukaryote it shares many functional pathways with mammalian cells; the genome is annotated and large knockout collections exist. In addition, *Saccharomyces* has a short doubling time of about two hours and is quite easy to handle.
There are two ways of aging in yeast cells: replicative and chronological aging. Yeast cells divide asymmetrically by budding. Thereby the mother cell retains for each daughter produced a bud-scar. A yeast cell can only bud off a limited number of daughter cells. Yeast cells therefore age while dividing until they lose their replicative potential. Replicative aging in yeast is studied as a model for actively dividing cells.
After entry into stationary phase or under nutrient deprivation yeast cells stop dividing and slowly loose their ability to reenter a new growth phase upon replenishment of nutrients. This process is called chronological aging and used as a model system for non-dividing cells, such as neurons.

In the beginning of my project the objective was to measure Hsp90 activity in aging yeast-cells. Due to technical hurdles and priority changes, only few measurements on Hsp90 were done. Instead the method was extended to the measurement of pH and redox-homeostasis which will be described in "Part C" of the thesis.

This part of my thesis describes the development of a flow-cytometry based approach to derive replicatively aged yeast cells. I created a strain background which is a suitable model-system for addressing age associated changes. Finally, I will demonstrate robust measurement of fluorescent reporters in old cells.

1.2 Methods to access replicative aging in yeast

There are several ways to analyze replicative aging in yeast cells. The classical dissecting method where cells are grown on agar plates and daughters are removed via micromanipulator is in use since the 1960s and still the gold standard to analyze mutants (Mortimer and Johnston, 1959). Nevertheless, it is limited to very few cells and the cell division and morphology are the only readouts you can get. Strains for higher throughput analysis of lifespan were designed, like the W303-K6001 (Ralser et al., 2012). This stain expresses the essential CDC6 gene, a component of the pre-replicative complex, under the Gal1-promoter and under the mother cell-specific promoter of the homothallic endonuclease. The strain can be maintained by growth on galactose. When shifted to glucose, daughter cells cease to divide and culture growth becomes linear. As an advanced system the mother enrichment program was developed (Lindstrom and Gottschling, 2009). Here part of the CDC20 and the UBC9 genes are flanked by LoxP-sites. A modified Cre-recombinase, which is inducible by Estradiol, is expressed under the daughter-cell specific SCW11-promoter. By the addition of Estradiol, daughter cells arrest in cell-cycle. Colony forming at different time-points gives a typical survival curve and is an indirect measure of the replicative lifespan. To analyze just the old mother cells one takes advantage of the properties of the yeast cell-wall. During division, new cell-wall material is deposited at the bud - which forms the daughter cell – while the mother cell keeps the old material. By using reactive biotin, an initial population can be coated and later retrieved by affinity purification on streptavidin coated magnetic beads (Smeal et al., 1996);(Chen et al., 2003) . To cover the whole replicative lifespan of a yeast cell, the procedure has to be repeated several times, depending on the strains background. In combination with the mother enrichment program, it is even possible to follow the whole lifespan within on single exponential culture.
Problems arise when adaptive processes, like heat-stress, osmotic stress, pH or environmental signals should be monitored. Magnetic sorting involves a temporary depletion of medium and transfer into PBS solution. Cells will react to the altered conditions and subtle changes could be masked. Alternatively the medium could be depleted for biotin to prevent cross-reaction with the steptavidin-beads. A further disadvantage is the fact that beside dividing and senescent cells also dead mother cells will be enriched and can introduce artifacts, especially when cell-lysates are analyzed.
Flow chambers where mother-cells are trapped due to their increased size and daughters are drained away by medium flow are ideal for protein or organelle localization studies (Lee et al., 2012); (Xie et al., 2012); (Zhang et al., 2012); (Fehrmann et al., 2013), but are restricted to very few cells and once treated with substances or shocks they are lost for further unbiased measurements.

2 A flow-cytometry approach to aging

To overcome the above-mentioned limitations I made use of high speed sorting capabilities of flow-cytometers to enrich for old mother-cells. Instead of biotin I chose an amine-reactive Alexa-dye to stain an initial young population of yeast-cells and retrieve them after growth by the cytometer. This has the advantage that cells could be measured directly from an aliquot of the culture, without altering conditions and dead cells can be excluded from both the measurement and the passage. The principle of the assay is depicted in [Fig.B1]

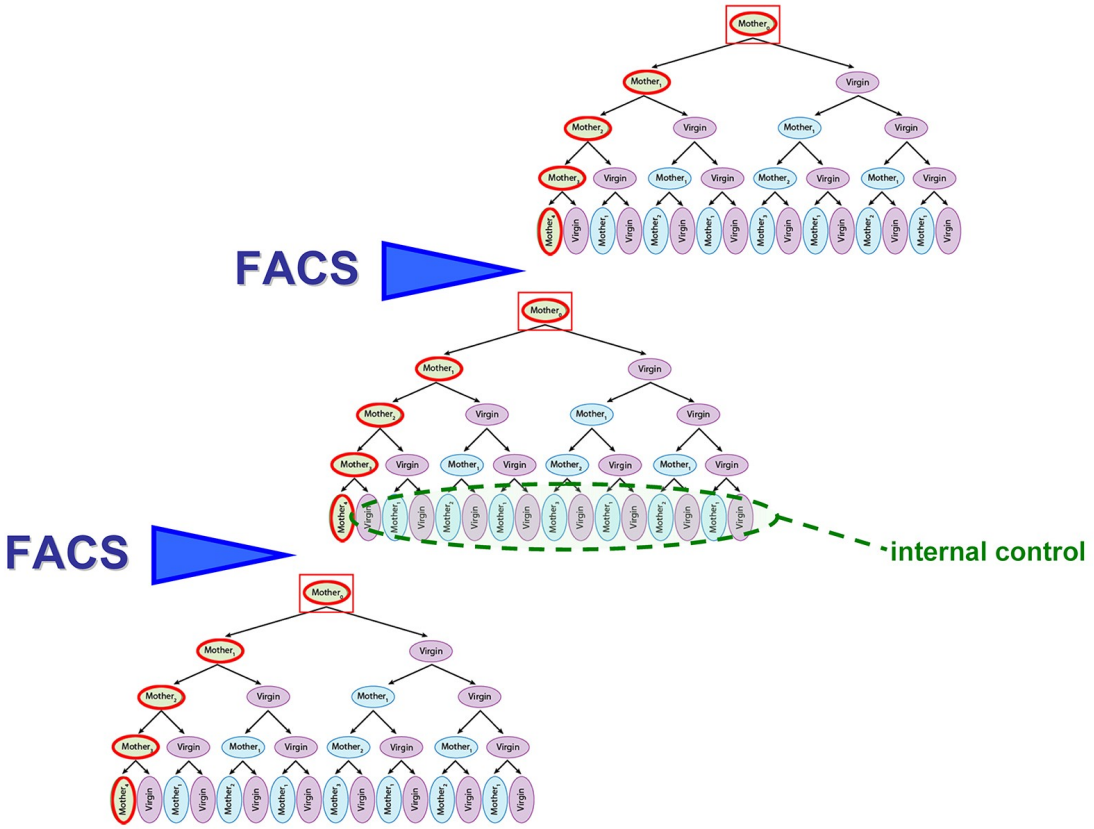

Fig.B1
Schematic representation of the flow-cytometry based aging assay. An initial population is stained with an amine-reactive Alexa633 dye and inoculated in medium. After several divisions the initial population is retrieved and enriched by flow cytometry. Rejuvenated offspring serve as an internal control for signal quantification. The image was adapted from (Steinkraus et al., 2008).

2.1 Proof of principle

For the establishment of the method I used the heat-shock-reporter described in "Part A". The aging-protocol, cell-treatment and the reporters were a co-development and used to gain experience. Therefore, the early experiments have not been standardized and the results should be considered as such. For a detailed description of the method and the final protocol, please refer to the "*Aging by Flow-Cytometry*" section.

Initial experiments were done with BY4741 expressing the pRS303-HSE1-sf4x reporter. Cells were labeled with Alexa633 and single-cells were sorted for inoculation in SC-medium at 25°C. In intervals of about 20h Alexa-positive cells were enriched again by FACS and budscars were counted after staining with Solophenylflavin. With increasing age the cells clearly accumulate budscars although the age distribution becomes very broad with time [Fig.B2].

From the liquid culture, aliquots were taken and expression of the heat-shock reporter before and after 1h at 37°C was quantified for Alexa-positive and Alexa-negative cells. In [Fig.B3] results from three independent experiments are shown. The graph shows that basal reporter expression goes up with the age of the cells (left), whereas the young cells in the culture stay at a constant expression level (middle). The reporter expression after heat-shock mildly increases

in the old cells. The induction calculated as the ratio of 37°C to 25°C (right) steadily declines in old cells, while the trend of the young cells stays constant. The population averaged budscars over time however showed a very large variation [Fig.B4]. The age distribution from [Fig.B2] suggests that some cells divide very slowly.

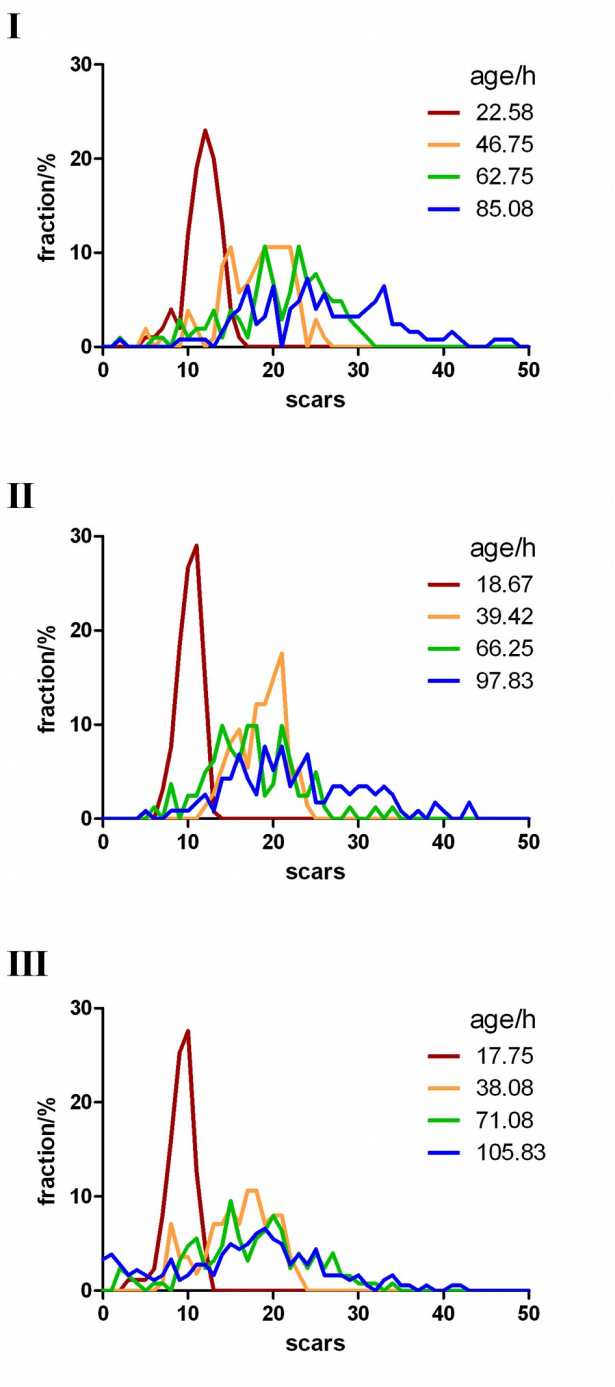

Fig.B2
Distribution of budscars in aging BY4741 cells. Buds of enriched cells were counted at the indicated time-points for three different experiments (I-III).

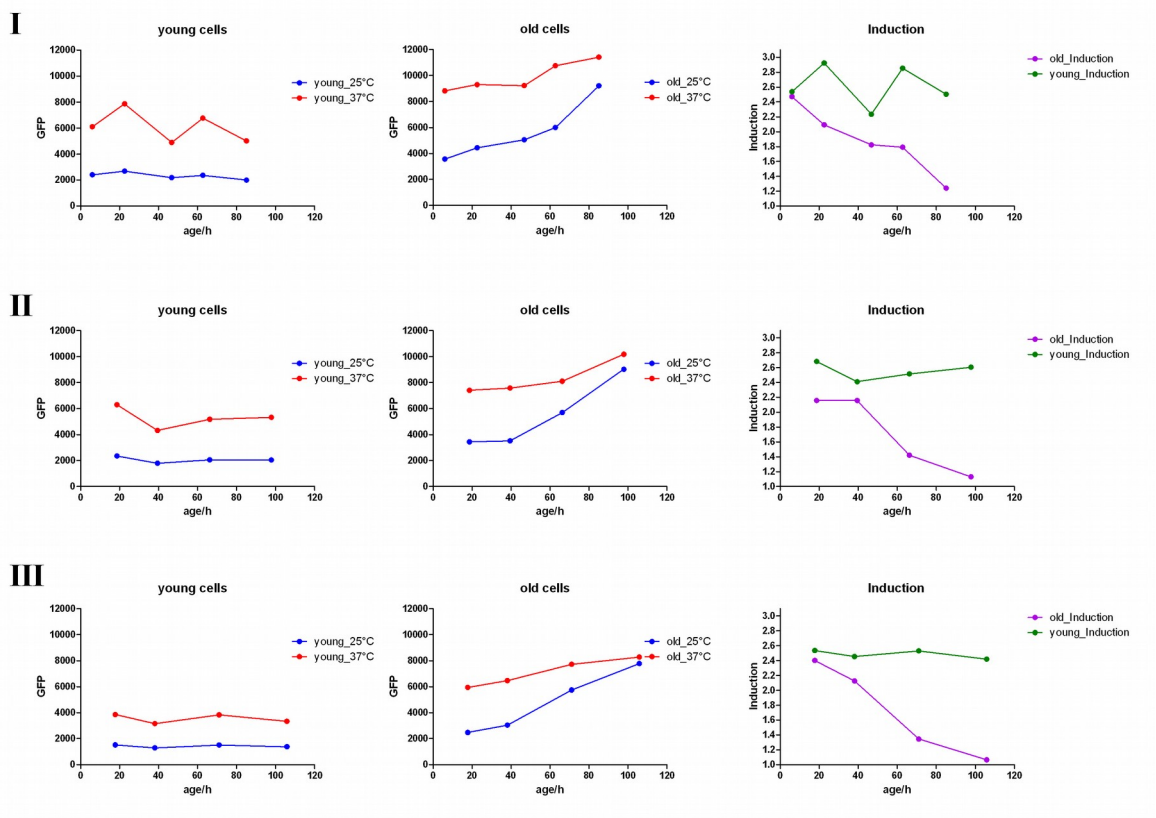

Fig.B3
Heat-shock response measured in aged BY4741 with the HSE1 reporter. Data from three independent experiments is shown (I-III). The corresponding budscar distribution is given in [Fig.B2]. The aging culture was grown at 25°C. Basal reporter fluorescence was measured before (blue) and after 1h heat-shock at 37°C (red). Data is shown for the young cells (left) and the old mother cells (middle). On the right, the reporter induction (fluorescence at 37°C/25°C) is plotted for the young (green) and the old (violet) cell population.

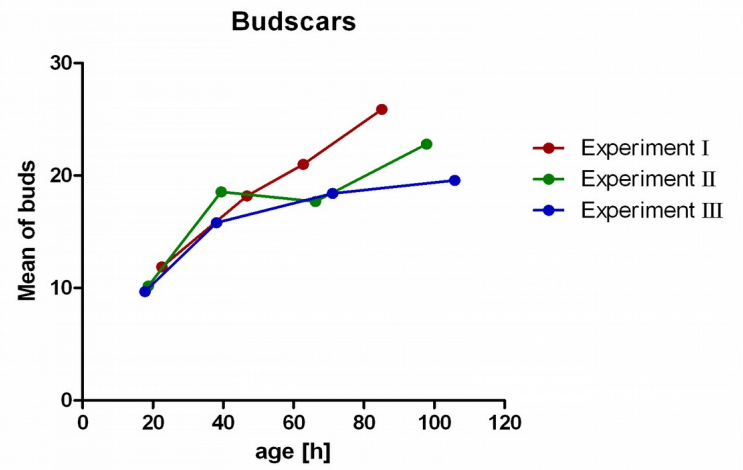

Fig.B4
Average number of budscars of aging BY4741 cells from three independent experiments (I-III). The corresponding budscar distributions are given in [Fig.B2].

To investigate the growth properties of the old cells, single Alexa-positive cells were spotted on YPD-Agar-plates and colony forming was addressed [Fig.B5]. Here it became obvious that many cells formed small colonies in an age dependant manner. To test if this is due to a defect in the strain I was using, I repeated the sorting in a Ppt1-knockout which should originally also be used for Hsp90 studies. In this strain the same behavior was observed [Fig.B6a].

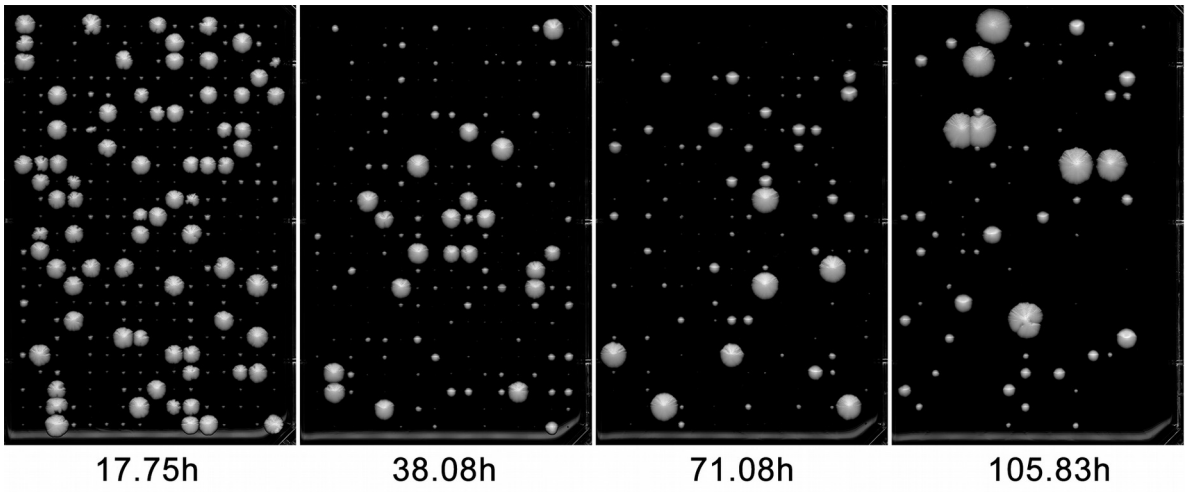

Fig.B5
Accumulation of petite cells during aging of BY4741. Old mother cells from experiment III (see Fig.B2) were sorted on YPD plates at the indicated time-points and grown to colonies. Small colonies are petite cells, large colonies are grande.

The assumption was that small colonies were respiratory deficient and show the “petite” phenotype (Ephrussi et al., 1955). Those cells form small colonies and fail to grow on non-fermentable carbon sources. Many common lab strains are prone to petite formation. Small and large colonies from the Δ*ppt1*-experiment were picked and replica-pated on YPD, SC(-His) and SG-Plates. SG-plates contain glycerol instead of glucose which can only be utilized from respiratory competent yeast cells. SC(-His) was used to account for the unlikely loss of the integrated reporter-plasmid. Whereas large colonies are able to grow under all given conditions, small colonies fail to grow on the glycerol-medium [Fig.B6b]. This clearly indicates that small colonies consist of petite-cells.

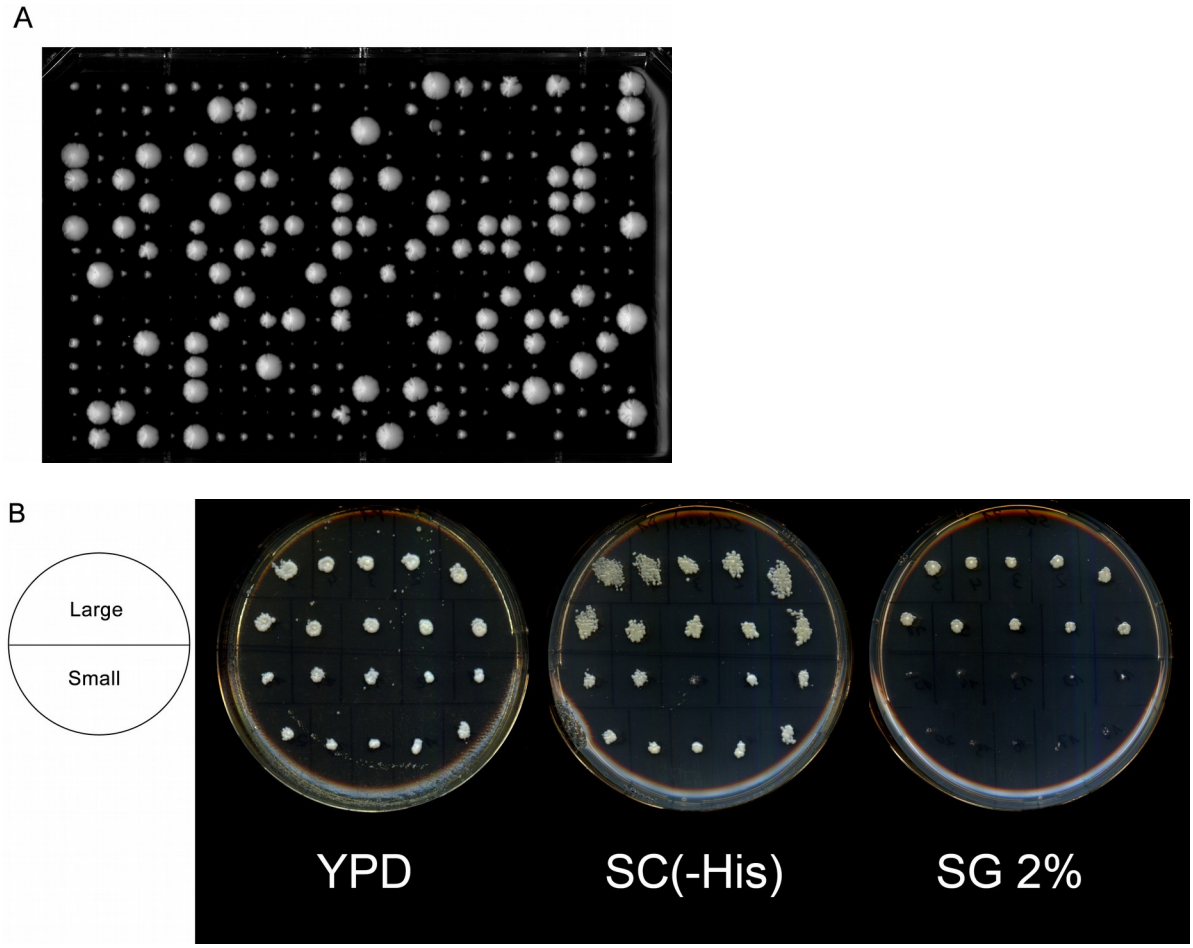

Fig.B6
High petite production is a general feature of BY4741.
a.) A freshly ordered strain from the stock center (BY4741 Δppt1 – pRS303-HSE1) also exhibits a high petite frequency.
b.) Ten large and ten small colonies were picked from a.) and tested on different media. The small colonies were confirmed to be respiratory deficient (right).

Since the common lab strain BY4741 turns nearly quantitatively into petite cells, age associated changes may be linked to this phenotype. To see whether petites have an influence on the heat-shock response or the budscar-distribution, a petite colony was picked and subjected to an aging experiment. Indeed the overall inducibility was slightly lower in both young and old cells but the onset of the aging phenotype must have started already before the first sort and only minor changes in inducibility take place later [Fig.B7a]. For the budscar-distribution, no clear pattern was detectable [Fig.B7b]. Cells seem to arrest in cell-cycle at any number of budscars and stay viable over the whole experiment. This indicates that statistic processes that take place in petite cells can lead to early cell-cycle arrest or even extreme replicative longevity (see also (Woo and Poyton, 2009); (Miceli et al., 2012)). Although respiratory competent cells (grande-phenotype) grow much faster than petites, the population of young cells – which are the rejuvenated offspring of the old mothers – would also be dominated by petites in later stages of the experiment and therefore would adulterate the impression of the young culture.
So it turns out that BY4741 is not a suitable model-system to address age-associated changes.

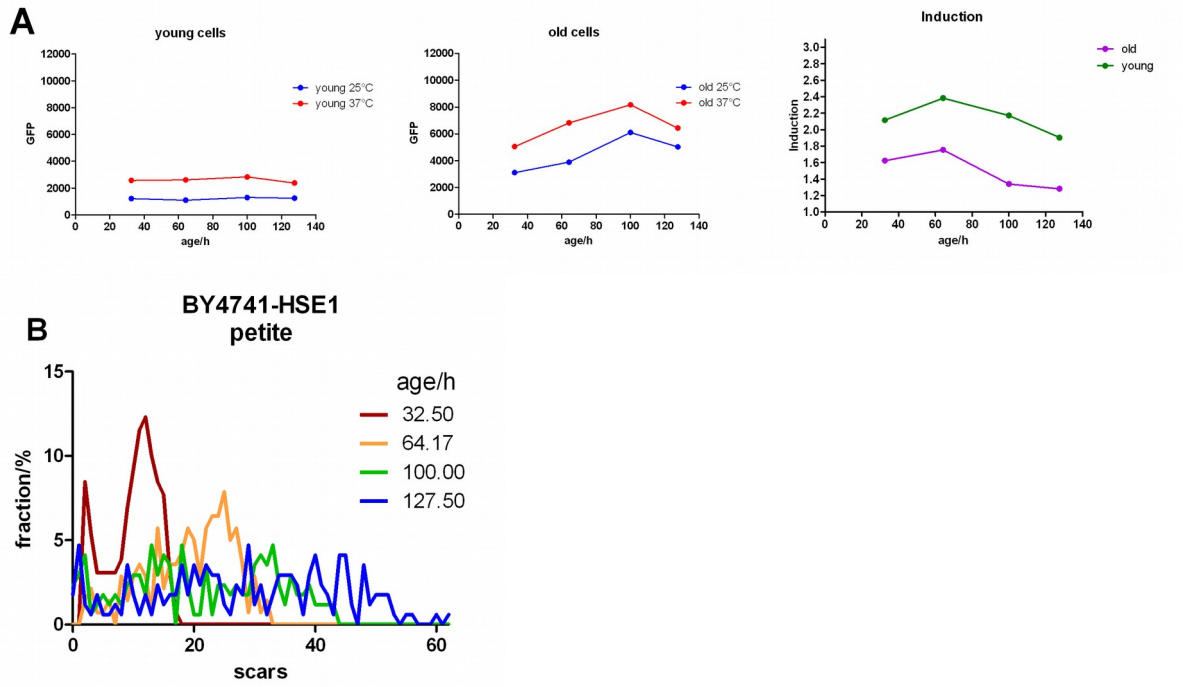

Fig.B7
Heat-shock response in aging petite cells (BY4741-pRS303-HSE1). A petite colony from a previous aging experiment was taken and subjected to an aging experiment.
a.) Heat-shock response followed over the aging process. The layout is the same as in [Fig.B3].
b.) Budscar distribution of the old cells at different time-points.

2.2 Aging with the mother enrichment strain

The mother enrichment program (MEP) was designed to overcome the need of enriching the mother cells on a daily basis but instead have the whole lifespan accessible in one culture. Nevertheless for my aging experiment at least one enrichment-step would be necessary because otherwise the density of old cells would be too small to acquire enough events in a reasonable timescale. The haploid MEP-strain Ucc5179 was transformed with pRS303-HSE1-sf4x, Alexa633-labelled and subjected to an aging assay. The MEP was induced with 17β-Estradiol 2.5h after inoculation and one sole enrichment-step was done after about 27h. For the old mother cells a similar picture like in the BY4741-background emerges [Fig.B8a]. A peculiarity of the MEP-strain is that young cells which directly originate from old mothers are prevented from dividing and thus from rejuvenation. Although trapped in cell-cycle, the young cells are still metabolically active and persist in the culture and their heat-shock response resembles the response of the old mother cells. The budscar-distribution seems to be more focused than in the BY4741-strain [Fig.B8b] but also the MEP-strain shows a variety of colony size [Fig.B8c], indicating that it also turns petite with time. The MEP-strain Ucc5179 harbors a deletion of the ade2 gene which leads to accumulation of a red pigment in the cell when grown on low adenine concentrations and makes colonies appear red. Because the red color of the pigment is dependent on an oxidation step, only respiratory competent cells show this color and petite cells remain white.

Although the MEP-strain would make most of the enrichment steps dispensable, it has little benefits over BY4741 for heat-shock measurements. First, sorting of old cells on agar-plates and for budscar-counting becomes inefficient if the sorted population is of low abundance and at least one or two enrichment steps would still be necessary. Second, the problem of "contaminating" petite-cells is not solved. Third, the Ucc5179 strain gets slightly older than BY4741, which makes it more difficult and time-consuming to count budscars. Fourth, due to the genetic manipulation of the MEP, many common selection markers are already in use, which complicates studies with further genetic manipulations. And last, although the "aged"-young-cells of the MEP-strain show similar properties than the old mothers, it is unclear since when they are in the arrested state. They could originate from early divisions or even from the most recent ones. And they are also useless to serve as an internal standard to monitor the day-to-day variation either of the instrument or the culture.
In conclusion, the MEP-strain confirms the results of the heat-shock response observed in BY4741 but, at least due to the petite-formation, it is not a suitable to serve as an unbiased model system for measuring age-associated changes.

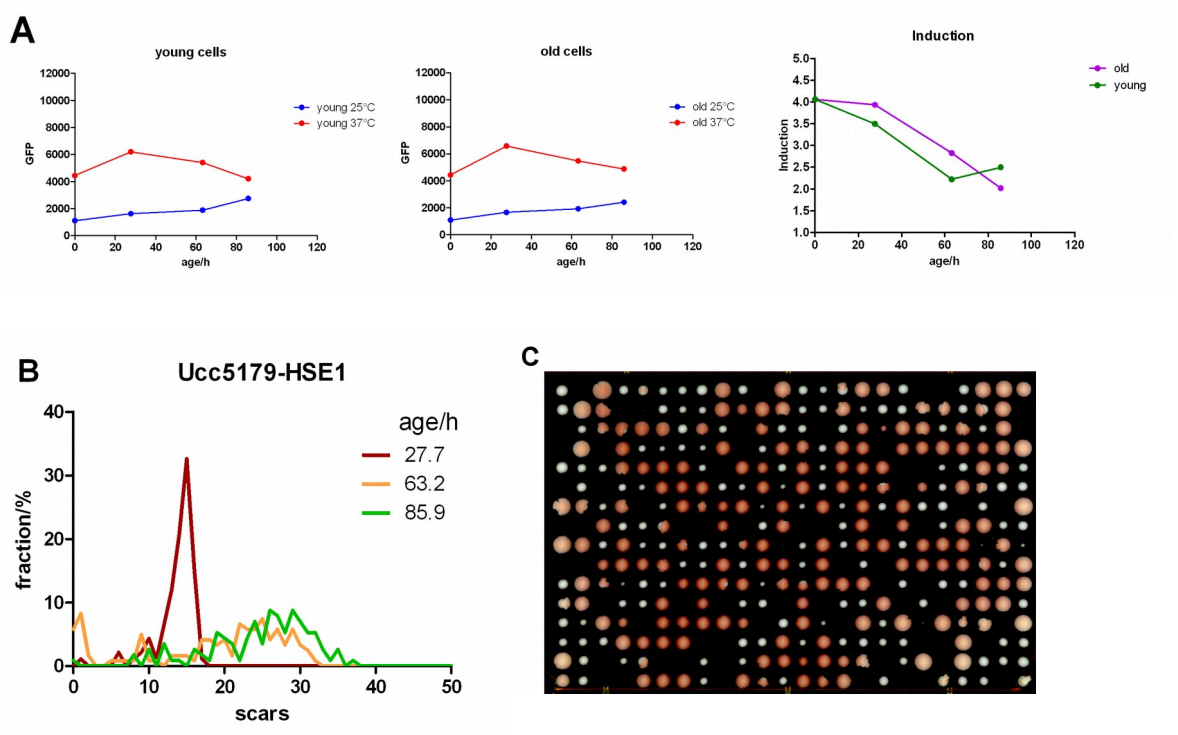

Fig.B8
Heat-shock response in the mother-enrichment strain Ucc5179 - pRS303-HSE1. The mother enrichment program was induced with 17β-Estradiol 2.5 h after inoculation of the initial population.
a.) Heat-shock response followed over the aging process. The layout is the same as in [Fig.B3]. Note that the offspring cannot rejuvenate in this system.
b.) Budscar distribution of the old cells at different time-points.
c.) Petite production of Ucc5179. Cells were sorted on YPD-agar. In petite cells the red metabolite occurring in ADE2 cells cannot be produced under limiting adenine conditions and cells stay white.

2.3 Creation of WΣ

Petite formation is a quantitative trait with a large number of genes contributing to it. Any mutation that impairs the respiratory chain can lead to petite formation. In most cases, the loss of mitochondrial DNA is the outcome which also leads to loss of the mitochondrial membrane potential and subsequently to chromosome rearrangements triggered by impaired iron-sulfur-cluster biogenesis (Veatch et al., 2009). Common lab strains often show a higher petite frequency than their relatives in natural habitats and some mutations of laboratory strains have been identified to increase this frequency (Baruffini et al., 2010); (Dimitrov et al., 2009). BY4741 harbors critical single nucleotide polymorphisms in the mitochondrial DNA-polymerase Mip1 which is also present in other lab-strains like W303 and can severely affect petite formation. Moreover it has a transposon insertion in the Hap1 transcription factor which regulates cytochrome c level and also has some other defects related to petite formation (Baruffini et al., 2007); (Young and Court, 2008). Therefore studies involving yeast respiration can be problematic in this background. W303-1A is described to have a functional HAP1 allele and a lower petite frequency than S288C or BY4741 but still higher compared to more wild-type-like strains (Baruffini et al., 2010); (Dimitrov et al., 2009).
Most natural yeast isolates have very low petite rates but are barely characterized and no auxotrophy markers exist. The strain Σ1278b was sequenced in 2010 (Dowell et al., 2010) and was shown to be very similar to S288C but has wild-type versions of most of the petite-rate affecting genes including MIP1. Unfortunately, this strain flocculates and shows invasive growth on agar-plates [*http://www.yeastgenome.org/community/sigma.html*] and therefore is unsuitable for my aging studies.
Considering all of those advantages and disadvantages, W303 seemed to be the best compromise. In order to get rid of the defective MIP1[S] in W303 (the "S" refers to S288C), I cloned the functional MIP1[Σ] gene from Σ1278b and used it to replace the MIP1[S]. As a selection marker, I chose the ade2 gene which also abolishes the red color of the strain when grown at low adenine concentrations. The resulting strain I called WΣ.

2.4 Aging with WΣ

2.4.1 Hsp90 reporter in fermenting cells

The new WΣ-strain was transformed with the HSE1-reporter construct and in addition the meanwhile established constitutive P_{TEF}-T-Sapphire reporter (*see Part A*). WΣ produced very few small colonies and the budscar-distribution looked much more narrow [Fig.B9a,b]. Heat shock response was measured in old and young cells. Both the HSE1-induced GFP-signal and the constitutive P_{TEF}-T-Sapphire signal were recorded. Increased basal expression of the GFP-reporter [compare Fig.B3] now turned out to be an effect of general translation as normalization to the constitutive signal resembled the signal of young cells, except for the last time-point [Fig.B10a-c]. As cells aged inducibility of the heat-shock response declined [Fig.B10d]. For comparison, the inducibility considering only the GFP-channel is shown [Fig.B10e]. Although the raw-data sometimes were very noisy, most likely due to air bubbles in the flow-cell, stringent gating revealed results consistent with previous experiments.

Another Hsp90-reporter was measured in WΣ. Cells expressing P_{TEF}-T-Sapphire were transformed with the PRE-reporter (*see Part A*) and subjected to a replicative aging experiment. The reporter was induced by the addition of alpha-factor (f.c.5.9µM) for 2h at 25°C. To prevent

further induction during measurement, translation was blocked with cycloheximid (f.c. 15µg/ml) 15 minutes before measurement. Results are shown in [Fig.B11]. With increasing age a population of cells unresponsive to alpha factor emerged. The data indicates a severely impaired pheromone signaling and supports the hypothesis of limited chaperone availability in aged cells.

Due to its very low rate of petite-formation, a much sharper budscar-distribution than BY4741 and robustness of phenotypes, WΣ seems to be a suitable model-system to monitor age-associated changes.

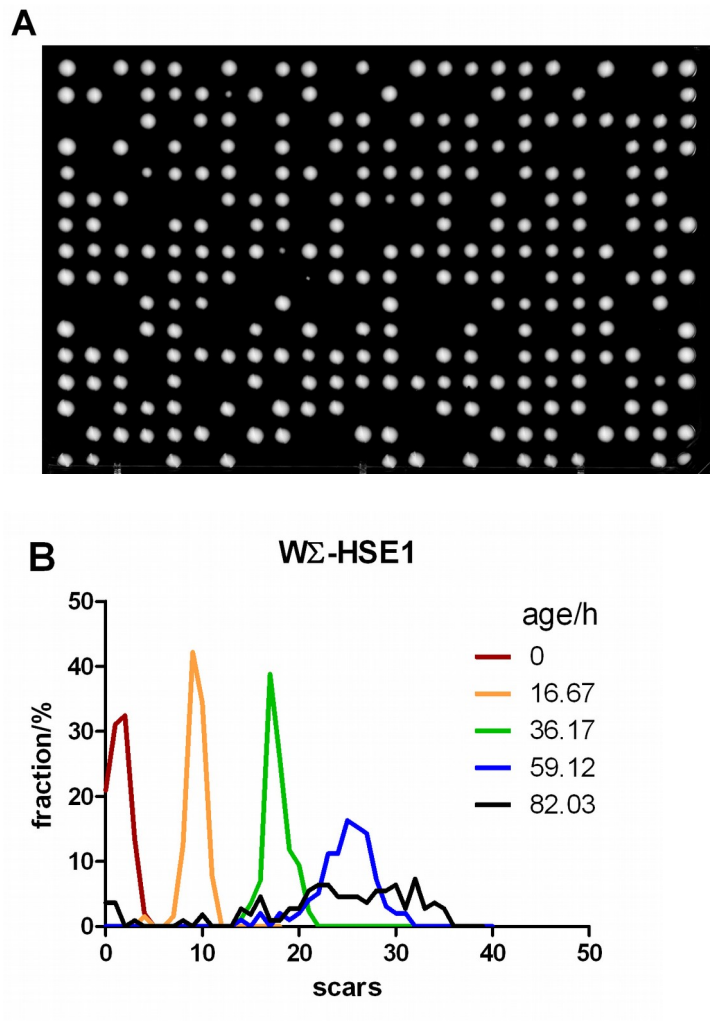

Fig.B9
Replicative aging in WΣ - pRS303-HSE1 cells.
a.) Colony forming on YPD-plates of a 59.1h old culture.
b.) Budscar distribution of the old cells at different time-points.

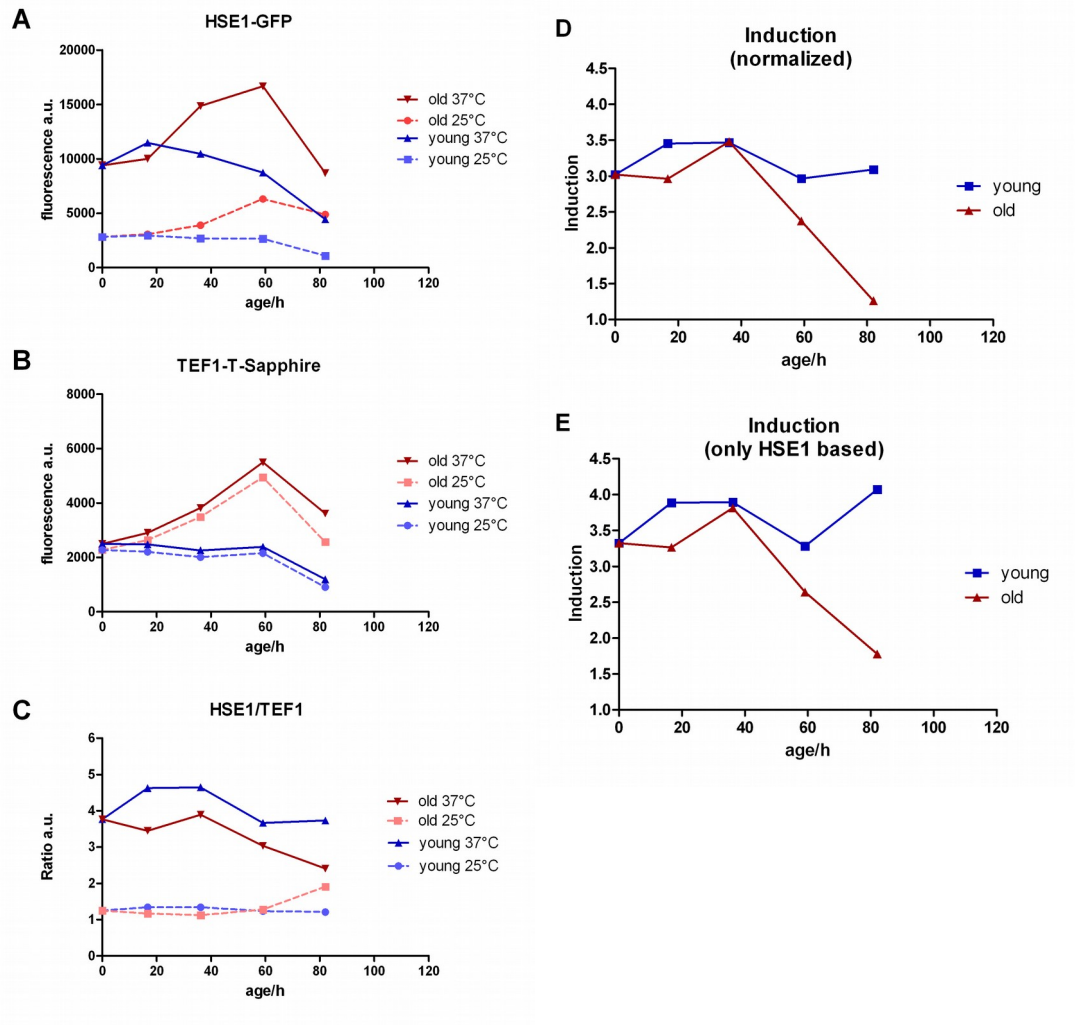

Fig.B10
Heat-shock response in aging WΣ cells expressing pRS304- P_{TEF1}-T-Sapphire4x and pRS303-HSE1-sfGFP4x. Data is shown for the young cells (blue) and old cells (red) at 25°C (dashed lines) and after 1h heat-shock at 37°C (solid lines).
a.) Signal of the HSE1-reporter
b.) Signal of the TEF1-reporter
c.) HSE1-signal normalized to the TEF1 signal
d.) Reporter induction based on the normalized HSE1-signal from 37°C relative to 25°C
e.) Reporter induction based on only the HSE1-signal from 37°C relative to 25°C

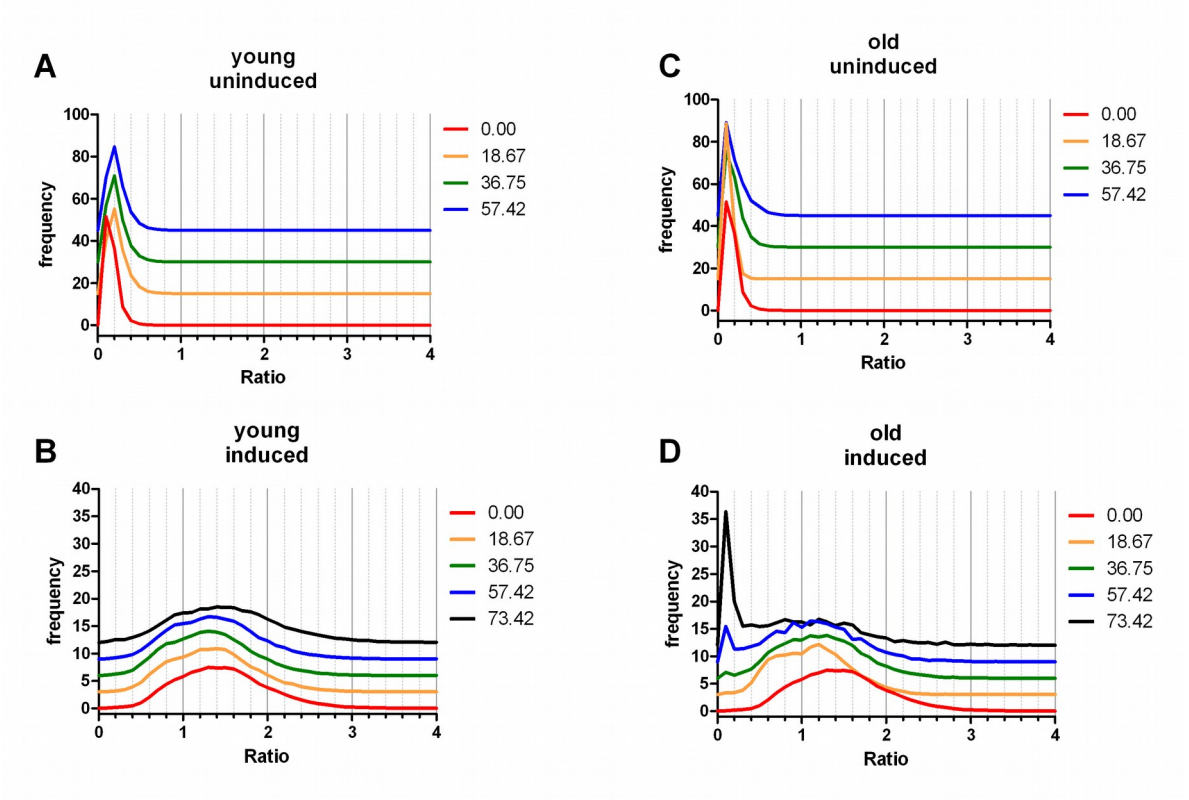

Fig.B11
Pheromone response in aging WΣ cells expressing pRS304- P_{TEF1}-T-Sapphire4x and pRS303-PRE-sfGFP4x. The PRE-signal normalized to the TEF1-signal in individual cells is shown.
a.) Signal distribution of uninduced young cells
b.) Signal distribution of young cells induced with 5.9 µM alpha factor
c.) Signal distribution of uninduced old cells
d.) Signal distribution of old cells induced with 5.9 µM alpha factor

2.5 Compare FACS-method with classical dissecting

To prove that WΣ ages naturally with the FACS-method, a classical aging-assay with a micromanipulator was performed. In this assay the strain is grown on an agar plate and freshly budded cells are arranged at numbered positions with a glass needle attached to a micromanipulator. Every time a cell divides, the daughters are dissected away with the needle and the event is scored. Over-night the plates are stored a 4°C. The experiment is finished when all cells cease to divide.
In my case I wanted to show that first, the age-distribution of FACS-enrichment is comparable with dissecting and second, whether the labeling with Alexa633 has any influence on aging itself. Instead of taking freshly budded daughter cells from the plate, the cells were prepared like for a FACS-aging experiment either including Alexa633 or omitting it. Then solophenylflavin and propidiumiodide were added to the prepared cells. Gatings were set to sort PI-negative, Solo-negative single cells for the Alexa633-positive and Alexa633-negative sample directly on the side of an YPD-agar-plate. These gatings ensure to start with healthy, freshly budded single cells. The survival curves of the two preparations were nearly identical

[Fig.B12]. Median life spans were calculated for Alexa633-labelled and unlabelled cells to be 21 and 20 respectively. The combined median lifespan of both preparations was 21. The published life spans of W303 show a large variance but the results from my experiments are compatible with the literature values [Table B1].

Table B 1 – Published replicative lifespans of W303

Replicative lifespan (median)	Reference	Strain details
13.6	(Barros and Bandy, 2004)	
17	(Ringvoll et al., 2007)	
18,3	(Sharma et al., 2011)	W303-1A HMRΔE::TRP1 rDNA::ADE2 CAN1 VR TEL::URA3
~20	(Ünal et al., 2011)	
20.2	(Kirchman and Botta, 2007)	
~21.5	(Kaeberlein et al., 1999)	*W303-1A MATaRDN1::ADE2 RAD5*
23.9	(Lamming et al., 2006)	*W303-1A MATaRDN1::ADE2 RAD5*
24.6	(Kaeberlein et al., 2006)	*W303-1A MATaRDN1::ADE2 RAD5*
23.2 - 25	(Medvedik et al., 2007)	*W303-1A MATaRDN1::ADE2 RAD5*
26.3	(Zadrag et al., 2008)	

Because the FACS-method allows excluding dead cells from enrichment, a culture-age higher than the median-lifespan is possible.

Taken together, Alexa633-labeling did not impair the normal aging of the yeast-cells and according to [Fig.B9b] the FACS-method is able to enrich cell-populations older than the median replicative lifespan of the strain.

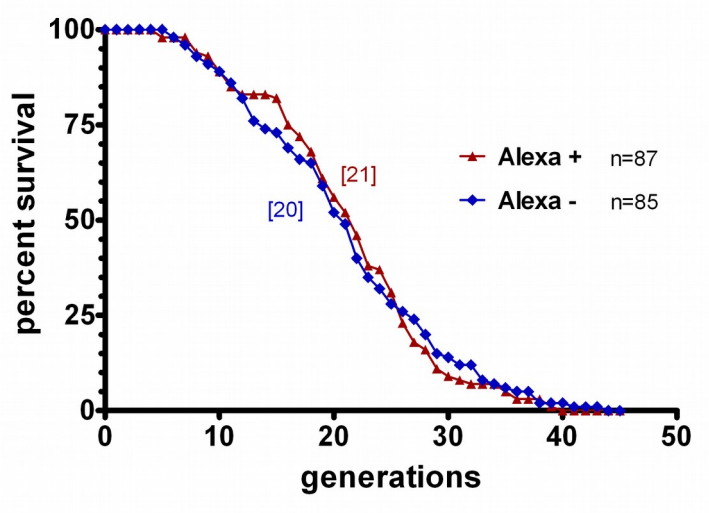

Fig.B12
Survival curve of WΣ determined by micromanipulation. Alexa633 labeled cells were compared to unlabeled cells. The median of budscars (shown in square brackets) was 21 for Alexa-labelled cells and 20 for unlabelled cells.

2.6 Autofluorescence

A critical parameter when quantifying fluorescence is the fluorescent background produced by the cells or the medium (Billinton and Knight, 2001). For FACS measurements medium fluorescence is usually not an issue because it can be considered constant when the experimental conditions are unchanged. Furthermore, the hydrodynamical focusing of the cells in the flow cytometer will dilute the medium so its contribution to the signal is strongly reduced. The cellular fluorescence, however, cannot be considered constant as cells are constantly growing and adapting to altered conditions. Therefore, it is crucial to determine and subtract the autofluorescence especially when reporter fluorescence is low.

2.6.1 Autofluorescence in fermenting cells

To measure autofluorescence in WΣ an untransformed wild-type strain was used and cellular fluorescence was measured over the aging process for the relevant spectral channels. To exclude dead cells from the measurement, propidiumiodide (PI) was added and only PI negative cells were used for quantification. To account for instrumental changes, fluorescent standard beads were recorded and used to normalize the signals. The results for cells grown in synthetic complete medium with 2% glucose at 25°C are shown in [Fig.B13a,b]. A sigmoid curve was fitted to the data using the following formula

$$Y(x) = Y_{\min} + \frac{(Y_{\max} - Y_{\min})}{(1 + 10^{\hat{}}((a - x)\cdot b))}$$

The fit parameters and the standard errors (for CST bead lot 14755) are given in [Table B2]

Table B 2 – Fit parameters for the autofluorescence in fermenting cells

Fit	Ex_{488nm}	Ex_{405nm}
Y_{min}	0.005545	0.003514
Y_{max}	0.03403	0.03366
a	50.83	44.18
b	0.03084	0.03059
Std. Error	Ex_{488nm}	Ex_{405nm}
Y_{min}	0.0004203	0.0006170
Y_{max}	0.001584	0.001433
a	2.163	1.882
b	0.003772	0.003953

This formula, adapted to the current bead lot was used for subtraction of the autofluorescence in all aging experiments under fermentative conditions. When a strain had a substantial growth difference, indicated by the increase in budscars over time during the first 45h, a scaling factor was applied to the "age" parameter to match the conditions of the wild-type strain.

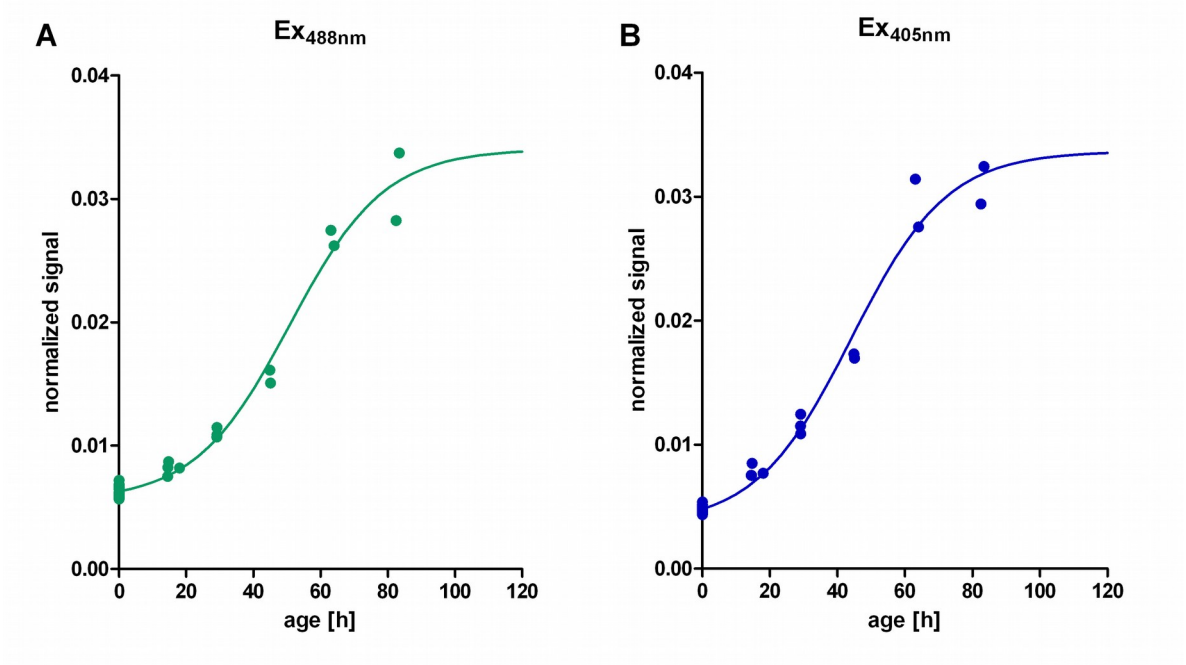

Fig.B13
Measurement of autofluorescence in aging WΣ cells grown at 25°C by the FACS-Canto II. The population averaged signal was normalized to CST standard-beads. Sigmoidal curves were fitted to the data (see text).
a.) Signal of the autofluorescence in the 488-E channel
b.) Signal of the autofluorescence in the 405-A channel

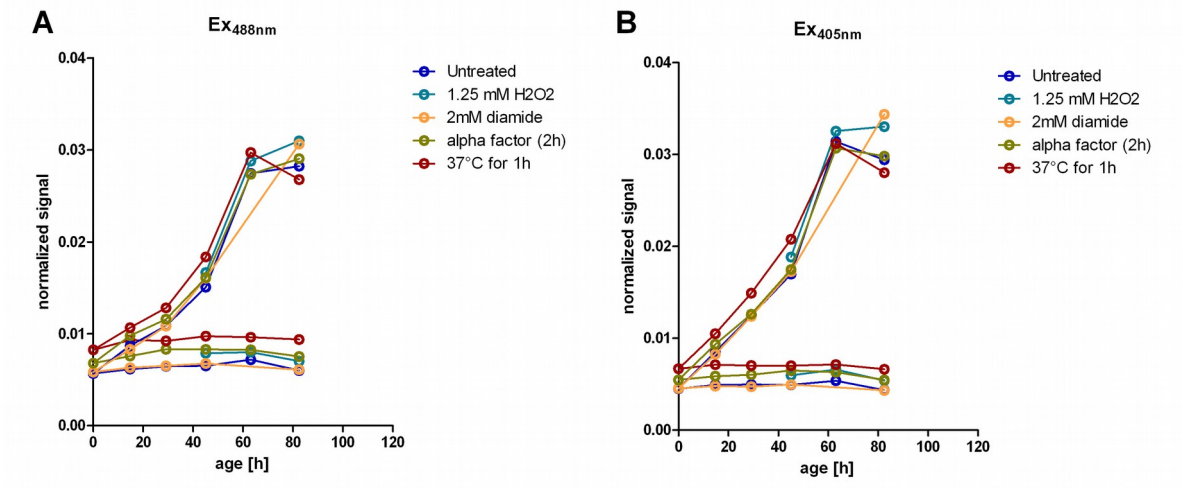

Fig.B14
Measurement of autofluorescence in aging WΣ cells after different stimuli. The population averaged signal was normalized to CST standard-beads. Data for young cells (curves at the bottom) and old cells (ascending curves) are shown in one graph.
a.) Signal of the autofluorescence in the 488-E channel
b.) Signal of the autofluorescence in the 405-A channel

During the aging experiments, different treatments had to be applied to the cells. To check whether they significantly influence the autofluorescent signal they were also tested in one experiment [Fig.B14a,b].
The data indicates that cells under all treatments show a similar autofluorescence although heat-shocked cells have a slightly increased signal. The larger differences between the treatments on the last day may be the result of killing a fragile subpopulation. Because PI is not the ideal vital dye for old cells, as it sometimes misses some of the dead cells (Pereira and Saraiva, 2013); and undocumented observation], membrane permeability could also be altered by the treatments. Since the differences for the remaining data-points are small and within the error of the fitting, the model described above was used in every context.

2.6.2 Autofluorescence in respiring cells

Under respiratory conditions cell growth is much slower and a different model for autofluorescence is needed. From the previously conducted aging experiment with the three different promoters (see above) the autofluorescence was extracted. Spectral spillover from the fluorescent proteins was eliminated by a compensation-matrix and autofluorescence in the remaining channels was determined. The results are shown in [Fig.B15a,b]. A sigmoid function (see previous section) was fitted to the data. The parameter "b" was globally shared for all fluorescent channels (only the relevant two are shown) as otherwise the sigmoid fit would be ambiguous. The results for the fitting are given in [Table B3] (for CST bead lot 57599).

Table B 3 – Fit parameters for the autofluorescence in respiring cells

Fit	Ex_{488nm}	Ex_{405nm}
Y_{min}	-0.002540	-0.004617
Y_{max}	0.02576	0.1124
a	94.55	215.0
b	0.005305	0.005305
Std. Error	Ex_{488nm}	Ex_{405nm}
Y_{min}	0.002053	0.001621
Y_{max}	0.003424	0.04015
a	24.60	47.31
b	0.0008113	0.0008113

Since the model was only built from one experiment, one should be critical with this data especially at later time-points where the data is extrapolated.

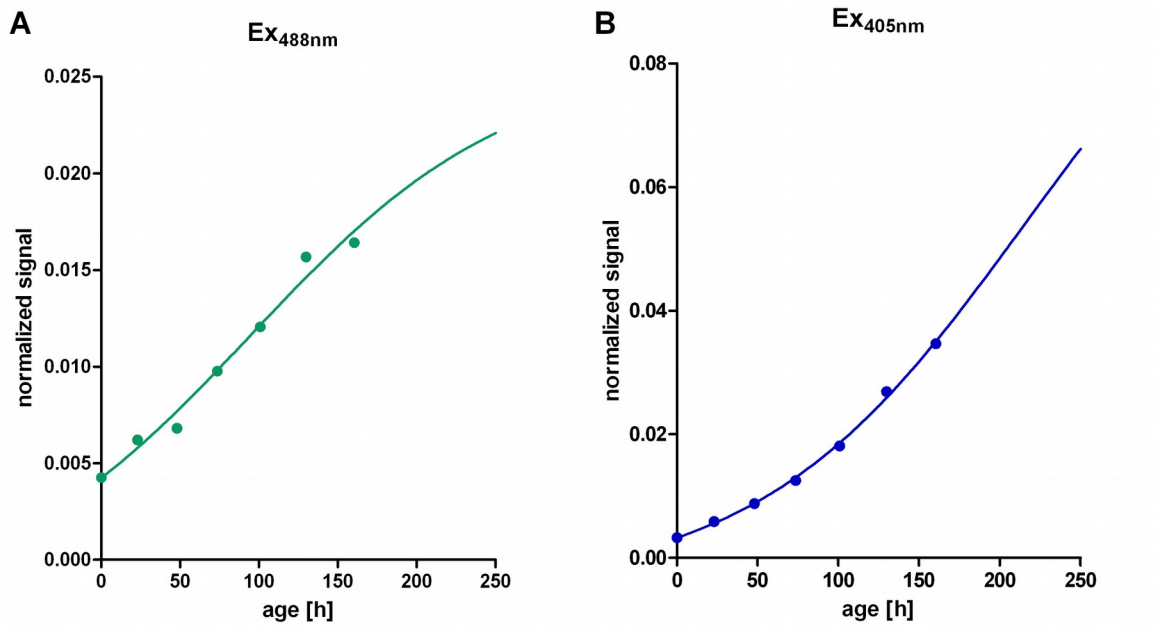

Fig.B15
Measurement of autofluorescence under respiratory conditions in aging WΣ cells grown at 25°C by the FACS-CantoII. The population averaged signal was normalized to CST standard-beads. Sigmoidal curves were fitted to the data (see text).
a.) Signal of the autofluorescence in the 488-E channel
b.) Signal of the autofluorescence in the 405-A channel

2.6.3 Constitutive promoters in respiring cells

In the presence of glucose yeast cells produce their energy by fermentation. When glucose is depleted cells undergo a diauxic shift and metabolize alternative carbon sources like glycerol or ethanol and produce ATP by oxidative phosphorylation. Under those conditions the cell cycle time is largely increased. Therefore, a suitable model for the autofluorescence is needed (see below). The determination of the autofluorescence was also an opportunity to test the expression of constitutive promoters in the same setup. As discussed in "*Part A"*, normalization to housekeeping genes is a necessary step to evaluate the readout of a reporter. To make use of the multispectral analysis of the flow cytometer, three different strains were used for an aging experiment in the same culture each expressing a different fluorescent protein under a different constitutive promoter [Table B4]. The aging experiment for respiratory growth was done in synthetic complete medium containing 3% glycerol and 2% ethanol at 25°C.

Table B 4 – Fluorescent proteins expressed by different promoters

Promoter (systematic name)	Fluorescent protein
ACT1 (YFL039C)	T-Sapphire
TDH3 (YGR192C)	sfGFP
TEF1 (from Ashbya)	TagBFP

The data showed a continuous increase in fluorescence for all tested promoters [Fig.B16a]. The ACT1 promoter had the strongest induction whereas the TDH3 promoter was less variable and the fluorescent protein expressed by the TEF1 promoter from *Ashbya gossypii* showed an intermediate accumulation [Fig.B16a,b].

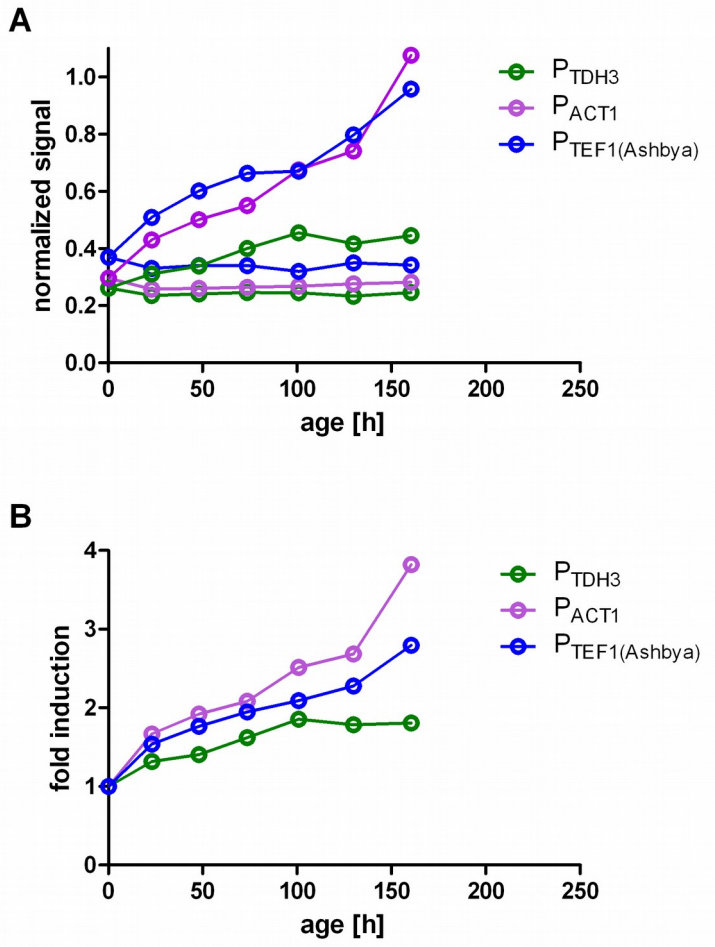

Fig.B16
Measurement of constitutive promoters under respiratory conditions in aging WΣ cells. Cells were expressing pRS304-P_{TDH3}-sfGFP4x, pRS304-P_{Act1}-T-Sapphire4x or pRS304-P_{TEF1}-TagBFP4x respectively and grown in the same culture.
a.) Reporter expression during aging. The population averaged signal was normalized to CST standard-beads. Data for young cells (curves at the bottom) and old cells (ascending curves) are shown in one graph.
b.) Reporter induction during aging determined relative to the young cells.

3 Discussion

3.1 Pros and cons of the method

Fluorescent signal quantification in living cells is always challenging and fixation for microscopic imaging is sometimes not an option. The here described flow cytometry based approach to enrich and measure fluorescently labeled cells and follow them over their replicative lifespan eliminates several problems of the conventional detection methods.
First, cells can be measured directly from the medium without altering the conditions. This is important for environmental sensitive probes as their status often cannot be fixed when cells are prepared for measurement. Second, dead cells can be quantified and eliminated during the passage. Third, measurement of distinguishable populations (e.g. Alexa labeled old cells and unlabeled rejuvenated daughter cells) from the same culture is possible to visualize subtle differences. Fourth, statistically relevant amounts of cells can be quantified to get an impression of the whole natural variation. And fifth, kinetic measurements can easily be done without purification or loss of the whole aging culture.

On the other hand there are also some limitations and drawbacks of this method which should be discussed here.
The first and maybe most severe disadvantage is the passage of the cells itself. Starting with 4 million cells for an aging experiment, seven divisions will increase the number to roughly 500 million cells that have to pass the flow cytometer. With a sorting speed of 30 000 events per second this takes about 5 h. During this time cells are kept at high densities at 4°C during the sort and in PBS solution after the sort until finally inoculated into fresh medium. Although agar plates for the classical micromanipulator based aging experiments are usually kept in the cold over night and cells can survive for several weeks in water when subjected to chronological aging experiments, this procedure will undoubtedly apply stress to the cells which could alter the "natural" aging behavior. However, after sorting the cells had a recovery phase of at least 12 h in media before any measurement.
Conventionally old cells are biotinylated and enriched by paramagnetic steptavidine-coated beads over magnetic columns. It should be possible to combine biotin labeling with fluorescent labeling on the surface to allow both magnetic enrichment and discrimination in the flow cytometer at the same time. However this can be problematic as the surface attached beads can get lost during several enrichment steps especially when cells need to be sonicated to separate mother from daughter cells. Whether a combined approach could increase yield or speed remains to be tested.

Another issue of using flow cytometry is the mother-daughter separation. As a flow cytometer does not detect cells but only can detect events, the single cell population has to be identified by the observed parameters. For ratiometric measurements in young cells this normally is not a problem but an old cell could easily be surrounded by a cluster of attached offspring and would be completely dominated by their signal. Furthermore, an accurate subtraction of autofluorescence will require a defined population. Therefore it is absolutely essential to separate the old cells from the daughters. The most effective way is mild sonication (already discussed in *Part A*). This treatment could apply a mechanical stress to the cells (on the other hand the classical dissection will do the same as cells are separated by the rapid movement of a glass needle). More important, the single-cell gating only defines a sub-population of cells – namely those cells that are single. Cells that are arrested in a budded state (at least those cells

were the bud is of comparable size to the mother cell) are excluded by the gating. It should be kept in mind, that some aspects of aging may be missed by this analysis.

Although analysis of the old cells is convenient with this aging assay, due to their low abundance purification efficiency is poor. The current technical limitations of the flow cytometer do not allow a high yield and a high precision at the same time. When sorting with a high precision all events that do not match the strict sorting criteria are discarded which can lead to a substantial loss of material. A pre-enrichment with a high yield followed by a high precision sort is possible and recommended for the passage of the cells but the pre-enriched cells will always be diluted in the sheath-fluid (PBS) of the cytometer were an unbiased growth condition is not given anymore. This may be tolerable for a translation-based reporter but is not compatible with environmental sensitive probes that are influenced by the medium. Pre-enrichment into a medium filled tube will be a compromise at the cost of an extended sorting time caused by the high dilution.

3.2 Reporter measurements

3.2.1 Pheromone response

The pheromone-response in old yeast cells showed a clear dichotomy in reporter activation [Fig.B11]. One population of old cells could be induced to the same level as young cells whereas an increasing population of the old-fraction emerged which was not inducible at all.

It was reported before that old cells become sterile maybe due to chromatin remodeling. It is thought that chromatin maintenance gets less efficient resulting in increased expression of the formally silenced mating-type loci. By this mechanism the cells would lose its mating-type identity and become MAT**a**/α. (Smeal et al., 1996). The authors of the study showed that Ste12-mRNA level in enriched old yeast cells become lower, most likely due to de-repression of the hidden MAT-loci.
The results of my reporter-measurements are in line with this interpretation. On the other hand the general observation was made (see *Part C*) that colony formation of metabolically active cells declines with age. It is likely that stationary cells may also fail to induce the mating response. It should be possible in future experiment to sort cells of both populations on plates to see if they differ in colony formation.

3.2.2 Heat-shock response

The same argument raised in the context of the pheromone response can also be applied to the heat-shock response. A global loss of gene silencing, which seems to be a general hallmark of aging cells (Wood and Helfand, 2013), would lead to an increased protein production. This may also involve an elevated expression-level of chaperones as well and thus reducing the dynamic range of the heat-shock induction. The preliminary data from the heat-shock reporter [Fig.B10] supports this argumentation.

4 Aging by Flow-Cytometry

The following sections will describe in detail how to perform an experiment. The protocols are the result of successive optimization to increase the yield and speed of the assay. Specific caveats and recommendations are included to aid the experimenter.

4.1 Labeling of cells

Reagents to prepare:

- 200 µM Alexa633-Succinimidyl ester in water-free Dimethyl-formamide (DMF). Aliquots can be stored for about 2 years at -70°C but labeling efficiency may go down.
- 200 mM $NaHCO_3$-Buffer, pH 8.4
- PBS pH 7.4
- 500 mM Tris/HCl, pH8.4

1. Grow cells for at least 12h in early log-phase from a starter culture at 25°C
2. Leave an aliquot of culture for analysis on the flow-cytometer (see below)
3. Harvest about 5 OD-units (roughly 10^8 cells) by centrifugation (4800g or lower)
4. Wash twice with 5 ml PBS
5. Resuspend in 5 ml $NaHCO_3$-Buffer
6. Add 50 µl of Alexa-dye and incubate for 15-20 min at room temperature. If the Alexa-stock is already old, label first with 30 µl for 5 min, then centrifuge and resuspend in fresh $NaHCO_3$ and label again with 70 µl Alexa for 15 min.
7. Centrifuge and resuspend cells in 5 ml Tris/HCl and incubate for about 5 min
8. Centrifuge and resuspend cells in 3 ml PBS
9. Proceed with preparation of the cytometer

4.2 Sort of initial cell-population

For the sorts, a FACS-Aria I and later (since June 2012) the upgraded Aria IIIu with Diva 6.1.3 Software (BD-biosystems) was used.
Preparation:

- YPD-Agar-plates (96-well-plate format)
- Solophenylflavin 100 µg/ml in water
- Poly-lysine-coated microscope-slides or ConcanavalinA-coated coverslips
- 0.2% Agar
- Synthetic complete (SC)-medium

1. Transfer labeled cells to a FACS-tube with 70 µm cell-strainer and shortly sonicate them
2. Record some cells to adjust gating - the optional compensation-matrix should have been established before. Always use the 70 µm Nozzle in the sorter to enable high-speed sorting and keep the drop size as small as possible.
3. Select for Alexa-positive, GFP and/or T-Sapphire-positive, single-cells with a low FSC-A to preferentially sort virgin daughters. Exclude cells with very bright Alexa-fluorescence as they might have taken up the dye. The sorting gate will be at about 10-30% of the total population. Caution: Since the Laser and the PMTs in the cytometer are not

constant over time, and also cells may adapt to the PBS conditions, gatings should be adjusted, if necessary.

4. Sort about $3*10^6$ to maximal $1*10^7$ cells with "single-cell" precision (*Note: not to confuse with the single-cell gate*). The sorting speed or the sample dilution can be adjusted. If the speed is too high, the efficiency of the sort will drop. The best trade-off is at about 700 to 1500 sorted cells/sec, with an efficiency of about 40%.
5. Keep some of the cells for microscope and plate sorting (*see below*).
6. Take a sterile graduated cylinder and fill-in 100 ml SC-medium. Pour about 3/4 of the medium in the Erlenmeyer flask and pipet the cells carefully into it. Then use the rest of the medium to rinse the FACS-tubes several times to transfer as many cells as possible. Do not splatter cells to the Erlenmeyer walls as they would dry out and stop dividing. If the Shaker is exposed to light during incubation, wrap it with some aluminum foil to prevent bleaching of the Alexa dye.
7. Incubate at 25°C at 140 RPM. It is crucial not to shake with more than 160 RPM, otherwise cells will stick to the glass above the meniscus and will not age properly.
8. Use the rest of the cell-suspension (see step 5) to spot some cells (500-1000) on a sticky microscope-slide or coverslip (coated with ConcanavalinA) and add 3 µl of Solophenylflavin solution to the spot. Let the spot dry, then add some melted 0.2% Agar and immediately assemble coverslip and microscope slide. If budscar counting is not performed directly, add some water to the slide after the agar is solidified and/or freeze the slide at -70°C.
9. To test for cell viability, spot 384 single-cells on a YPD-agar-plate and incubate at 30°C until colonies appear. Then calculate the percentage of formed colonies.

4.3 Measuring young and old cells

For analysis of cells a FACS-CantoII and Diva 6.1.3 Software (*BD-Bioscience*) was used.

1. Take aliquots of the overnight culture at $OD_{600} < 0.2$ for every condition you want to measure. If the cells should be induced or shocked for some time, be sure that the final cell density does not exceed 10 000 events/sec in the "Fast-Flow"-mode (at 120 µl/min). Calculate to have about 20 000 old cells in the tube but not more than 2 ml total volume (*see section 4.5.*). It is useful to have an established timing schedule and judge the cell density by eye rather than wasting cells for OD measurement.
2. Apply shocks to the aliquot. For heat-shock, aliquots were kept in 2 ml Eppendorf tubes and transferred to a thermomixer at 37°C for 1h at 1000 rpm shaking frequency. If needed, add Cycloheximid (f.c. 15 µg/ml) to the cells at the end of the shock to stop further induction and incubate for additional 15 minutes.
3. To account for instrument variability, it is recommended to record standard beads before and after every measurement, to normalize the data.
4. Transfer the samples to FACS-tubes by pouring. Avoid pipetting, as many cells would stick to the pipet-tip.
5. Sonicate the samples to ensure mother-daughter separation. The older the cells get, the harder they are to separate. This needs some experience to judge, how long the sonication should be without killing the cells. Always try to find the resonance spot in the sonicator bath where energy transfer to the sample is maximal. As sonication also heats up the sample, vortex in between to ensure cooling,
6. For measuring young cells in the culture, record 20 000 – 30 000 Alexa633 negative cells.

7. For measuring old cells, record only Alexa633 positive cells. Depending on the age of the culture, they will make up around 3% (for the first passage) to 0.2% (for late passages) of the total cells. Since the young cells can be in more than 100 fold excess over old cells and the cytometer (or the software in the current version) is not able to discard a certain percentage of a gating, it is not recommended to record old and young cells in parallel. Do not include too many statistics and gatings on the recording-worksheet, because this will lead to massive abort-counts due to limiting computing power!
8. Always try to acquire the data as fast as possible (Flow-rate "Fast") to minimize instrument fluctuations during recording. Nevertheless, if a live kinetic should be acquired, flow rate can be adjusted while recording. I would strongly recommend plotting the fluorescent parameters (GFP, T-Sapphire and/or the ratio) over time as a live-view with a reference line in the worksheet to see if the measurement is stable.

4.4 Recovering cells

This part describes how to recover as many old cells as possible. This can be up to 70% of the inoculated culture and it is highly recommended to put much effort in these steps to have enough material for the measurement of the oldest cells.
Transfer the rest of the over-night culture (after taking out the aliquots) in 50 ml Falcon-tubes and pellet cells. (For the experiments 4800g or lower was used). If two Falcon tubes are in use, mark one for the final pellet. As the pelleting takes about 30-60 min, centrifugation and sample storage should be done at 4°C to prevent cell-division.

1. Write down the time when cells are put to 4°C, to later calculate the "sort-brake".
2. Carefully take off about 2/3 to 3/4 of the supernatant with a 25-ml-glass-pipet and save it in the Erlenmeyer-flask. Resuspend the cells in the unmarked Falcon and transfer them to the marked one. Be sure to rinse the Falcon-walls with supernatant from the Erlenmeyer. Important: Here contamination is not a problem because cells will be sorted afterwards – so the same pipet can be used for the whole procedure.
3. Fill up the unmarked Falcon with supernatant and repeat steps 1-3 until the marked Falcon contains only 1ml volume. Take a 2-ml-glass-pipet and transfer the gently resuspended pellet in a FACS-Tube with 70-µm-cell strainer. Rinse Falcon tube with some supernatant and also transfer this into the FACS-tube. The cell strainer is extremely important; otherwise the Nozzle in the sorter will clog eventually. The whole procedure can be repeated, while the first batch is running on the sorter.

4.5 Passage of old cells

Preparation: YPD-Agar-plate, SC-medium, coated coverslips, Solophenylflavin and 0.2% Agar as described in (*Section 4.2.)*. Optional: Propidium iodide 200 µg/ml

1. Set up the Cell-Sorter with the 70-µm-Nozzle. Cool down the sorting chamber to 4°C. Be sure to have the optimal settings of the drop-delay with the Accudrop-beads.
2. Sonicate the sample shortly to reduce cell-aggregates. Do not sonicate too long because killing cells here will reduce the yield of the whole experiment!
3. Select for Alexa633-positive, Propidium iodide negative (*see comment section below*), T-Sapphire-positive cells. Do not use a single-cell-gate at this step. It is recommended to already have a template-worksheet for the passage to estimate where the cells will be, so the sort could be stared immediately.

4. A first round of enrichment is necessary, because sorting efficiency is poor, if the sorted population is less then 10%. Therefore, use the "Sort-precision: Yield"-setting. The sort-rate should be less than 30 000 events/sec, otherwise the abort-rate will increase - adjust the sorting speed accordingly.
5. Always keep an eye on the cytometer! If the stream becomes instable, the sorting will stop, but the sample-flow will still proceed. This leads to the loss of cells. With the sort-precision: "Yield" and "Purity" maximal $2.5*10^6$ cells will fit into a FACS-collecting tube (5 ml) – so be sure to change them on time. I do not recommend collecting in Falcon tubes, because their surface seems to be much stickier to cells than the FACS-tubes.
6. Alexa633-labelled cells seem to have a high affinity for surfaces. If not agitated, many sorted cells will stay in the place, where they first hit the FACS-tube. To increase yield of the enrichment one can make use of this behavior. Before starting the final enrichment, I recommend to sort the agar-plate and the microscope-sample. Set up an additional single-cell gate in the T-Sapphire-positive hierarchy and choose "Sort-precision: Single-cell". Then take an un-agitated tube with the first enrichment and set the sorting rate to minimum. If the tube was vortexed before, the event-rate would be unnecessarily high and would lead to substantial cell-loss. Sort and prepare single cells for the Agar-plate and the coverslip as done in *(Section 4.2.)*.
7. Proceed with the second round of enrichment. Be sure not to use the single-cell gate here. Check the position of the sort output, as it may have changed during plate-sorting. Set the Sort-precision to "Purity" and start the sort.
8. As mentioned above, many cells will stick on the tube walls. Be sure always to rinse them. A good way to do this is to use the PBS from the stream in the sorting chamber.
9. For inoculating the enriched cells, calculate to have a minimum of about 10 000 cells/ml final concentration. Consider that a Falcon-tube could hold about 55 ml of volume, so try to make use of all the capacity for the next enrichment. Inoculate the cells as carefully as described in *(Section 4.2.)*.
10. Put the culture to 25°C and shake with 140 RPM.
11. Write down the time of the inoculation for calculation of the "sort-break".

4.6 pHluorin & roGFP-measurements

Measurement of pHluorin or roGFP reporters (described in *Part C*) can be performed directly from the medium without further pre-incubation. When measuring kinetics it is recommended to handle the sample as fast as possible.

1. Record an untreated sample before the kinetic to know the basal reporter activity
2. Consider how long the recording of the kinetics should be and how much culture volume you would need at a given flow-rate to cover this time (not more than 2 ml). The flow rates for the CantoII cytometer are assigned to be (High: 120 µl/min, Medium: 60 µl/min, Low: 10 µl/min). For kinetic measurements of young cells try to dilute the sample to about 100 events/sec at medium flow rate. When measuring different cell-types in the same culture consider a higher density (ideally 100 events/sec for each cell-type).
3. If the instrument-parameters should be monitored during the recording, fluorescent standard beads can be added to the tube. Calculate that the bead-type you want to normalize your sample to have not less than 1/10 of the density of the cells. Be aware that standard beads usually contain sodium azide as a preservative. If you think this could influence the reporter, wash the beads first (in the centrifuge they should pellet like normal cells).

Consider also that the standard beads could be prone to bleaching at ambient light. The Sphero-Rainbow beads seem to be critical in this respect. For the CST beads I have not observed any indication for bleaching.

4. Prepare an appropriate stock solution of the chemical you want to treat the cells. I usually used stocks of about 50 – 200x.
5. Prepare the FACS-tube with the cells (and beads) and be sure they are already sonicated.
6. Record a sample with reference beads before the kinetics
7. Wipe the sample collection tubing to get rid of hanging drops of FACS-Flow.
8. Prepare all the setting in the software. Ensure that you do not start with the lowest flow rate, as this would increase the instrument delay. Be sure that you have not set any recording constrains (maximal time or limited amount of cells to record) which could abort the measurements too early.
9. Pipet the shock solution not directly to the cells but rather on the wall of the FACS-tube in a way that they do not mix yet.
10. When everything is prepared, mix the FACS tube and the drop of shock solution quickly but thoroughly on the vortexer and start recording as fast as possible. The delay from mixing to recording was always about 10 seconds for my measurements. This time is later needed for the data processing.
11. Monitor the response of the cells by an appropriate dot-plot in the software (e.g. ratio over time) to judge the current state of the kinetic.
12. The flow rate can be adjusted during the recording to cover fast changes with more datapoints if needed.
13. After the kinetic record another sample with reference beads

4.7 Probe calibration

For pH determination by the pHluorin probe a calibration curve has to be established to calculate the exact pH from the fluorescent ratios. For roGFP constructs, fully oxidized and fully reduced samples have to be measured.
It is a matter of debate whether calibration should be done with old cells as well or whether the calibration of the young cells could be transferred to the old cells. I would argue that it is legitimate to use the data from young cells for several reasons. First, the ratiometric probes are thought to be independent of the expression level and should give reproducible results at a physiological environment. Second, the calibration itself is performed under completely unphysiological conditions. For pHluorin this is a pH buffered solution with protonophors or detergents which would change the cytosolic conditions anyway. For roGFP cells are treated with high concentrations of oxidant and reducing agents, which would impair global protein function and homeostasis at least temporarily. It is therefore unlikely that altered cytosolic conditions in old cells would have a big impact on the reporter normalization. Third, autofluorescence in old cells is a critical parameter. Especially when the ratiometric reporters are calibrated to their extremes, at least one fluorescent parameter would exhibit low fluorescence. A substantial uncertainty in autofluorescence could completely ruin the accuracy of calibration. In addition it needs to be shown that the autofluorescence of old cells is not changed by the calibration itself. Fourth, old cells are already fragile. Extreme conditions as applied by the calibration could easily kill a subset of cells, which would then be missed by the analysis and therefore calibration would never be unbiased.

4.7.1 Calibration of pHluorin

Standard buffers in a range of pH 5.7 to pH 8.5 should be prepared using a 100 mM MES/Tris or HEPES/Tris system. Buffers can be stored for several months in the cold but the pH might change a bit over time so it is recommended to check the buffers before every new calibration curve. I preferred the simple buffer system for my experiments but there may be better solutions containing salts (Orij et al., 2009), stabilizers, preservatives and protonophors (Diakov et al., 2013); (Ayer et al., 2013).
For calibration, cells were grown in SC medium harvested and washed once with water. The standard buffers were prepared in FACS-tubes using 267 µl buffer and 3 µl digitonin (stock 16% in DMSO). To the buffer 30 µl cells were added and incubated for 1-5 minutes. pH equilibration was followed in the flow-cytometer and data was recorded when the condition was stable. I observed that buffers in the range of pH 6 to pH 7 maintained the stable signal over several minutes but at higher pH cells started to lyse shortly after equilibration and lost reporter fluorescence. This is why the equilibration process should always be followed when this simple buffer is used. Here the other buffering systems might provide more stable results.
A sample calibration curve for pHluorin is shown and described in "*Part C*" [Supp.C10].

4.7.2 Calibration of roGFPs

To fully oxidize the roGFP probes, a 10x stock solution of diamide (stock 200 mM in H_2O) or DTT (stock 2 M in H_2O) was added directly to the cells in the medium and allowed to equilibrate for 5-10 minutes. The samples were then analyzed on the cytometer. For the aging experiments an aliquot of 180 µl was taken from the culture, supplemented with 20 µl of diamide/DTT and only young cells were used for calibration.
Details on the redox calculations are given in "*Part C*" where the reporters are introduced.

4.8 General comments and precautions

4.8.1 Spectral-compensation

If two fluorophores with overlapping emission-spectra are analyzed, a compensation-matrix has to be built. In case of GFP, T-Sapphire and TagBFP (Alexa633 has no significant overlap to the other fluorophores) this can be done either by the built-in function in the Diva-software or manually, which is the method I preferred. To do this, cells expressing each fluorophore separately and one sample without any fluorophore (blank) are recorded. For each sample, select a gate of single-cells, expressing the fluorophore. Open a statistics view and show the mean-value of the respective channels. The blank-sample is the reference. Write down the blank-values and go through the fluorophore-expressing samples to adjust the spectral overlap until the blank-values in the relevant cannels are reached. As compensation will also affect the autofluorescence, blank values will be changed a bit. Write down the changed values, and fine-tune the matrix again. The matrix can then be used for quite a long time as long as the PMT-voltages remain unchanged and the relative detection sensitivity is constant.

4.8.2 Special issues of spectral compensation

If a strain with a severely affected autofluorescence is used (messed-up metabolism with e.g. elevated flavonoid-level or increased cell-size), compensation may be done separately. For old cells that might be an issue, but as long as the fluorophore expression is high, the effect should be negligible. If one would really need high accuracy, autofluorescence calculations would have to be done with exactly the same compensation matrix as the experiments. But since autofluorescence determination itself is subject of high biological variation, such an excessive effort might not improve the quality of the data.

If the fluorophores are independent of each other, and fluorescence resonance energy transfer (FRET) is constant or negligible, each fluorophor can be compensated. In the case of environmental-sensitive probes like pHluorin and roGFPs, the two detection channels have to be excluded from compensation. Other fluorophores that are expressed in addition to roGFPs & pHluorin, have of course to be compensated.

If standard beads are used, compensation should be disabled. The beads are usually coated with different fluorophores and are fluorescent in all channels. Since normally one does not have individually labeled beads to compensate for, a cell-adapted compensation would adulterate the standardization. Therefore beads should be measured independently of the cells, or, if they are used together with cells, either be processed with their own matrix or only be used to correct for relative changes.

4.8.3 Instrument and sample handling

Sometimes it can happen that the bubble-filter of the FACS-CantoII is already filled with large amounts of air. This may affect the flow of the sheath-fluid and mess-up with the timing of the detectors. I recommend to purge the filter before starting a measurement.
If a FACS-tube runs empty, the FACS-Aria will (*in most cases*) shut-off the stream (*in the other cases it will flood your sample*), whereas the FACS-CantoII will keep-on acquiring data. In the latter case, meaningless data is recorded and air enters the flow-cell. Air bubbles may remain in the tubings and can affect the next measurement. If this happens, nudge the tubings to get rid of the air or run the “degass-flow-cell” option.
In most flow-cytometers, cells are hydrodynamically focused by sheath-fluid. The pressure-difference between sample-flow and sheath-flow determines how narrow the cells line up and how they pass the laser-beam. A population normally becomes broader when measured at higher flow-rates and this also affects the mean fluorescence intensity that is calculated by the program. This becomes evident, if ratiometric measurements are taken. In the CantoII the difference of the 488E/405A ratio-values between High-flow and Low-flow, is below 5%, mainly attributed to the 405A-channel. In the FACS-Aria IIIu the difference (488B/405B compared to flow-rate=1) can be more than 15% mainly attributed to the 405B-channel [Fig.B17].
The Aria IIIu should therefore only be used for measurements, if extremely low flow-rates are applicable.

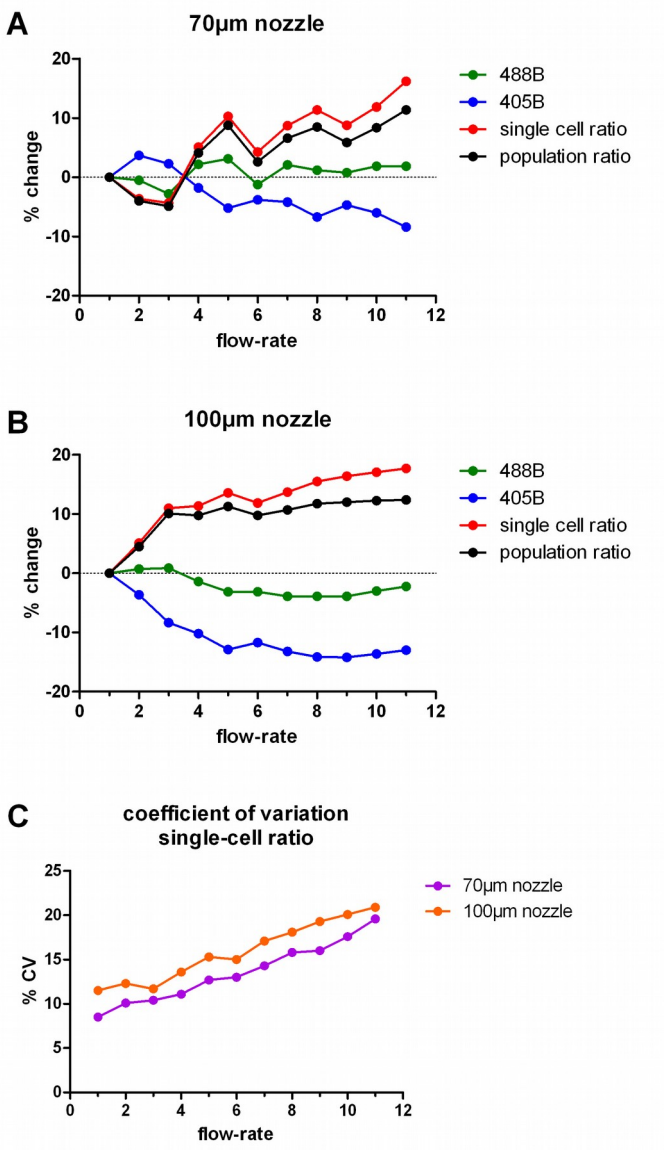

Fig.B17
Flow-rate dependency of the fluorescent signal in the FACS-Aria IIIu. WΣ-cells expressing the ratiometric pHluorin reporter were analyzed on the cytometer at different flow-rates. The signal of the 488-B and the 407-B (in the figure "405-B" is written) channels (green and blue), the signal ratio based on population averages (black) and the signal ratio based on individual cells (red) are shown.
a.) Relative flow-rate dependency in the high-pressure setup with the 70-µm-nozzle
b.) Relative flow-rate dependency in the low-pressure setup with the 100-µm-nozzle
c.) Coefficient of variation for 70-µm and 100-µm-nozzle, based on the single-cell ratio signal

4.9 Standard beads

Flow cytometers are complicated machines with many fine-tuned subsystems. To maintain accuracy timings and voltages have to be adjusted from time to time. The machine has an internal routine to derive those parameters by measuring standard beads. These beads are called

"BD™ Cytometer Setup & Tracking Beads", (BD-Bioscience Cat.no. 641319) or short CST-beads. The CST mixture contains fluorescent beads of three defined intensities, covering the whole spectral range of the detectors. The instrument adjustment with the CST beads was performed once a week by the FACS-facility. In the beginning of this work I assumed this would ensure a constant and reproducible signal quality. It later turned out that despite of the regular calibration the instruments showed a substantial day-to-day variation. Since the instrument calibration is based on CST beads I utilized them also as a standard to normalize my measurements. By measuring the CST beads regularly I even could see severe fluctuations within one experiment day. The fluctuations may be attributed to temperature changes, laser instability or accumulation of particles or microscopic air-bubbles in the flow cell. For precision demanding measurements these fluctuations (in a few cases more than 10% signal amplitude) could completely render an experiment useless. It is therefore most important to keep track of the instrumental variation. In the final state of my work I made it a good-practice to measure CST beads about every 20 minutes.
To normalize the data, the CST species with the brightest fluorescence was chosen and gated to show one sharp peak. The averaged fluorescence of this peak in the respective spectral channels was used as a reference for the cells. It should be mentioned that some beads come in doublets which cannot be separated by sonication. By a stringent gating in the forward-scatter signal, those beads can be excluded.

In some cases when a constant kinetic was recorded (not for the aging experiments) I included standard beads directly in the cell suspension. For that I used *"Sphero™ Rainbow Calibration Particles",* (Spherotech Cat no. RCP-30-5A (8 peaks)).

4.10 Budscar counting

To access the replicative age of a culture, the budscars on the surface of the cells can be counted. For that purpose an Olympus IX81 cell^{R} PointFRAP microscope with PLAPO 100x/1.45 Oil DIC objective was used. Fluorescence of Solophenylflavin shows a bright emission in the violet to green range. A filter set suitable for CFP detection (transmission at around 460 nm) was chosen as it provided the best visual contrast. Budscars were counted by eye with permanent focusing through the z-plane. This is a very tricky part and unfortunately much experience is needed to reliably determine the number of scars. It helps to define an axis on one half-sphere of the cell and then counting around the surface in one direction until reaching the axis again. Counting becomes easier when the loss of water under the coverslip compacts the cells in z-direction and brings more scars into focus. But care should be taken as invading air-bubbles can drain the cells away. Before this happens find an eye-catching point in the vicinity of the current cell, carefully unmount the specimen and add a drop of water on the side of the coverslip to prevent dehydration of the sample. Then find the last object position again and continue with the counting. If there is confusion whether a cell is a mother or a daughter cell (sometimes cells stick together for many generations, even when the mother cell already died and the daughter continues dividing), a picture of the Alexa633 dye can help to decide. Unfortunately, this is not always possible when propidium-iodide was used for the sort as it can interfere with the weak Alexa633 fluorescence. Don't get discouraged! Counting becomes better after a few hundred (or thousand) cells.
Because of the ease of use I chose the solophenylflavin dye. But this dye also shows a strong signal in the cellwall, which decreases the contrast to the buds. Maybe FITC-coupled wheat-germ agglutinin, which is often used to visualize budscars, will give better results. I also

observed a decline in image quality when changing from Polysin® covered microscope slides to manually ConcanavalinA (ConA)-coated coverslips. This was done because yeast cells stick much better to ConA than Poly-L-lysine. I expect that machine-coated coverslips will give better results for imaging.

4.11 Microdissection

The microdissection of yeast cells was done with a Singer MSM Manual Micromanipulator. For the assay, cells were prepared in the same way as for a flow-cytometry based aging experiment. For the Alexa633 negative sample, only DMF was used for mock-labeling. Cells were then supplemented with propidium-iodide to exclude dead cells and solophenylflavin to exclude cells with budscars. Single new-born daughter cells were then sorted on the edge of a YPD plate and in addition on a microscope slide for controlling the population. Unbudded cells on the YPD plate were then arranged by the micromanipulator in defined positions and the plate was incubated at 30°C for 2 h. When a cell accomplished a division, daughter cells were separated by the glass-needle and placed on a deposit position on the plate. When all cells were dissected, the plate was wrapped in parafilm and incubated again at 30°C for 1 - 4 h (depending on the age of the cells). Every cell division was scored. A cell was considered dead when it did not divide for more than 12 h. Over night the plate was stored at 4°C.

Part C – Redox homeostasis in old yeast cells

1 Introduction

Aging is a multidimensional phenotype and far from being understood. A still controversial discussion is lead about the involvement of free radicals and their implication in affecting cellular integrity. As a consequence of energy production, free radicals are natural by-products or intermediates of metabolic pathways. Their origin is largely attributed to the respiratory chain. For that reason they mostly contain oxygen and were termed reactive oxygen species (ROS). Beside ROS, there are also other reactive bio-molecules like carbon monoxide (CO), nitrogen monoxide (NO) or alkyl-radicals. Because of their unpaired electrons, radicals readily react with other molecules. Most of the biological relevant radicals finally result in the formation of oxidized proteins or lipids. In the worst case, they can react with DNA and cause mutations. As organisms age they accumulate damaged proteins and DNA mutations, which are tightly correlated with their oxidative turnover (rate of living hypothesis). This led to the formulation of the free radical theory of aging (Harman, 1956), stating that oxidative stress is thought to be responsible for age associated phenotypes. On the other hand, serving also as signaling molecules or as cellular defense against intracellular parasites, free radicals play the role of a double-edged sword and cells have evolved mechanisms to control their toxicity. It is undoubted, that high concentrations of oxidants are toxic to cells but at low doses, through their role in cell signaling and differentiation, they seem to have beneficial effects. This observation was termed “hormesis” or more specific to the mitochondrial ROS production “mitohormesis”. In fact, through recent studies it became more and more clear that avoiding ROS or the use of radical scavengers can even lead to shorter lifespans as ROS signaling will not get activated (Ristow and Schmeisser, 2014).

1.1 ROS in yeast cells

Saccharomyces cerevisiae is a facultative anaerobe organism, which uses fermentation when glucose is present. Under those conditions the respiratory chain is dispensable and only the basal functions of the mitochondria have to be maintained. When glucose levels are low and non-fermentable carbon sources are available, yeast activates oxidative phosphorylation and higher levels of ROS are generated.
I present here only a short overview of ROS production and the redox-buffers in yeast cells. A more detailed insight is given in (Morano et al., 2012).

1.1.1 Superoxide

The respiratory chain transfers electrons from reduction equivalents to oxygen. During this process, electrons can leak out of the system and react with other molecules and reactive species like the superoxide anion $O_2^{\cdot-}$ can be formed. Although, this molecule is weakly reactive on proteins, it can readily react under catalysis of transition metals or iron-sulfur cluster containing enzymes.
Superoxide can also be produced on purpose by NADPH-oxidases in the lysosomes of mammalian macrophages where phagocytosed bacteria are killed and degraded. Recently, a

NADPH-oxidase (termed Yno1) was discovered in the yeast endplasmatic reticulum, which was shown to account for about 20% of the total ROS production under fermenting conditions (determined by Dihydroethidium staining) (Rinnerthaler et al., 2012). It is thought to mediate apoptosis via yeast caspase 1 and also seems to play a role in actin remodeling.

1.1.2 SOD & Catalase

As a line of defense against $O_2^{\cdot-}$ induced damage, cells use special enzymes to dismutate the radical to H_2O_2. All superoxide dismutase (SOD-) enzymes possess a coordinated metal-ion (Cu , Zn, Fe, Mn, Ni) to catalyze the reaction (Abreu and Cabelli, 2010). In *S. cerevisiae* there are two SOD enzymes, the cytosolic CuZnSOD (Sod1) and the mitochondrial MnSOD (Sod2).
The H_2O_2 produced by SOD enzymes is an uncharged molecule and can diffuse across membranes to act as a signaling molecule or react to other species. The most dangerous species, although at very low rate, can be produced by Fenton-types of reaction also using metals (mostly Fe^{2+} and Fe^{3+}) for catalysis. Thereby hydroxyl radicals (•OH) are formed, which react with most of the biological molecules. To control the peroxide levels, cells express another type of enzymes called catalases (Zamocky et al., 2008). These enzymes use a catalytic heme group to decompose H_2O_2 to H_2O and O_2. In *S. cerevisiae* there are two genes coding for catalase (*cta1* and *ctt1*).

1.1.3 Redox-buffers

Many proteins are post-translationally modified and regulated in their biological activity making those sites critical for oxidative events. A special case of modification takes place at the protein thiol groups from cysteine moieties. As disulfide bridges can be formed, these residues critically influence the 3D structure of proteins. Depending on their pKa value and their accessibility, disulfide formation is in equilibrium with the local environment provided by the cellular redox buffers. Being constantly restored, the protein thiols can extend the buffering capacity of the cellular thiol redoxsystem.
Redox buffers not only serve the purpose of reverting protein damage but also provide a stable environment for proper protein folding. Every cellular compartment or organelle has its own demands on the redox buffers and is therefore regulated individually.

The ubiquitous small molecule glutathione (GSH) and its oxidized dimeric form GSSG represent such a buffering system. Under physiological conditions the cytosol is always kept at a highly reducing state. In yeast cells this is accomplished by active removal of oxidized cytosolic glutathione into the vacuole (Morgan et al., 2013) or by reduction via glutathione reductase. The electrons for the reduction are provided by NADPH.

1.1.4 Glutathione peroxidase

Glutathione can itself scavenge many radicals and can therefore act as an antioxidant.
In addition reactive molecules like H_2O_2 or their reaction products (hydroperoxides) with proteins or lipids (R-OOH) can be removed by glutathione peroxidases (GPx) utilizing the reducing power of GSH

R-OOH + 2GSH → GSSG + H_2O + R-OH.

In *S.cerevisiae* there are three glutathione peroxidases (Gpx1, Gpx2, Gpx3). Whereof Gpx2 (Tanaka et al., 2005) and Gpx3 (Delaunay et al., 2002) are atypical in that way, as they use the thioredoxin system as electron donors and therefore are more similar to peroxiredoxins described next.

1.1.5 Peroxiredoxins

Peroxiredoxins belong to the peroxidase family and can also reduce hydroperoxides. Usually these proteins are homodimers. Instead of using glutathione as electron donor, a catalytic (peroxidatic cysteine) thiol-group (-SH) gets directly oxidized to sulfenic acid (-SOH). This group either reacts with an adjacent –SH group (resolving cysteine) in the same protomer or in the other protomer to a disulfide. Regeneration of the thiols is in most cases achieved by the thioredoxin system. At high doses of peroxides a hyperoxidation of the thiol to sulfinic acid (-SOOH) can occur which inactivates the enzyme. Regeneration is then performed by sulfiredoxins.
In *S. cerevisiae* there are five peroxiredoxins (Ahp1, Dot5, Prp1, Tsa1, Tsa2).

1.1.6 Thioredoxin/Thioredoxin reductase

Thioredoxins are enzymes that catalyze the resolving of protein disulfides. They can either facilitate disulfide isomerization or reduce target proteins by donating electrons from their catalytic cysteines. Reduction of the thioredoxins itself is usually performed by a thioredoxin-reductase in a redox relay. The electrons are finally taken from the oxidation of NADPH. In *S. cerevisiae* are three thioredoxins (Trx1, Trx2, Trx3) and two thioredoxin-reductases (Trr1, Trr2).

1.1.7 Glutaredoxins

Because of its high reduction potential (of -280 mV at pH 7) and high intracellular concentration (about 10 mM) glutathione can directly be used as an electron donor for the reduction of oxidized proteins

R-S-S-R + 2GSH → 2R-SH + GSSG

These kind or reactions are catalyzed by glutaredoxins. Beside their role in protein reduction they are also involved in iron homeostasis and iron-sulfur-cluster biogenesis. In *S. cerevisiae* there are eight enzymes encoding for glutaredoxins (Grx1-8).

1.1.8 Glutathione reductase

The most effective glutathione reducing enzyme in yeast is the homodimeric glutathione reductase (Glr1). The reaction catalyzed by Glr1 is the following:

$GSSG + NADPH + H^+ \rightarrow 2GSH + NADP^+$.

In a first step, NADPH reduces a flavin group (FAD), which then generates two free thiol groups in the active centre of the enzyme. During the catalysis GSSG reacts with the charge-

transfer thiols and takes up the two electrons and a proton from an acid-base catalytic residue. In the last step two molecules GSH are released (Veine et al., 1998).
The *glr1* gene has two alternative starting sites. The first start codon includes a mitochondrial targeting sequence localizing the gene product to the mitochondrial matrix (Outten and Culotta, 2004). Since glutathione is only synthesized in the cytosol and needs to be imported into the mitochondria an active regenerating system is important for the maintenance of the mitochondrial redox buffer.

1.1.9 Oxidation and heat-shock

Reactive species are also involved in the regulation of the heat-shock response under stress conditions. The peroxiredoxin Tsa1 was shown to play a dual role as a chaperone and antioxidant. At low ROS conditions it forms small oligomers, which are associated with the ribosome to work as a local antioxidant. At severe stress conditions the peroxidatic cysteine gets hyperoxidated to sulfinic acid and leads to the formation of high molecular-mass oligomers, which acts as a chaperone (Trotter et al., 2008). Hyperoxidation of Ssa1 (a Hsp70) in yeast was also shown to interfere with its inhibitory effect on Hsf1 and subsequently leads to induction of the heat-shock response (Wang et al., 2012).

1.2 Objective of this work

1.2.1 Oxidation in aging yeast cells

For higher organisms it is reported that old cells accumulate damaged or misfolded proteins and their ability to induce the heat-shock response or degrade proteins declines (Calderwood et al., 2009).

It was shown that old yeast cells exhibit markers of apoptosis (staining with Annexin V and TUNEL) and were enriched for oxidized molecules (staining with dihydrorhodamine 123), (Laun et al., 2001) . Partially contradicting results were reported by (Wang et al., 2014) as they could not detect Annexin V and only weakly increased Rhodamine 123 staining in 48h old W303-1A cells. On the other hand the authors found a substantial increase in fragmented mitochondria, elevated level of mitochondrial DNA and a larger amount of cells that stain with $O_2^{\cdot-}$ sensitive compounds like dihydroethidium dye (DHE) and MitoSOX Red staining which could be reduced by adding the radical scavenger resveratrol. Another study shows that cells with strong budscar staining (FITC coupled to wheat germ agglutinin) also have a stronger staining with DHE (Lam et al., 2011). Finally flow chamber measurements indicated a higher ROS level demonstrated by an increased staining of old cells with DCFH-DA (Xie et al., 2012).

These studies provide convincing evidence that aging cells have to cope with higher oxidative stress which raises the question whether the redox buffers declines while cells are getting old. Since we had the chance to use the recently optimized redox-sensitive GFPs we wanted to test this hypothesis. In addition, a ratiometric pHluorin was utilized to measure the cellular pH. I will only focus on the cytosolic changes because, firstly, the aging assays are extremely time-consuming, secondly, although interesting to study, the expression-level of mitochondrial-targeted redox-probes were too low for reliable subtraction of autofluorescence and thirdly, most of the cellular proteins are localized in the cytosol or transit through the cytosol and a global change would most likely affect other organelles as well.

In this work I made use of my previously established flow-cytometric approach (*please refer to "Part B"*) to measure these parameters with high accuracy by a single method in a (hopefully) unbiased replicatively aged yeast strain. The major advantages of this method are that cells could be measured directly from the culture without any preparation, contamination with young cells is impossible - in fact they serve as an internal standard – and dead cells can be directly excluded from the measurement.

1.2.2 The roGFP redox sensor

Fluorescence of GFP is generated by a three amino-acid-derived fluorophore located within the β-barrel of the protein. The molecular environment around this central structure determines the fluorescence and the spectral properties of the fluorophore. In redox sensitive GFPs (roGFPs) environmental accessible cysteines were introduced into the protein structure, linking the central fluorophore to the oxidation-status of the protein (Dooley et al., 2004). The cysteines are in equilibrium with the cytosolic glutathione pool and a change in this equilibrium results in an altered excitation spectrum of the roGFP. The roGFP used in this study was a slightly modified version called roGFP2. For higher specificity and faster responses a human glutaredoxin (Grx1) was fused to the protein catalyzing the equilibration of the cysteines with the GSH/GSSG buffer (Gutscher et al., 2008). Though the probe normally is sensitive to glutathione the replacement of the Grx1 enzyme with the yeast thiol-peroxidase Orp1 (also known as Gpx3) switches specificity to H_2O_2 instead (Gutscher et al., 2009). For better expression levels, the DNA-sequence of roGFP2 had been codon-optimized for yeast. The readout of the roGFP2 is done at an emission wavelength typical for GFP at around 510 nm. There are two inverse correlated excitation maxima at about 390 nm and 490 nm. The ratio between the emission signals at the two excitations carries the information about the protein oxidation. For setting the range of the fully oxidized and fully reduced probe a measurement is done after addition of diamide and DTT, respectively. From those values the probe oxidation (OxD) can be calculated using the following equation (Meyer and Dick, 2010):

$$OxD = \frac{I405 \cdot I488_{red} - I405_{red} \cdot I488}{I405 \cdot I488_{red} - I405 \cdot I488_{ox} + I405_{ox} \cdot I488 - I405_{red} \cdot I488} \qquad \textit{Equation (C1)}$$

I405 and I488 is the emission of the probe at the excitation at 405 nm and 488 nm. The respective $I_{red/ox}$ values are the calibration parameters obtained from a fully oxidized and fully reduced probe.

Knowing also the midpoint-potential of roGFP2, and the temperature, a redox potential for standard conditions can be calculated from the OxD values:

$$E_{GSH} = E^{\circ'}_{roGFP2} - \frac{RT}{2F} \ln\left(\frac{1 - OxD_{roGFP2}}{OxD_{roGFP2}}\right) \qquad \textit{Equation (C2)}$$

Where $E^{\circ'}_{roGFP2}$ is the midpoint-potential of roGFP2 at standard conditions, R is the gas constant (8.3145 J mol^{-1} K^{-1}), T is the absolute temperature (295,15 K), and F is the Faraday constant (96485.3 C mol^{-1}).

The electrochemical potential can be determined by considering the pH:

$$E_{GSH}^{pH} = E_{GSH} - (59.1\,mV \cdot (pH - pH\,7)) \qquad \textit{Equation (C3)}$$

The midpoint-potential of roGFP2-Grx1 has been described elsewhere and assumed to be $E^{\circ'}_{roGFP\,2}$ = -280 mV. The midpoint potential of glutathione (see below) was given as $E^{\circ'}_{GSH}$ = -240 mV (Meyer and Dick, 2010). Because all measurements were done at room temperature, a temperature of 22°C (T=295,15 K) was used for the calculation. The dependency of the redox-potential at standard conditions on the probe-oxidation is shown in [Fig.C1]. The remaining parameter, the pH, has to be determined independently. For this purpose another GFP derivate, the ratiometric pHluorin (Miesenböck et al., 1998) was used. When measured in buffers of known pH, a calibration curve can be determined and the ratiometric measurements can be transferred to the cells of interest. Due to a similar pK_a of the thiol groups from roGFP2 and glutathione (about 9), the probe equilibrates to the ratio of oxidized to reduced glutathione to the same extend when the pH is changed. Events seen by the probe are therefore pH independent changes (Meyer and Dick, 2010).

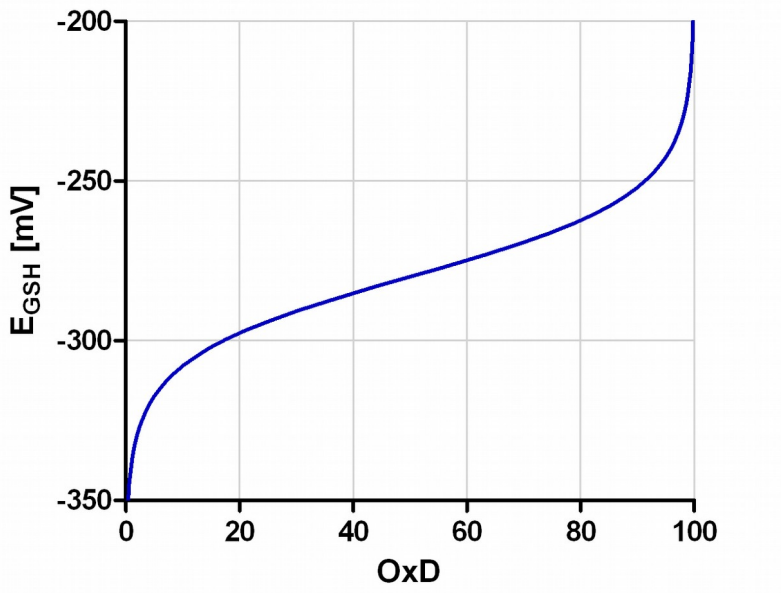

Fig.C1
a.) Dependency of the redox potential E_{GSH} on roGFP2-Grx1 oxidation (OxD) assuming standard conditions (pH 7, 22°C, 10 mM total glutathione, roGFP2 midpoint potential -280 mV)
b.) Calculation of oxidized glutathione (GSSG) based on roGFP2-Grx1 oxidation (OxD) assuming standard conditions

For all the measurements it should be kept in mind that the ratiometric redox-reporters are not able to monitor absolute concentrations as they are in equilibrium with the respective pools. Because of the relation

$$[GSH_{total}] = [GSX] = 2[GSSG] + [GSH] \qquad \textit{Equation (C4)}$$

and

$$E_{GSH} = E^{\circ\prime}_{GSH} - \frac{RT}{2F} \ln\left(\frac{[GSH]^2}{[GSSG]}\right) \qquad \textit{Equation (C5)}$$

the total glutathione concentration influences the redox-potential significantly. For that reason most of the results are given in percent probe oxidation (OxD) only. For measurements where a redox-potential is calculated, the total glutathione concentration was assumed to be 10 mM. From the redox potential at a given total glutathione concentration, the amount of oxidized glutathione can be calculated by

$$[GSSG] = \frac{e^{\Delta} + 4[GSX] - \sqrt{(e^{\Delta} + 4[GSX]^2 - 16[GSX]^2}}{8} \qquad \textit{Equation (C6)}$$

and

$$e^{\Delta} = \exp\left(\frac{nF}{RT}\left(E^{\circ\prime}_{GSH} - E_{GSH}\right)\right) \qquad \textit{Equation (C7)}$$

For a measured probe oxidation of OxD=36.5% the (uncorrected) redox potential at 22°C and a total glutathione concentration of 10 mM is E_{GSH} = -287 mV. From this the GSSG concentration calculates to 56.4 µM. The molar ratio of GSSG:GSH would therefore be about 1:175. The dependency of the redox potential on the total glutathione concentration at a fixed molar GSSG:GSH ratio of 1:175 is exemplarily shown in [Fig.C2].

Also nothing can be concluded for the amount of reduction equivalents like NAD(P)H which are the main electron donors to regenerate the redox buffers. Nevertheless, all redox systems are somehow coupled and measuring the main pools will give valuable information about general changes in redox-homeostasis.

All the roGFP2 constructs were obtained from Tobias Dick (DKFZ-Heidelberg). The pHluorin probe was a kind gift from Matthias Seedorf (ZMBH, University of Heidelberg).

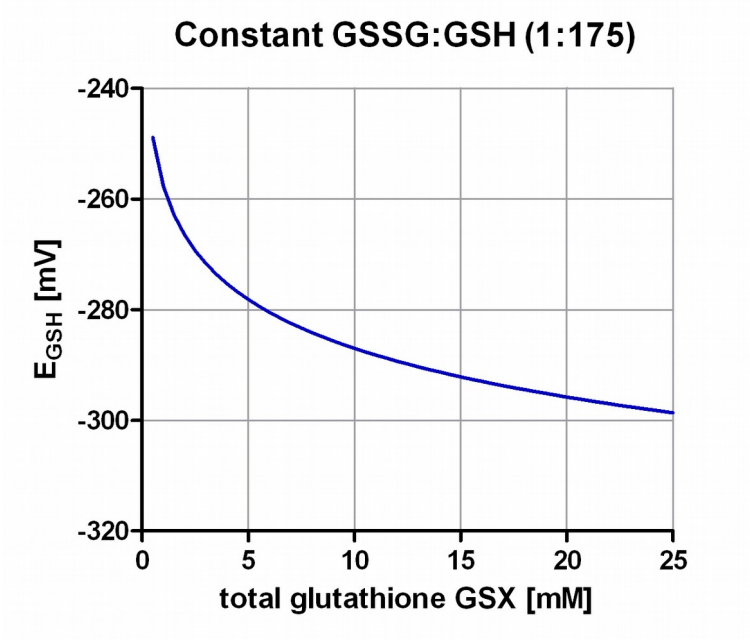

Fig.C2
Concentration dependency of the glutathione potential. Assuming a constant molar ratio of GSSG:GSH = 1:175, the redox potential changes upon the total glutathione concentration.

2 Steady-state Measurements in Replicative Aging

2.1 Redox-homeostasis – fermentative growth

2.1.1 Lifespan and viability

The FACS-method allows different measures of the vitality of the old culture. Because the labeling with a surface bound fluorophore is still present when a cell dies and dead cells can be distinguished by the lack of roGFP expression, it is easy to quantify the fraction of metabolically active cells. The second measure comes from the possibility to sort single cells on agar plates and observe colony-formation. The third measure can be taken from the number of buds determined by fluorescent microscopy. An illustration of the vitality parameters is given in [Fig.C3]. For more details, please refer to "Part B".

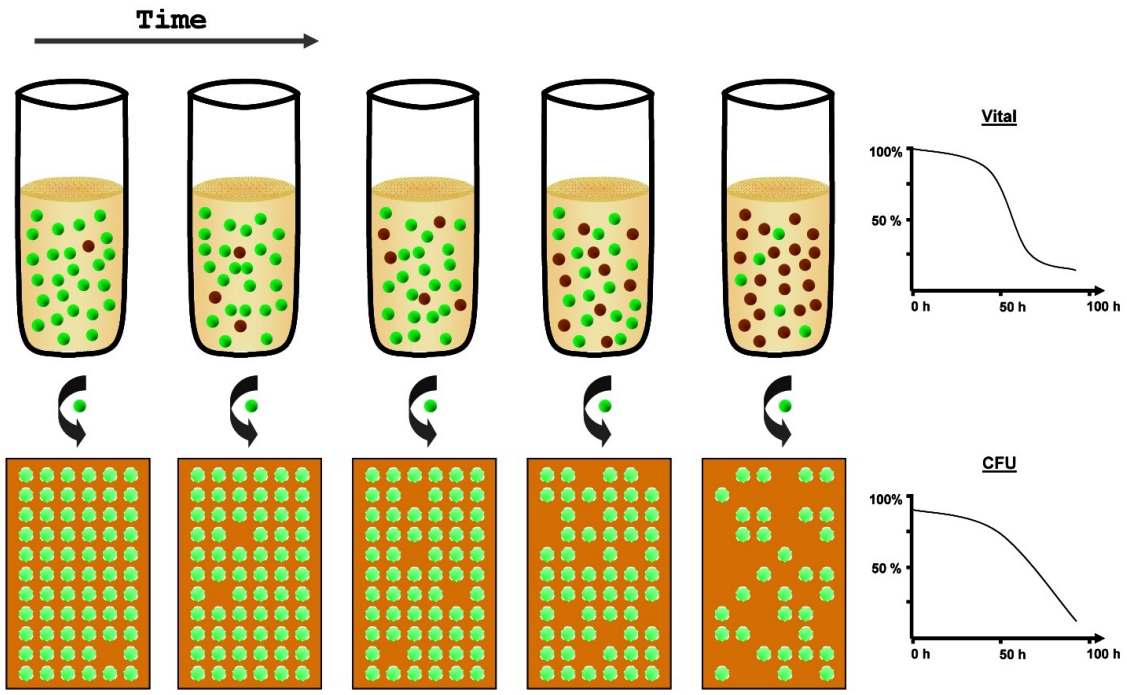

Fig.C3
Schematic representation of the vitality parameters determined by flow-cytometry and cell-sorting. Fraction of living cells is determined by roGFP-reporter expression, the colony forming units (CFU) are determined by single cell sorting of living cells on YPD plates.

An interesting observation was made when cells expressing roGFP2-Grx1 and roGFP2-Orp1 are compared by their vitality parameters. In all experiments the roGFP2-Orp1 cells exhibited a longevity phenotype compared to roGFP2-Grx1. The effect was seen in the average numbers of buds [Fig.C4a], the fraction of living cells in the culture [Fig.C4b] and the colony-forming assay [Fig.C4c]. Fitting parameters for the maximal number of budscars are given in [Table C1]

The Orp1-protein is a peroxidase, which facilitates the transfer of peroxides to the Yap1 transcription factor to induce the oxidative stress-response in yeast. In unstressed conditions

Yap1 is excluded from the nucleus but upon oxidation, a nuclear localization-signal is exposed (Kuge et al., 2001). It is known that mild oxidative stress can up-regulate the cellular defense mechanisms and lead to lifespan extension (hormesis effect). Overexpression of Orp1 by the roGFP-peroxide sensor could accelerate the response to oxidative stress and thus lead to higher stress resistance and a longer lifespan.
Targeting the roGFP2-Orp1 reporter to the mitochondria by an N-terminally fused mitochondrial targeting sequence abolished the lifespan extension [Fig.C4a-c], indicating a cytosolic activity of the probe.
Because there was no alternative to the roGFP2-Orp1 reporter at that time, no further investigations on this phenomenon have been done in this study. Therefore, it should be kept in mind that the results of the roGFP2-Orp1 reporter may be biased by its own expression.

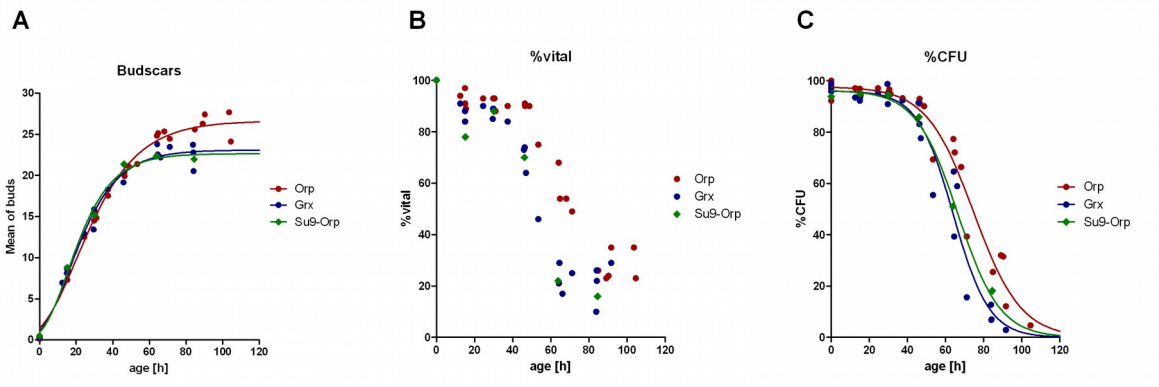

Fig.C4
Replicative aging of WΣ wild type expressing cytosolic roGFP2-Orp1 (red), roGFP2-Grx1 (blue) and the mitochondrial inter membrane space targeted Su9-roGFP2-Orp1 (green). Data from independent experiments are shown. Orp n=4; Grx1 n=4; Su9-Orp n=1
a.) Average number of budscars from the living, single cell population of the culture. The data was fitted by a Gompertz-function to guide the eye
b.) Fraction of living cells determined by roGFP-reporter expression
c.) Colony forming units (CFU) determined by single cell sorting of living cells on YPD plates. Data was fitted with a sigmoidal function to guide the eye

2.1.2 roGFP2-Orp1 reporter

Cells expressing the roGFP2-Orp1 probe were monitored over the aging process. A weak increase in H_2O_2 could be detected. Several biological replicates differ in the amplitude of oxidation but all showed a positive trend [Fig.C5]. Although a more prominent signal has been expected, the data is consistent with the general believe of higher oxidative stress in old cells.

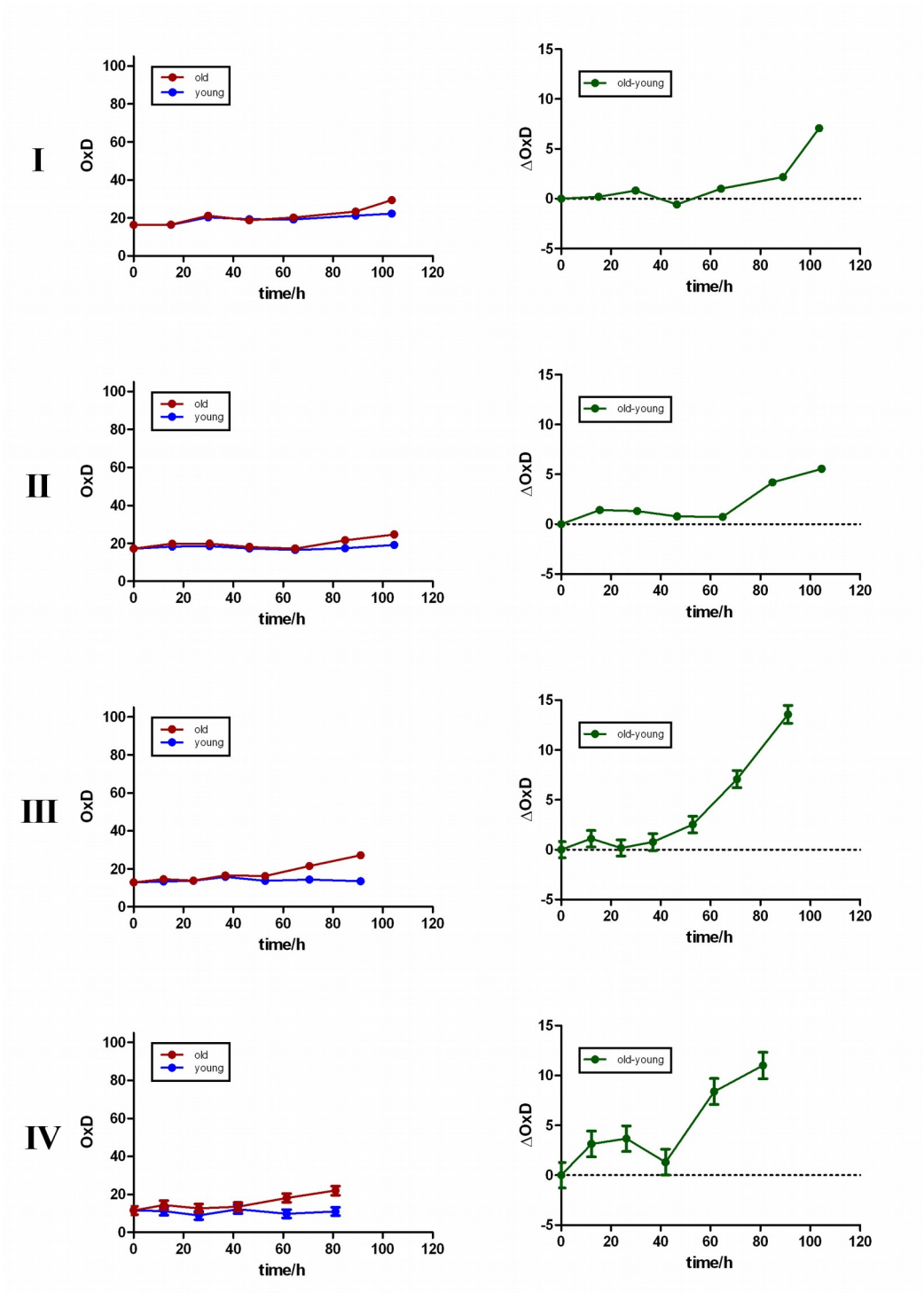

Fig.C5
Measurement of roGFP2-Orp1 in WΣ wild-type cells over their replicative lifespan. Average probe oxidation (left side) of four independent experiments (I-IV) is shown for the old cells (red) and the internal young-cell control (blue). On the right the difference in probe oxidation between young and old cells is plotted (green). Error bars (when available) represent the standard error of repeated probe calibration during the experiment. In graphs without error-bars, the fully oxidized and fully reduced standard was only measured once.

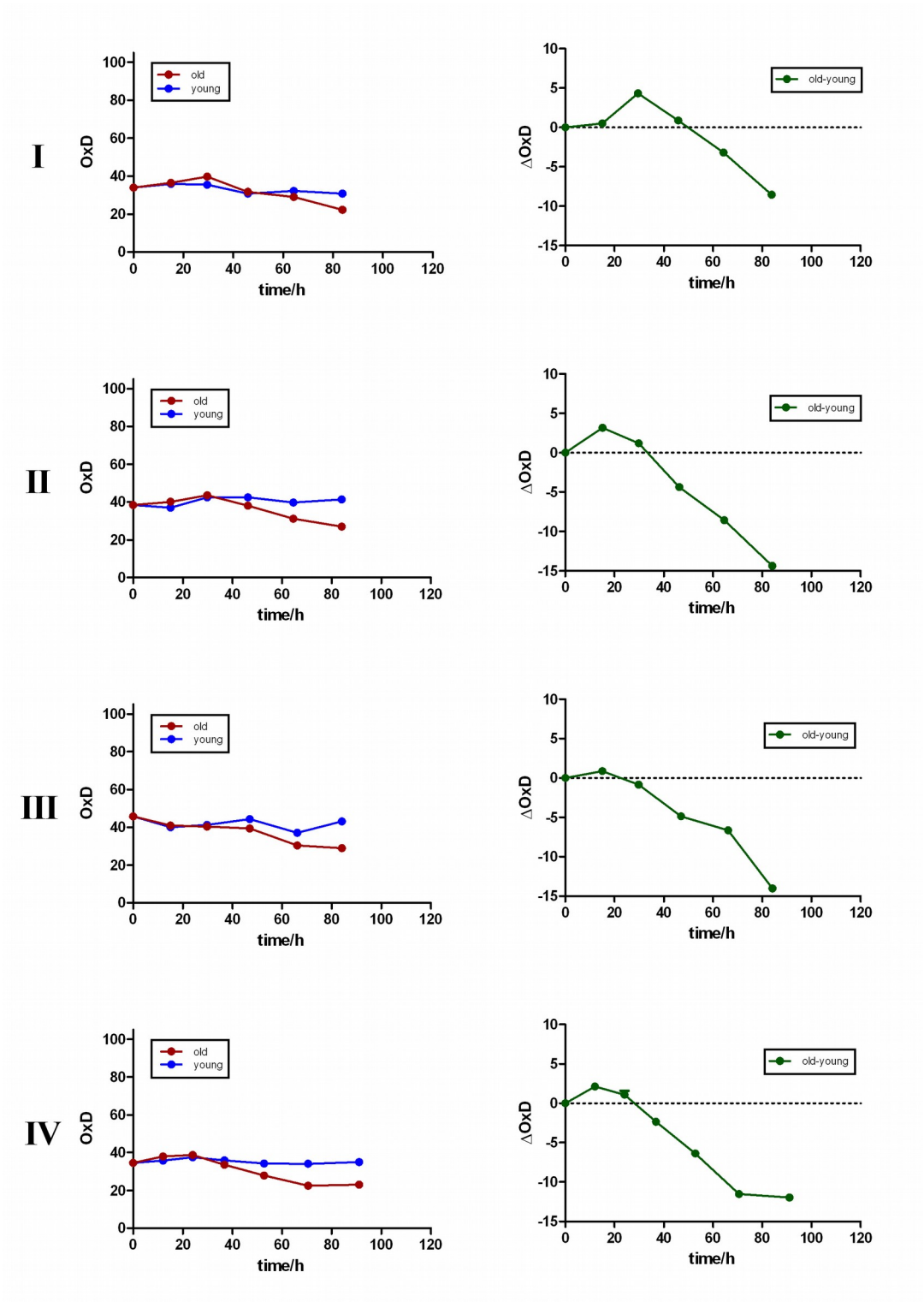

Fig.C6
Measurement of roGFP2-Grx1 in WΣ wild-type cells over their replicative lifespan. Average probe oxidation (left) of four independent experiments (I-IV) is shown for the old cells (red) and the internal young-cell control (blue). On the right the difference in probe oxidation between young and old cells is plotted (green).

2.1.3 roGFP2-Grx1 reporter

Next the roGFP2-Grx1 probe was measured in old cells. Surprisingly, probe oxidation was decreased when cells are getting older. This phenotype was robust in several independent experiments [Fig.C6]. It seems that the cytosolic glutathione-pool creates a more reducing environment in old yeast cells.
To see if the reduction-phenotype is strain specific the experiment was repeated with the mother-enrichment strain Ucc5179 (*see Part A*). To have a proper internal control, the mother enrichment program was not induced so that the offspring is able to rejuvenate. Despite the high rate of petite-cells in this strain background, the reduction phenotype was reproducible for the glutathione reporter already at very early cellular age [Fig.C7a].
However, in contrast to the WΣ-strain, no increase in H_2O_2 could be observed in Ucc5179 using the roGFP-Orp1-reporter [Fig.C7b].

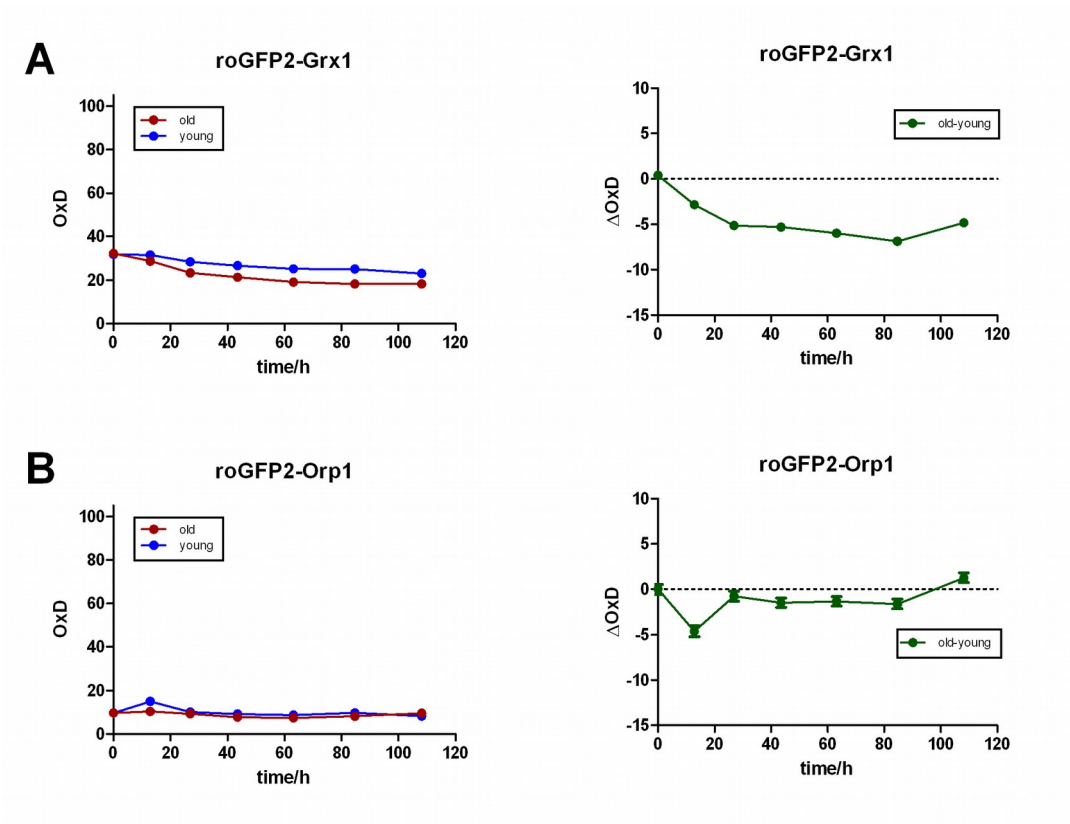

Fig.C7
Replicative aging. Measurement of the redox-reporter. The layout is the same as in [Fig.C5].
a.) Measurement of roGFP2-Grx1 in Ucc5179
b.) Measurement of roGFP2-Orp1 in Ucc5179

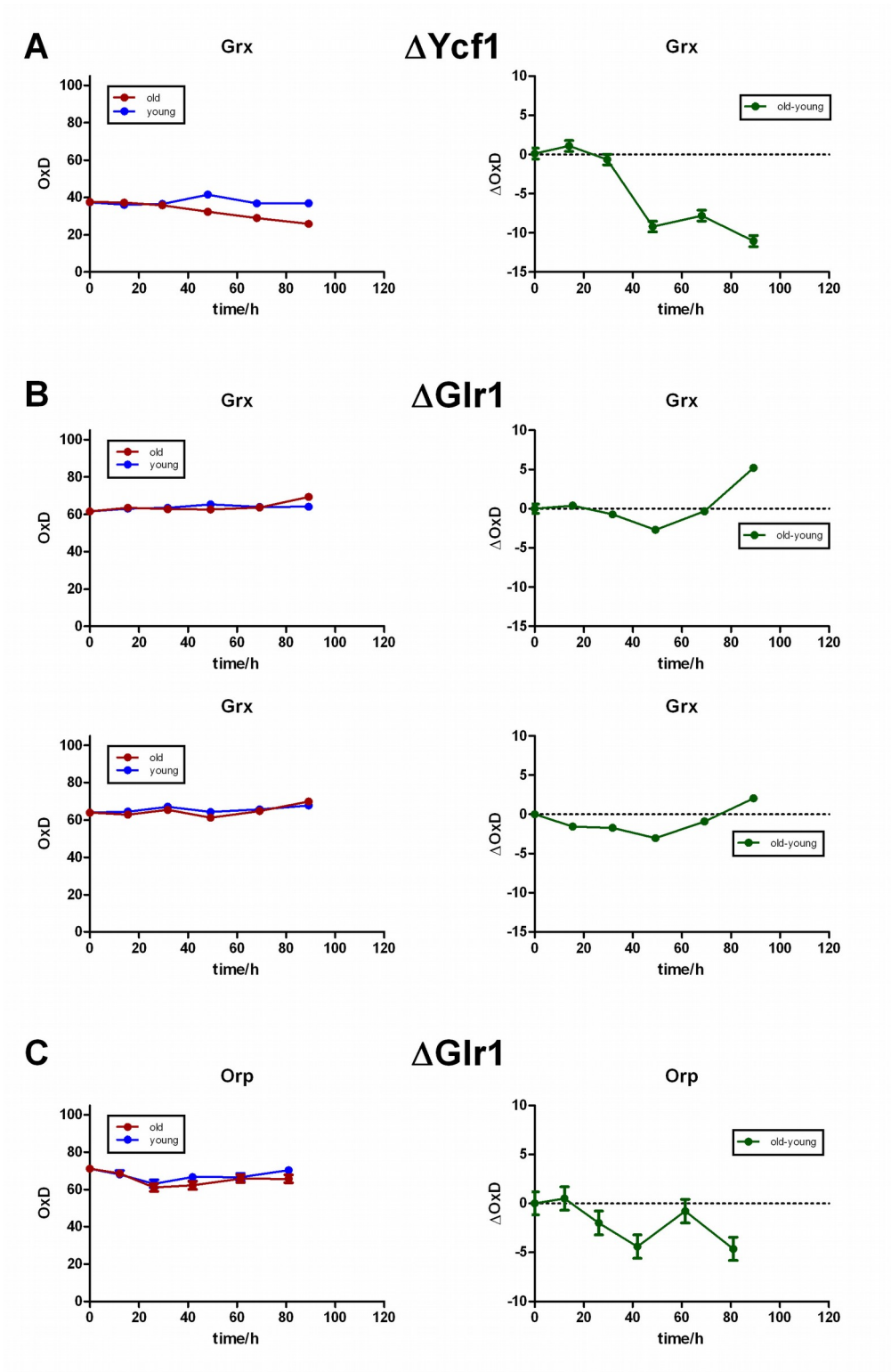

Fig.C8
Replicative aging. Measurement of the redox-reporter. The layout is the same as in [Fig.C5].
a.) Measurement of roGFP2-Grx1 in WΣ Δycf1
b,c.) Measurement of roGFP2-Grx1 in WΣ Δglr1 in two independent experiments.
d.) Measurement of roGFP2-Orp1 in WΣ Δglr1

2.1.4 Glr1 contributes to reduction phenotype

The glutathione redox-buffer is tightly regulated and the oxidized glutathione is rapidly removed from the cytosol. This can be achieved either by sequestering GSSG into the vacuole via the Ycf1-transporter or by reduction to GSH by several reductases from which the glutathione reductase Glr1 is the most efficient and loss of Glr1 leads to severe oxidation of the yeast cytosol (Ayer et al., 2012).
Knockout of Ycf1 had no effect on the age associated glutathione-reduction phenotype [Fig.C8a] so it can be ruled out that GSSG is transported into the vacuole in old cells.
Knocking out the *glr1* gene in contrast showed a much more oxidized cytosol and no distinct reduction during aging – very old cells were even more oxidized compared to the young control [Fig.C8b]. Interestingly the vitality parameters did not differ from the wild-type strain [Fig.C9a-c].

The roGFP2-Orp1 probe was also tested in a *Δglr1* background where the H_2O_2 level was dramatically increased. Here it seems that, at least for the one measurement done, no further H_2O_2 is produced was old cells [Fig.C8c]

Taken together, the data indicates that Glr1 is involved in the age-associated reduction of glutathione.

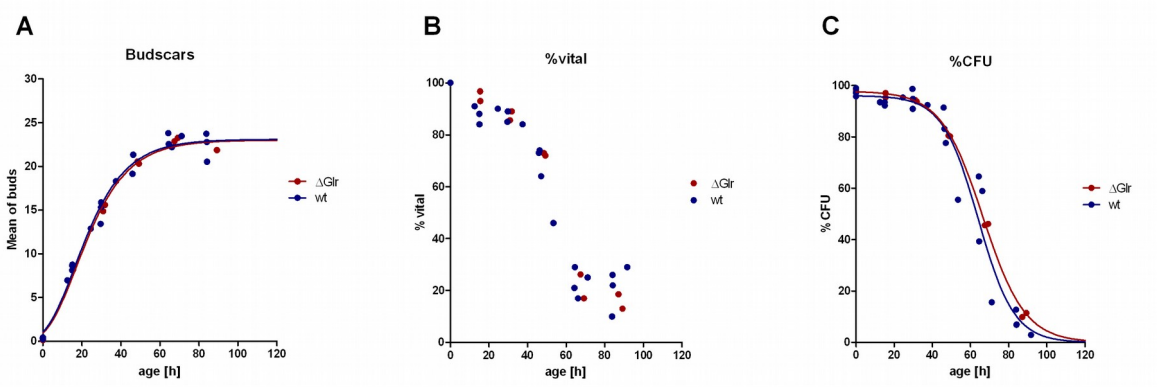

Fig.C9
Replicative aging of roGFP2-Grx1 expressing cells grown in medium with 2% glucose. Comparison of WΣ-wild-type (blue) and WΣ Δglr1 (red).
a.) Average number of budscars of living cells. The data was fitted by a Gompertz function to guide the eye
b.) Fraction of living cells determined by roGFP-reporter expression
c.) Colony forming units (CFU) determined by single cell sorting of living cells on YPD plates. Data was fitted with a sigmoidal function to guide the eye

2.1.5 Caloric restriction

Limiting the amount of glucose in the growth-medium is a condition, which promotes longevity in nearly all organisms (Roth and Polotsky, 2012). To see whether the onset of the glutathione reduction is delayed when cells live longer, an aging experiment was performed in low-glucose medium (0.1% instead of 2%). Unexpectedly, WΣ showed no increase in mean budscar number (replicative longevity) under this condition [Fig.C10a]. In contrast, the percentage of living

cells was slightly increased [Fig.C10b] and counter intuitively also the fraction of colony forming cells was increased [Fig.C10c]. A slower division rate especially in very old cells might delay the onset of cell death which would shift the survival curves to later time-points without significantly changing the mean of budscars. However, a minor replicative longevity effect is not ruled out. There may still be an effect if one could extend the experiment by enriching cells of later time-points.
The age associated glutathione reduction phenotype remaind robust in the low glucose medium [Fig.C11].

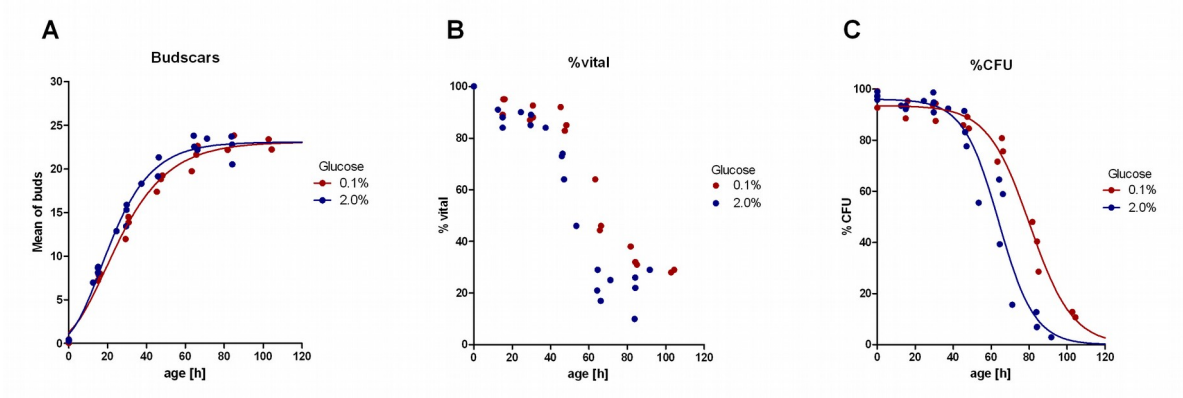

Fig.C10
Replicative aging of WΣ wild-type, comparing roGFP2-Grx1 expressing cells grown in medium with 2% glucose (blue) and in 0.1% glucose (red). The layout is the same as in [Fig.C4]. Data from independent experiments are shown. 2% glucose n=4; 0.1% glucose n=3.
a.) Average budscars of living cells
b.) Percentage of living cells
c.) Colony forming units of living cells (F-test: $p=5.2*10^{-9}$)

Because the knockout library was done in the S288C and not in the W303 background, most aging assays had been done in BY4741 and BY4742. There are studies where W303 is reported to be susceptible to lifespan extension by caloric restriction (Lamming et al., 2006) but also reports where no longevity was observed (Kaeberlein et al., 2006). It may well be that several branches of this strain exist or that the cells are influenced by my aging assay. Because of time constrains and priority issues the control experiments (testing caloric restriction on BY4741 with my assay and WΣ with dissection) have not been performed so far.

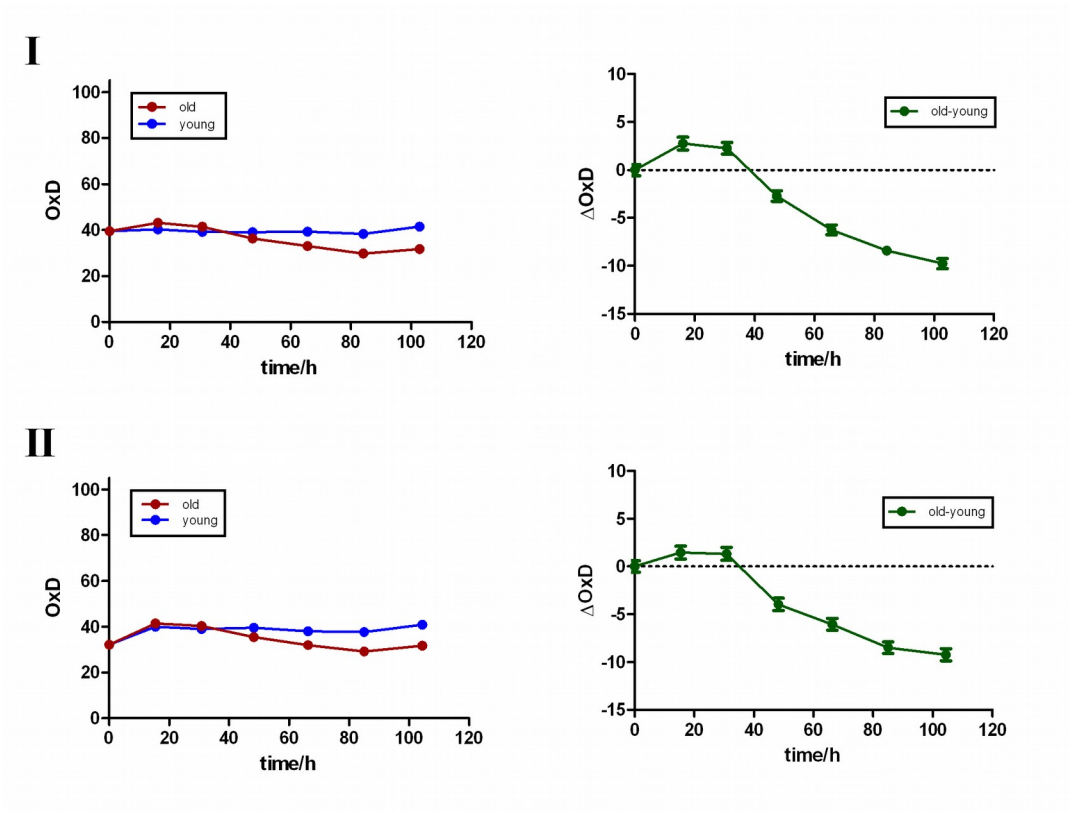

Fig.C11
Replicative aging. Measurement of roGFP2-Grx1 in WΣ wild-type cells under caloric restricted conditions (medium with 0.1% glucose). Two independent experiments are shown (I, II). The layout is the same as in [Fig.C5].

2.1.6 Longevity in Δfob1

To test whether lifespan extension with WΣ can be seen at all in my aging assay, a knockout of the replication-fork blocker Fob1 was created in WΣ, which is a known longevity mutation (Defossez et al., 1999). Indeed, the *Δfob1*-cells showed a significant lifespan extension seen by the average number of budscars [Fig.C12a] (see also [Table C1]) and the colony forming assay [Fig.C12c]. On the other hand, the fraction of living cells resembled the wild-type [Fig.C12b], which indicates that *Δfob1*-cells have no extended post-replicative lifespan.
Glutathione homeostasis measured by the roGFP2-Grx1 reporter did not differ from wild-type cells [Fig.C13].

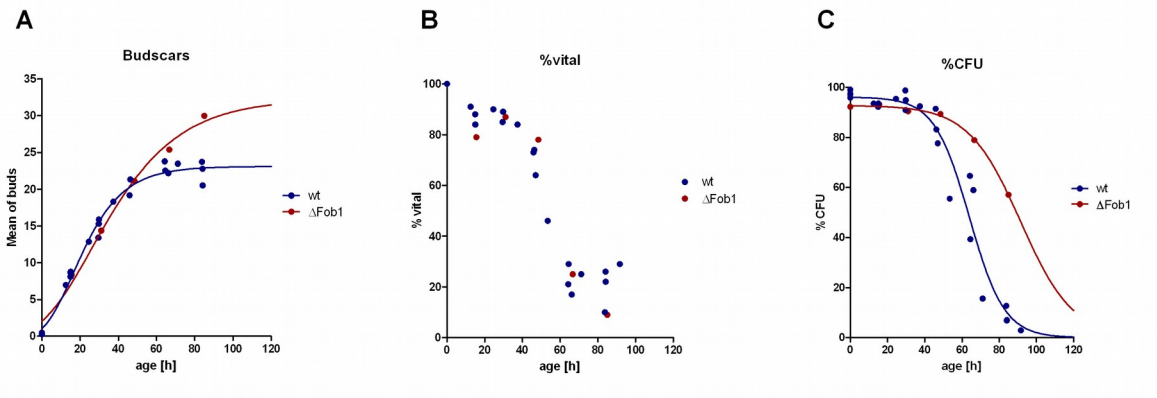

Fig.C12
Replicative aging of WΣ cells expressing roGFP2-Grx1, comparing wild-type (blue) with Δfob1 (red). The layout is the same as in [Fig.C4]. Data from independent experiments are shown; wild-type n=4; Δfob1 n=1
a.) Average budscars of living cells
b.) Percentage f living cells
c.) Colony forming units of living cells

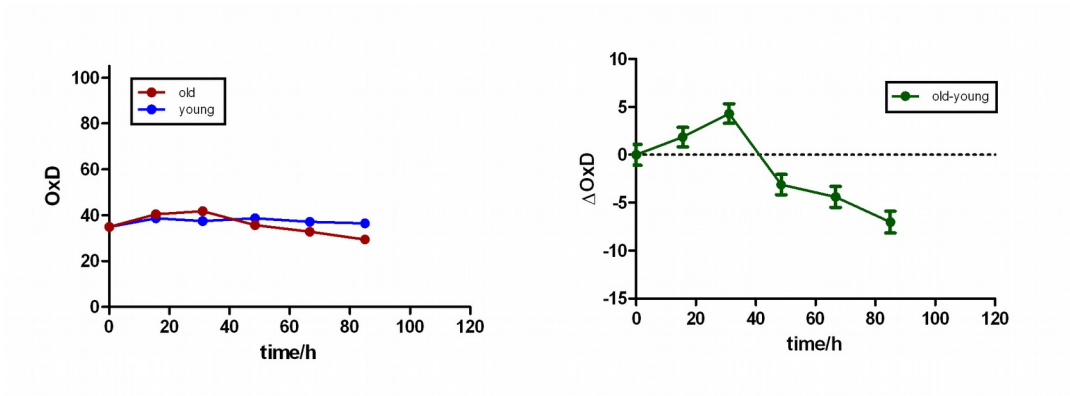

Fig.C13
Replicative aging. Measurement of roGFP2-Grx1 in WΣ Δfob1 cells. The layout is the same as in [Fig.C5].

2.1.7 Restoration of Ybp1 in WΣ

When WΣ was created, the objective of my work was the study of Hsp90 and its co-chaperones. As the project changed I missed the fact that W303 harbors a critical mutation in the *ybp1*-gene, which abrogates the activation of the main redox-transcription factor Yap1 (Veal et al., 2003) by the redox-sensor Gpx3 (*also known as Hyr1 or Orp1, see discussion*). To rule out that the phenotypes I observed are due to this defect, I restored the defective *ybp1-1* allele with the wild-type *ybp1* allele from BY4741. The repaired strain was called W2Σ. Overexpression of the wild-type ybp1 in young WΣ or W2Σ cells did not show any effect on the roGFP2 reporter [Fig.C14a-b].

The response of the roGFP2-Grx1 and roGFP2-Orp1-reporter was tested in W2Σ during aging and found to be comparable to WΣ [Fig.C15a,b].

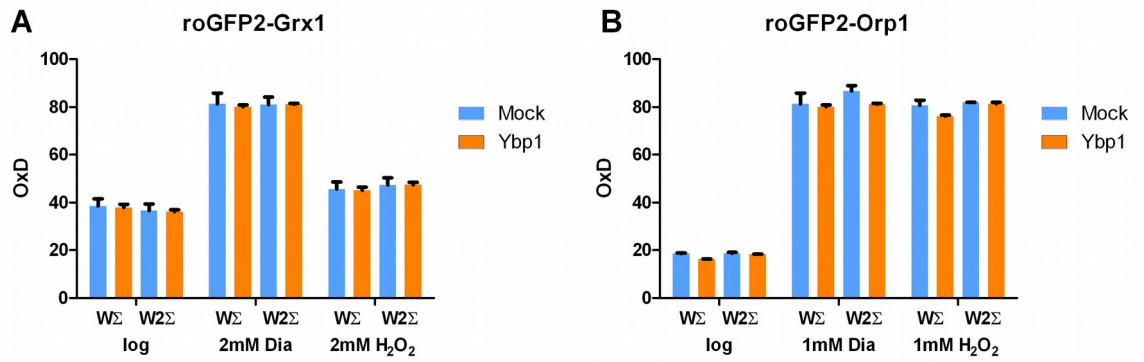

Fig.C14
Overexpression of Ybp1. Comparing WΣ with W2Σ transformed with pRS425-ybp1 (orange) or mock transformed (blue). Cells were either measured untreated (log), oxidized by diamide (Dia) or after treatment with H_2O_2.
a.) Cells expressing roGFP2-Grx1. Error bars represent the SEM from three separate clones.
b.) Cells expressing roGFP2-Orp1. Error bars represent the SEM from two separate clones.

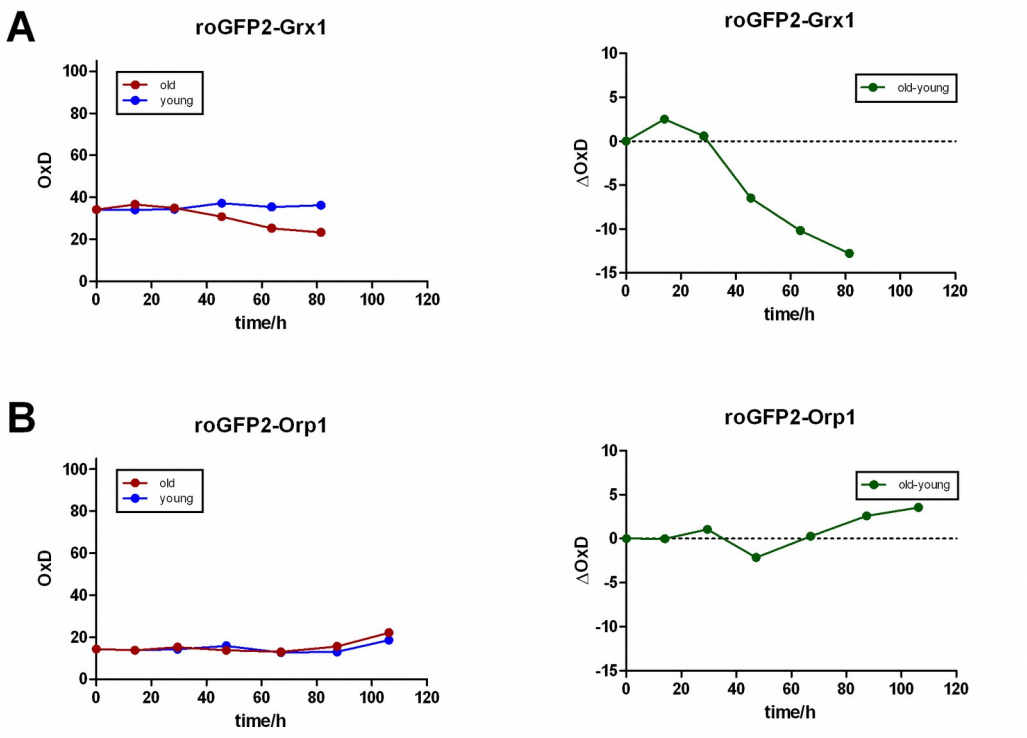

Fig.C15
Replicative aging in W2Σ cells. The layout is the same as in [Fig.C5].
a.) Measurement of roGFP2-Grx1
b.) Measurement of roGFP2-Orp1

Strangely the W2Σ strain seems to show a reduced replicative lifespan compared to WΣ [Fig.C16a,d]. For roGFP2-Grx1 expressing cells the difference was not significant (F-test with P=0.093) but for the roGFP2-Orp1 expressing cells the effect was more prominent (F-test with $P=2.3*10^{-4}$).

Noteworthy, the lifespan extension by expression of the roGFP2-Orp1 probe can also be seen in the W2Σ background [Table C1] defined by the "a"-parameter of the Gompertz function [Equation D1].

Table C 1 – Average number of budscars determined by a Gompertz fit-function

	roGFP2-Grx1	roGFP2-Orp1
WΣ	23.09±0.48	26.64±0.477
W2Σ	20.73±0.745	22.61±0.632
WΣ Δfob1	32.28±2.72	n.d.

The fraction of living cells in the W2Σ background however, seems to be slightly increased for both reporters [Fig.C16b,e], whereas no difference could be seen in the colony forming assay [Fig.C16c,f].
The vitality parameters can be interpreted in that way that W2Σ arrests at lower budscar-numbers and cannot divide anymore, but stays viable for a longer time in this state. Since the correct *ybp1*-locus in W2Σ was confirmed by sequencing, the strain may have acquired a mutation elsewhere in the genome or WΣ was already adapted to the corrupted *ybp1-1* allele and restoration interferes with this adaptation. The fact that roGFP2-Orp1 can extend lifespan already in WΣ argues for the adaptation hypothesis. Addressing these questions however, would be part of a different study.

I also wanted to test if the mother enrichment strain Ucc5179 also harbors a wild-type allele of ybp1. Unfortunately, the locus seems to have severe sequence alterations as it was not possible to amplify the gene by PCR with the primers used for BY4741.

Taken together, the defective *ybp1-1* allele in WΣ does not seem to contribute to the age associated glutathione reduction phenotype and the previous results remain valid.

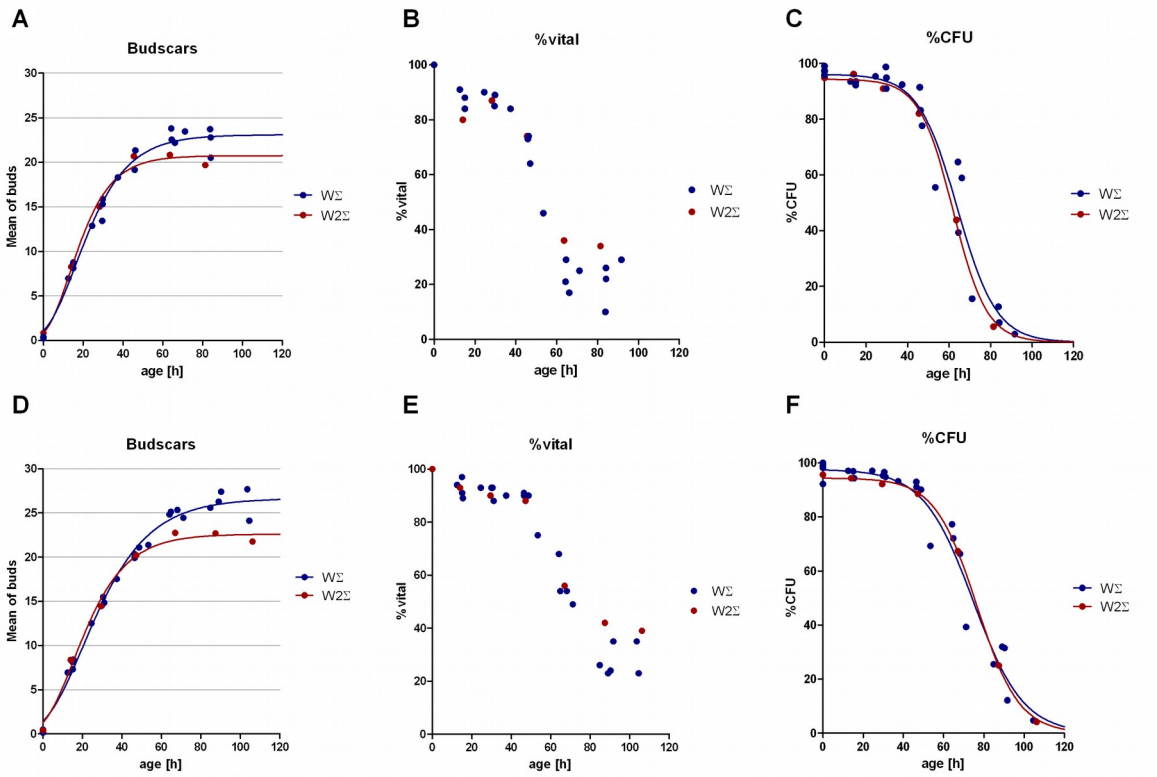

Fig.C16
Replicative aging of WΣ and W2Σ. The layout is the same as in [Fig.C4]. Data from independent experiments are shown.
a-c.) Measurement of roGFP2-Grx1 (WΣ n=4; W2Σ n=1)
a.) Average budscars of living cells
b.) Percentage of living cells
c.) Colony forming units of living cells
d-f.) Measurement of roGFP2-Orp1 (WΣ n=4; W2Σ n=1)
d.) Average budscars of living cells
e.) Percentage of living cells
f.) Colony forming units of living cells

2.2 Redox-homeostasis – respiratory growth

Unlike most of the higher organisms, yeast preferentially uses a fermentative energy metabolism while glucose is available and the respiratory chain becomes dispensable under those conditions. Supplemented with glucose, cells can survive without mitochondrial DNA as petite cells. The contribution of mitochondrial reactive oxygen species during fermentative growth should therefore be negligible. To see how the redox-state changes during aging when mitochondria are active, yeast was grown on glycerol/ethanol-medium, which forces them to respire.

An initial experiment on young cells showed that the cytosol becomes more reducing while grown in glycerol/ethanol-medium, seen by the response of both the roGFP2-Grx1 and roGFP2-Orp1 reporter [Fig.C17a,b].

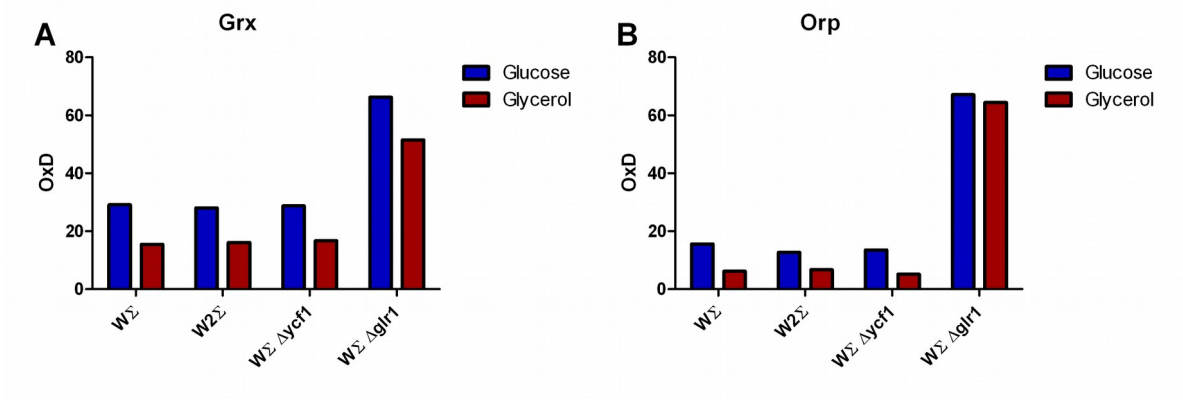

Fig.C17
Redox probe oxidation under fermentative (glucose) and respiratory conditions (glycerol) in different strain backgrounds.
a.) Measurement of roGFP2-Grx1
b.) Measurement of roGFP2-Orp1

2.2.1 Lifespan & viability in glycerol

Forcing yeast cells to respire in glycerol/ethanol-medium slows down the division rate by a factor of about 1.8 seen by the increase of budscars over time as compared to experiments in glucose. Interestingly, lifespan was prolonged under respiratory conditions, seen by the average budscars, the percentage of living cells and the colony-formation [Fig.C18a-c].

For the glycerol condition both wild-type and *Δglr1* cells expressing the roGFP2-Grx1 and the roGFP2-Orp1 reporters were compared by their vitality parameters [Fig.C19]. First it can be seen that roGFP2-Orp1 expression slowed down the division rate compared to roGFP2-Grx1 expressing cells but also raised the vitality parameters of the culture. The second conclusion, which can be drawn from these data, is that the Glr1 knockout has no influence on lifespan under respiring conditions.

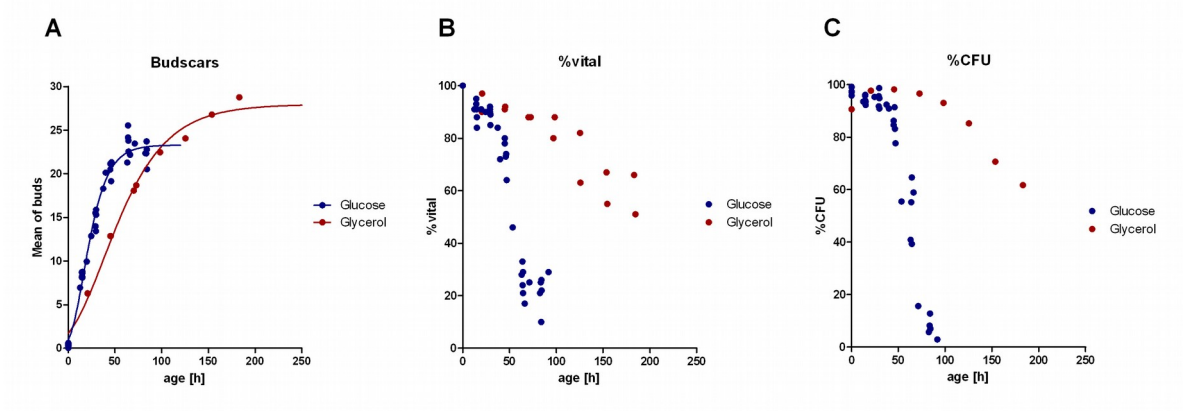

Fig.C18
Replicative aging of WΣ wild-type cells under fermentative (blue) and respiratory conditions (red). The layout is the same as in [Fig.C4]. Data from independent experiments are shown.
a.) Average budscars of living cells (glucose n=8; glycerol n=2)
b.) Percentage of living cells (glucose n=8; glycerol n=2)
c.) Colony forming units of living cells (glucose n=8; glycerol n=1)

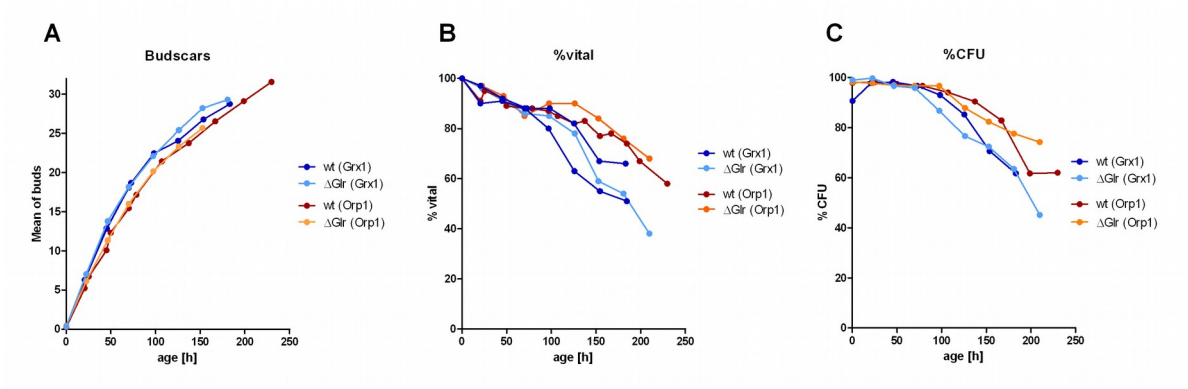

Fig.C19
Comparing vitality parameters of replicatively aging WΣ cells under respiratory conditions. Data from partially parallel-experiments are shown.
a.) Average budscars of living cells
b.) Percentage of living cells
c.) Colony forming units of living cells

Only very few papers are published reporting replicative aging on glycerol-medium (Kirchman and Botta, 2007), most likely due to the high petite-rates of the common laboratory strains, which would lead to growth-arrest of respiratory deficient cells in this medium. Indeed, aging with Ucc5179 did not show any lifespan extension for the budscars in glycerol/ethanol [Fig.C20a, c] in concordance with its high rate of petite production. The percentage of living cells is not shown because the population of dead cells was ambiguous in some experiments. However, the data obtained from this strain seems to contain an internal contradiction which will be discussed in the supplements.

I have to emphasize that the lifespan extension by glycerol was only addressed by my aging setup. To really prove that this is not due to a decreased lifespan of glucose grown cells in my assay a classical lifespan experiment with a micromanipulator needs to be done.

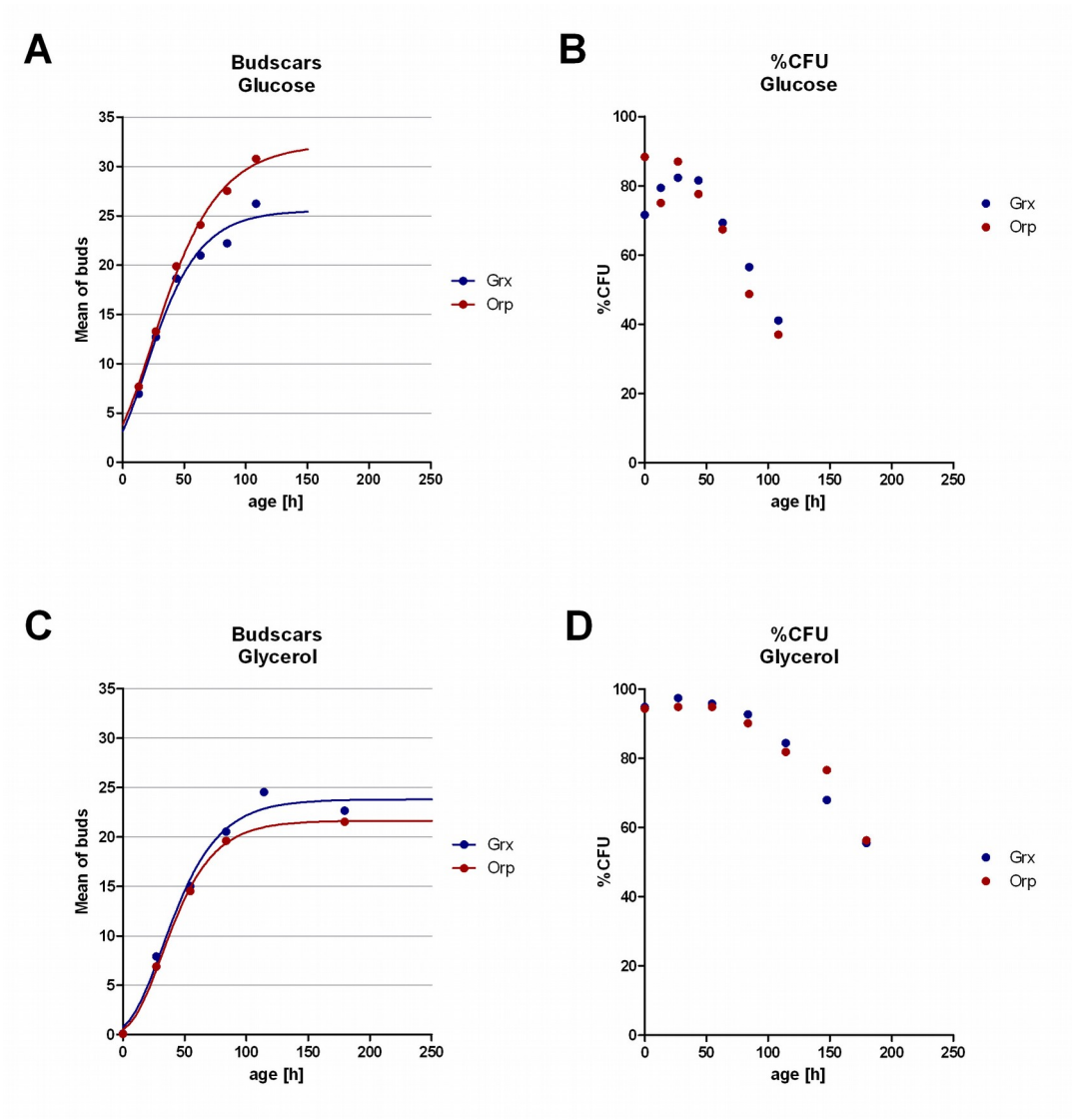

Fig.C20
Replicative aging of Ucc5179 cells expressing roGFP2-Grx1 (blue) or roGFP2-Orp1 (red). The budscar data was fitted by a Gompertz function to guide the eye.
a.) Average budscars of living cells grown under fermentative conditions
b.) Colony forming units of living cells grown under fermentative conditions
c.) Average budscars of living cells grown under respiratory conditions
c.) Colony forming units of living cells grown under respiratory conditions

2.2.2 Redox measurements during respiration

A roGFP2-Orp1 expressing yeast culture was aged in glycerol/ethanol-medium and its oxidation was monitored. In contrast to cells grown in glucose [compare Fig.C5] the cytosol of old cells became quickly oxidized and then stayed at a constant level [Fig.C21].

By looking at the roGFP2-Grx1 probe a striking difference between glucose [compare Fig.C6] and glycerol/ethanol grown cells became apparent [Fig.C22]. Here cells started more reduced but then became more oxidized when getting older.

One experiment was conducted measuring both roGFP2-Orp1 and roGFP2-Grx in a *Δglr1* background in glycerol/ethanol medium. In contrast to cells grown in glucose [compare Fig.C8b-c] a strong oxidation of old cells could be seen both in the roGFP2-Orp1 and roGFP2-Grx1 reporter adding up to the already highly oxidized basal level [Fig.C23a,b]. Similar to the growth on glucose, vitality parameters of the Δglr1 cells showed no difference to the wild type strain [Fig.C24a-c].

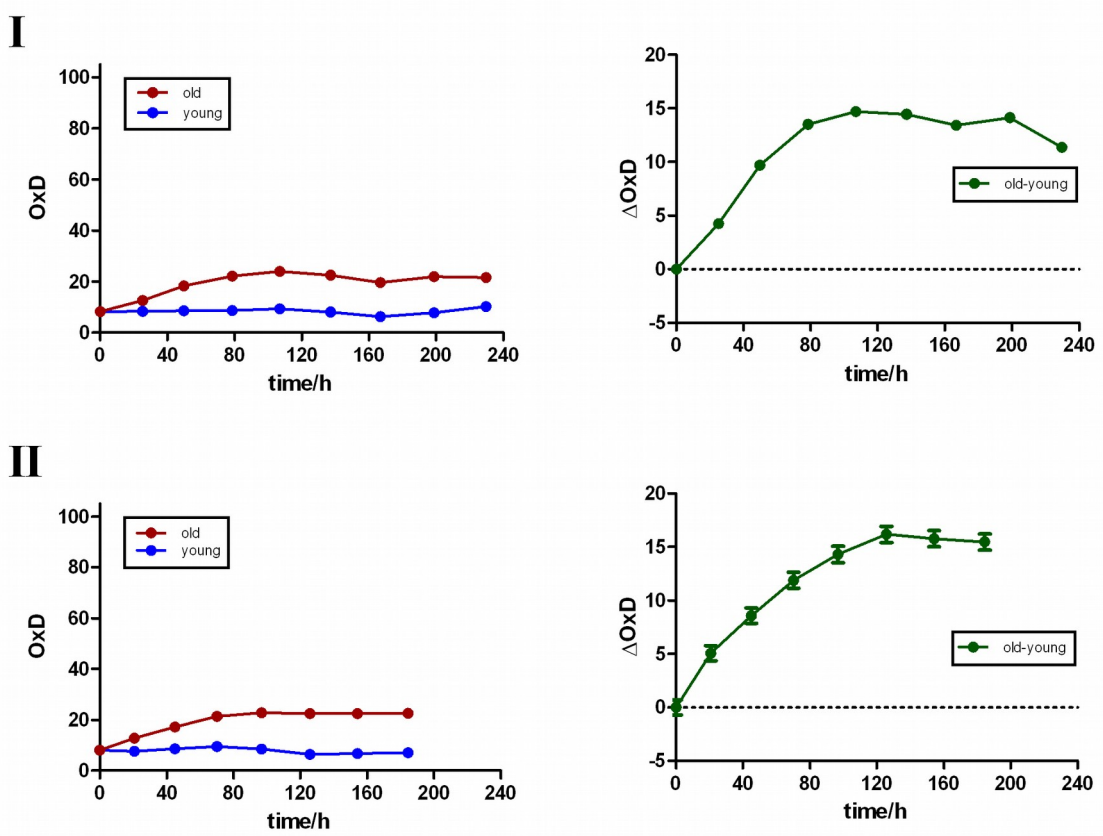

Fig.C21
Replicative aging. Measurement of roGFP2-Orp1 in WΣ wild-type cells under respiratory conditions. Two independent experiments are shown (I, II). The layout is the same as in [Fig.C5].

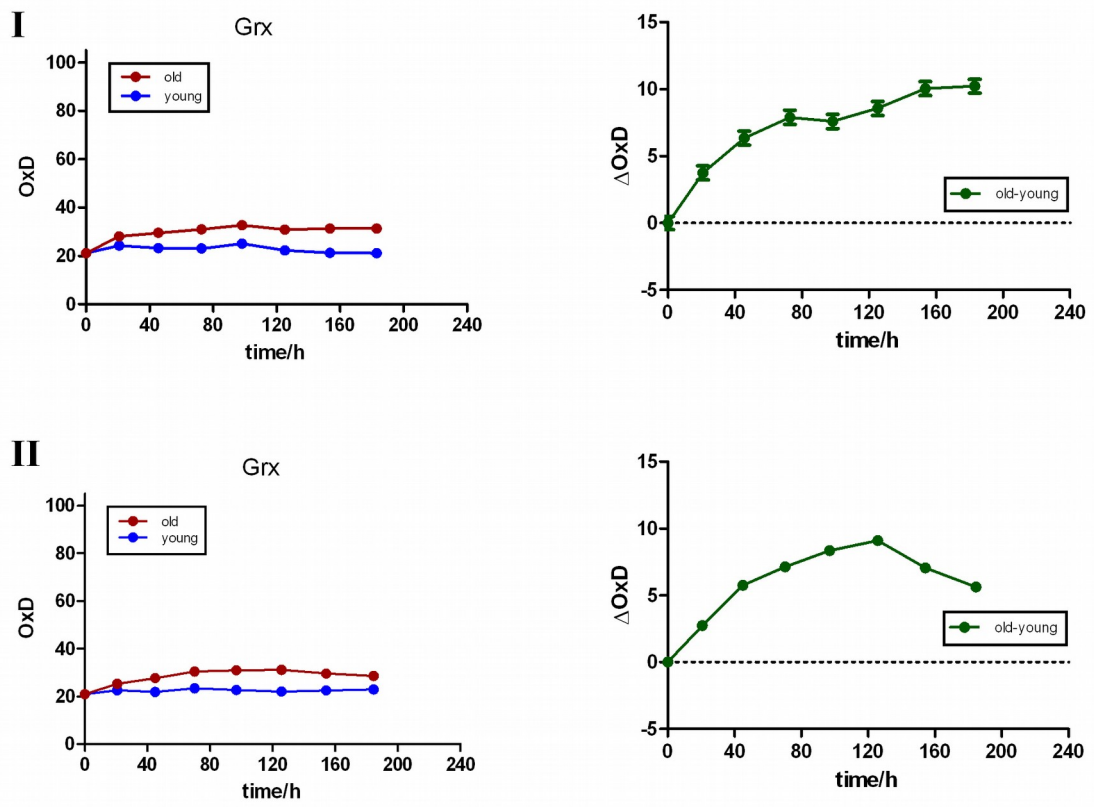

Fig.C22
Replicative aging. Measurement of roGFP2-Grx1 in WΣ wild-type cells under respiratory conditions. Two independent experiments are shown (I, II). The layout is the same as in [Fig.C5].

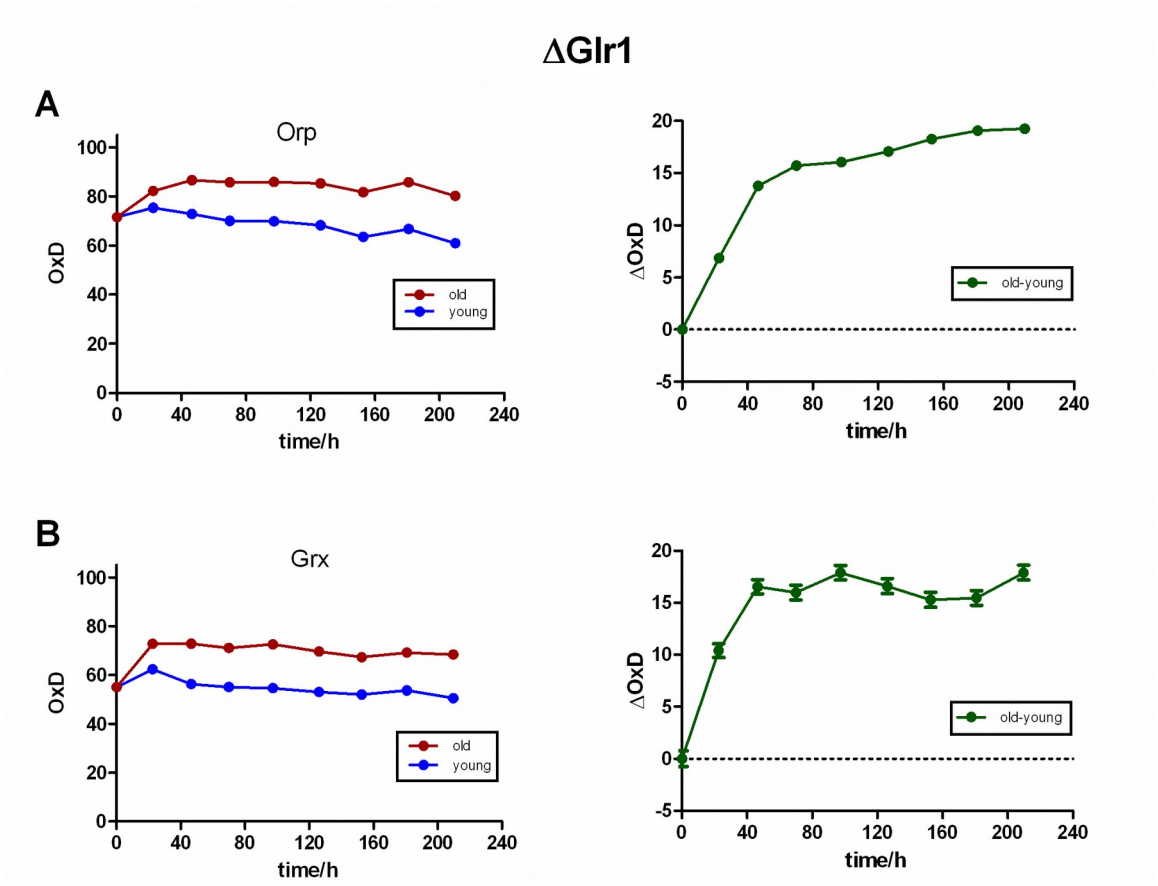

Fig.C23
Replicative aging in WΣ cells deleted for Glr1 under respiratory conditions. The layout is the same as in [Fig.C5].
a.) Measurement of roGFP2-Orp1
b.) Measurement of roGFP2-Grx1

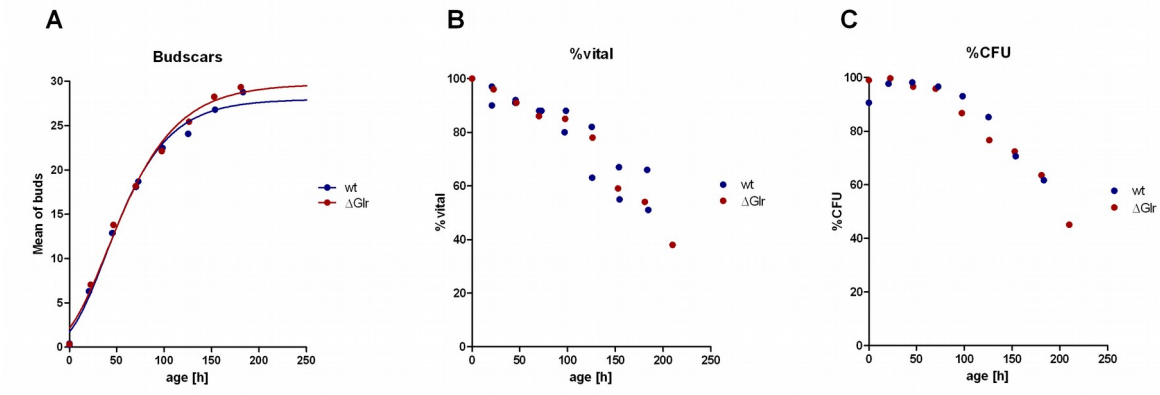

Fig.C24
Replicative aging of roGFP2-Grx1 expressing cells grown in glycerol/ethanol medium. Comparing WΣ-wild-type (blue) and WΣ Δglr1 (red).
a.) Average number of budscars of living cells. The data was fitted by a Gompertz function to guide the eye
b.) Fraction of living cells determined by roGFP-reporter expression
c.) Colony forming units (CFU) determined by single cell sorting of living cells on YPD plates.

2.3 pH-Measurements in old cells

2.3.1 A general comment on pH and redox potential

The roGFP2-Grx1 reporter is able to measure the ratio between oxidized and reduced glutathione, which can be transformed into a glutathione-potential. This potential is normally calculated for standard conditions, i.e. pH 7 and 293.15 K. For a different pH the redox-potential can be corrected by using *Equation (3)*. The pH dependency of the electrochemical redox-potential is depicted in [Fig.C25]. To determine the chemical redox potential of the glutathione-pool in old cells, it is therefore essential also to determine the pH. To do so, I made use of a pH-sensitive GFP-reporter also known as pHluorin (Miesenböck et al., 1998). This reporter can be measured with the same fluorescent configuration as the roGFPs, which unfortunately makes it impossible to access both reporters in the same cell. The ratio of fluorescence by two different excitations can then be transformed into a pH using a standard curve, which can be determined independently.

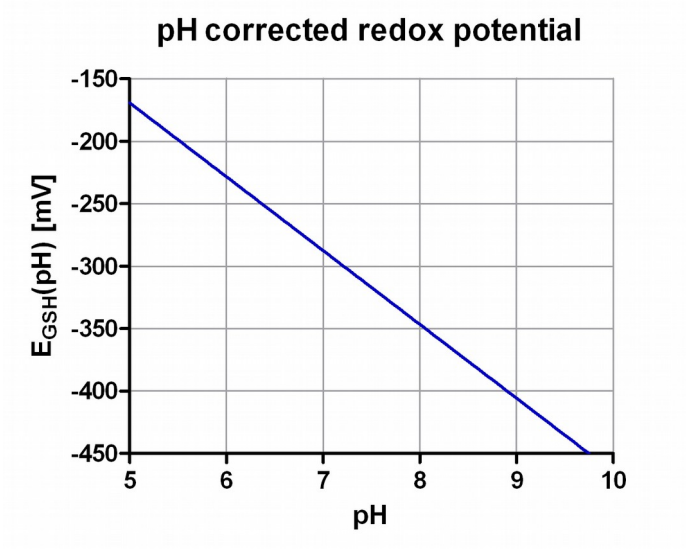

Fig.C25
Calculation of the redox potential for the 2GSH:GSSG couple corrected for the pH

2.3.2 Acidification in old cells (Fermentation)

Measurement of the pHluorin reporter showed a strong acidification in old cells starting at around 45 h of aging [Fig.C26a,b]. Single-cell data seem to reveal two populations - one with a low pH and the other with a pH similar to young cells. The latter becomes less abundant the older the cells get. Knockout of the Glr1-gene had no influence on the pH-phenotype demonstrated by differentially tagged cells grown in the same culture [Fig.C26c].

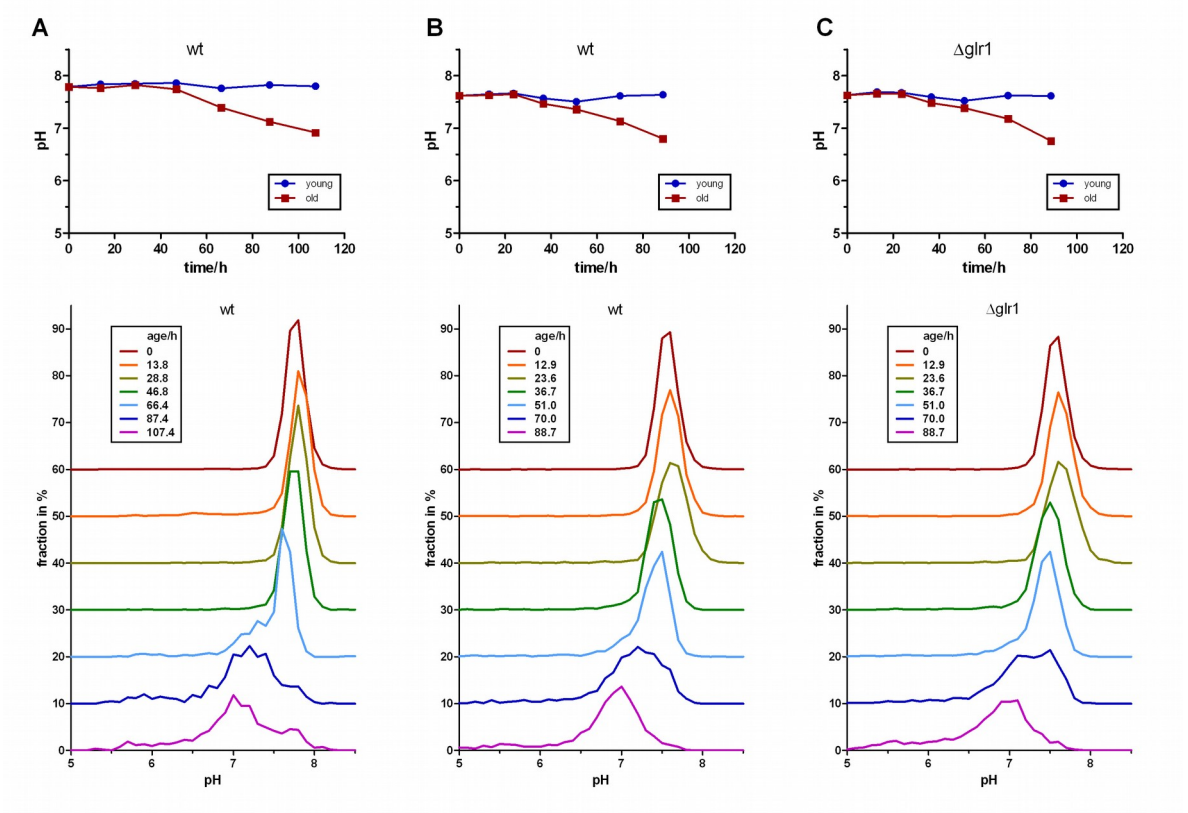

Fig.C26
Replicative aging of WΣ cells expressing the pHluorin reporter. In the upper panels the average pH of the population is shown for the old cells (red) and the young cells (blue) in the culture over their replicative lifetime. The lower panels show histograms of the pH distribution in the old population at the indicated time-points (inset).
a, b) Measurement of the pH in WΣ wild-type cells in two independent experiments.
c.) Measurement of the pH in WΣ-Δglr1

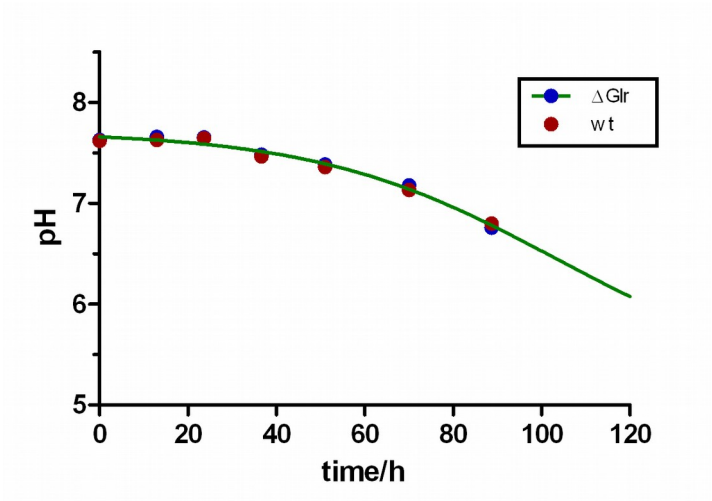

Fig.C27
Sigmioidal fitting (green) of average pH development in WΣ wild-type (red) and Δglr1 (blue) during replicative aging. The fit parameters were used to exemplarily calculate a pH-corrected redox-potential in [Fig.C28].

2.3.3 pH corrected redox-potential

As mentioned above, the roGFP-Grx1-probe cannot detect pH-changes. If one would assume a constant $[GSH]^2/[GSSG]$ ratio over the yeasts lifetime, the cytosol will get strongly oxidized when the pH goes down in old cells. By correcting the glutathione-potential of [Fig.C6-IV] and [Fig.C8b] with the pH, approximated by a sigmoidal fit of the data from [Fig.C26a,c] – the fitting is shown in [Fig.C27], it can clearly be seen that the absolute electrochemical potential would completely be dominated by the cellular pH [Fig.C28-I,II].

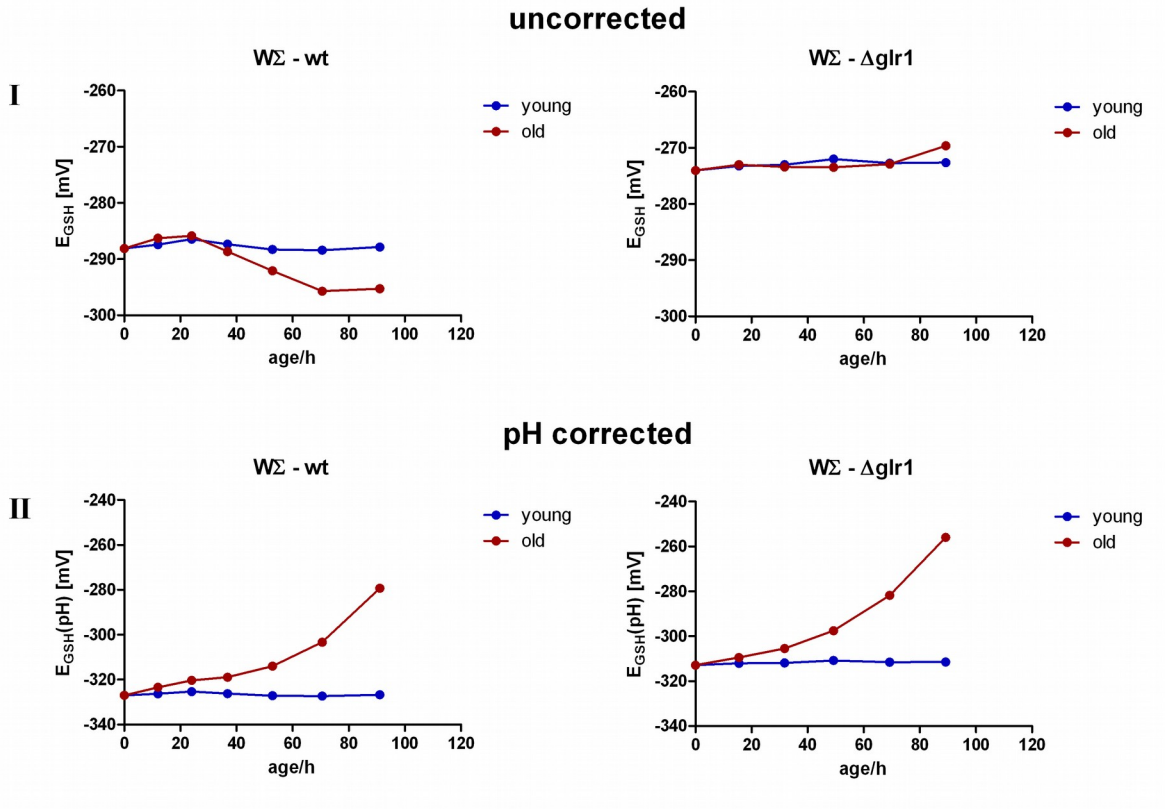

Fig.C28
Glutathione redox-potential during replicative aging for WΣ wild-type (left) and WΣ-Δglr1 (right) as calculated for standard conditions (I) or pH-corrected (II) with parameters obtained from [Fig.C27].

2.3.4 Acidification in old cells (Respiration)

Cells grown in glycerol/ethanol-medium were found to have a slightly decreased steady-state pH compared to the growth in glucose-medium and the knockout of Glr1 had no effect on the pH under both conditions [Fig.C29]. To see whether the pH is changing in old cells, an aging experiment was planed. Unfortunately, the flow-cytometric sorter then entered a phase of continued technical problems, which made it impossible to finalize the project. The measurement of the pH in old cells under respiratory conditions therefore remains to be done.

Fig.C29
Measurement of the steady state pH with the cytosolic pHluorin probe in glucose and glycerol containing medium for WΣ wild-type (green) and WΣ Δglr1 (blue).

3 Kinetics Measurements in Replicative Aging

3.1 A general comment on kinetics measurements

A constant steady-state level of a regulated parameter could either mean that there is no change in the observed parameter at all or that there are regulatory processes which hold the parameter constant. In the latter case a change in adaptation to stress may reveal changes in the regulatory processes. To see whether this is the case in aging yeast cells, the redox-reporters were tested under oxidant treatment. Because centrifugation of an aliquot from the logarithmic culture and removing supernatant would lead to a considerable loss of old cells due to weak pelleting, it was not possible to perform recovery measurements. Instead, the dynamics of adaptation by the addition of the oxidant was recorded, allowing measurements directly from the undisturbed logarithmic culture.

3.2 roGFP2-Orp1 Reporter-Kinetics

3.2.1 H_2O_2-shocks seen by roGFP2-Orp1

3.2.1.1 Fermentative growth

For shock-experiments aliquots of the fermentative grown aging culture were taken and oxidant was added directly to the medium. With a delay of about 10 seconds kinetics could be acquired by flow-cytometry. Note the different density of the data points in the kinetics is the result of an adjusted sample flow. This was done to monitor fast changes with higher resolution and prevent wasting sample on phases with little changes.

Adding 1 mM H_2O_2 to roGFP2-Orp1 expressing cells leads to a rapid probe oxidation reaching equilibrium after about 500 seconds [Fig.C30]. The numbering of the measurements corresponds to the age of the culture where M0 is the logarithmic starter culture and higher numbers are measurements of the aged culture separated by at least 12h. To guide the eye, the

data was fitted with a two-phase exponential. The steady-state oxidation of old cells is represented by the dashed grey line. Since it was not possible to record the kinetics of old and young cells in parallel (the relative abundance of young:old could go up to 1000:1), the saturated signal of the young cells was recorded at the end of the old-cell kinetic and used to compare the plateaus. Steady-state and saturated values for the young cells from the culture are given as dashed green lines.

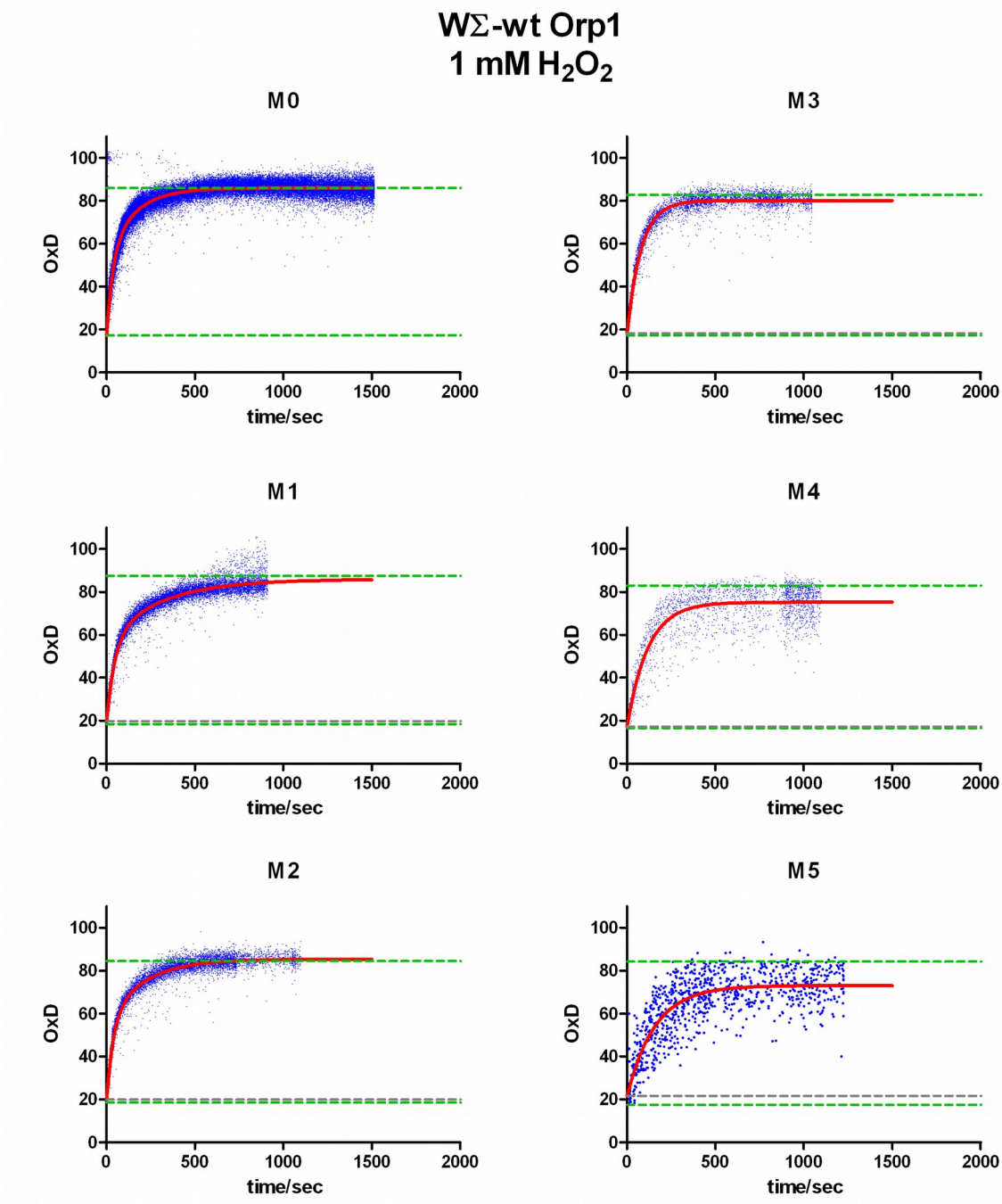

Fig.C30
Replicative aging in glucose medium. Kinetics of roGFP2-Orp1 oxidation in WΣ wild-type upon addition of 1 mM H_2O_2. The graphs represent measurements at the different stages of the aging process (M0 is a logarithmic young culture, M5 are the oldest cells measured). Double exponential fittings were performed to guide the eye. Green dashed lines show the basal reporter oxidation and the maximal oxidation after peroxide treatment for the internal young cell-control. Grey dashed lines show the basal oxidation of the old cells.

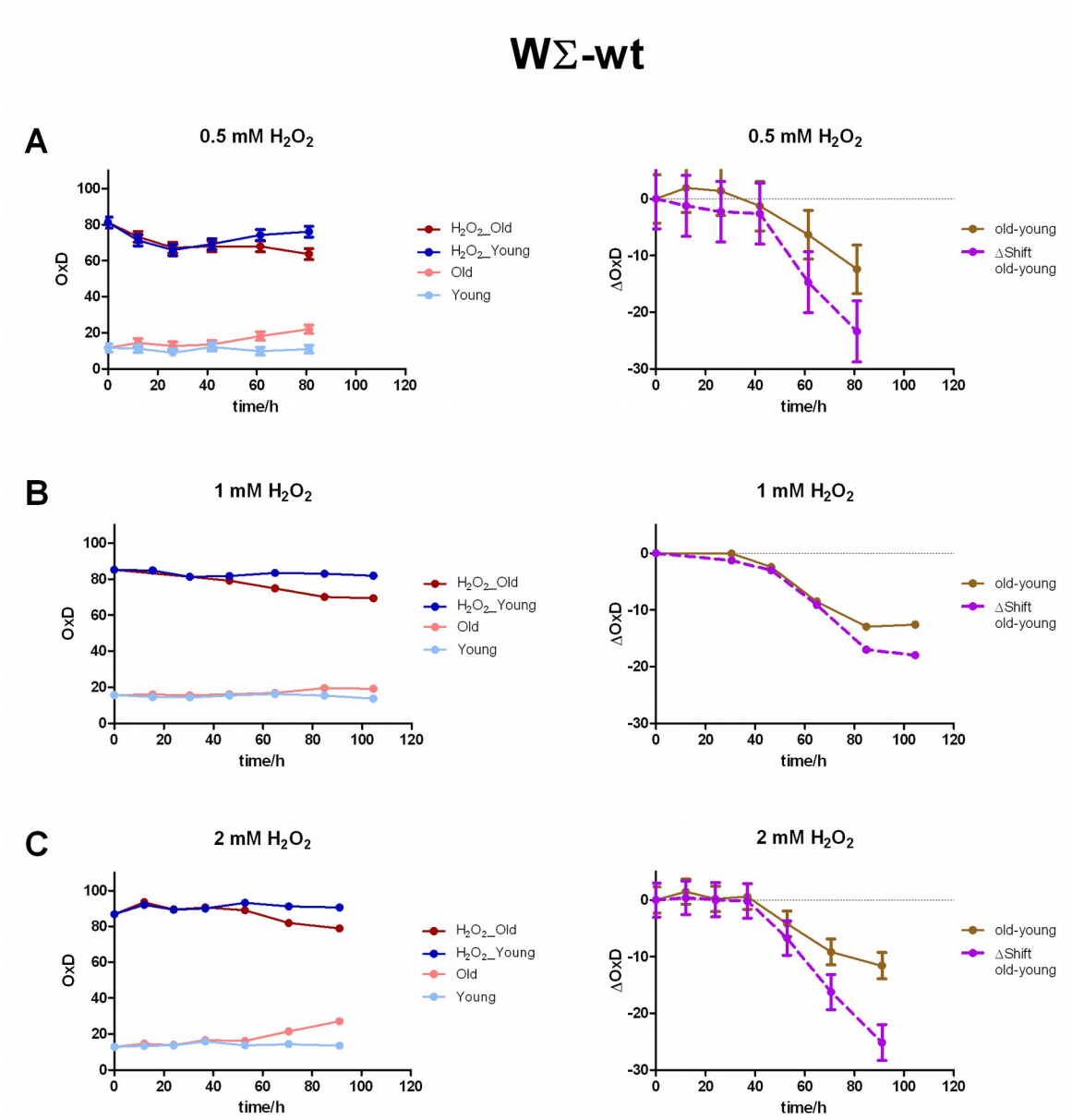

Fig.C31
Basal and maximal roGFP2–Orp1 oxidation after H_2O_2 treatment during replicative aging in glucose medium for WΣ wild-type cells.
On the left side basal probe oxidation for young (light colors) and old cells (dark color) is shown. On the right side the difference of the maximal oxidation between old and young cells (light brown) or the differences in the oxidation shifts after peroxide treatment for old and young cells is plotted (dashed violet).
Error bars (when available) represent the standard deviation of repeated probe calibration during the experiment. In graphs without error-bars, the fully oxidized and fully reduced standard was only measured once.
a.) Treatment with 0.5 mM H_2O_2
b.) Treatment with 1 mM H_2O_2
c.) Treatment with 2 mM H_2O_2

Because the young cells in the culture were subjected to day-to-day fluctuations the response of the old cells is likely to be influenced in a similar way so it is useful to show the data of the old cells relative to the young cells [Fig.C31a-c-left]. The differences in the plateaus are shown in [Fig.C31a-c-right]. In addition, the differences in the shift relative to the steady-state oxidation are plotted. Here an increased resistance to H_2O_2 in old cells becomes clearly visible. The W2Σ strain was also measured and found to be similar to WΣ [Fig.C32a].

In WΣ cells where the glutareductase Glr1 is deleted, the kinetic already started at a high basal oxidation and the probe was completely oxidized by 0.5 mM of H_2O_2 [Fig.C32b], whereas the parallel recorded wild-type was able to keep probe oxidation below 80% [Fig.C31a].

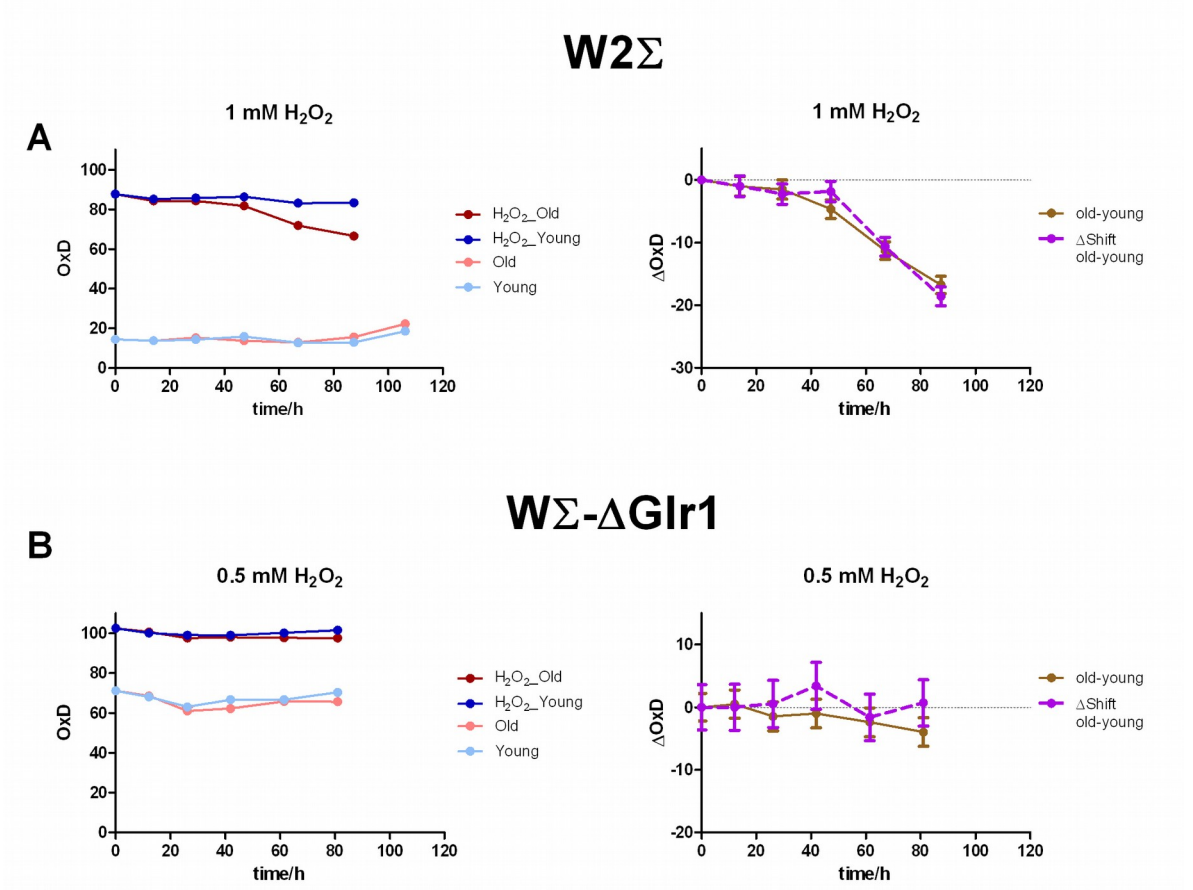

Fig.C32
Basal and maximal roGFP2–Orp1 oxidation after H_2O_2 treatment during replicative aging in glucose. The layout is the same as in [Fig.C31].
a.) W2Σ treated with 1 mM H_2O_2
b.) WΣ Δglr1 treated with 0.5 mM H_2O_2

One caveat about the OxD plots should be mentioned here. Because of the nonlinear relationship between OxD and E_{GSH} [Fig.C1] the values get compressed near 0% and 100% oxidation. Differences that appear to be small could therefore be quite large when expressed as redox potential and the shock-shifts could be misleading. If one would be interested in events happening at high oxidation, other types of roGFPs working in this range should be used. The

OxD representation was chosen because it illustrates first the position of the measurement in the dynamic-range of the probe and second it is independent of other parameters like absolute concentrations or pH, which are not accessible within the same cell with current techniques.

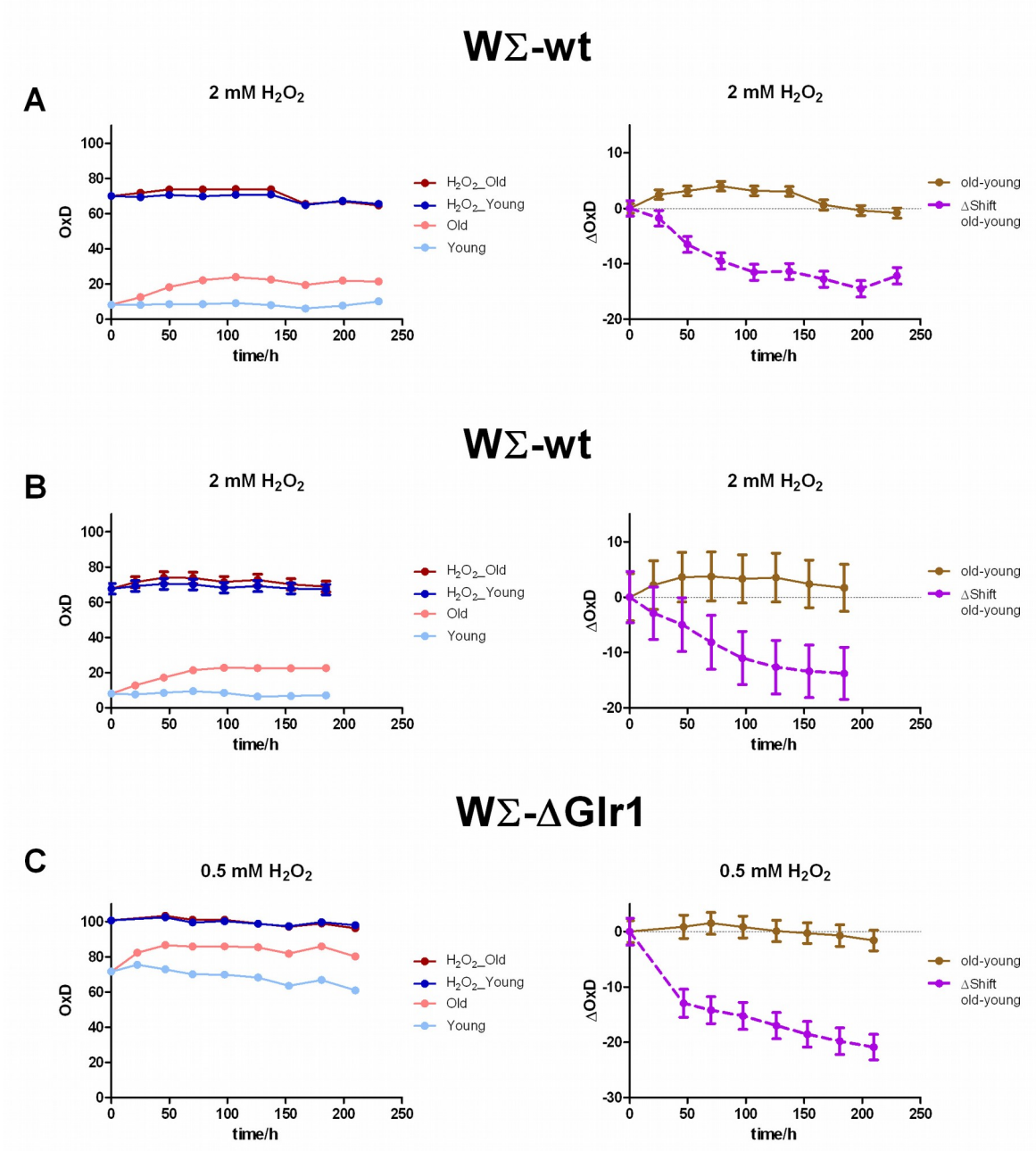

Fig.C33
Basal and maximal roGFP2–Orp1 oxidation after H_2O_2 treatment during replicative aging under respiratory conditions. The layout is the same as in [Fig.C31].
a. and b.) WΣ treated with 2 mM H_2O_2
c.) WΣ Δglr1 treated with 0.5 mM H_2O_2

3.2.1.2 Respiratory growth

Wild type cells grown under respiratory conditions showed an increase in basal roGFP2-Orp1 oxidation during aging but, unlike cells grown in glucose, they did not become more resistant to H_2O_2 [Fig.C33a,b]. Oxidative shifts by H_2O_2 addition were dominated by the increasing basal level.
A similar behavior was observed in the Glr1 knockout [Fig.C33c].

3.2.2 Diamide-shocks seen by roGFP2-Orp1

3.2.2.1 Fermentative growth

As a strong oxidant diamide is able to oxidize glutathione and the roGFP2-probes directly so the signal should be closely linked to the capacity of the cell to deal with oxidative stress. Kinetic measurements after addition of 2 mM diamide to aging cells showed a complete probe oxidation within a few minutes [Fig C34]. The data of the plateaus is also shown in [Fig.C35c] together with a biological replicate [Fig.C35b].
There seems to be a resistance phenotype in very old cells but the oxidation by diamide may be too high to tell. An experiment done with a lower diamide concentration seems to confirm the result [Fig.C35a] but here the variation in the young cells was too large to draw conclusions from the data. However, another experiment done in the W2Σ-background with an intermediate diamide concentration confirmed the trend seen in the previous experiments [Fig.C36a].

For the Glr1-knockout strain, 0.5 mM diamide already lead to complete oxidation with no resistance trend in old cells [Fig.C36b].

Given the high sensitivity of the Δglr1 strain and cells expressing the roGFP2-Orp1 reporter, lower diamide concentrations should be considered in future experiments to verify the resistance phenotype in old cells.

3.2.2.2 Respiratory growth

During the respiratory growth unshocked cells increased their H_2O_2-production with replicative age. In parallel, the sensitivity to diamide-treatment in wild-type cells increased [Fig.C37a, b]. Here it seems that the oxidation by diamide just adds up to the basal level as the oxidative shift of old and young cells was nearly the same.

Cells lacking the glutareductase Glr1 also became fully oxidized by 0.5 mM diamide under respiratory conditions [Fig.C37c].

These results indicate that there is no up-regulation of the oxidative defense during aging under respiratory conditions.

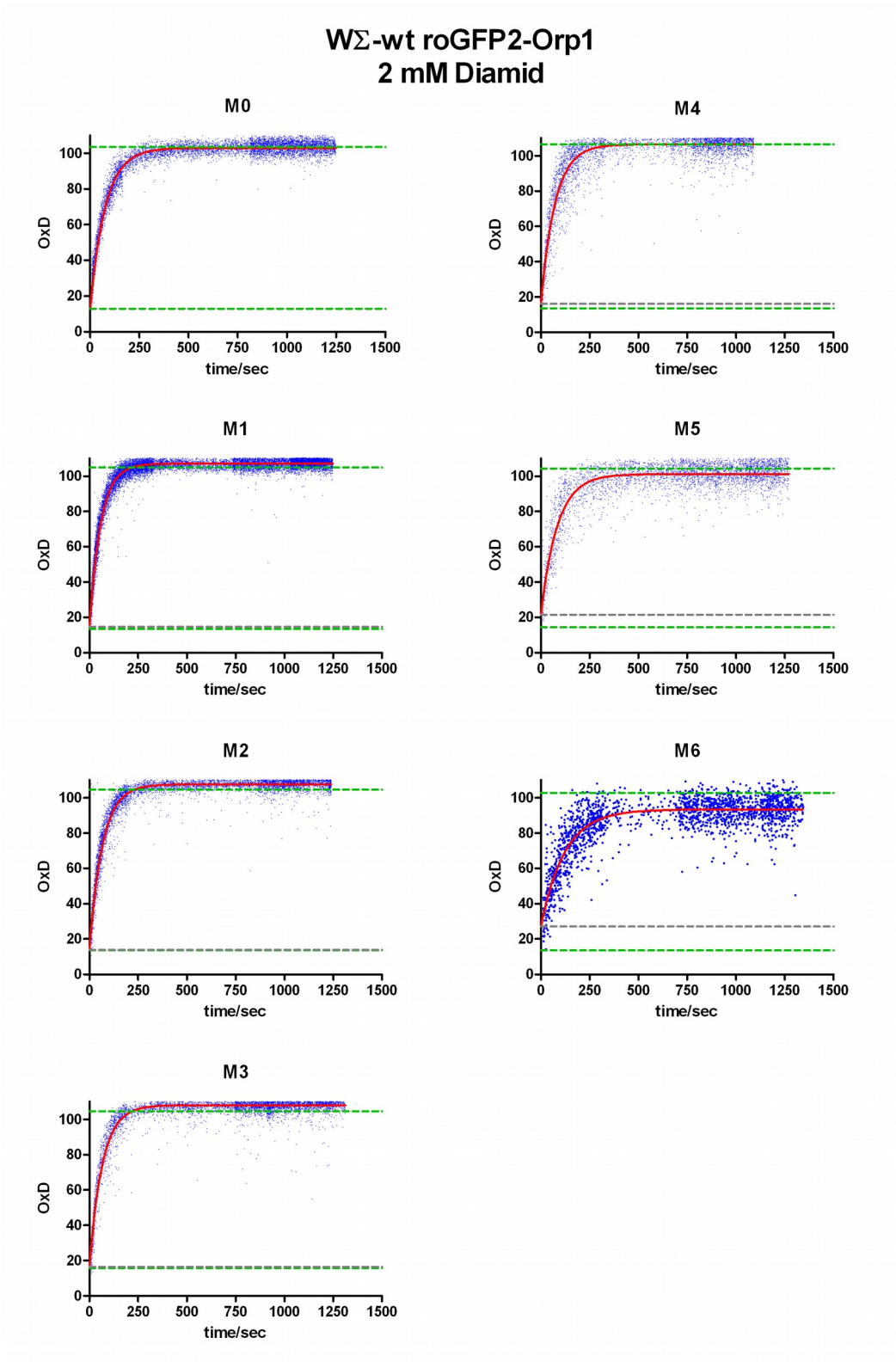

Fig.C34
Replicative aging in glucose medium. Kinetics of roGFP2-Orp1 oxidation in WΣ wild-type upon addition of 2 mM diamide. The layout is the same as in [Fig.C30].

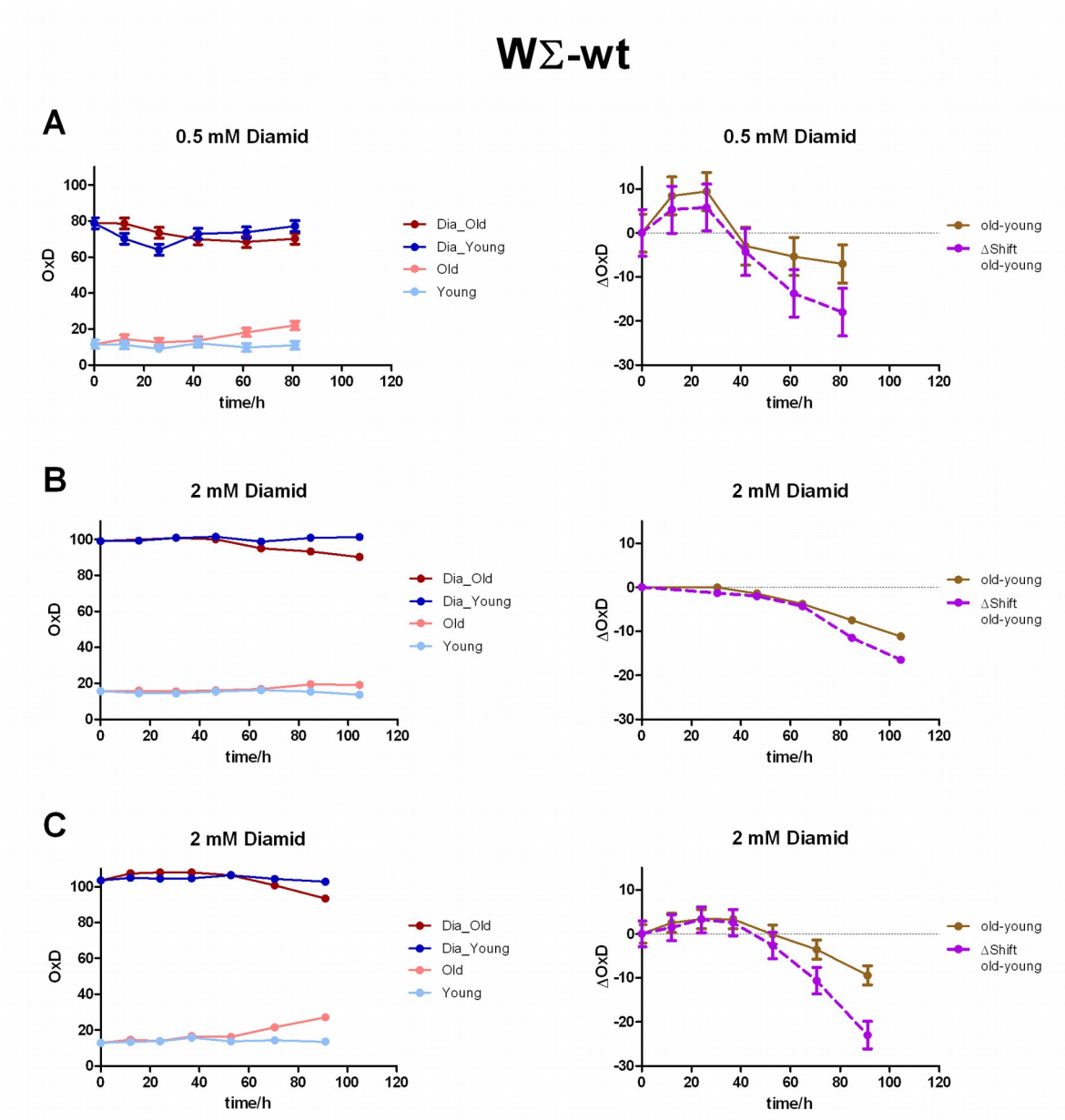

Fig.C35
Basal and maximal roGFP2–Orp1 oxidation after diamide treatment during replicative aging in glucose. The layout is the same as in [Fig.C31].
Three independent replicates in WΣ wild type are shown.
a.) Treatment with 0.5 mM diamide
b. and c.) Treatment with 2 mM diamide

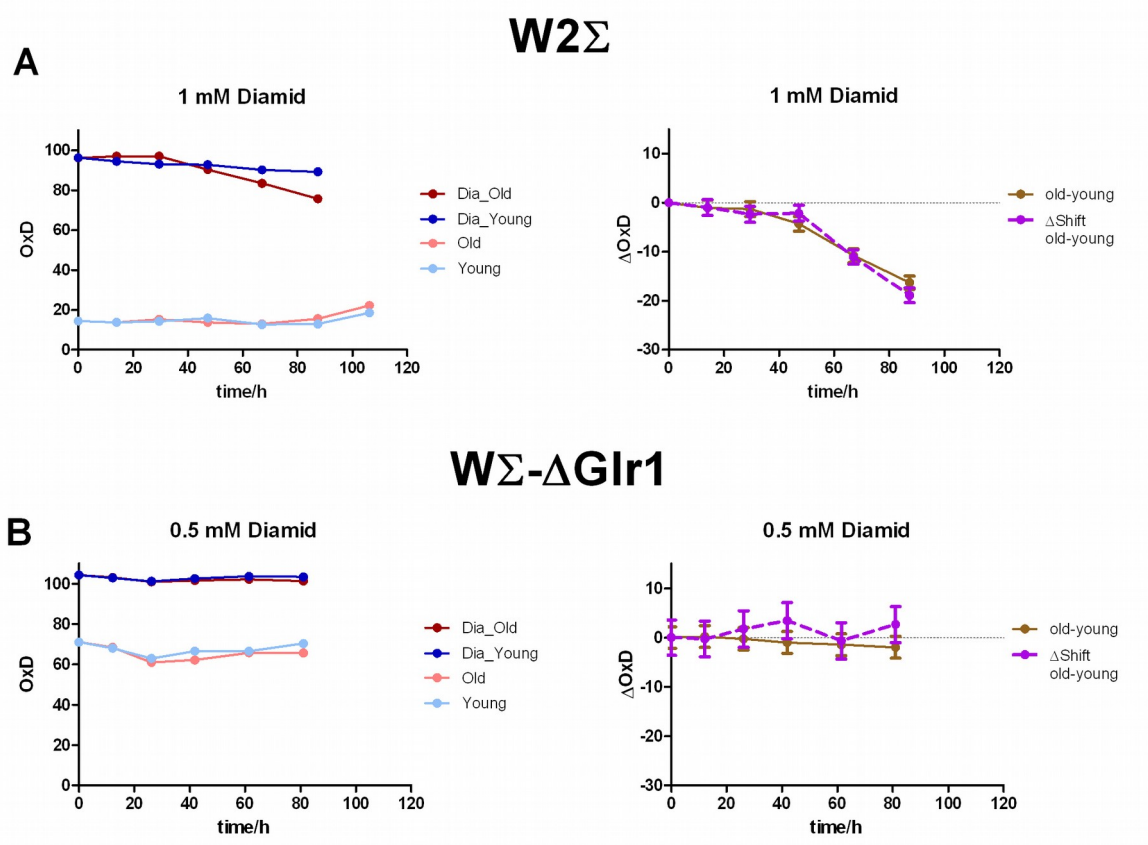

Fig.C36
Basal and maximal roGFP2–Orp1 oxidation after diamide treatment during replicative aging in glucose medium. The layout is the same as in [Fig.C31].
a.) W2Σ treated with 1 mM diamide
b.) WΣ Δglr1 treated with 0.5 mM diamide

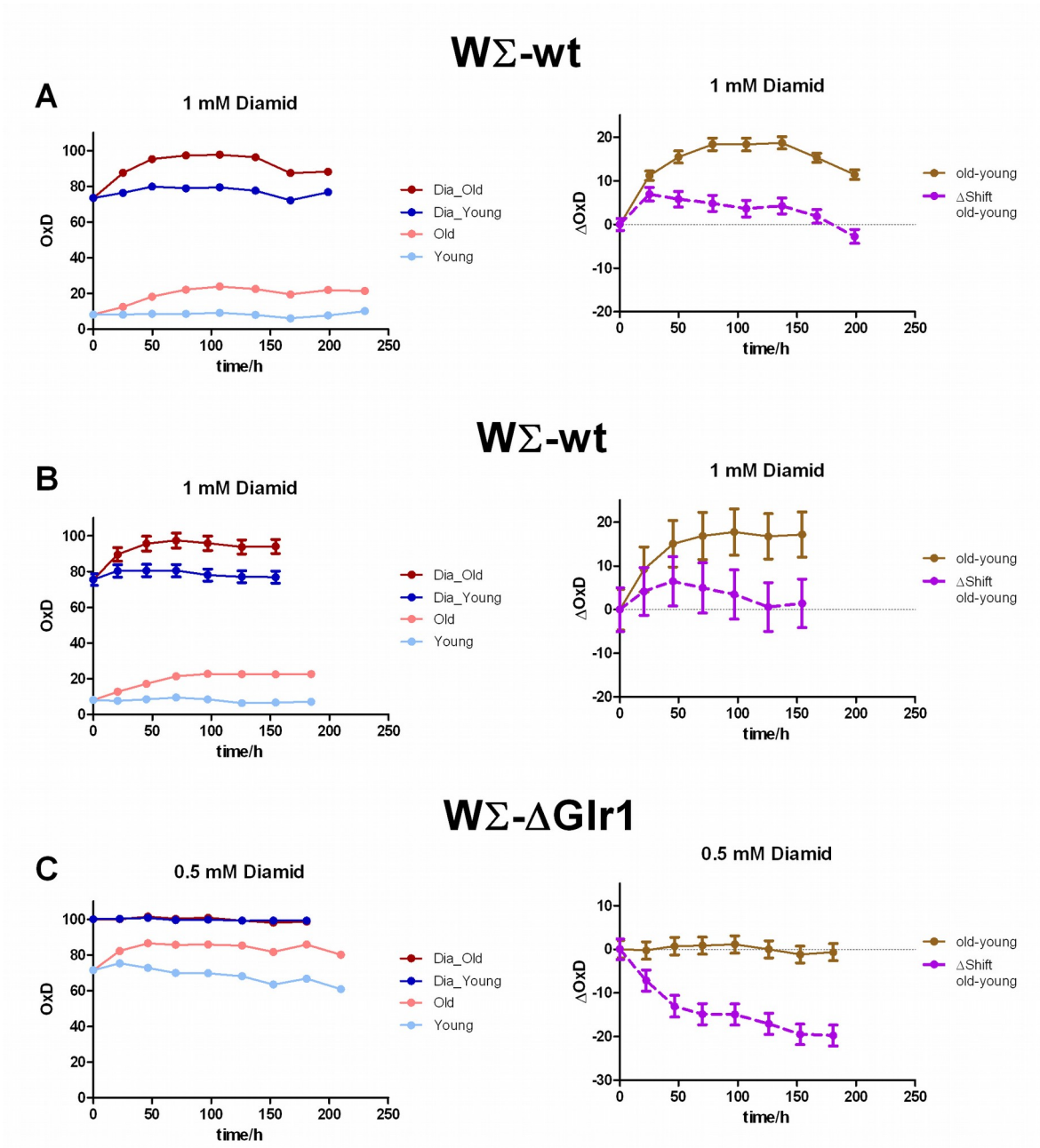

Fig.C37
Basal and maximal roGFP2–Orp1 oxidation after diamide treatment during replicative aging under respiratory conditions. The layout is the same as in [Fig.C31].
a. and b.) WΣ treated with 1 mM diamide
c.) WΣ Δglr1 treated with 0.5 mM diamide

3.3 roGFP2-Grx1 Reporter-Kinetics

3.3.1 H_2O_2-shocks seen by roGFP2-Grx1 (Fermentation and Respiration)

The response of the roGFP2-Grx1 glutathione-reporter to H_2O_2-treatment showed a more complex kinetic than the roGFP2-Orp1 reporter [Fig.C38]. To compare results in one graph, box-smoothed data averaged over 25 cells are shown [Fig.C39]. Upon 2 mM H_2O_2 treatment, a fast glutathione oxidation could be observed in young cells, followed by a quick reduction phase. With increasing age, the steady-state oxidation was lower and the fast transient oxidation peak disappeared. Instead cells at all ages seem to end up at a similar degree of oxidation in the observed timeframe.

In the Ycf1 knockout and in the W2Σ-strain, the oxidation of the glutathione probe by H_2O_2 followed the same pattern seen in wild-type [Fig.C40a,b] and [Fig.C41a,b], arguing against the involvement of Ycf1 and Ybp1 in the redox-homeostasis in old cells.
Cells in a Glr1 knockout background were extremely sensitive to oxidation. Already 1 mM H_2O_2 was sufficient to overwhelm the glutathione redox-buffer [Fig.C42]. A lower H_2O_2 concentration however, allowed partial adaptation in young cells. With increasing age, more and more old cells lost the ability to compensate for the H_2O_2 influx [Fig.C43].

Under respiratory conditions in wild type cells a weak oxidation phase was observed upon H_2O_2-treatment followed by a slow reduction phase. Boxed smoothened data average over 25 cells are shown in [Fig.C44]. Except for the higher basal oxidation and a slightly slower recovery in old cells, no major change in kinetics could be observed over the aging process.

Taken together, the data indicates a coupling of H_2O_2-levels to the glutathione-pool seen by the first fast oxidation phase of the roGFP-Grx1 reporter and a compensatory mechanism, which leads again to glutathione reduction under fermentative conditions. In old cells this compensatory mechanism seems to be replaced by a general up-regulation in peroxide-defense or a weaker coupling to the glutathione-pool. In glycerol-medium cells appear to have a stronger general peroxide defense, seen by the lower signal amplitude but only a weak compensation seen by the slow recovery after H_2O_2-induced glutathione oxidation.

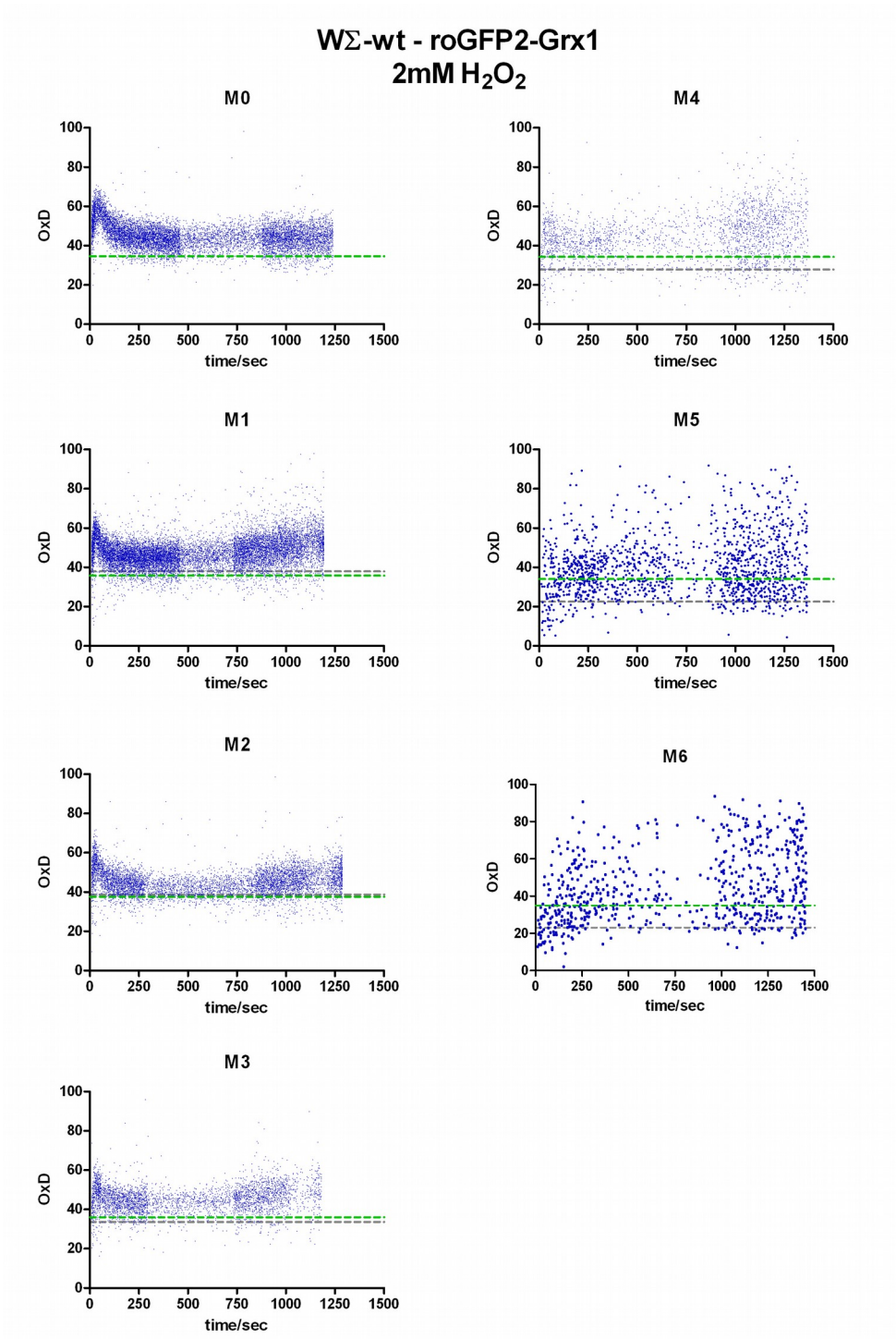

Fig.C38
Replicative aging in glucose medium. Kinetics of roGFP2-Grx1 oxidation in WΣ wild-type after addition of 2 mM H_2O_2. The graphs represent measurements at the different stages of the aging process (M0 is a logarithmic young culture, M6 are the oldest cells measured). Green dashed lines show the basal reporter oxidation for the internal young cell-control. Grey dashed lines show the basal oxidation of the old cells.

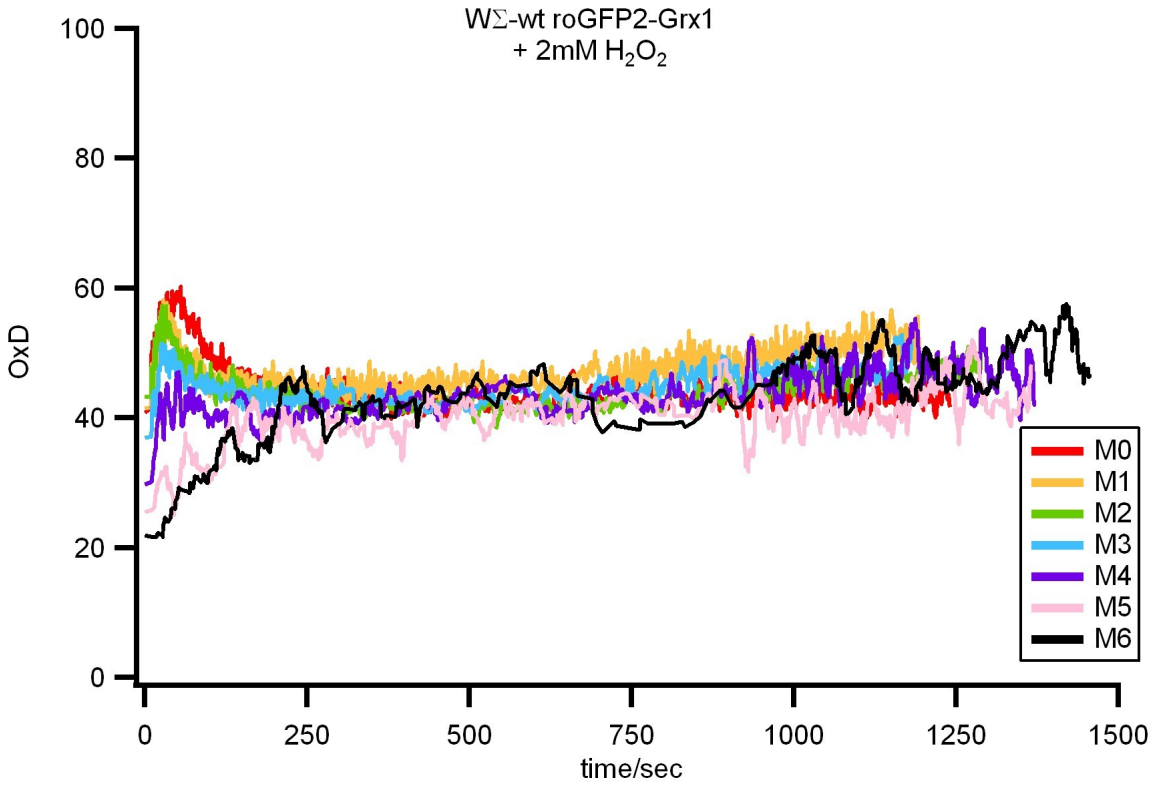

Fig.C39
Same data as in [Fig.C38] but box-smoothened over 25 cells.

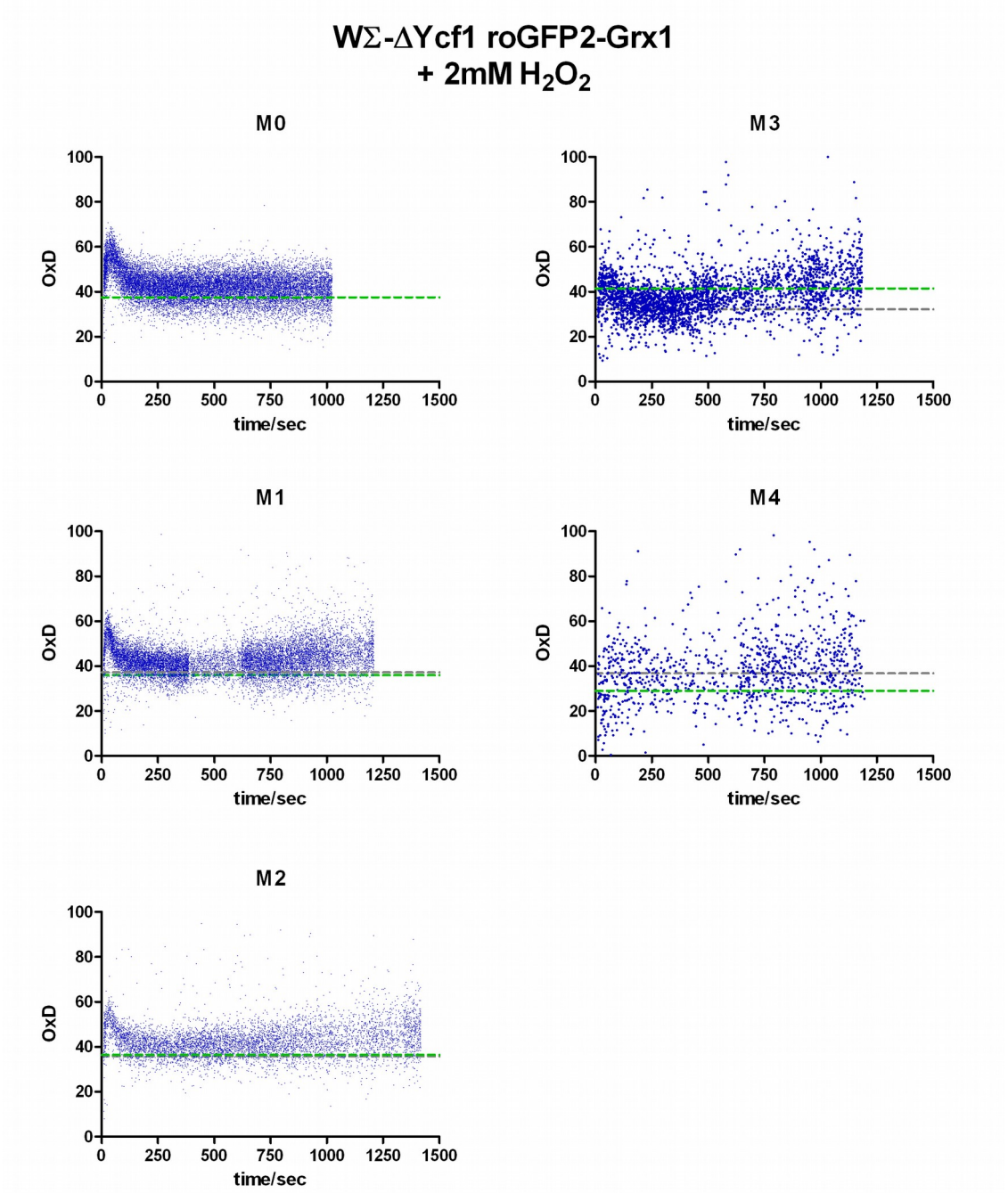

Fig.C40a
Replicative aging in glucose medium. Kinetics of roGFP2-Grx1 oxidation in WΣ Δycf1 cells after addition of 2 mM H_2O_2. The layout is the same as in [Fig.C38].

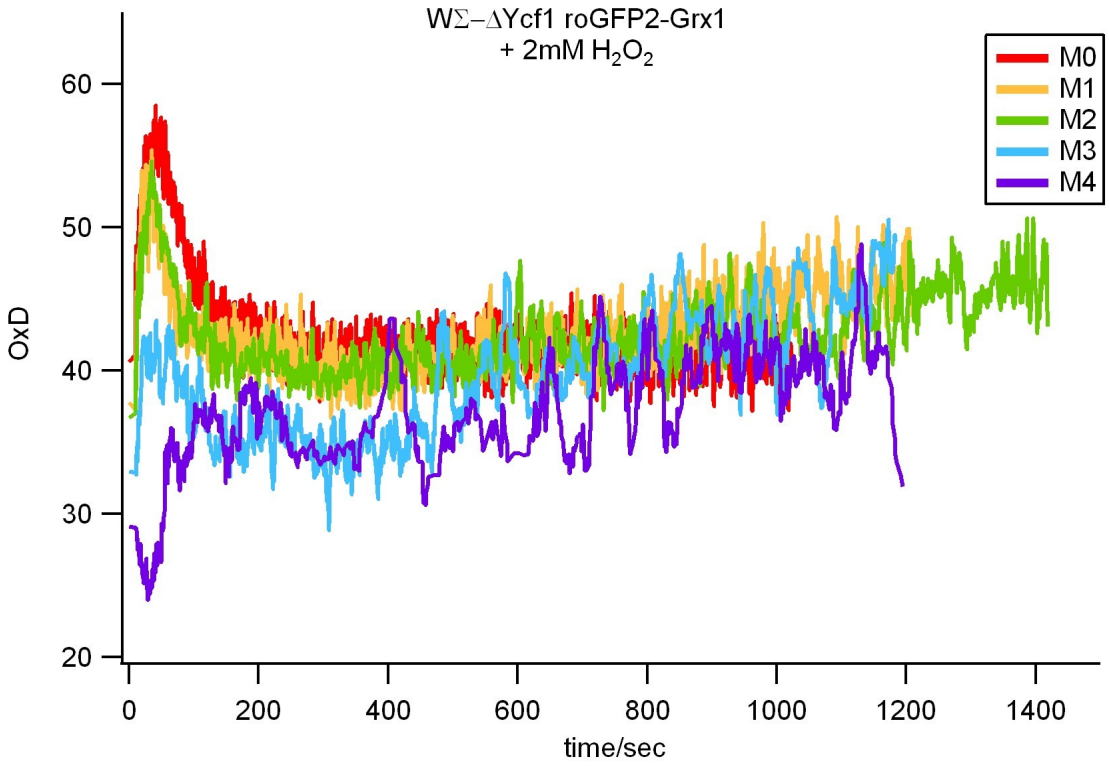

Fig.C40b
Same data as in [Fig.C40a] but box-smoothened over 25 cells.

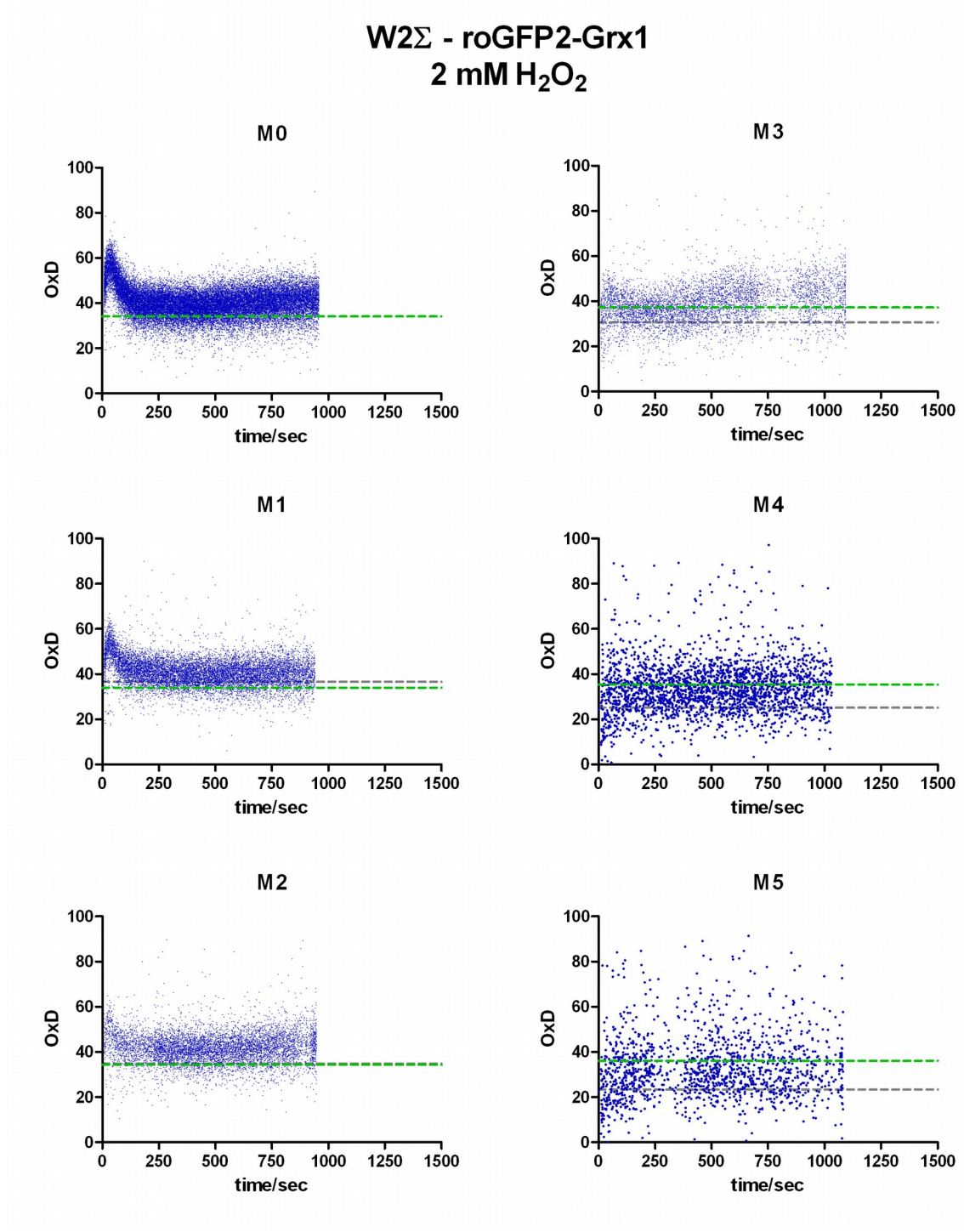

Fig.C41a
Replicative aging in glucose medium. Kinetics of roGFP2-Grx1oxidation in W2Σ cells after addition of 2 mM H_2O_2. The layout is the same as in [Fig.C38].

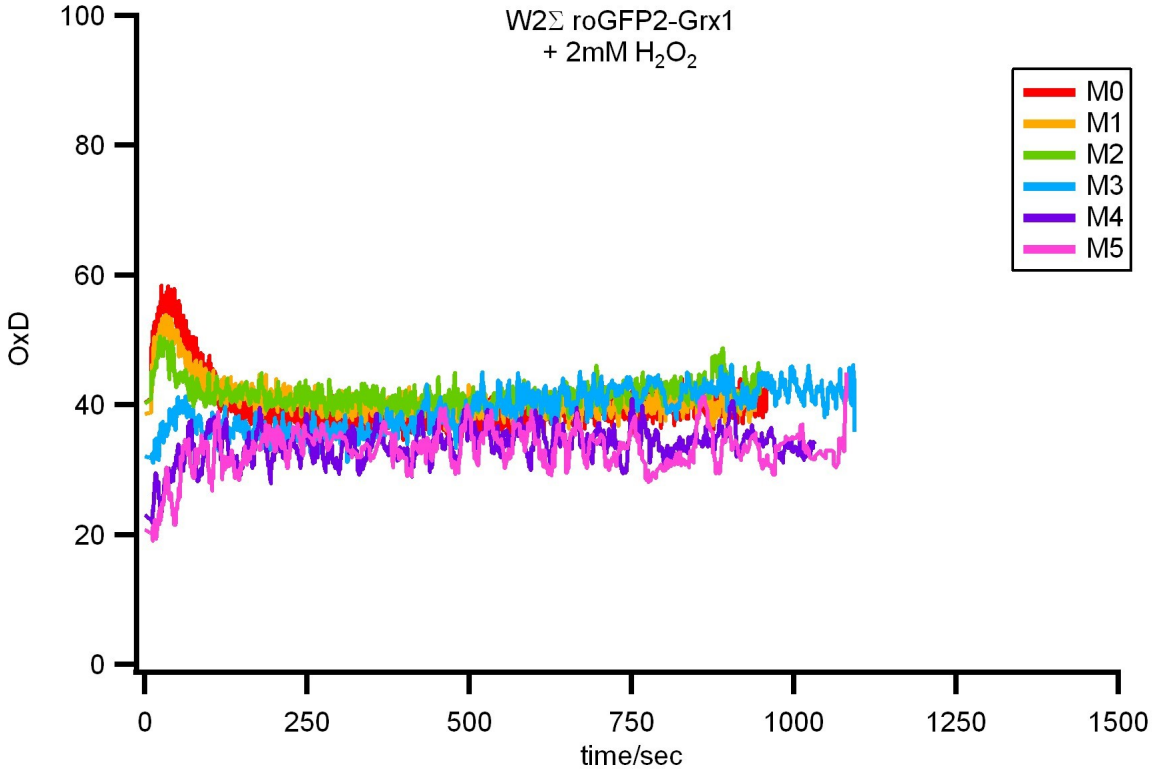

Fig.C41b
Same data as in [Fig.C41a] but box-smoothened over 25 cells.

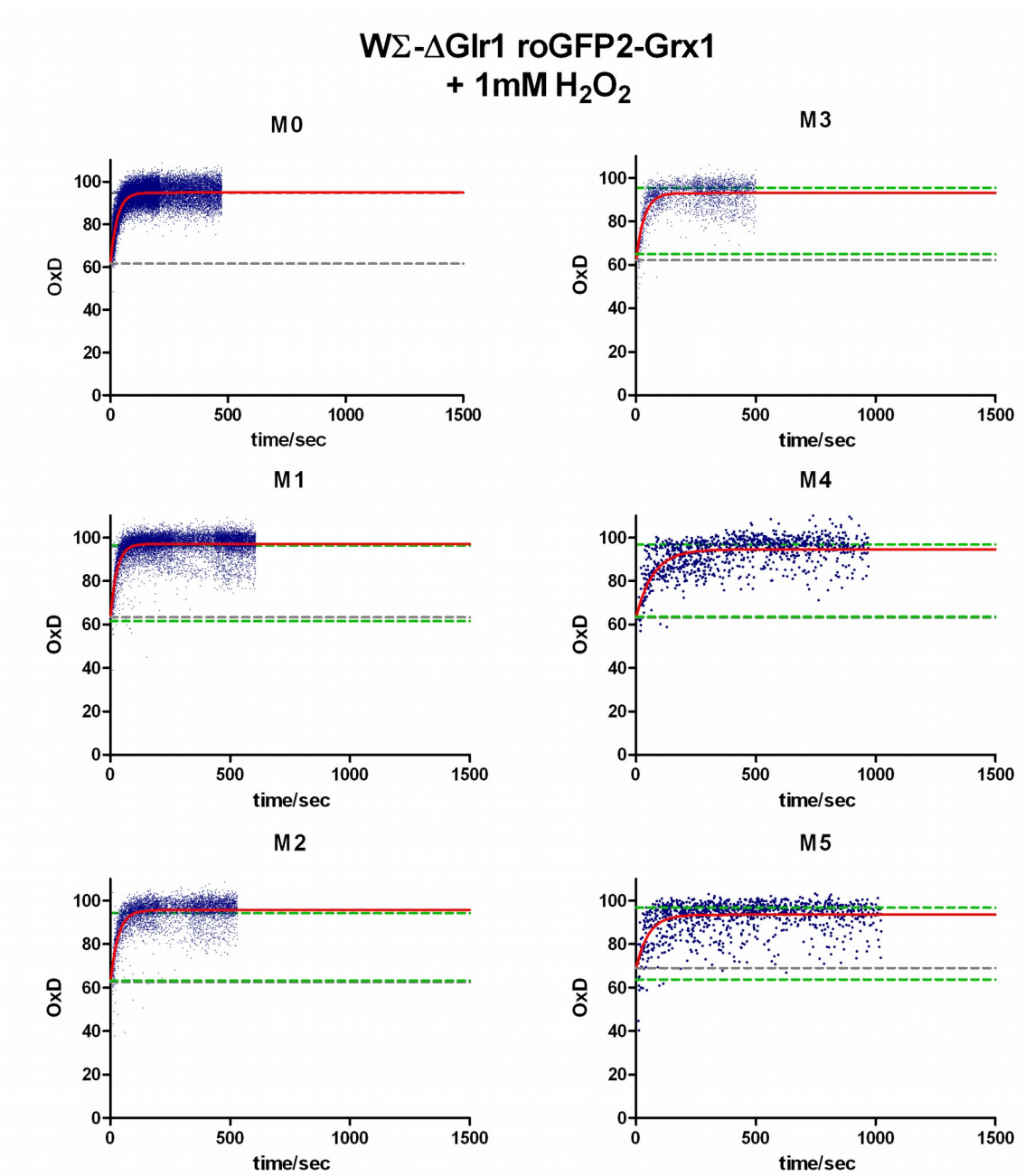

Fig.C42
Replicative aging in glucose medium. Kinetics of roGFP2-Grx1 oxidation in WΣ Δglr1 cells after addition of 1 mM H_2O_2. The graphs represent measurements at the different stages of the aging process (M0 is a logarithmic young culture, M5 are the oldest cells measured). Single exponential fittings were performed to guide the eye. Green dashed lines show the basal reporter oxidation and the equilibrated oxidation after peroxide treatment for the internal young cell-control (directly after measurement of the old cells). Grey dashed lines show the basal reporter oxidation in the old cells.

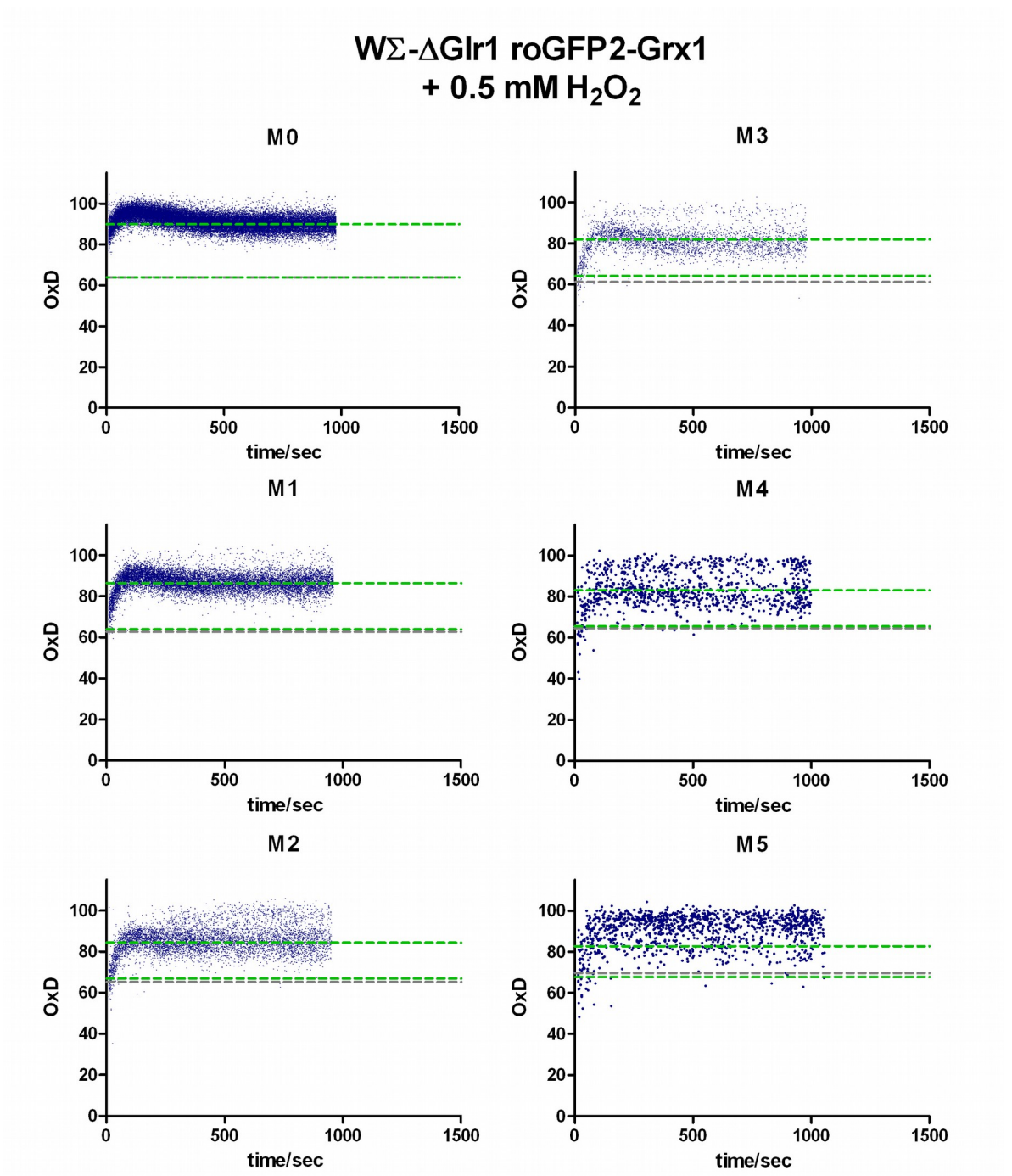

Fig.C43
Replicative aging in glucose medium. Kinetics of roGFP2-Grx1 oxidation in WΣ Δglr1 cells after addition of 0.5 mM H_2O_2. The layout is the same as in [Fig.C42] except that no fitting was applied to the data.

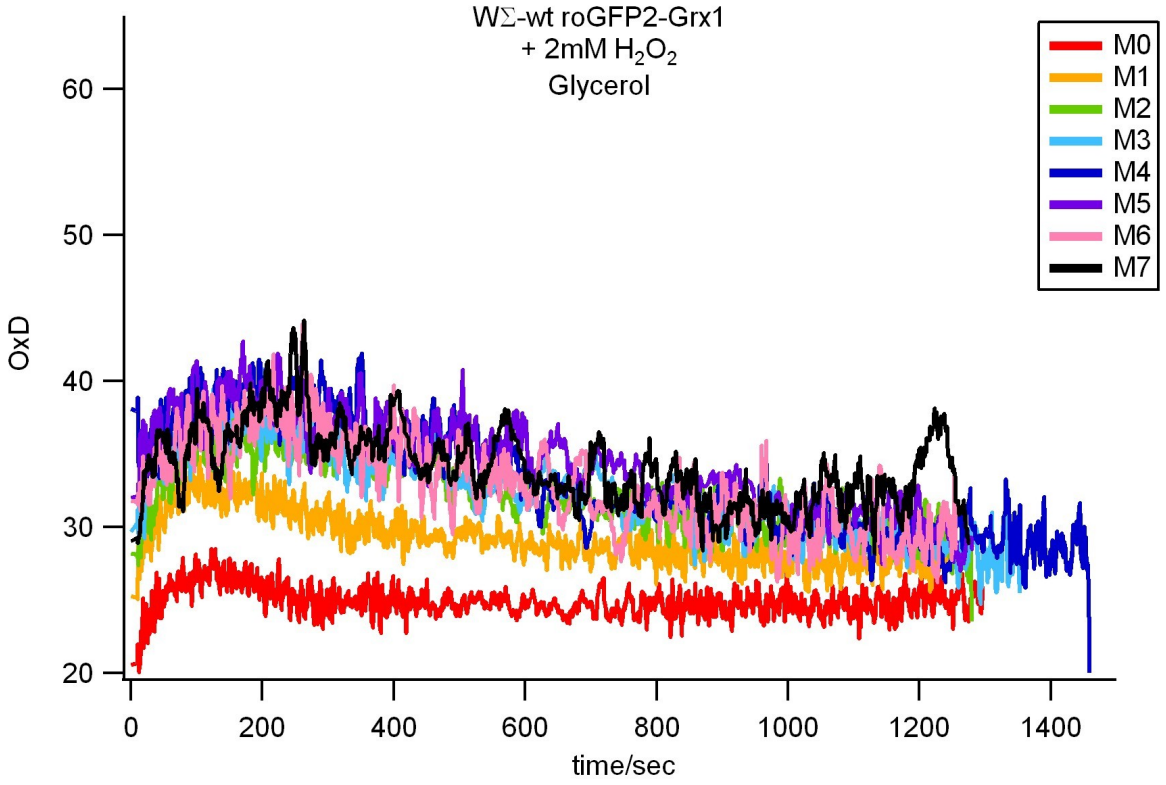

Fig.C44
Replicative aging under respiratory conditions. Kinetics of roGFP2-Grx1 oxidation in WΣ wild-type cells after addition of 2 mM H_2O_2. Data smoothened over 25 cells is shown for different stages of the aging process. M0 represents young cells from a logarithmic culture and M1-M7 older species in increasing order.

3.3.2 Diamide-shocks seen by roGFP2-Grx1 (Fermentation and Respiration)

Treatment of glucose-grown cells expressing the roGFP2-Grx1 reporter with diamide results in similar kinetics [Fig.C45] as seen with the roGFP2-Orp1 reporter (compare [Fig.C34]. Here 2 mM diamide did not lead to complete oxidation so the resistance phenotype in old cells is more reliable. In [Fig.C46a-e] the plateaus of the kinetics are plotted for different strain backgrounds. For WΣ wild-type and W2Σ, the plateaus behave similar with age. The more reduced steady-state of old cells seem to be transmitted to a resistance behavior, seen by the similar shift differences between old and young cells. For the *Δycf1* and the *Δfob1* strain not enough cells were left on the last day to measure the stress response kinetics but within the error they seem to behave equivalent. The Glr1-knockout is already too highly oxidized for conclusions.

Measurements were also performed under caloric restricted conditions for WΣ and W2Σ and the results were similar [Fig.C47a-c] although W2Σ seem to have a slightly stronger resistance in old cells.

Under respiring conditions the shift in oxidation induced in wild-type cells by diamide increased significantly on top of the already increasing basal level of the roGFP-Grx1 reporter during the first 50 h of aging and then seems to stay constant [Fig.C48a,b]. In the *Δglr1* background the signal was again near saturation after diamide addition and the differences between old and young nearly became compressed to identity and therefore the shift-differences in OxD appeared to be inverted [Fig.C48c]. Except for the absolute values the responses are identical with the diamide shocks seen by the roGFP2-Orp1 reporter (compare [FigC37]).

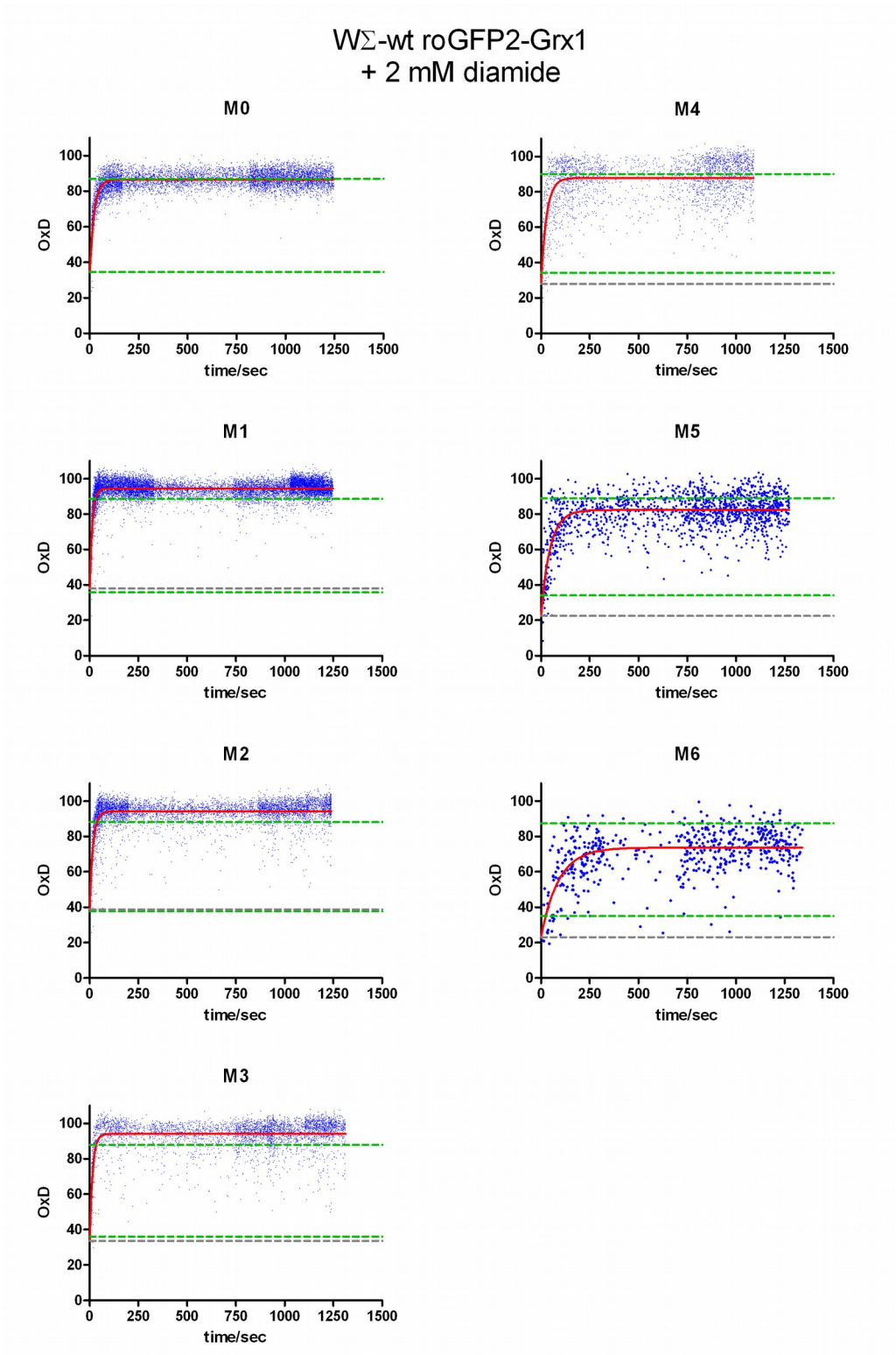

Fig.C45
Replicative aging in glucose medium. Kinetics of roGFP2-Grx1 oxidation in WΣ wild-type after addition of 2 mM diamide. Single exponential equations were fitted to the data to guide the eye. The layout is the same as in [Fig.C30]

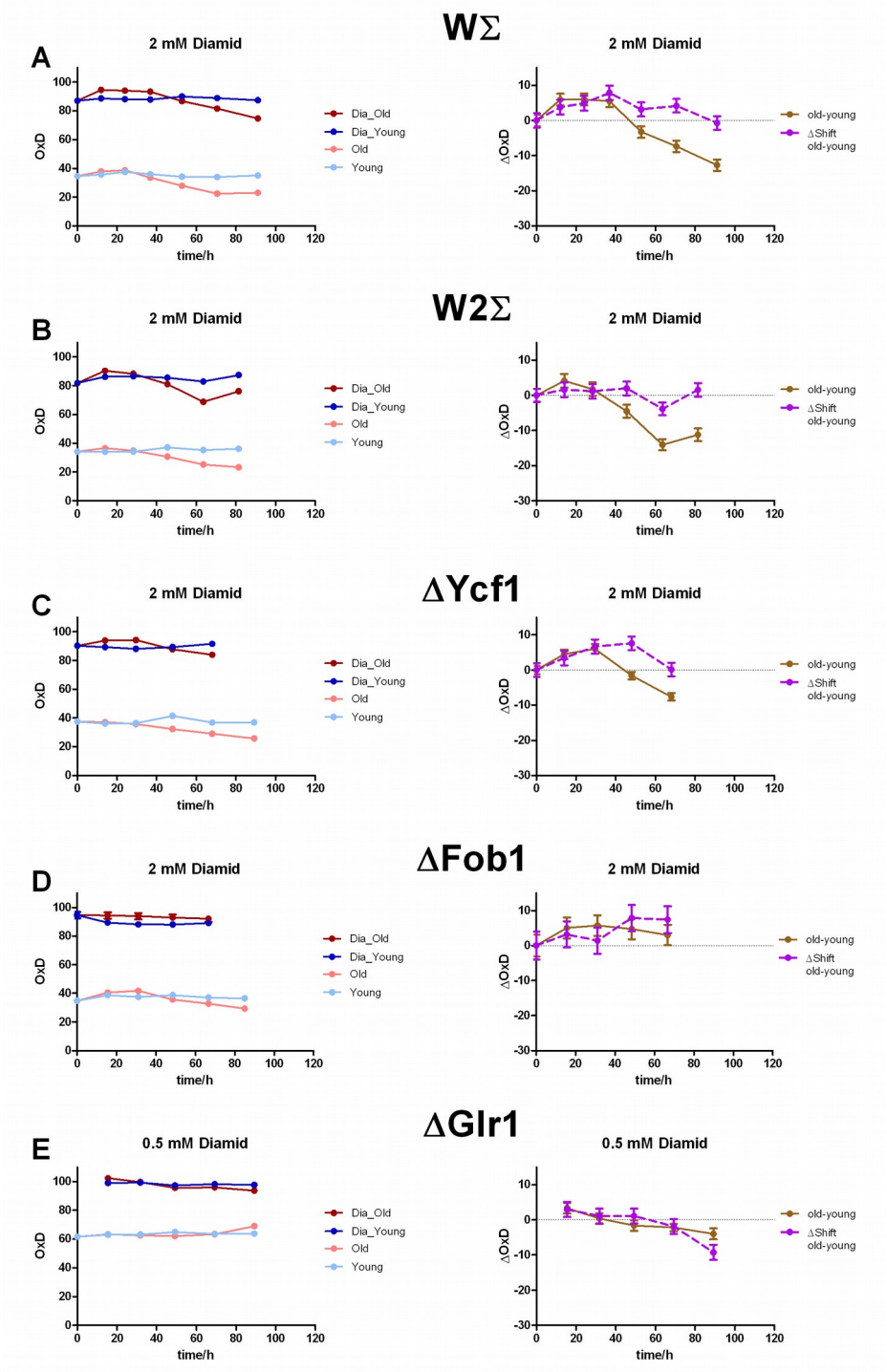

Fig.C46
Basal and maximal roGFP2–Grx1 oxidation after diamide treatment during replicative aging in glucose. The layout is the same as in [Fig.C31].
a.) Treatment of WΣ wild-type with 2 mM diamide
b.) Treatment of W2Σ with 2 mM diamide
c.) Treatment of WΣ Δycf1 with 2 mM diamide
d.) Treatment of WΣ Δfob1 with 2 mM diamide
e.) Treatment of WΣ Δglr1 with 0.5 mM diamide

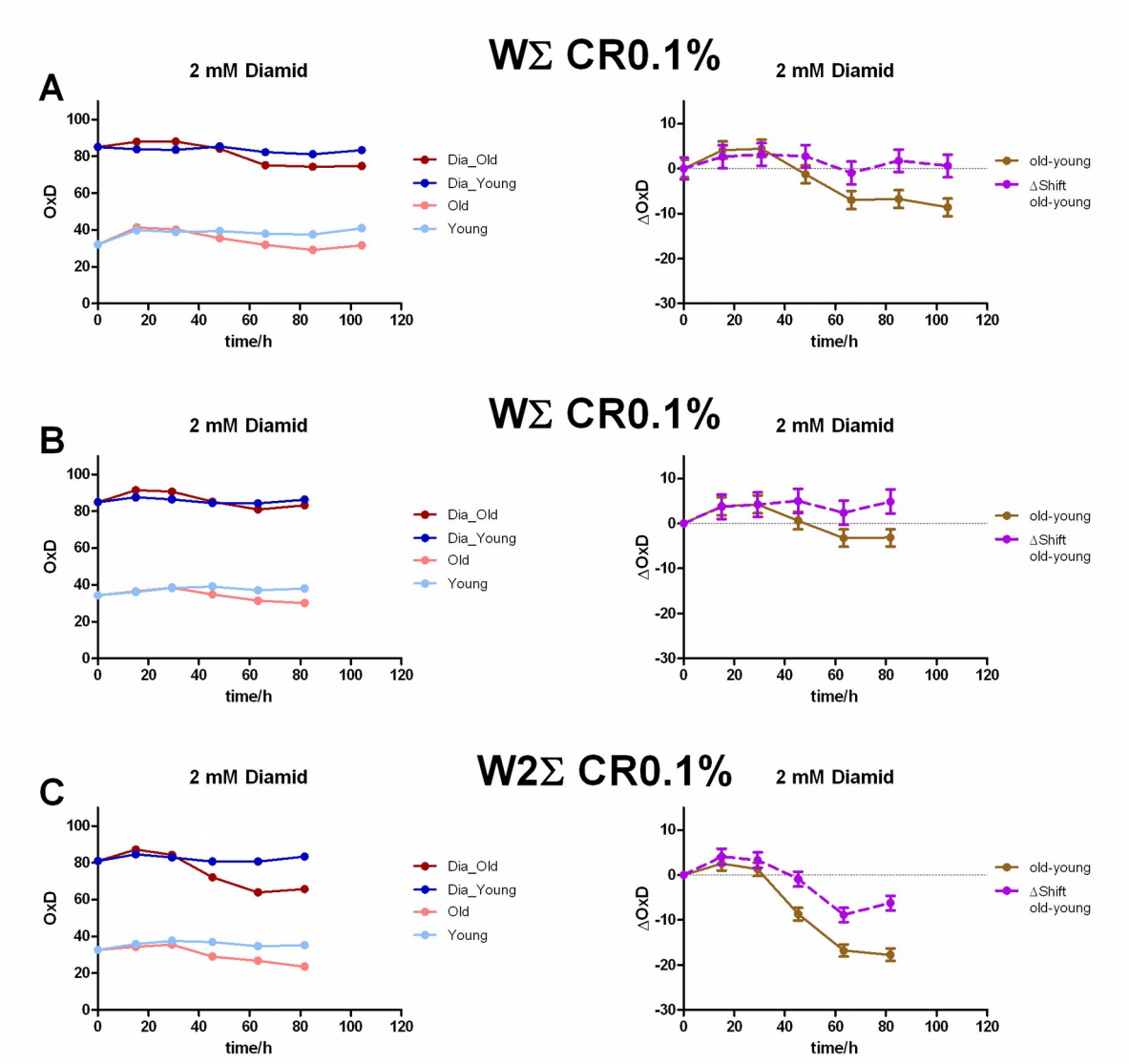

Fig.C47
Basal and maximal roGFP2–Grx1 oxidation after diamide treatment during replicative aging under caloric restricted conditions (0.1% glucose). The layout is the same as in [Fig.C31].
a, b.) Treatment of WΣ wild-type with 2 mM diamide
c.) Treatment of W2Σ with 2 mM diamide

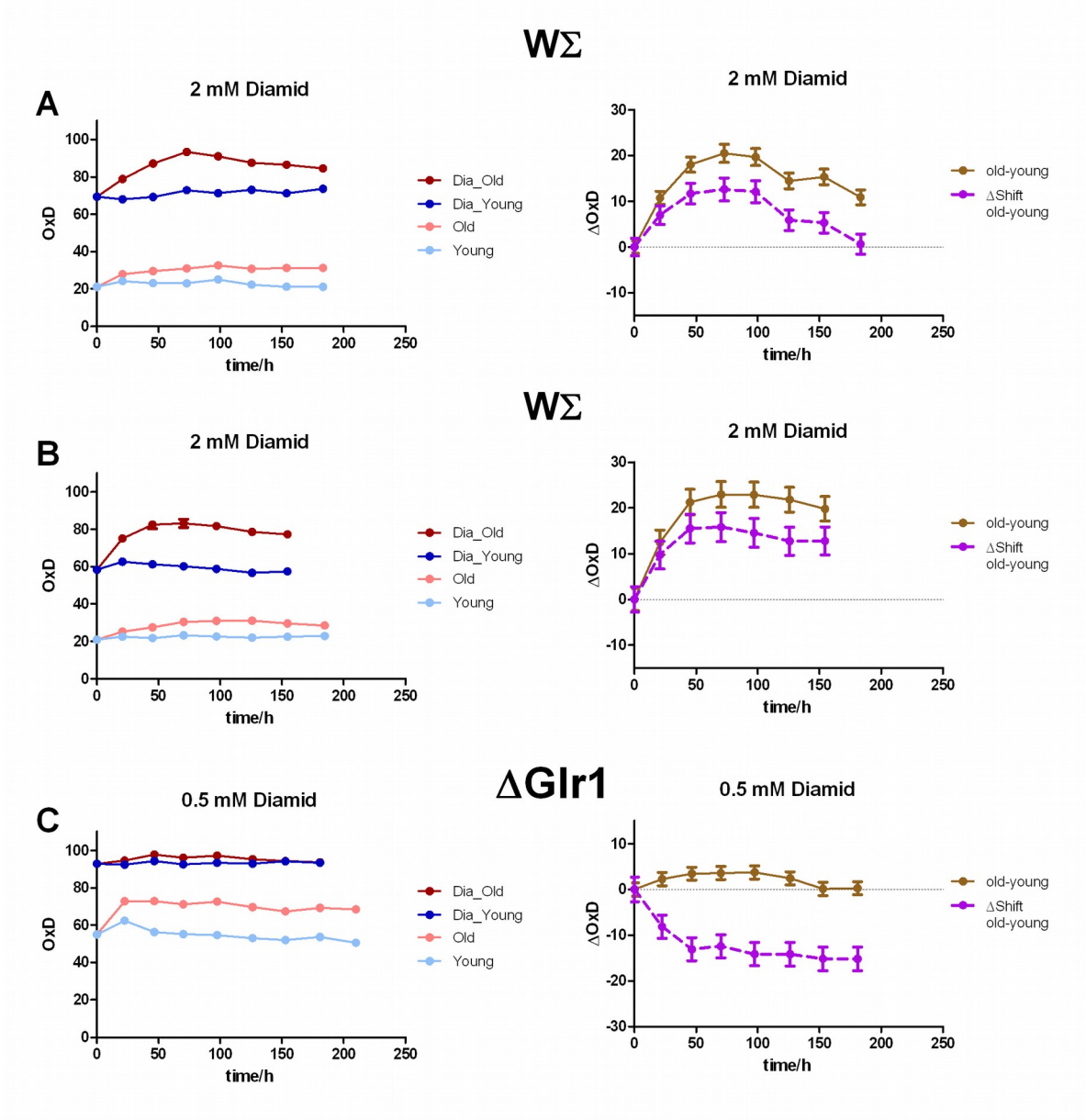

Fig.C48
Basal and maximal roGFP2–Grx1 oxidation after diamide treatment during replicative aging in respiratory medium. The layout is the same as in [Fig.C31].
a, b.) Treatment of WΣ wild-type with 2 mM diamide
c.) Treatment of WΣ Δglr1 with 0.5 mM diamide

3.4 pHluorin Reporter-Kinetics

Synthetic yeast medium is usually quite acidic. In the recipe I used the pH was 3.92. In this medium yeast cells constantly have to export protons from the cytosol to keep the cytosol in a physiological range. Like the redox-reporters, the objective was to challenge the cells and monitor their reaction. To test the buffering capacity of the medium together with the respective shock-substances, a titration with 1 M Tris or 10% acetic acid was performed [Fig.C49].

Kinetics-measurements of the pH in old cells came in focus very late in the project, so the graphs presented here are derived from only one experiment containing wild-type and *Δglr1* cells differently tagged in the same culture. Due to the technical problems with the FACS-instrument, there is only data from young cells grown in glycerol-medium.

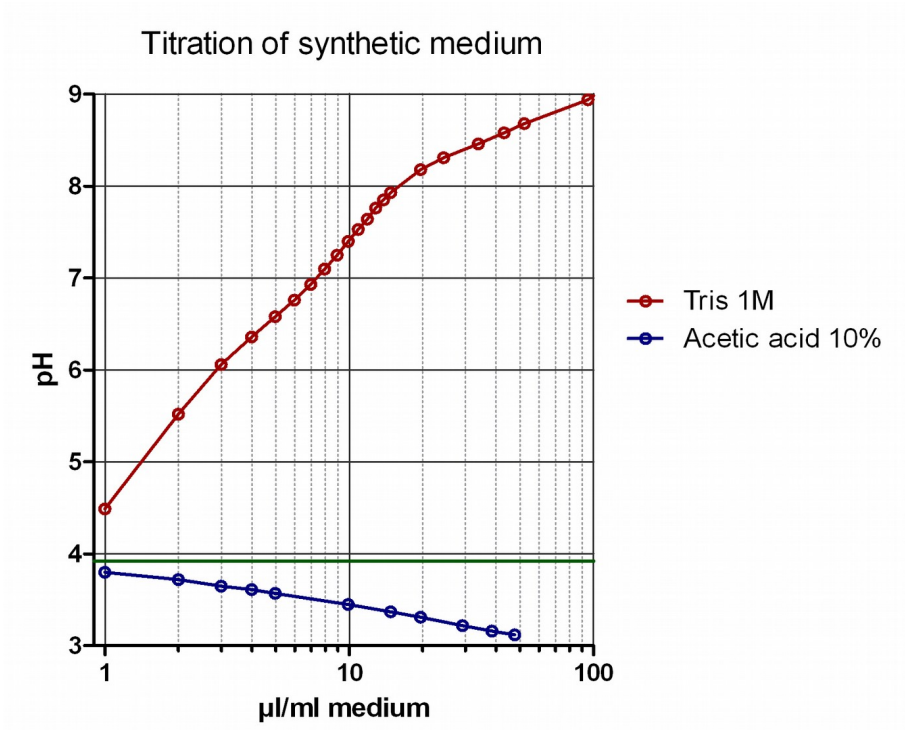

Fig.C49
Titration of synthetic medium with 1M Tris (red) and 10% acetic acid (blue). Untreated medium pH 3.92 (green).

3.4.1 Acetate-shocks seen by pHluorin

The shock with 500 parts per million (ppm) acetic acid showed complex kinetics with a fast acidification and a multiphase recovery [Fig.C50a]. The most severe effect could be seen in the oldest cells tested where recovery failed for a substantial fraction of cells. Interestingly, while the average steady-state pH goes down with age (dashed grey line), addition of the acid does not seem to acidify the recovery competent cells much further but rather increase the likelihood of cells to lose recovery completely (within the observed timeframe). The parallel culture of *Δglr1*-cells behaved identical [Fig.C50b].

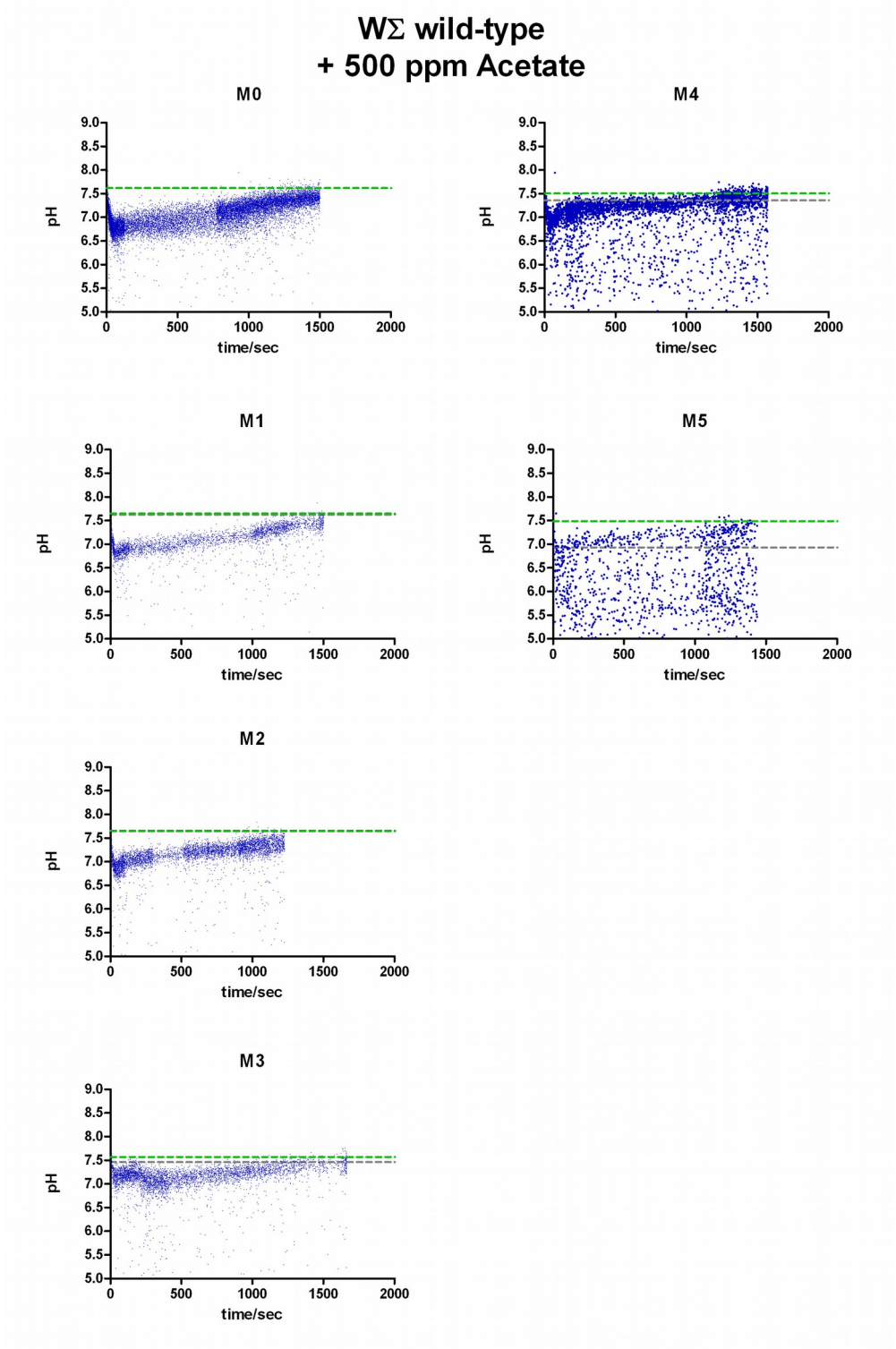

Fig.C50a
Replicative aging of WΣ wild-type in glucose medium. Kinetics of pH changes measured by the pHluorin reporter after addition of 500 ppm acetic acid. The graphs represent measurements at the different stages of the aging process (M0 is a logarithmic young culture, M5 are the oldest cells measured). Green dashed lines show the pH of the untreated young cell (internal control). Grey dashed lines show the average cytoplasmic pH in untreated old cells.

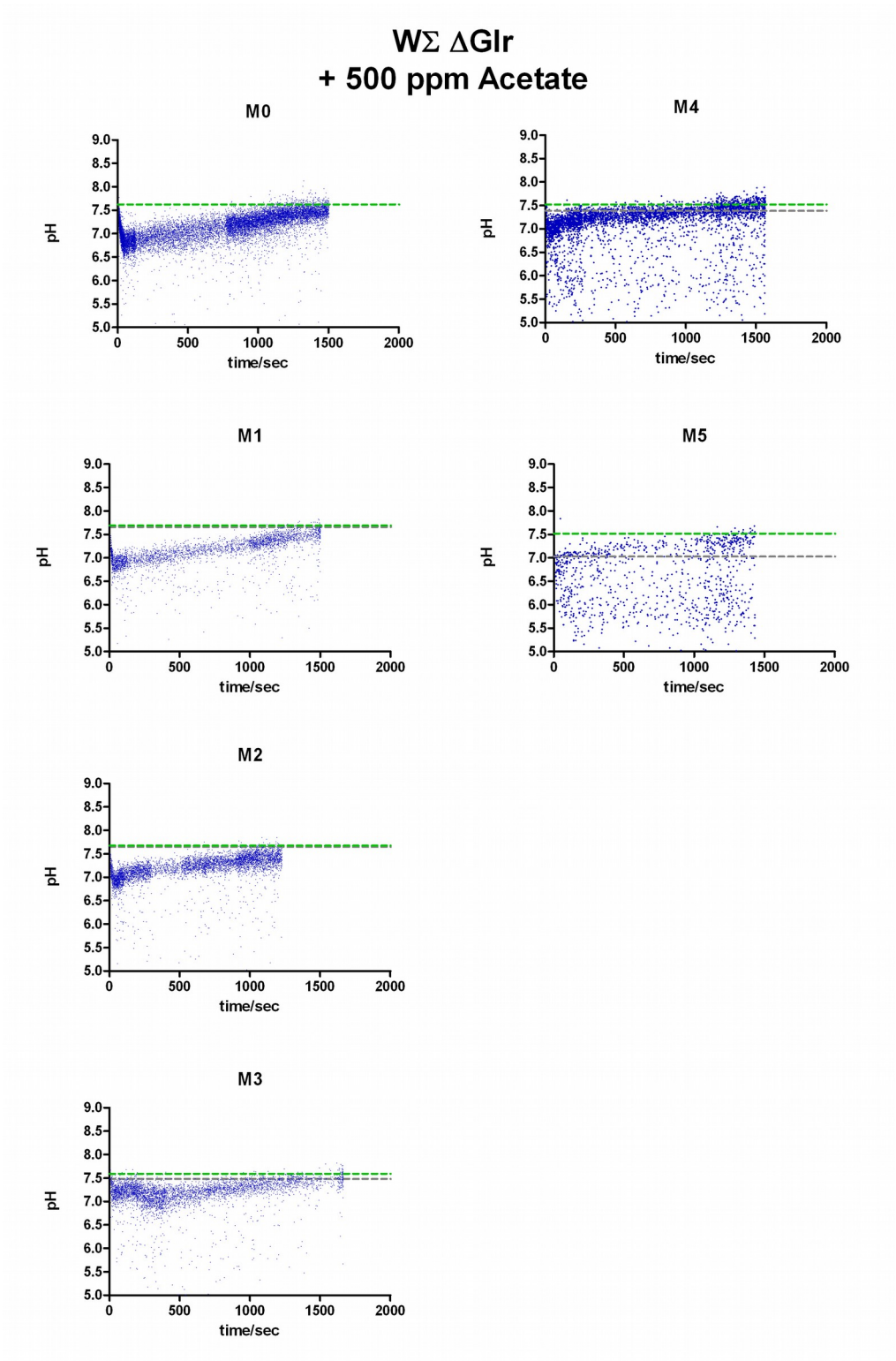

Fig.C50b
Replicative aging of WΣ-Δglr1 (these cells were differentially tagged and measured in parallel to wild type cells) in glucose medium. Kinetics of pH changes measured by the pHluorin reporter after addition of 500 ppm acetic acid. The layout is the same as in [Fig.C50a].

3.4.2 Tris-shocks seen by pHluorin

A Tris-shock at low concentration (5 µl/ml 1M Tris) resulted in a fast alkalization with a rapid recovery, which did not change significantly during aging [Fig.C51a]. Surprisingly, in middle-aged and old cells a second population with a very low pH appeared upon addition of Tris and equilibrated at about pH 6.7. Referring to the medium titration curve from [Fig.C49], addition of 5 µl/ml Tris (1M) would shift the medium to a pH of 6.6. It is most likely that this low-pH population consists of cells that just became leaky and pHluorin was quenched by the acidic medium. The addition of Tris would then restore pHluorin fluorescence again. To test whether these cells are already dead, one would have to add a vital dye in future experiments. If this assumption is true, this would demonstrate a pitfall when working only in buffered medium and emphasizes how important it is to tightly control the observed population.
Again no differences between wild-type and *Δglr1* cells were observed [Fig.C51b]

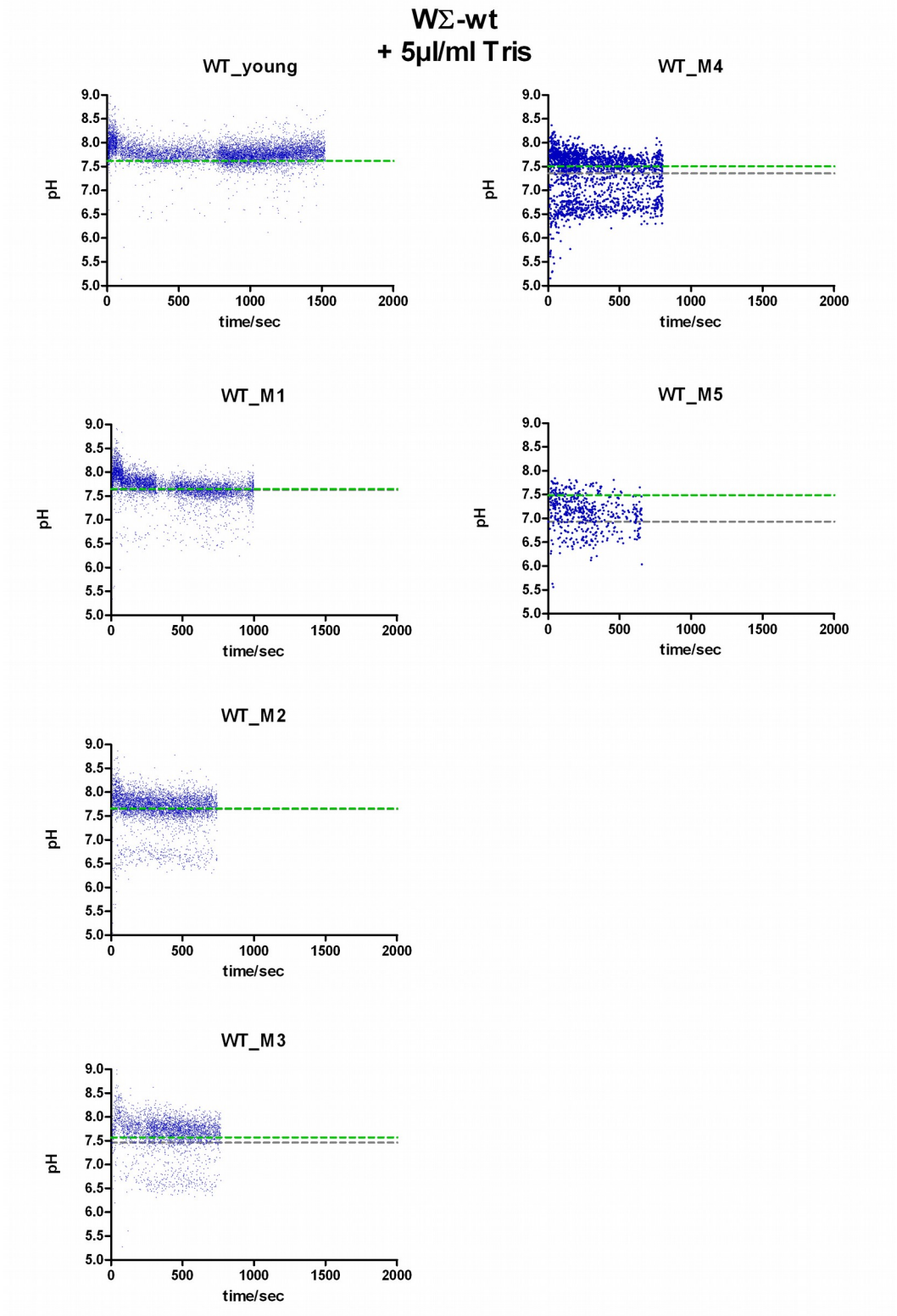

Fig.C51a
Replicative aging of WΣ wild-type in glucose medium. Kinetics of pH changes measured by the pHluorin reporter after addition of 5 µl/ml 1M Tris. The layout is the same as in [Fig.C50a].

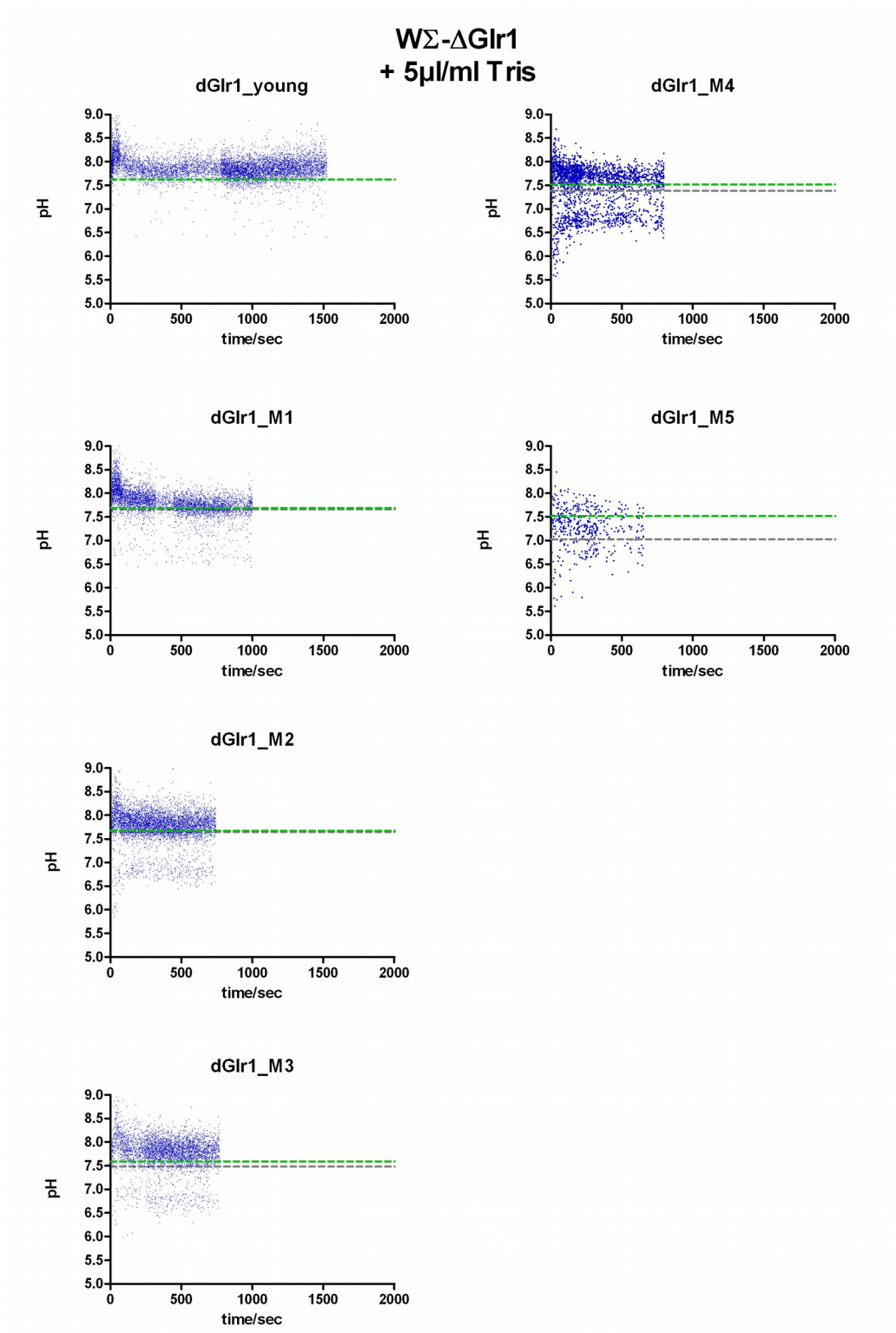

Fig.C51b
Replicative aging of WΣ-Δglr1 (these cells were differentially tagged and measured in parallel to wild type cells) in glucose medium. Kinetics of pH changes measured by the pHluorin reporter after addition of 5 µl/ml 1M Tris. The layout is the same as in [Fig.C50a].

3.4.3 H_2O_2-shocks seen by pHluorin

A fermenting aging culture was shocked by the addition of 1 mM H_2O_2 to the medium and the response of the intracellular pH was followed [Fig.C52a]. The response of the cells was not homogenous. There seems to be a subpopulation, which was able to maintain the pH, and a more prominent subpopulation, which strongly acidified upon peroxide treatment. (*Note that in most of the previously described aging experiments with the roGFP2-reporters 2 mM H_2O_2 was used. Under these conditions most of the cells end up in the low-pH subpopulation. 1 mM seems to be a critical concentration, at which some cells are able to maintain cytoplasmic pH and some are not [Fig.C76 – see discussion]. In this experiment the lower concentration was chosen on purpose to visualize this phenomenon*.)
A subpopulation of cells with peroxide resistance apparent at measurement M3 (about 36h old) and disappeared again at M5 (72h old). The opposing wedge-shaped subpopulations indicate that the cells are not different per se but rather resist the pH-drop for different time intervals. An identical behavior was observed in the parallel recorded Glr1 knockout cells [Fig.C52b] arguing against any involvement of Glr1 in pH regulation in old cells.

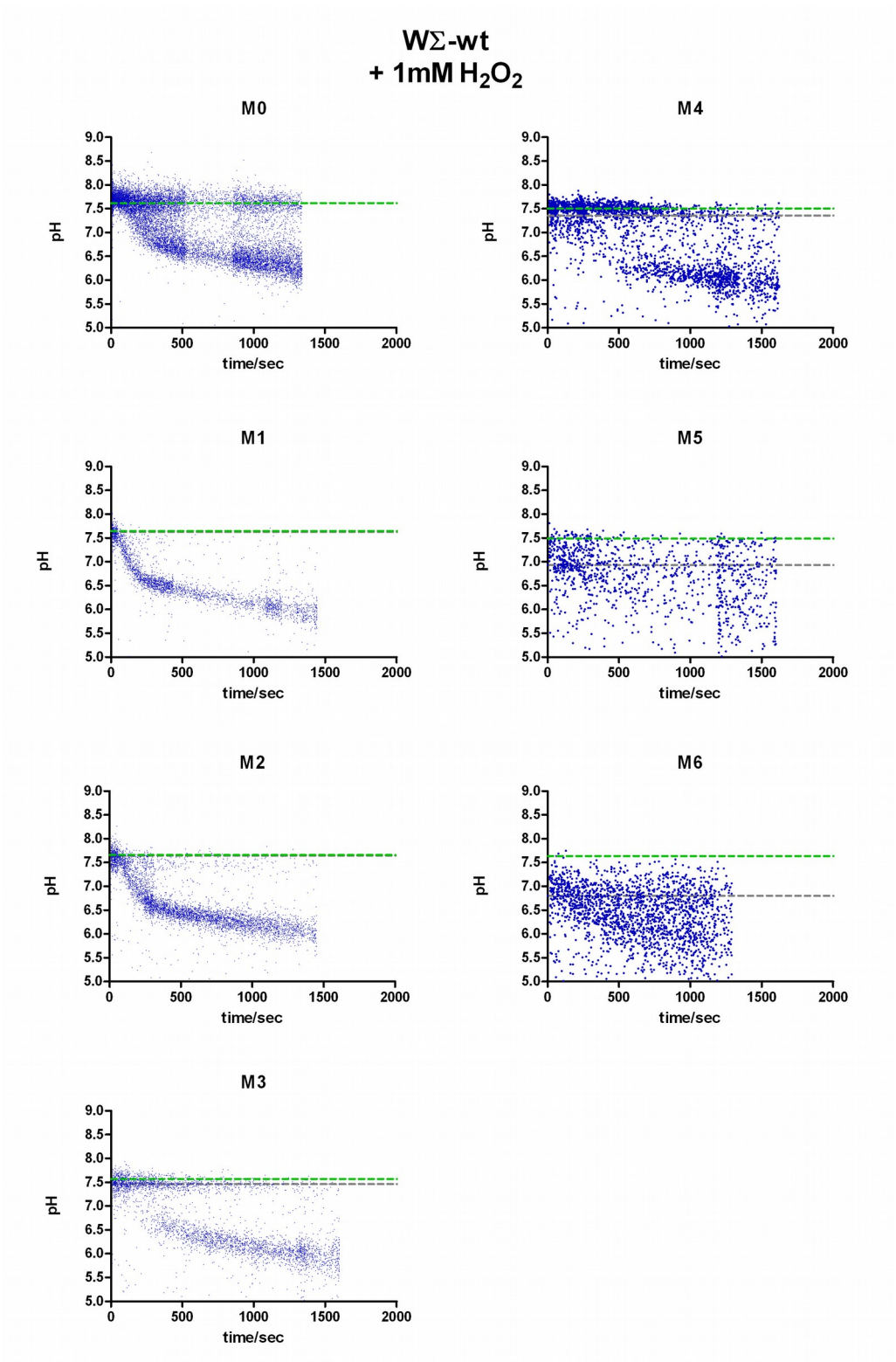

Fig.C52a
Replicative aging of WΣ wild-type in glucose medium. Kinetics of pH changes measured by the pHluorin reporter after addition of 1 mM H_2O_2. The layout is the same as in [Fig.C50a].

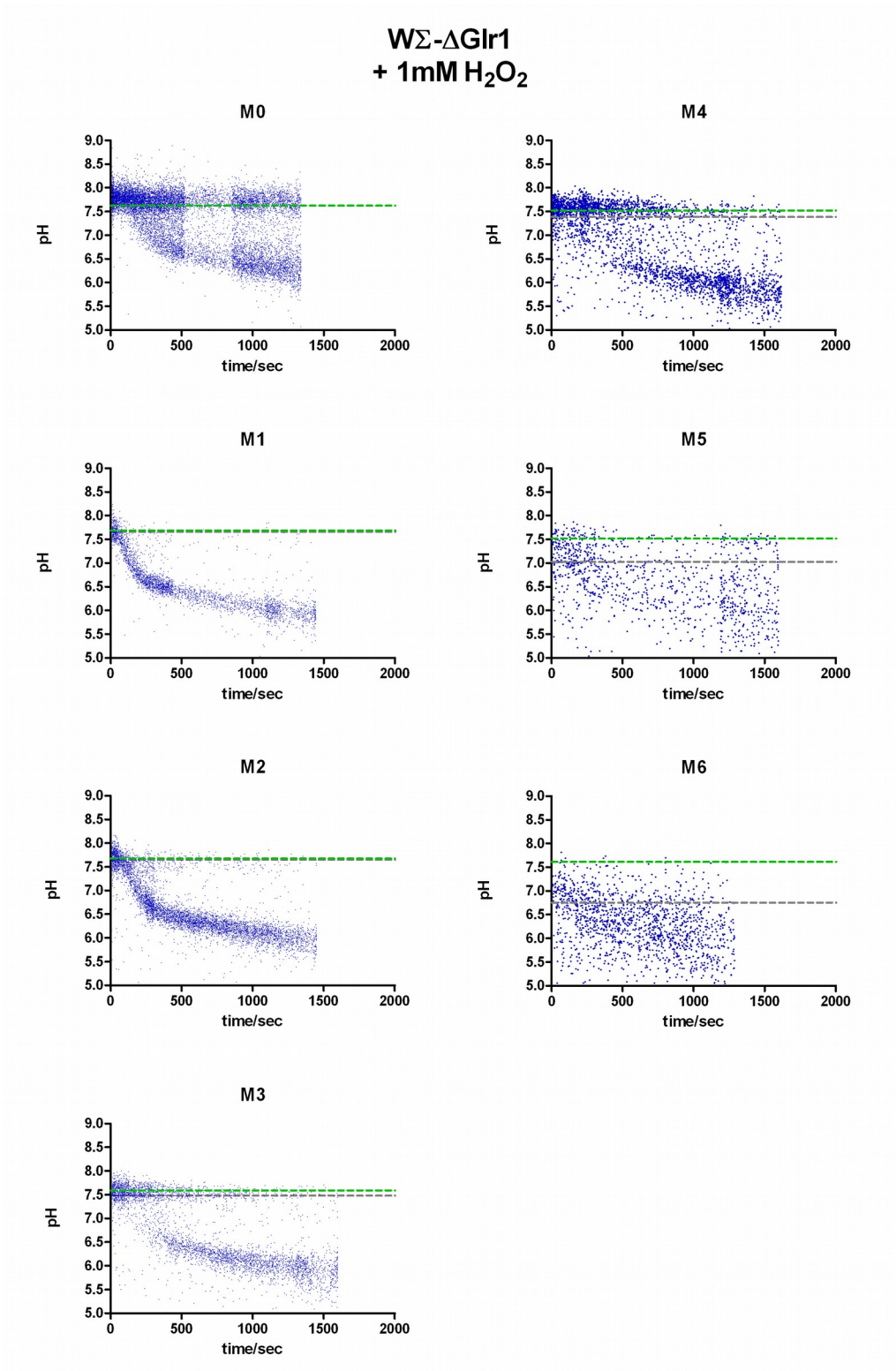

Fig.C52b
Replicative aging of WΣ-Δglr1 (these cells were differentially tagged and measured in parallel to the wild type cells) in glucose medium. Kinetics of pH changes measured by the pHluorin reporter after addition of 1 mM H_2O_2. The layout is the same as in [Fig.C50a].

3.4.4 pH-shocks in young respiring cells

Although no aging experiment with the pHluorin reporter in glycerol medium could be performed, the kinetics of a young culture should still be presented here in this section and compared with the previous kinetics in glucose.
The first obvious difference between glucose and glycerol grown cells can be seen in the H_2O_2-shock (compare [Fig.C52 – young cells] with [Fig.C53a]). Whereas the glucose cells react with a pH-drop, no effect even with a higher peroxide concentration is visible in the glycerol culture.
The next considerable difference can be seen when cells are shocked with acetic acid (compare [Fig.C50 – young cells] with [Fig.C53b]). While it took more than 1500 seconds to recover for glucose cells, the recovery in glycerol was with less than 200 seconds much faster.
In contrast to the acetate or the peroxide shock, the shock with 10 µl/ml Tris (1M) showed no difference to the glucose grown cells (compare [Fig.C54] with [Fig.C53c]).

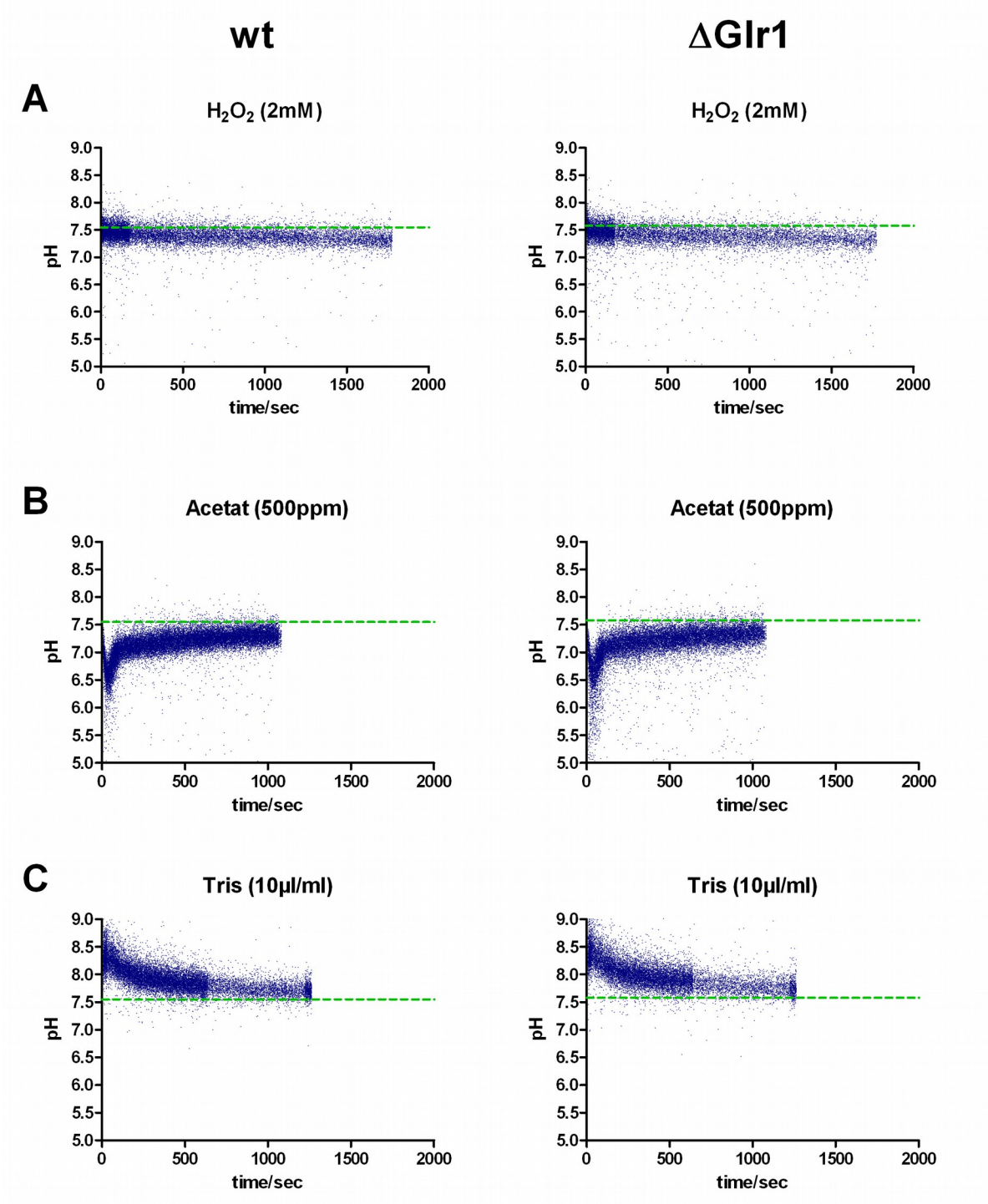

Fig.C53
Kinetics of pH changes measured by the pHluorin reporter under respiratory conditions in young cells. WΣ wild-type (left) and WΣ Δglr1 (right). WΣ Δglr1 cells were differentially tagged and measured parallel to the wild type. Green dashed lines mark the steady-state pH of untreated cells.
a.) Addition of 2 mM H_2O_2
b.) Addition of 500 ppm acetic acid
c.) Addition of 10 µl/ml 1M Tris

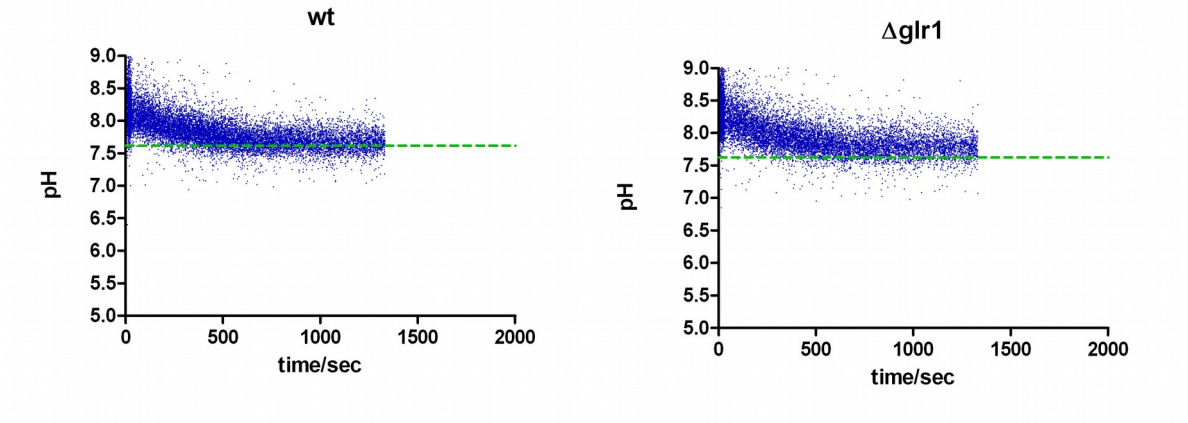

Fig.C54
Kinetics of pH changes measured by the pHluorin reporter in glucose medium in young cells. WΣ wild-type (left) and WΣ Δglr1 (right). Addition of 10 µl/ml 1M Tris. WΣ Δglr1 cells were differentially tagged and measured in parallel to the wild type cells. Green dashed lines mark the steady-state pH of untreated cells.

4 Redox & pH in young cells

4.1 Overexpression of Glr1 does not reduce the cytosol

As aging experiments are technically very challenging, time consuming and the amount of cells are limited, my next approach was to reproduce the observed phenotypes in young cells. Since the GSSG/GSH ratio decreased upon aging [Fig.C6], it was tempting to speculate that Glr1 might be up-regulated in old cells. To test weather overexpression of Glr1 leads to a more reduced glutathione-potential in young cells, glr1 genes from W303 and BY4741 (the protein from of W303 has an A213V substitution and the protein from BY4741 was found to have a E399V substitution compared to the S288C reference sequence), were cloned under the control of the TEF-promoter in pRS415 and expressed together with the redox-reporters.
Cells overexpressing Glr1 did not show a more reduced glutathione-potential than untransformed cells [Fig.C55a] but were more resistant to diamide treatment [Fig.C55b]. Overexpression was able to restore the redox-potential of a Glr1-knockout to wild-type-level and even lead to a better resistance to diamide, which means that Glr1 equilibrates the GSSG/GSH ratio independently of its concentration. The slightly different proteins from BY4741 and W303 both behaved identical.

The data suggests that up-regulation of Glr1 cannot explain the glutathione-reduction phenotype seen in old cells but is compatible with the observed diamide-resistance.

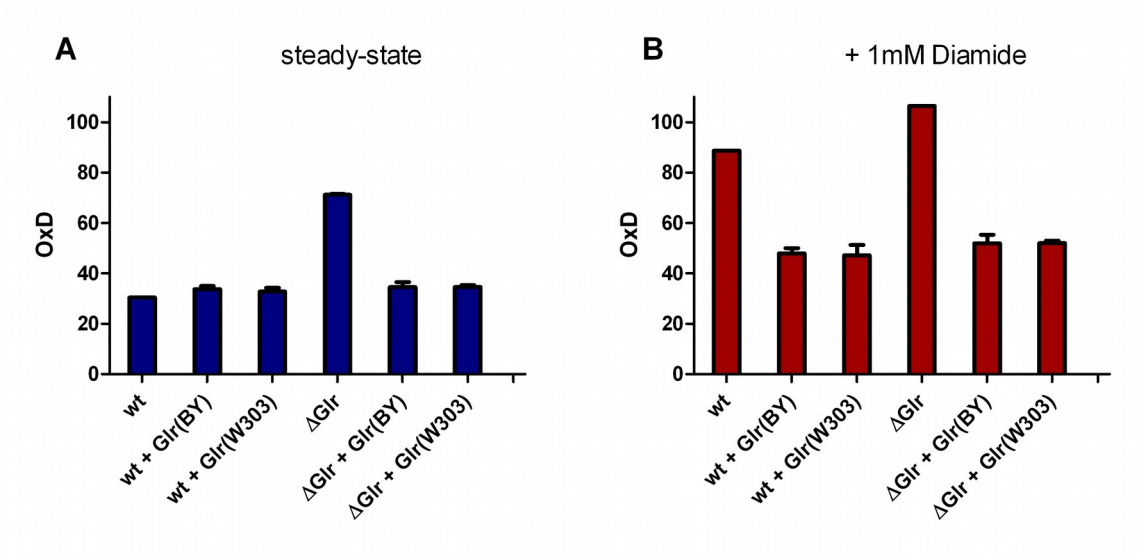

Fig.C55
Measurement of roGFP2-Grx1. Overexpression of Glr1 expressed from pRS413-TEF (cloned either from BY4741 or from W303) in WΣ wild-type and in WΣ Δglr1. Error bars represent the standard deviation. wt n=1; wt + Glr(BY) n=4; wt + Glr(W303) n=4; Δglr n=2; Δglr + Glr(BY) n=4; Δglr + Glr(W303) n=4.
a.) Measurement in untreated cells
b.) Measurement after addition of 1 mM diamide

4.2 Glr1 influences the redox kinetics

Next I wondered, if the dynamic properties of the redox response would be changed by the overexpression of Glr1. To have a more stable expression, the *glr1*-gene from W303 was cloned under the control of the TDH3-promoter and was integrated into the LYS2-locus. To directly compare overexpressing cells with wild-type in the same culture, a TagBFP was expressed in wild-type cells also harboring the roGFP2-Grx1 reporter.
The response after addition of H_2O_2 was followed in wild-type [Fig.C56a] and overexpressing cells [Fig.C56b]. In wild-type cells the percent oxidation first rapidly increased, peaked at around 40 seconds after addition of H_2O_2 and then returned close to the steady-state level. In the Glr1 overexpressing cells the initial increase and subsequent decrease in oxidation was much faster and the probe gets dramatically reduced below the steady state level until eventually returning to steady-state levels.

This data suggests that in the presence of high concentrations of Glr1 the glutathione-potential is more dramatically influenced by the presence of H_2O_2. Glr1 therefore seems to play an important role in linking H_2O_2 to the glutathione pool.

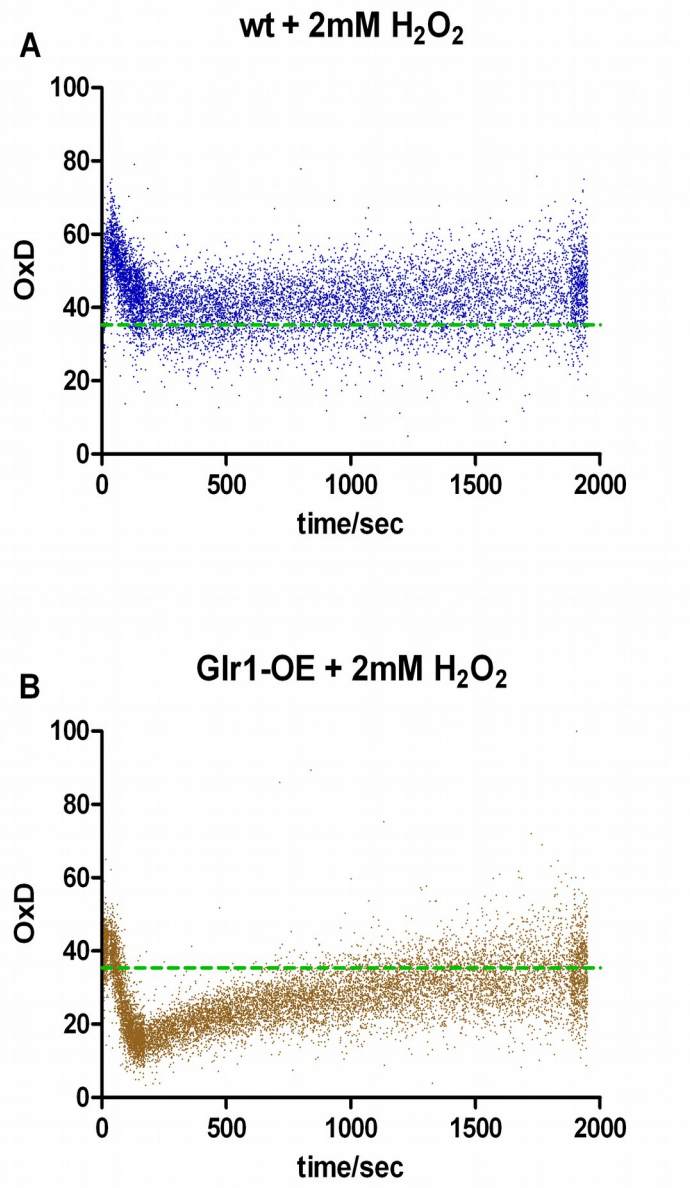

Fig.C56
Kinetics of roGFP2-Grx1 oxidation after addition of 2 mM H_2O_2. Dashed lines represents probe oxidation of untreated cells.
a.) WΣ wild-type
b.) WΣ overexpressing Glr1 from the GPD promoter (integrated in the genome). The cells were differentially tagged and measured in parallel to the wild-type.

4.3 pH dependency of Glr1

Looking carefully at the H_2O_2-kinetics obtained from the aging experiments [see Fig.C38] the data from old wild-type cells seems to be similar to the Glr1 overexpression in young cells except for the lack of the initial oxidation peak. On the other hand overexpression alone would not lead to a more reduced glutathione pool – so there must be another parameter, which impacts the response.

As I could see from previous data, which is also supported by literature (Ayer et al., 2013), treatment of cells with H_2O_2 leads to a decrease in cytosolic pH. Additionally, the cytosolic pH in old cells is also lower than in young cells. Although the roGFP2-Grx1 probe itself is reported to be independent of pH, the glutathione pool may show such dependence. To bring Glr1 back to this picture, I noticed that a *Δglr1* strain in an aging experiment shows the same pH drop as observed in the wild-type strain but no glutathione reduction in old cells. Based on these observations I hypothesized that Glr1 gets activated by lower pH and therefore would lead to a more reduced cytosol under acidic conditions.

To test this hypothesis, I co-cultured cells expressing either pHluorin and TagBFP or roGFP2-Grx1 and transiently lowered the cytosolic pH by adding acetic acid. It can clearly be seen that a drop in pH [Fig.C57-left] is accompanied by a strong reduction of the glutathione reporter when Glr1 is present [Fig.C57-right]. In the absence of Glr1, acidification rather has a slightly oxidizing effect.

To further support the hypothesis I reasoned that an altered pH may also alter the response to oxidants. A mixed culture was set-up: one cell-line expressing the roGFP2-Grx1 probe and the other cell-line the pHluorin reporter together with TagBFP. To alter the cytosolic pH I used the protonophor 2,4-Dinitrophenol (DNP) for acidification or increased the pH by adding Tris to the medium. After 300 seconds of pre-treatment, either H_2O_2 or diamide was added to the cells and the further response was monitored for the pHluorin [Fig.C58] and the roGFP2-Grx1 reporter [Fig.C59]. As expected DNP and Tris pre-treatment altered the cytosolic pH and the effect of the H_2O_2-shock on pH was directly dependent on the actual pH status of the cells. The diamide-shock had no additional effect on the pH.

Cells expressing the roGFP2-Grx1 reporter showed the known response when a neutral pre-shock was applied but when the pH was lowered by DNP, peroxide treatment led to oxidation in the same pattern as observed in old cells until the pH completely breaks down after about 1000 seconds. The lower pH shows little protective effect for a subsequent diamide-shock – at least in the recovery phase. When the pH is raised by a Tris pre-treatment, the glutathione-pool became severely oxidized and additional H_2O_2 did not lead to further oxidation. Similar results were obtained by the diamide-shock where only a marginal increase in oxidation of the glutathione-pool was observed.

The data strongly suggest that pH is the main regulator of the cytosolic glutathione-pool in fermentatively growing cells and the coupling seems to be accomplished by Glr1.

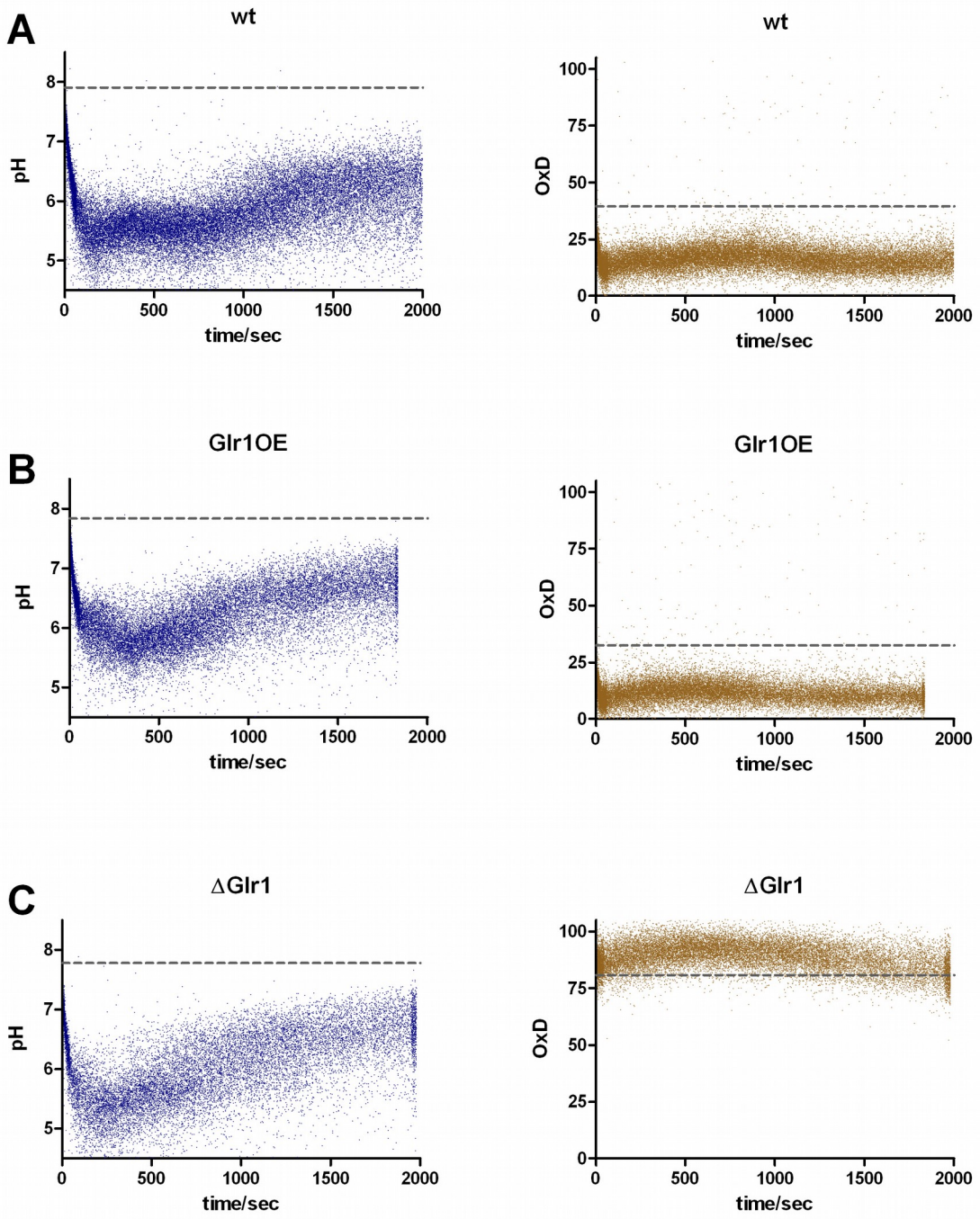

Fig.C57
Kinetics of changes in pH and relative oxidation of the GSH/GSSG buffer for cells grown in glucose medium after addition of 1000 ppm acetic acid. pHluorin measurements (left) and roGFP2-Grx1 (right). Cells were differentially tagged and measured in parallel. Grey dashed lines represent the values in untreated cells.
a.) WΣ wild-type
b.) WΣ overexpressing Glr1 from the GPD promoter (integrated in the genome)
c.) WΣ Δglr1

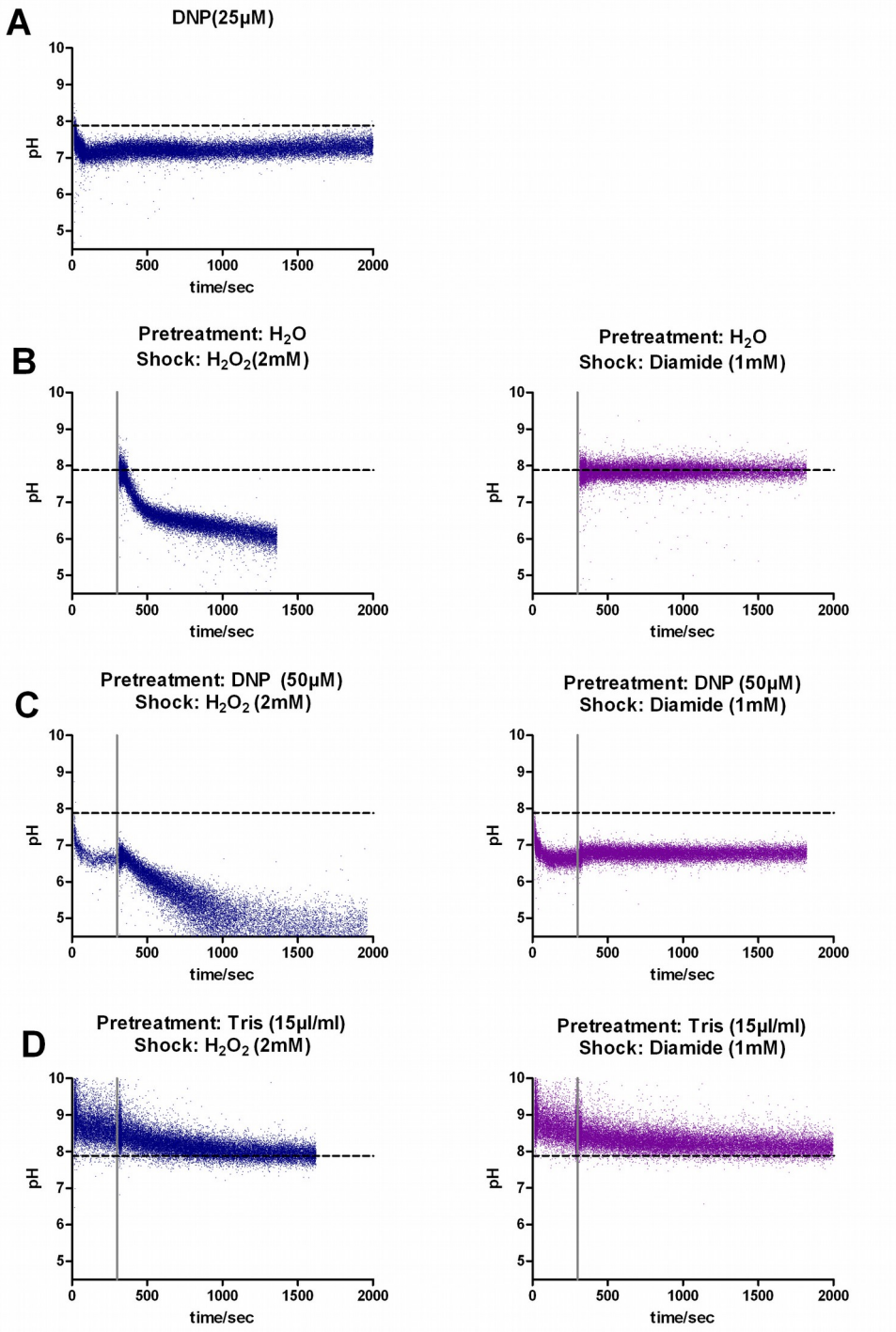

Fig.C58
Kinetics of pH changes with different pH-changing pre-treatments in WΣ grown in glucose medium. Dashed black lines represent conditions in untreated cells. Grey line marks the time-point of the application of oxidant treatment.
a.) Addition of 25 µM DNP
b.) Pretreatment with water and shock with 2 mM H_2O_2 (left) or 1 mM diamide (right)
c.) Pretreatment with 50 µM DNP and shock with 2 mM H_2O_2 (left) or 1 mM diamide (right)
d.) Pretreatment with 15 µl/ml 1M Tris and shock with 2 mM H_2O_2 (left) or 1 mM diamide (right)

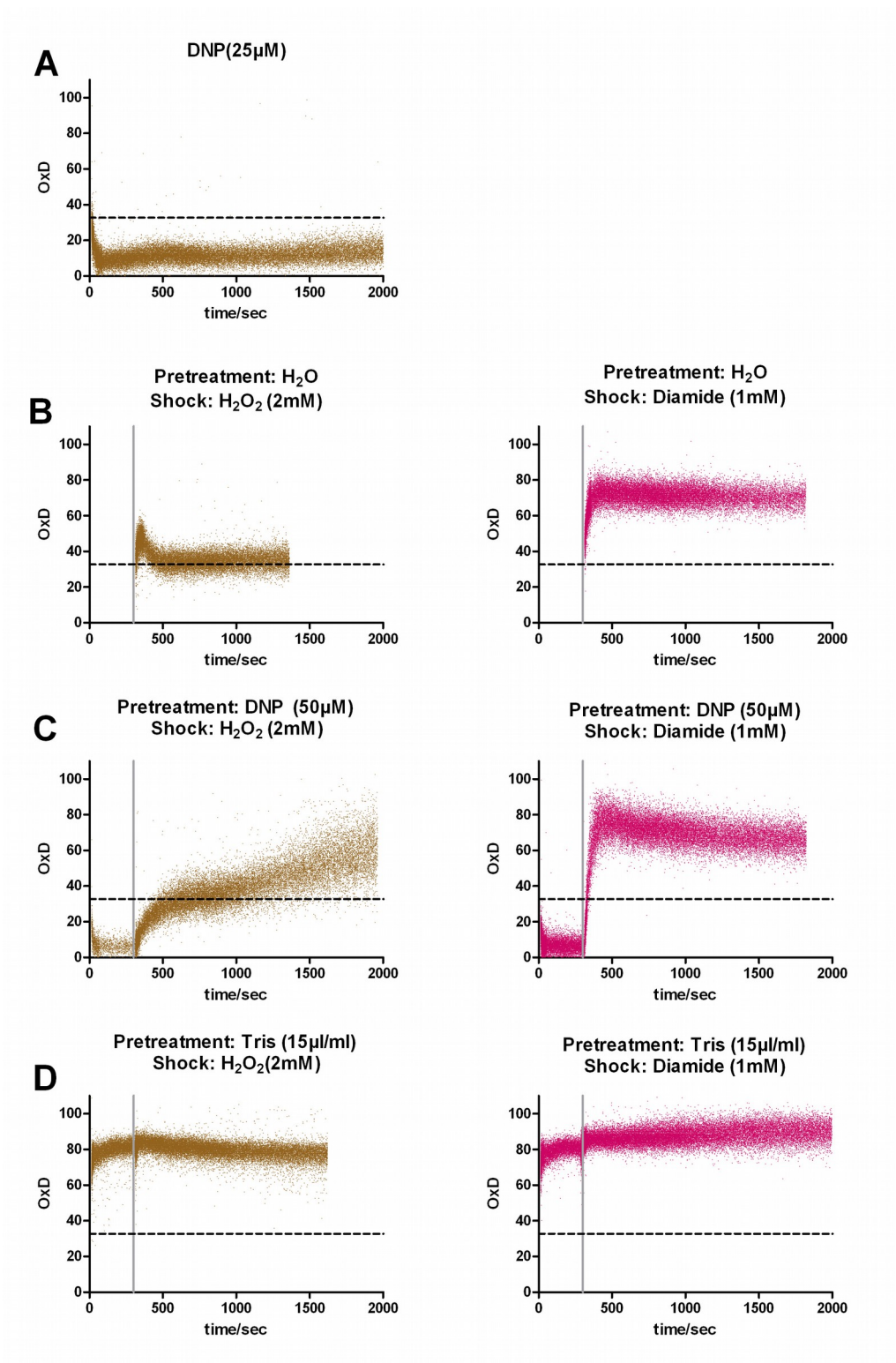

Fig.C59
Kinetics of GSH/GSSG-buffer oxidation as measured by roGFP2-Grx1 with different pH-changing pre-treatments in WΣ grown in glucose medium. Cells were differentially tagged and measured in parallel to the cells from [Fig.C58]. The layout and shocks are identical.

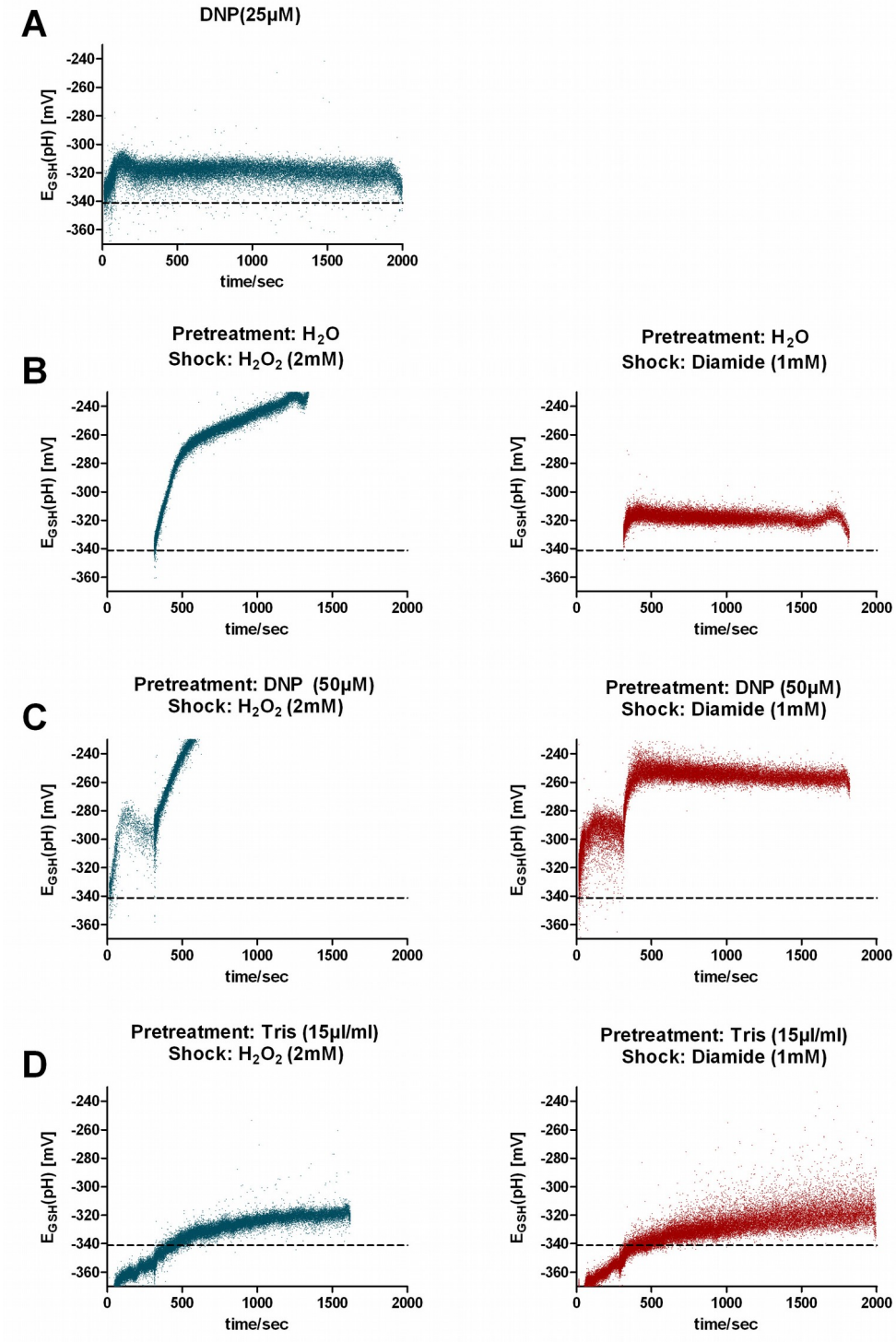

Fig.C60
pH corrected E_{GSH} kinetics with different pH-changing pre-treatments in WΣ grown in glucose medium. Data from [Fig.C58] was fitted with a spline function and used to calculate the pH corrected glutathione potential in the parallel recorded cells form [Fig.C59]. The layout and shocks are identical. The kinks on the end of the kinetics are artifacts from the spline-fitting.

4.4 Cellular pH does not protect against H_2O_2 induced damage

To visualize the change in kinetics of the chemical pH-corrected glutathione-potential, a spline-fit of the pHluorin data from [Fig.C58] was performed and the obtained values were applied to the data of the roGFP2-Grx1 reporter from [Fig.C59]. The results are shown in [Fig.C60]. This representation suggests that a pretreatment that lowers the pH would make cells extremely prone to peroxide induced oxidation whereas a higher pH would attenuate those effects. To test, whether this has any relevance for surviving a peroxide shock, a H_2O_2 concentration that kills about 90% of wild-type cells within 5 minutes was determined [Fig.C61]. A pre-shock of 300 seconds with H_2O, DNP, acetate or Tris was performed and then the cells were treated for additional 300 seconds with the determined H_2O_2 concentration. The sample was then immediately diluted tenfold to reduce the amount of residual H_2O_2 and subsequently spotted on YPD-plates in serial dilutions. The spot-test clearly shows that no protection or additional harm is applied by the pre-treatment [Fig.C62]. Interestingly, the Δglr1 strain is not more sensitive to H_2O_2, although its cytosol is already more oxidizing. Surprisingly, overexpression of Glr1 seems to protect from acute severe oxidative stress.
Taken together, the results indicate that survival after acute peroxide induced damage is not dependent on the cytosolic glutathione potential or the cytosolic pH.

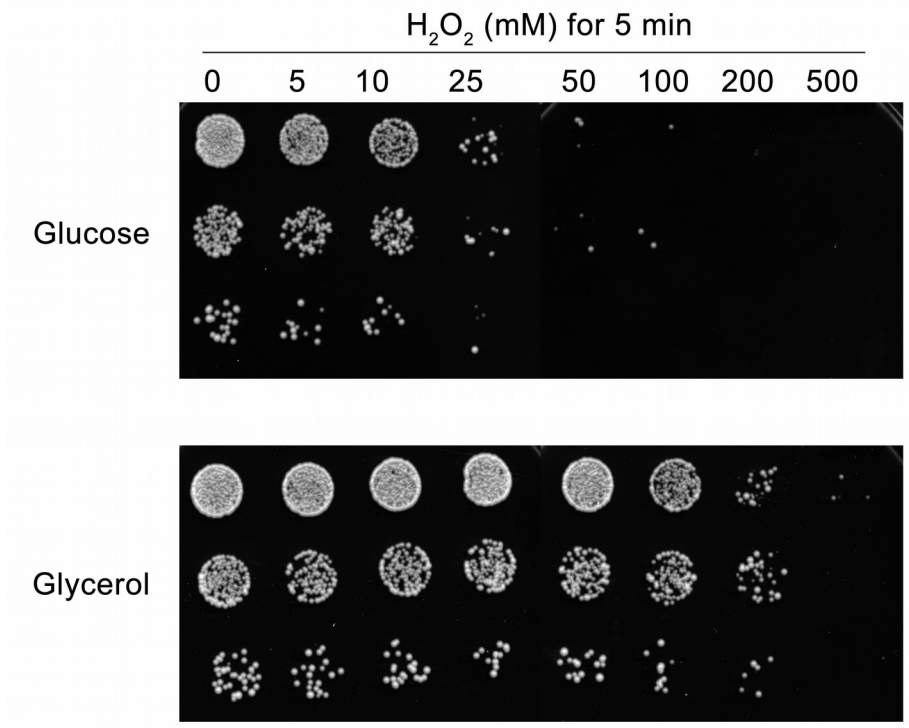

Fig.C61
Survival of acute peroxide stress. WΣ grown in glucose or glycerol/ethanol medium were treated with increasing amounts of H_2O_2. After 5 minutes exposure, the cells were spotted on YPD plates.

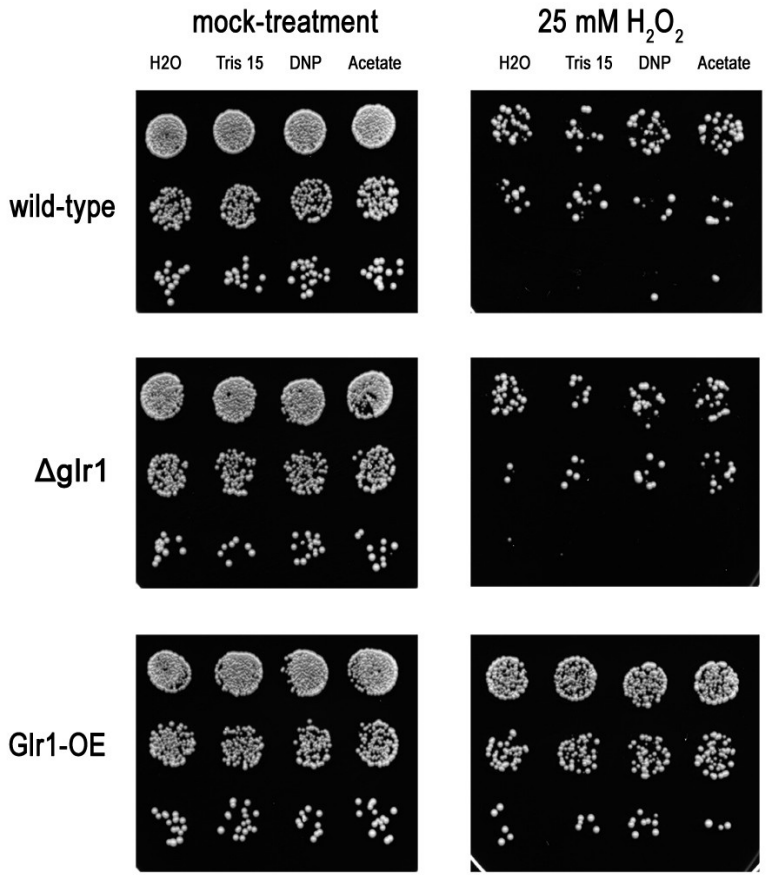

Fig.C62
Survival of severe peroxide shock after pH changing pre-treatment for WΣ wild-type (top), WΣ Δglr1 (middle) and WΣ overexpressing Glr1 (bottom). Cells were pre-treated for 5 minutes with H_2O, 15 µl/ml 1M Tris, 20 µM DNP or 500 ppm acetic acid. Mock treatment (left) and 25 mM H_2O_2 shock (right) was applied for 5 minutes prior to plating.

4.5 In vivo measurement of pH dependent Glr1 activity

When a cell acidifies, there are two opposing effects on the redox-potential. On the one hand, Glr1 gets activated and reduces the glutathione-pool; on the other hand, a lower pH chemically leads to a more oxidative redox-potential. We speculated that there may be an optimal pH where the redox-potential shows a minimum.

To address this question I gradually lowered the cytosolic pH by adding increasing amounts of DNP-protonophor to the cells or increasing it by the addition of 15µl/ml Tris and measured both the glutathione and the pH-reporter after 30 minutes of equilibration.
The data [Fig.C63a] shows a clear pH dependence of the uncorrected glutathione-potential with a minimum at around pH 6.5. Glr1 overexpression amplified this effect, whereas the uncorrected glutathione-potential in the Δglr1-strain did not show any substantial pH dependency. When the pH correction is applied to the measured potential [Fig.C63b] it becomes evident that the chemical effects of oxidation are always stronger than any reduction by Glr1 and that no local minimum exists.
The measurements were repeated with cells grown under respiratory conditions [Fig.C63c,d]. Here the steady state is already near the maximum of Glr1-activity so further lowering of the

pH did not lead to a stronger reduction. On the contrary, raising the pH with Tris led to oxidation. Again overexpression of Glr1 enhanced the effect whereas deletion showed no pH dependency within the physiologic range. It should be mentioned here that pHluorin calibration below pH 5.5 is not accurate anymore. Therefore all the lower values are just based on extrapolation of the fitting.
These results clearly show that the cytosolic glutathione pool is mainly regulated by the pH dependence of the Glr1 activity.

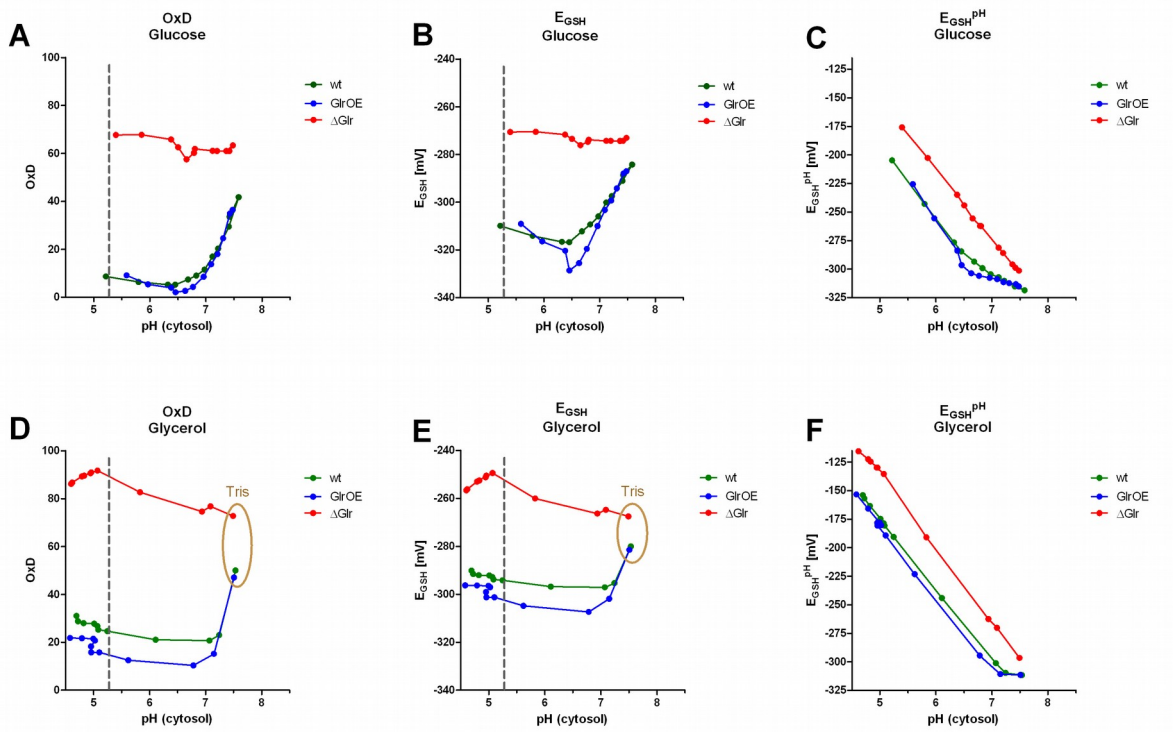

Fig.C63
The pH dependency of the glutathione pool. Differentially labeled cells expressing roGFP2-Grx1 and pHluorin respectively were treated with different amounts of DNP protonophor or 1M Tris for 30 minutes prior to measurement. The measured pH was plotted against the measured glutathione potential for WΣ wild-type, WΣ overexpressing Glr1 and WΣ Δglr1. Dashed grey lines indicate the limit for accurate pH detection by pHluorin. Encircled data-points should emphasize that the oxidation is due to a pH upshift by the addition of Tris.
a.) Probe oxidation for cells grown in glucose medium
b.) Uncorrected glutathione potential for cells grown in glucose medium
c.) pH corrected glutathione potential for cells grown in glucose medium
d.) Probe oxidation for cells grown under respiratory conditions
e.) Uncorrected glutathione potential for cells grown under respiratory conditions
f.) pH corrected glutathione potential for cells grown under respiratory conditions

4.6 pH dependence of roGFP2-Orp1

Similar to the roGFP2-Grx1 reporter I investigated whether the roGFP2-Orp1 reporter would also be affected by the cytosolic pH. The results for fermentatively growing cells are shown in [Fig.C64a]. Within the physiological pH range only little effects on the reporter were observed. Only at very low pH or when the cytosol pH was increased above the physiological range by

the addition of Tris, the roGFP2-Orp1 reporter showed a stronger oxidation. Overexpression of Glr1 showed the same pH dependency at a slightly more reduced reporter oxidation. No influence on roGFP2-Orp1 was observed in the Glr1 deletion background where the reporter oxidation is already at about 90%. Cells grown in glycerol medium exhibit a similar phenotype although intermediate pH values could not be achieved by the addition of DNP protonophor [Fig.C64b].

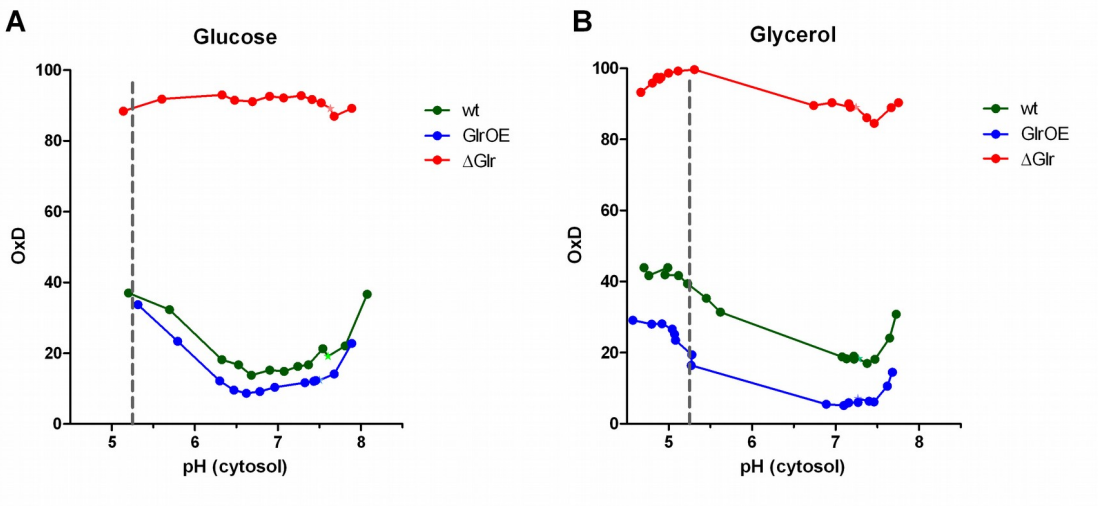

Fig.C64
The pH dependent oxidation of roGFP2-Orp1. Differentially labeled cells expressing roGFP2-Orp1 and pHluorin respectively were treated with different amounts of DNP protonophor or 1M Tris for 30 minutes prior to measurement. The measured pH was plotted against the measured roGFP2-Orp1 oxidation for WΣ wild-type, WΣ overexpressing Glr1 and WΣ Δglr1. Dashed grey lines indicate the limit for accurate pH detection by pHluorin. The differentially colored asterisk-shaped data-points indicate untreated cells. A pH-upshift was achieved by the addition of Tris.
a.) Probe oxidation for cells grown in glucose medium
b.) Probe oxidation for cells grown under respiratory conditions

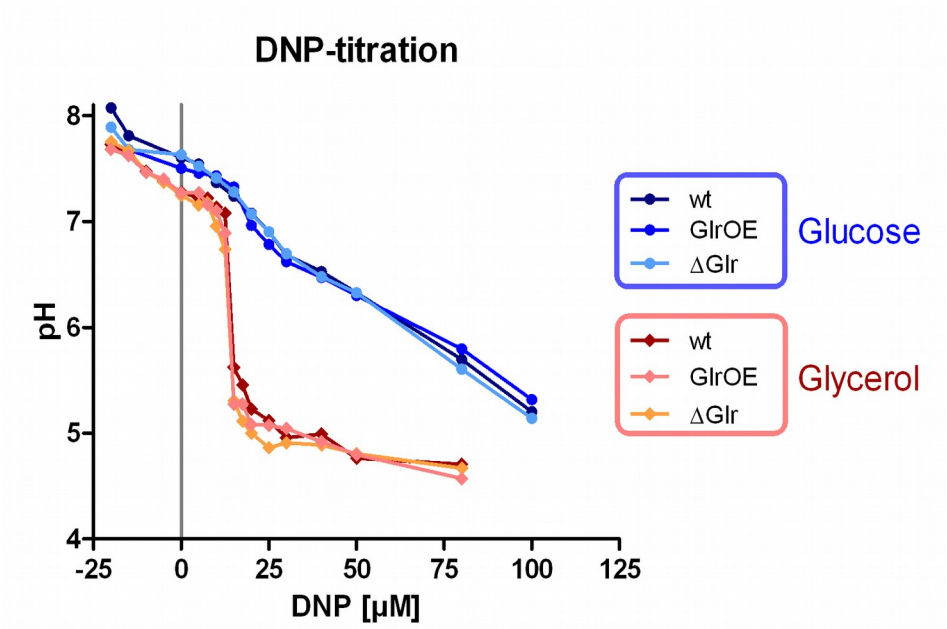

Fig.C65
Titration of cellular pH by DNP and Tris. Data-points for the pHluorin reporter are taken from [Fig.C64]. Positive values on the x-axis indicate the amount of DNP in µM, negative values indicate the amount of 1M Tris added in µl/ml.

4.7 Respiring cells are highly sensitive to protonophor

When treated with increasing concentrations of DNP protonophor, the cytoplasmic pH of cells growing on glucose gradually declines. Though the same range of DNP-concentrations was used on the glycerol-culture, the resulting cytosolic pH was dramatically different. Plotting the pH against the applied DNP-concentrations [Fig.C65] reveals that respiratory-grown cells are extremely sensitive to the DNP-protonophor compared to the fermenting cells (the negative value on the x-axis indicates the addition of 1M Tris in µl/ml instead of DNP). The most likely explanation for that is a short-circuit of the mitochondria and a break-down of ATP-production. Without ATP there will be no energy available for the plasma membrane ATPase Pma1 which pumps out protons. Cells with glucose as carbon source are not depending on the mitochondrial membrane-potential for ATP-production and therefore are still able to export protons.

If the proton concentration of the cytosol is relevant for the mitochondria as well, an outside pH change should be directly transferred to the mitochondria. To demonstrate that the mitochondrial intermembrane space is directly coupled to the cytosolic pH a response-kinetic was recorded by applying a Tris or an acetate shock to cell expressing either cytosolic or intermembrane-targeted pHluorin (Su9-targeting sequence) [Fig.C66]. It can clearly be seen that both intermembrane space and cytosol follow the same kinetic although at slightly higher pH in the mitochondrial intermembrane space.
Using DNP treatment and the pH-kinetics as readout for Pma1-activity it should be possible to estimate the ATP production of cells. This would be interesting to test in old cells.

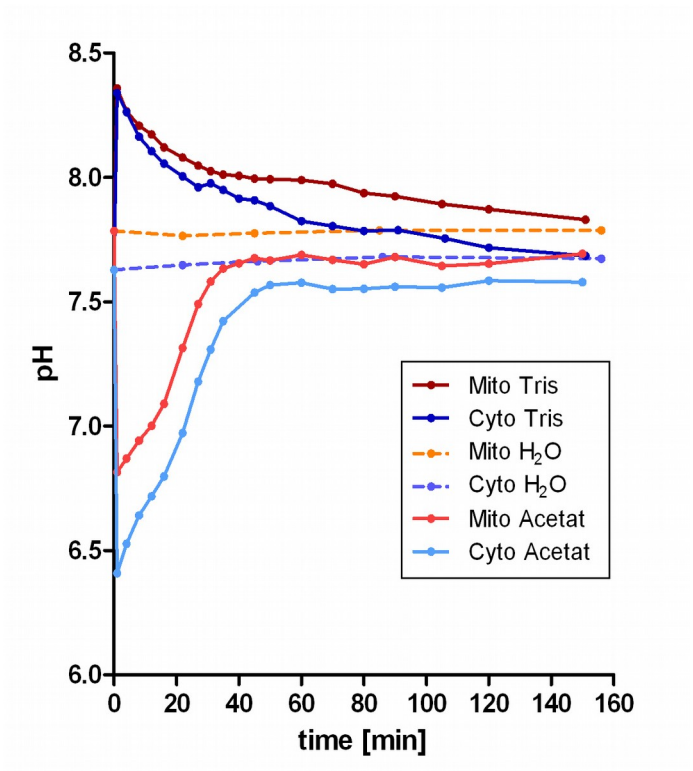

Fig.C66
Long term pH kinetic after addition of 15µl/ml 1M Tris, H_2O or 800 ppm acetic acid to pHluorin expressing WΣ wild-type cells. pHluorin was either expressed in the cytosol or in the mitochondrial inter-membrane space (via a Su9 targeting sequence).

5 Senescence

During a replicative aging experiment, more and more cells cease to divide but still persist in the culture for a considerable time interval – seen by the broadening of the budscar-distribution. Although the reasons for that may be plentiful, it is fact that the old culture becomes dominated by cells in a phase of post-replicative senescence. To test if the observed phenotypes are a general feature of senescence, I made use of a model-system for senescence caused by telomere shortening.

Telomeres in yeast are usually about 350 base pairs long and their length is maintained by the telomerase holo-enzyme and a complex regulatory process (reviewed in (Kupiec, 2014)). Deletion of the gene encoding the telomerase reverse transcriptase-component Est2 leads to the shortening of telomeres and subsequently to cell-cycle arrest and cell death. Some cells, however, escape from this fate by using telomerase independent ways to extend their telomeres. These mechanisms are based on recombination events between telomeric sequences using them as a template for extension by the DNA repair-machinery [reviewed in (Conomos et al., 2013). The additional knockout of the recombination protein Rad52 abolishes this alternative telomere-extension (Lundblad and Blackburn, 1993).

5.1 Creation of the senescent strain

The problem with a senescent strain is that it cannot be used for long time as it progressively "ages". A classical way to maintain this strain is to sporulate a diploid strain, which is haplo-insufficient of the respective genes. Since many test-crosses have to be done to chose the right spores, I tried a rescue-plasmid based approach.

I constructed a rescue-plasmid with a URA3-marker containing the genes encoding Est2 and Rad52 with their natural promoters and a TagBFP under control of the TDH3-promoter. This plasmid was transformed into WΣ wild-type and then the endogenous est2 and rad52 genes were knocked out subsequently using nourseothricin and hygromycin selection markers. Clones from both knockout orders ([rad52::NatMX then est2::HphNT] and [est2::NatMX then rad52::HphNT]) were collected and confirmed by sequencing using PCR-primers not present in the rescue plasmid. The redox and pHluorin reporters were then integrated into the HIS3-locus and confirmed by FACS-analysis. Afterwards the strains were plated on 5-FOA and individual clones were picked for the senescence experiments. The whole procedure is outlined in [Fig.C67].

5.2 Procedure for the senescence experiments

The senescence experiments were conducted as followed:

- Growing the strain with selection for the rescue-plasmid
- Streaking on a synthetic complete plate containing 5-FOA
- Picking a colony and re-streak in a patch to grow for one day
- Harvesting the patch and determining the cell-density by FACS (events/sec at medium flow-rate)
- Inoculation of cells into 5 ml synthetic medium to the desired density (based on the FACS-measurement)

- Growing the cells for about 20-24h at 25°C
- Taking aliquots for measurements and adding propidium-iodide (f.c. 0.5 - 1µg/ml)
- Measurement of the reporters and determining the cell density (events/sec at medium flow-rate)
- Re-inoculation from the remaining culture into fresh medium to a defined density
- Repeating the steps until the vast majority of cells is dead

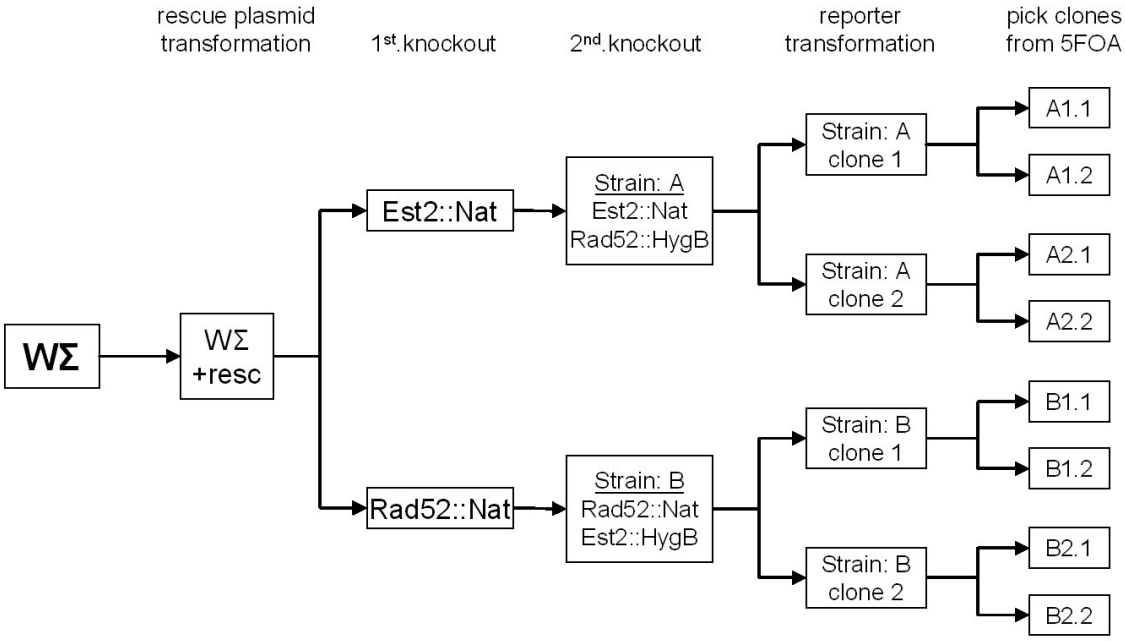

Fig.C67
Procedure of generating the strains for senescence experiments. To prevent premature senescence or adaption, a rescue plasmid containing the est2 and rad52 genes were introduced into WΣ first. In a second and third step, the chromosomal genes of est2 and rad52 were knocked out sequentially. The clones derived from both knockout orders were transformed with the reporter plasmids and two of each transformants were picked for rescue-plasmid elimination on 5FOA. Again two colonies from the 5FOA selection were chosen from each clone and subjected to a senescence experiment.

5.3 Experimental problems

The senescence experiments turned out to be more challenging than expected. The major drawback compared to the replicative aging-experiments was that the senescent cells lack an internal control of "young cells" grown in the same culture. This is not possible because each senescent clone which has lost the rescue-plasmid is unique and shows its own "kinetic of aging". In addition, a co-cultured wild-type would overgrow the senescent strain after several hours. Another problem is the autofluorescence which can not be coupled to a time-axis because of the individuality of the clones. Last, the redox-normalization (fully oxidized and fully reduced) would have to be measured directly on the senescent cells in contrast to the replicative experiments were this normalization was always performed on the internal young cells. At the first glance this appears to be an advantage but one has to consider that the senescent cells are already frail and application of high-molar DTT or diamide could change

their spectral properties or even kill a subset of cells. Moreover, the uncertainty in the autofluorescence will contribute three times to the calculation and last the pipetting errors will multiply. The compromise I resorted to was a parallel culture of wild-type cells from which the normalization was used but for comparison both types of representations will be shown (except for pHluorin where the calibration-curve was determined in an independent experiment on wild-type cells and then transferred to the aged cells).

5.4 Vitality parameters of a senescent culture

By keeping track on the density and dilution of the culture, a growth curve can be drawn over the whole senescent lifespan [Fig.C68a]. Keeping in addition the culture always logarithmic, the population doubling rate (PDs/h) can be calculated [Fig.C68b] and finally the fraction of living cells can be accessed by the flow-cytomertic measurement itself [Fig.C68c]. Colony forming cannot be addressed in these strains because the offspring of senescent cells will not rejuvenate and the colony size would get awfully small.

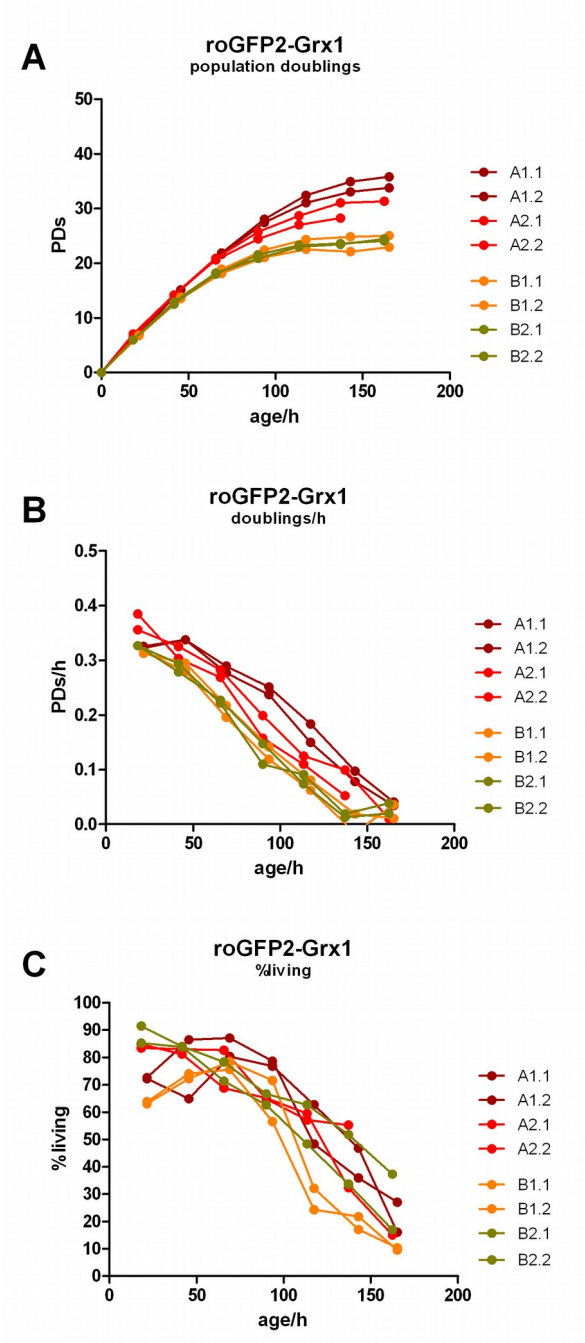

Fig.C68
Vitality parameters of WΣ Δrad52 Δest2 cells expressing the roGFP2-Grx1 reporter during senescent aging. Parameters for the individual clones [see Fig.C67] are shown.
a.) Population doublings of the culture since inoculation
b.) Averaged population doubling time over the senescent process
c.) Fraction of living cells determined by fluorescent reporter expression

5.5 Autofluorescence in senescent cells

In the model-system I used, senescence is triggered by the shortening of telomeres. The shortening starts when telomerase is lost. Since yeast has 16 chromosomes and not all have identical telomeres, the onset of senescence is strongly dependent on the initial conditions when the individual clone lost its rescue plasmid before getting picked for the experiment. Therefore, the time-axis is not a good choice to pin-down a value for the autofluorescence. When telomeres are getting short, cells experience a crisis and division slows down. Although no statements about individual cells can be made in the experimental setup, the average autofluorescence correlates well with the doubling time of the culture [Fig.C69]. A single exponential equation was fitted to the data and used to subtract autofluorescence from the fluorescence readings of cells harboring the reporters.

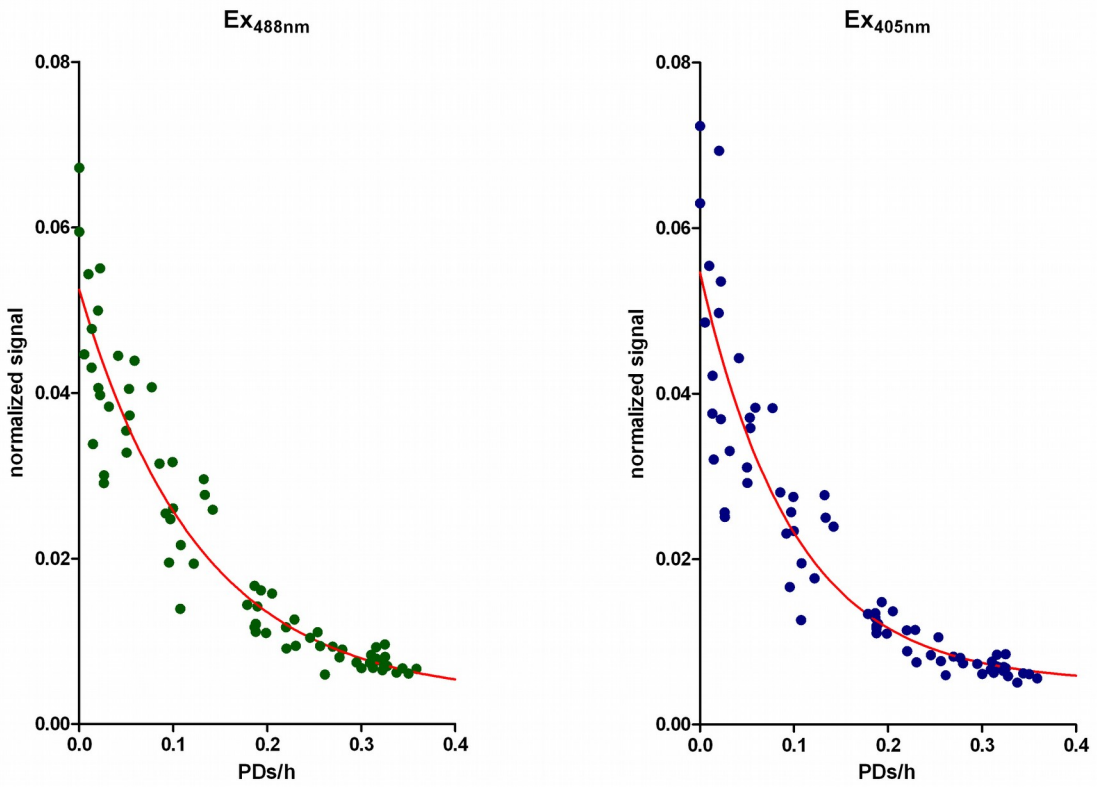

Fig.C69
Autofluorescence signal of WΣ Δrad52 Δest2 cells plotted against the averaged doubling time. The data was fitted by a single exponential function, which was used to subtract autofluorescence of reporter-expressing cells. The two relevant channels are shown.

5.6 The redox-state of senescent cells

Redox measurements with the glutathione reporter were determined in logarithmic cultures derived from different clones of the strain construction procedure (see above). The parameters of the population doublings, the doubling-rate and the fraction of living cells is given in [Fig.C68] and the results of the redox reporter is shown in [Fig.C70a]. A second representation

of the data is shown in [Fig.C70b] where the redox calibration of the parallel wild-type culture is transferred to the senescent strain (see above in 'Experimental problems').

It immediately becomes obvious that the redox-state differs in each clone except for the clones that were picked from the same 5FOA-plate. This means that either the clonal branches after the second knockout were heterogeneous or that transformation with the reporters somehow altered the redox-homeostasis. I have to emphasize here that I never observed this strong heterogeneity in wild-type cells. A rough uncalibrated ratio-plot of several roGFP2-Grx1 transformations of wild-type cells is given in [Fig.C71]. The cells from the senescence experiment are shown in color. Since Rad52 is a protein essential for recombination, expression from the rescue plasmid may not create a wild-type situation and making cells more prone to artifacts caused by the transformation procedure.

Neglecting the absolute values, the trend of oxidation did not indicate any substantial changes in these senescent cells. The large scattering in the "B" clones of the glutathione reporter can be explained by the poor signal to noise ratio - or in terms of the experiment, the fluorescence to autofluorescence ratio - and the ratio even gets smaller when DTT is applied to the cells. These values are given exemplarily for the most critical 405 nm excitation [Fig.C70c]. The negative OxD-values of the "B2" clones indicate that autofluorescence was overestimated for Ex_{405nm} in this case. Since the plasmid backbone was pRS303, different expression levels are due to multiple integrations of the reporters. In wild-type cells, where autofluorescence is well defined, the slight decline in the signal to autofluorescence ratio is most likely the effect of losing adjacent copies in some cells by recombination. For the senescent cells recombination events are unlikely because of the missing rad52 gene.

Next, the roGFP2-Orp1 was tested in the senescent-model. Results are shown in [Fig.C72] (at this time only half of the clones were tested). Here the signal to autofluorescence ratio was more opportune so the differences between the two normalization approaches are much smaller [Fig.C73]. There seem to be no change in the peroxide production over the whole senescent lifespan. It did not escape my notion that the vitality parameters of the reporter are cross-correlated between the 'A' and 'B' clones. Since a mix-up or a cross-contamination could not be ruled out, the data should be considered only preliminary.

Taken together, from the data it can be concluded that the glutathione-pool seems to remain stable in the telomere-based senescent model but the absolute values depend on the history of the strain. Also senescent cells don't seem to experience H_2O_2 stress as they age. The measurement shows that the accuracy of the redox data is strongly dependent on the reporter brightness and the model of the autofluorescence.

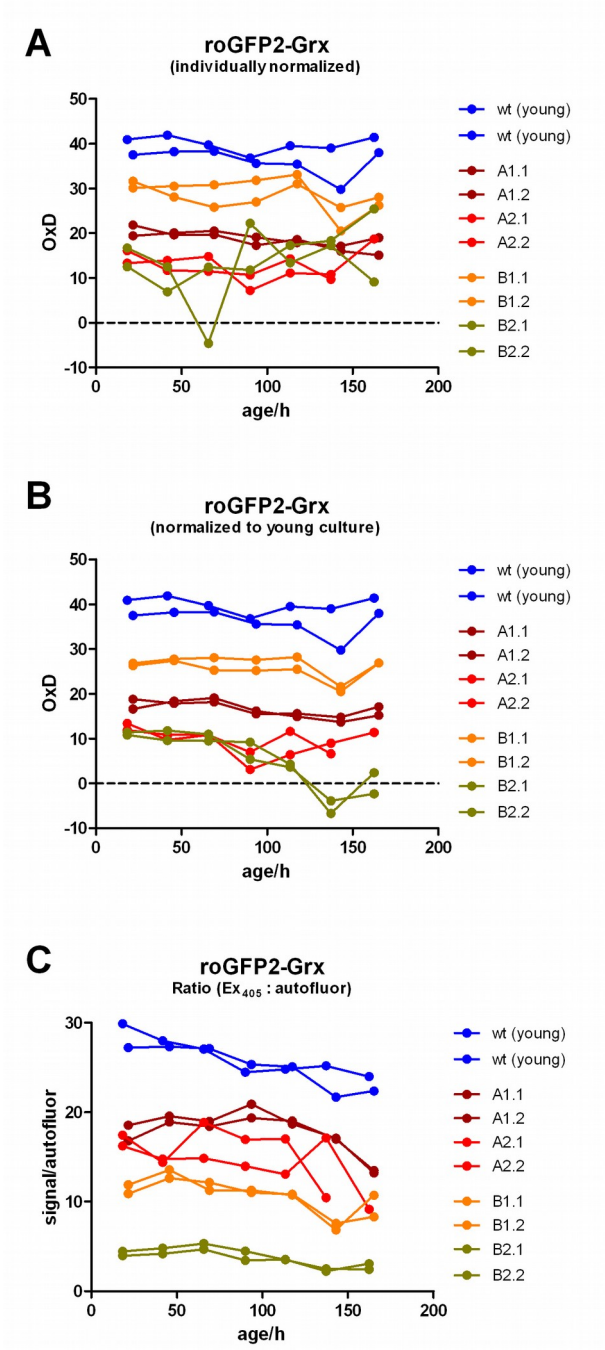

Fig.C70
The glutathione pool measured by roGFP2-Grx1 during senescent aging in WΣ Δrad52 Δest2 cells. Vitality parameters of the individual strains are given in [Fig.C68]. Numbering of the clones refers to [Fig.C67].
a.) Probe oxidation calculated from the clone-specific calibration
b.) Probe oxidation calculated from the averaged calibration of the young culture.
c.) Visualization of the reporter fluorescence to autofluorescence ratio of the individual clones. Only the critical spectral channel (excitation at 405 nm) is shown.

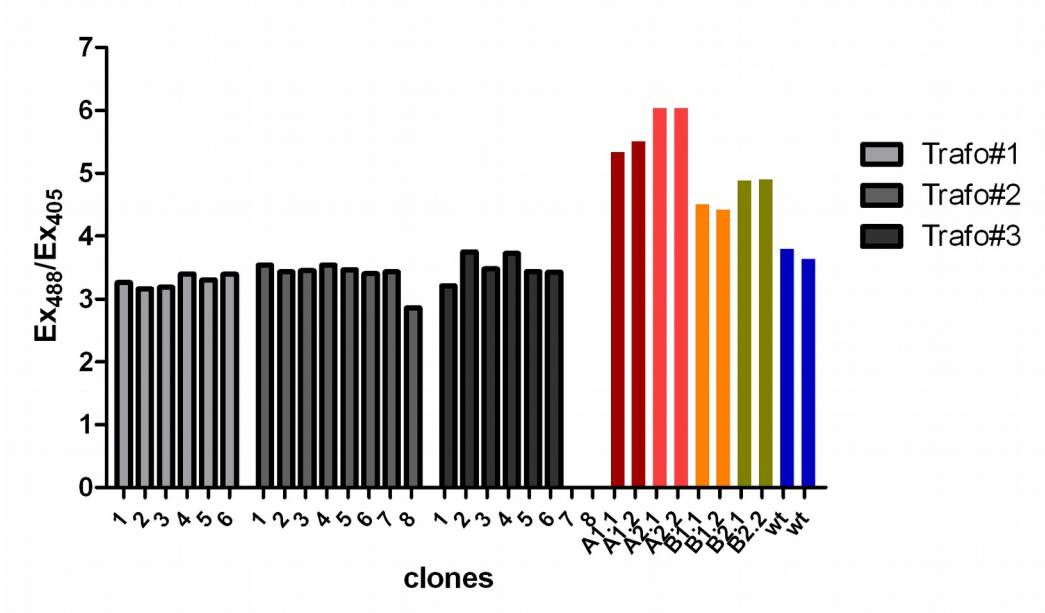

Fig.C71
Clone to clone variance of roGFP2-Grx1 transformed cells. The fluorescent ratio from the two excitations is shown. Grey bars represent individual clones from three different transformations. The colored bars show the values from the WΣ Δest2 Δrad52 strains (numbering of the clones refers to [Fig.C67]) and the wild-type control (blue).

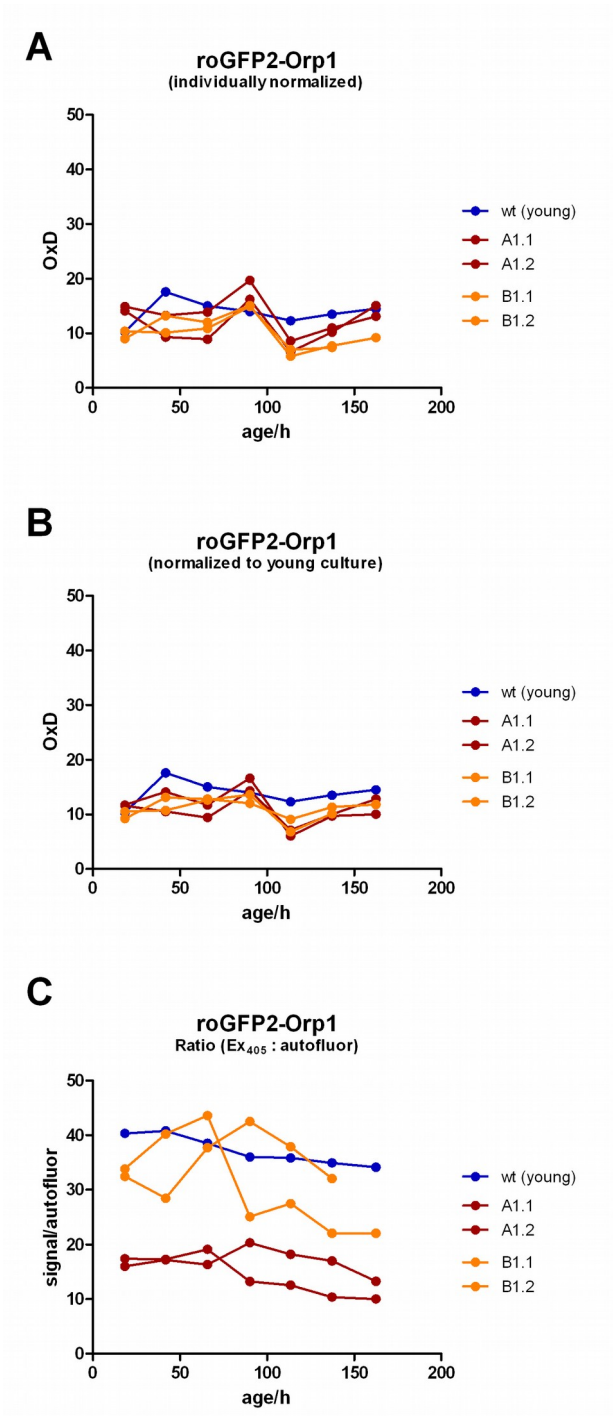

Fig.C72
Measurement of roGFP2-Orp1 during senescent aging of WΣ Δrad52 Δest2 cells. Vitality parameters of the individual strains are given in [Fig.C73]. Numbering of the clones refers to [Fig.C67].
a.) Probe oxidation calculated from the clone-specific calibration
b.) Probe oxidation calculated from the averaged calibration of the young culture.
c.) Visualization of the reporter fluorescence to autofluorescence ratio of the individual clones. Only the critical spectral channel (excitation at 405 nm) is shown.

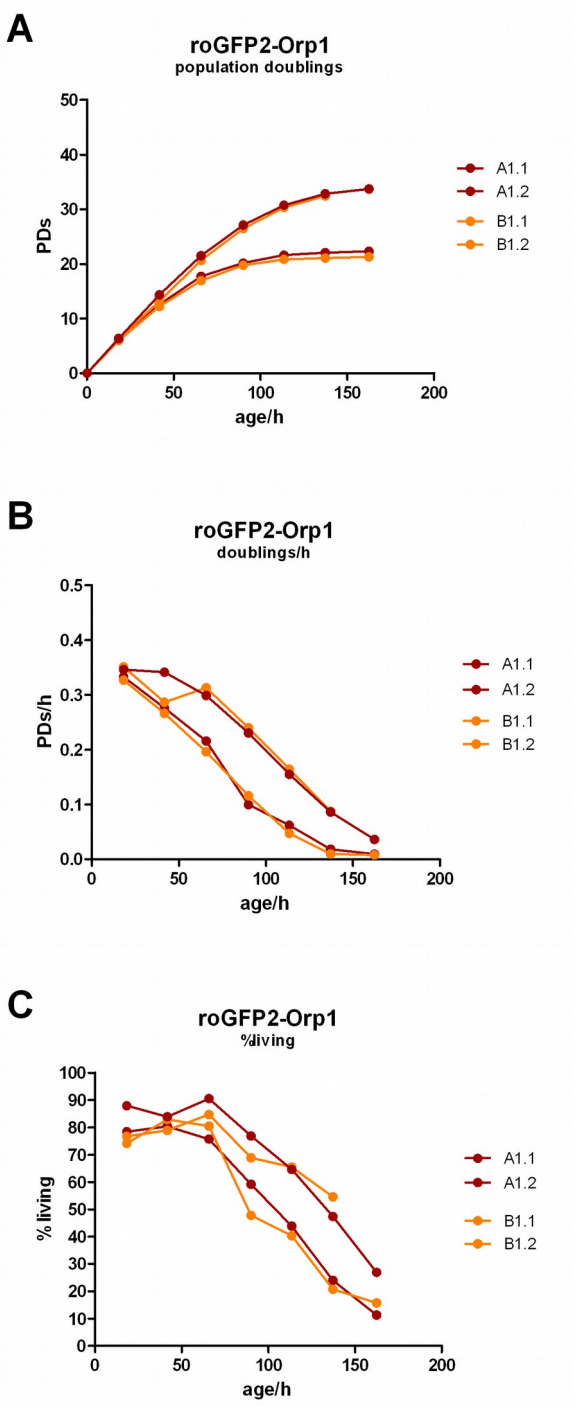

Fig.C73
Vitality parameters of WΣ Δrad52 Δest2 cells expressing the roGFP2-Orp1 reporter during senescent aging. Parameters for the individual clones [see Fig.C67] are shown.
a.) Population doublings of the culture since inoculation
b.) Averaged population doubling time over the senescent process
c.) Fraction of living cells determined by fluorescent reporter expression

5.7 pH measurement in senescent cells

As the cytosolic pH leads to Glr1-mediated glutathione reduction it is interesting to see, if the senescent cells, which appear to have a constant glutathione phenotype, also maintain pH constant. To test this, the pHluorin reporter was measured in the senescent model strains. The results of the pH distribution are plotted in [Fig.C74]. Unexpectedly, similar to replicative aging an acidification was observed. With the pHluorin reporter the signal was always way stronger than the autofluorescence (minimum 34 fold, maximum 127 fold) so the results are more reliable in this respect.
From the data it can be concluded that cytosolic acidification is a common feature of cellular frailty in yeast (seen both in replicative aging and senescence) but the glutathione homeostasis might be differentially regulated in different forms of aging.

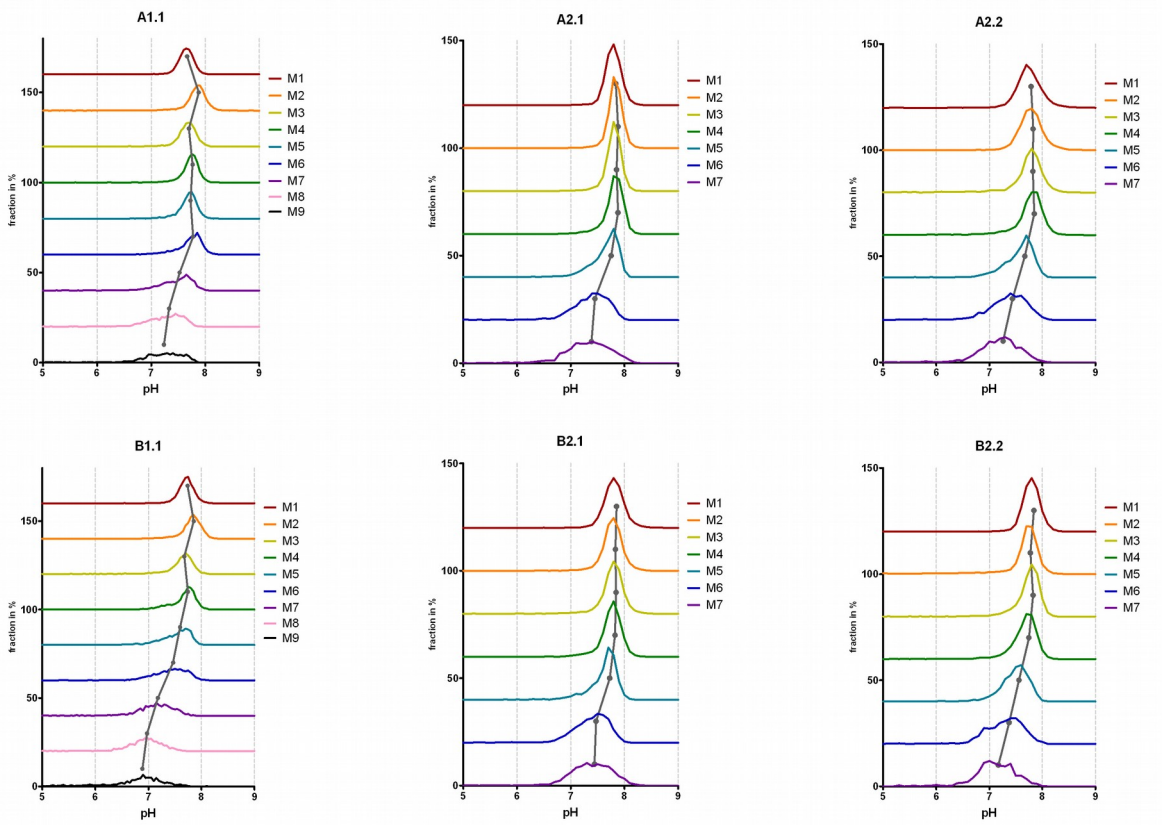

Fig.C74
The pH changes during senescent aging of WΣ Δrad52 Δest2 cells measured by the pHluorin reporter. The colored histograms show the pH distribution of individual cultures at different ages of the experiment (M1 = young to M9 = oldest). The connected grey data-points represent the population average. Numbering of the clones refers to [Fig.C67].

6 Discussion

The key question concerning replicative aging is whether intracellular oxidative stress is a cause or a consequence of the aging process. Cells contain many different reactive intermediates, several organelles with different physiology and considerable adaptations in the buffering-systems. Genetically encoded environmental sensitive reporters are therefore valuable tools to monitor the condition in an organelle-specific manner. Combined with an aging assay of single-cell resolution alterations can be spatio-temporally localized and this key question can be addressed.

6.1 Lifespan

6.1.1 Expression of roGFP2-Orp1 extends lifespan

Parallel to the reporter readout, observation of the vitality parameters gives additional information about the strain background and the age associated changes. The first striking observation is the longevity phenotype of cells expressing the cytosolic roGFP2-Orp1 probe [Fig.C4]. Orp1 (or its alternative names Gpx3 or Hyr1) is an important sensor for peroxide stress. Upon peroxide induced thiol oxidation it is able to transfer the oxidation to the Yap1 transcription factor by a transient intermolecular disulfide bridge (that was also the reason why this protein was chosen for the fusion with roGFP2). Resolving of the intermolecular disulfide leads to an intramolecular disulfide formation in the Yap1 transcription factor, which then masks its nuclear export signal. As a result Yap1 is trapped in the nucleus and activates genes for the peroxide stress-response. Overexpression of Orp1 as a part of the peroxide reporter could very well lead to a lifespan extension by increased peroxide resistance. However, the oxidation of Yap1 by Orp1 relies on the close proximity of the two proteins. This proximity is mediated by the Ybp1 protein, which was shown to be crucial for efficient Yap1 activation by Orp1. In the absence of Ybp1, a less efficient Yap1 activation is still possible by the peroxiredoxin Tsa1.
In the W303 background the ybp1-gene harbors a frameshift mutation at position 729 which leads to a short version of Ybp1 that is no longer able to promote Yap1 activation and therefore makes it solely dependent on Tsa1 (Tachibana et al., 2009). Seen in this light, lifespan extension by Orp1 overproduction is unlikely to work through Yap1. This is supported by the fact that roGFP2-Orp1-mediated lifespan extension is of similar magnitude in the W2Σ strain where Ybp1 was restored. In fact, W2Σ even accomplished a lower number of divisions than its parental strain WΣ [Fig.C16]. Whether Orp1 overexpression is able to induce the Yap1-mediated transcriptional response in WΣ could not be tested in this study.

6.1.2 Caloric restriction in WΣ makes cells more durable but not older

There is no doubt that caloric restriction is a universal condition, which increases lifespan in organisms from fungi to mammals (reviewed in (Fontana et al., 2010); (Roth and Polotsky, 2012). However, in WΣ the average number of budscars over time did not indicate any substantial increase in divisions when grown under nutrient restricted conditions [Fig.C10a]. On the other hand, the fraction of living cells [Fig.C10b] was slightly superior to cells grown in high glucose and paradoxically the ability to divide was significantly (F-test $P=5.2*10^{-9}$) enhanced [Fig.C10c]. One explanation would be that restricted cells divide slower when they

are old and thus shifting the vitality parameters to later time-points. Another explanation would involve the cytosolic acidification. Although not measured under caloric restriction conditions, it can be inferred from the identical behavior of the presumably pH-dependent phenotype of the roGFP2-Grx1 reporter [Fig.C11] and [Fig.C47a,b] that the cytosol acidifies under caloric restriction conditions in a similar manner as in cells grown at 2% glucose. If caloric restriction would just make WΣ more durable under low-pH conditions, then outgrowth to colonies at the more neutral pH of the YPD-plate (was measured to be about pH 6.2) could trigger the old cells to complete at least one division with is sufficient to form a colony. A possible way to test this would be the sort of aged single cells on both YPD and acidic synthetic-media-plates.

The lack of replicative lifespan extension by caloric restriction in WΣ is surely an issue that has to be addressed when the strain should further be used in genetic studies. In the controversy of (Lamming et al., 2006) and (Kaeberlein et al., 2006) it was argued that W303 might be very sensitive to nutrient depletion and that longevity could already be induced at high glucose concentrations and therefore not further be extended by lower concentrations. This may also explain the large variability of published lifespan in W303 (see Table B1). It could well be that the sorting procedure by FACS where the cells spend several hours in PBS (although at low temperature) already induces a starvation response. To test this, WΣ should be subjected to a classical dissection experiment to confirm or disproof the phenotype.

In a study on mitochondrial activity isolated from caloric restricted cells (Sharma et al., 2011), it was found that restricted mitochondria show an increased rate of oxygen consumption, dehydrogenease activity and H_2O_2 production. Concomitantly the ROS defense (Cu-Zn-SOD, Mn-SOD and Glutathione peroxidases) was upregulated. Interestingly neither the mitochondrial content nor their ATP production was increased. Replicative lifespan of a modified W303 was measured in non-restricted and restricted medium (18.27 to 25.5 generations respectively). The authors argue that increased NADH-dehydrogenase activity in the mitochondria leads to a higher NAD/NADH ratio, which activates the life extending Sir2-pathway. Parallel, increased respiration does not lead to more ATP production but rather the production of peroxide (by the respiratory complex III), which triggers upregulation of the redox defense.

In a different study it was described that increased peroxide production in old cells inactivates the peroxiredoxin Tsa1 by hyperoxidation in BY4742. During caloric restriction the PKA pathway is attenuated. This result in effective translation of the sulfiredoxin Srx1, which rescues the inactive Tsa1 and subsequently longevity pathways are activated. Deletion of Tsa1 prevents lifespan extension by caloric restriction (Molin et al., 2011). Since Tsa1 can also act as a backup for Orp1 to activate the Yap1 transcription factor (Tachibana et al., 2009), it seemed likely that WΣ may harbor a mutation in the Tsa1 gene. Indeed the “Saccharomyces genome database” (*http://www.yeastgenome.org* – dated October 2014) annotates a P182L mutation for W303. But this is most likely a misannotation derived from a previous publication (Timmermann et al., 2010) where a gain of function allele from a mutagenesis screen of an EMS-treated W303-K6001 strain was discovered. I have cloned and sequenced the *tsa1*-gene from WΣ and found it to be identical to the wild-type sequence.

Since it was not the primary aim of this study, I did not put further effort in the investigation of the nutrient sensing pathways and whether they are activated under restricting and non-restricting conditions.

6.1.3 Fob1 knockout

Fob1 is a unidirectional replication fork-blocking protein preventing collision between rRNA-polymerase and DNA replication at the repetitive ribosomal DNA-locus. This locus contains a large number of autonomously replicating sequences (ARS) and at the same time is heavily transcribed due to the high demand on ribosomes. The locus is therefore extremely prone to replication-associated events. It is assumed that the replication block by Fob1 stalls replication in one direction which facilitates DNA breaks and recombination in this region. As a by-product extrachomosomal rDNA circles (ERCs) are formed. These ERCs also contain further ARS which then lead to an increased replicative burden (sequestration of replication factors) and reduce lifespan by delaying or preventing cell-cycle completion. Introducing less efficient ARS in the rDNA locus could successfully extend lifespan also in the presence of Fob1 (Kwan et al., 2013). In the same study the authors demonstrate that caloric restriction reduces rDNA origin firing. It is argued that nucleosome occupancy of this locus is increased during restricting conditions and ribosome biogenesis, due to less active nutrient sensing pathways, is down-regulated. During cell division the whole genome has to be replicated and the gap between individual ARS determines the size of the replication fork and the time it takes to synthesize this region. Limiting amounts of replication factors in old cells could arrest cells in a stochastic manner leading to accumulation of senescent cells. Diminished sequestration at the ribosomal ARS would increase the available amount of replication factors in the cell and premature cell-cycle arrest is less likely.
Recently, it was stated that Δfob1-cells terminally arrest in an unbudded state whereas wild-type cells arrest during budding (Delaney et al., 2013).

In the Δfob1-background the WΣ strain showed a strong extension in replicative lifespan. Still more than 50% of the living cells were able to form colonies at the end of the experiment [Fig.C12c] and the average number of budscars did not reach saturation within the timeframe of the experiment ([Fig.C12a] see also [Table C1]). However, the post-replicative lifespan was not extended [Fig.C12b]. In this strain the cells seem to die directly after their last divisions. This is in agreement with the model by (Kwan et al., 2013). Old wild-type cells would preferentially not be able to complete cell-division but stay viable for a long time, whereas Δfob1 cells divide until limited by other aging factors and die quickly afterwards. However, the lack of replicative lifespan extension in WΣ under caloric restricted conditions (*see previous section*) does not apply to this mechanism.
It has to be pointed out here that the flow-cytometry based aging only focuses on single cells or cells that are separable by sonication. Especially for the colony formation assay, divisions of cells within aggregates cannot be addressed. If a strain contains cells with a different physiological state in cell aggregates, these events would be missed.

6.1.4 Lifespan during respiration

When grown in the absence of fermentable carbon sources, *Saccharomyces* restructures its metabolism to activate oxidative phosphorylation. Most likely due to high petite-rates of common lab strains and limited mother-daughter separation in this context there is virtually no literature reporting on replicative lifespan measurements under respiratory conditions. The flow-cytometry based assay allows overcoming this limitation.
Surprisingly, the growth in glycerol/ethanol-medium leads to a replicative lifespan extension and higher vitality of the old cells in the WΣ strain [Fig.C18].

In one rare case where microdissection on glycerol-plates has been performed (Kirchman and Botta, 2007), the authors observed that replicative lifespan extension in glycerol-medium is dependent on the supplementation of copper. By supplementing YPG-agar plates with 62 µM $CuSO_4$, the mean lifespan of W303-1A was extended from 20.2 to 23.6 generations whereas BY4742 showed a lifespan extension form 18.2 to 25.2 and the effect was even more dramatic in the SP-22 strain (33.4 to 57.4). In glucose-medium no effect of copper could be seen. The authors speculate that old cells may deplete their copper stores in the mitochondria, which could lead to inactivation of cytochrome c oxidase (Cox2). Synthetic medium however contains only 0.25 µM of copper. Although the authors did not show data for lower copper concentrations (they only comment that they tested several concentrations and 62 µM was chosen as optimal), it seems unlikely that the lifespan extension I observed for WΣ could be mediated by this mechanism.

One explanation would involve the mitohormesis theory, which states that mild oxidative stress is beneficial for the cells. At respiratory growth higher levels of ROS should be produced by the mitochondria and up-regulate oxidative defense mechanisms (similar to the observation in caloric restriction). Indeed as it can be seen by a plating assay, glycerol-grown cells tolerate much higher levels of H_2O_2 than cells from a glucose grown culture [Fig.C61].

A contradictory observation by (Ringvoll et al., 2007) should also be mentioned here, where the authors performed replicative and chronological lifespan assays in/on glucose and glycerol medium. The context of their work involves the role of helicases during DNA damage and aging. The wild-type control of the W303 background had a severely reduced replicative lifespan in glycerol compared to glucose (median lifespan of 9 for glycerol and 17 for glucose grown cells). For chronological aging however, median lifespan in glycerol was much longer (glucose 12 days and glycerol 47 days).

6.2 Redox homeostasis

The main results of the steady-state redox-conditions in replicative old cells are summarized in [Fig.C75]. For the roGFP2-Orp1 reporter an increase in peroxide can be detected only in the last third of the replicative lifetime of cells growing in glucose media. In contrast, cells growing in glycerol start slightly more reduced but already reach maximal oxidation after half of their lifespan where most of the cells are still abele to divide. By comparing these data the difference of the replicative timeline of cells grown in both conditions need to be considered. Firstly, glycerol-grown cells divide slower [Fig.C18] (for the first 15 divisions the division rate is about 55% of the rate of glucose grown cells at 25°C); secondly, the fraction of living cells and dividing cells is greatly increased in the glycerol-culture, making longer experiments possible. An alternative representation using budscars instead of time would not be appropriate because old cells, especially in glucose, get stationary while changes still proceed.

Diamide-stress, which oxidizes both the Grx1- and Orp1-probe directly, is likely to be buffered by the glutathione-pool. This explains the relative resistance of old cells as compared to young cells in glucose [Fig.C35] and the increased sensitivity of old cells as compared to young cells in glycerol [Fig.C37a,b], reflecting the steady-state GSH/GSSG-levels at the respective age.

From the perspective of the glutathione equilibrium, old cells exhibit a highly reproducible more reducing phenotype in glucose [Fig.C6], which is not mediated by vacuolar GSSG sequestration, because knockout of the Ycf1-transporter showed no change in the phenotype

[Fig.C8a]. The glutareductase Glr1 seems to be the key-player in this context as the knockout not only showed a highly oxidized cytosol but also no age dependent more reducing phenotype [Fig.C8b,c]. This phenotype can be explained easily by the drop in cytosolic pH in old cells [Fig.C26] and the pH dependent activation of Glr1 [Fig.C63]. In the absence of Glr1 the cytosolic acidification was not influenced [Fig.C26c] but the reduction-phenotype was lost [Fig.C8b,c], clarifying the cause-effect relationship. The increased diamide resistance observed in old cells is also compatible with an increased Glr1 activity.

The most striking discovery was the observation that cells knocked out for Glr1 showed no difference in the vitality parameters compared to wild-type cells ([Fig.C9] and [Fig.C24]), despite their highly oxidized state. This clearly indicates that the redox state of glutathione plays no role in the aging process of the WΣ-strain background.

The reductase activity of Glr1 is based on electron transfer from NADPH to GSSG. This raises the question, whether pH-dependent activation of Glr1 would deplete the pool of reduction equivalents and could even be harmful for old yeast cells. Since the replicative lifespan of the Glr1 knockout cells was not decreased in my aging assays, it is likely that the NADPH pool is not limiting in these cells and therefore not depleted by Glr1.

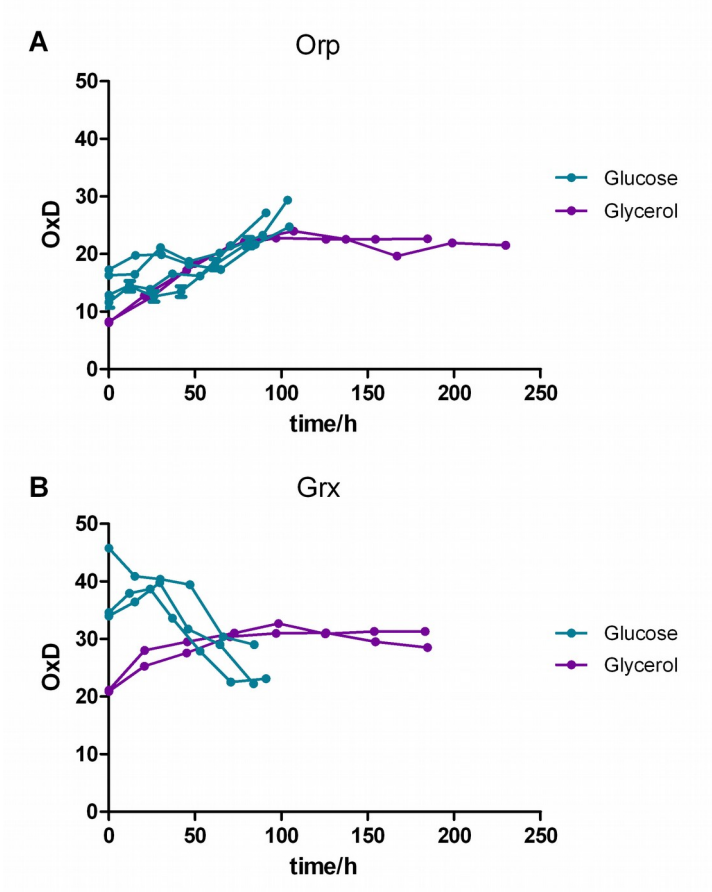

Fig.C75
Synopsis of all redox measurements in WΣ wild-type cells during replicative aging. Fermenting cells are colored in turquoise and respiring cells are drawn in violet.
a.) Measurement of roGFP2-Orp1
b.) Measurement of roGFP2-Grx1

6.2.1 Dissection of the peroxide-response kinetics (roGFP2-Grx1)

The dynamics of the H_2O_2-shocks seen by the glutathione-reporter is not easy to understand, especially the fast oxidation in the beginning [Fig.C56a]. The recovery-phase after the fast oxidation coincides with the drop in pH [Fig.C76c]. By overexpression of Glr1 [Fig.C56a] the recovery phase is much more prominent and even results in a roGFP oxidation level lower than the steady-state, suggesting that the recovery is due to pH-dependent Glr1 activation. At higher concentrations of H_2O_2 and longer stress exposure the pH may decrease too much for further Glr1 activation. The pH may even drop below the pH optimum of Glr1. Thereby, the oxidation level of the probe rises again. The re-oxidation of the glutathione-pool at high peroxide levels is also summarized in [Fig.C77]. Of course, Glr1 is not the only player in mediating the glutathione recovery from oxidation. It was shown that the vacuolar transporter Ycf1 removes oxidized glutathione from the cytosol and that deletion of Ycf1 or the thioredoxin Trx2 leads to a substantial decrease in recovery from peroxide-induced glutathione-oxidation in a *Δglr1* background (Morgan et al., 2013). Whether these processes are also pH dependent has to be tested.

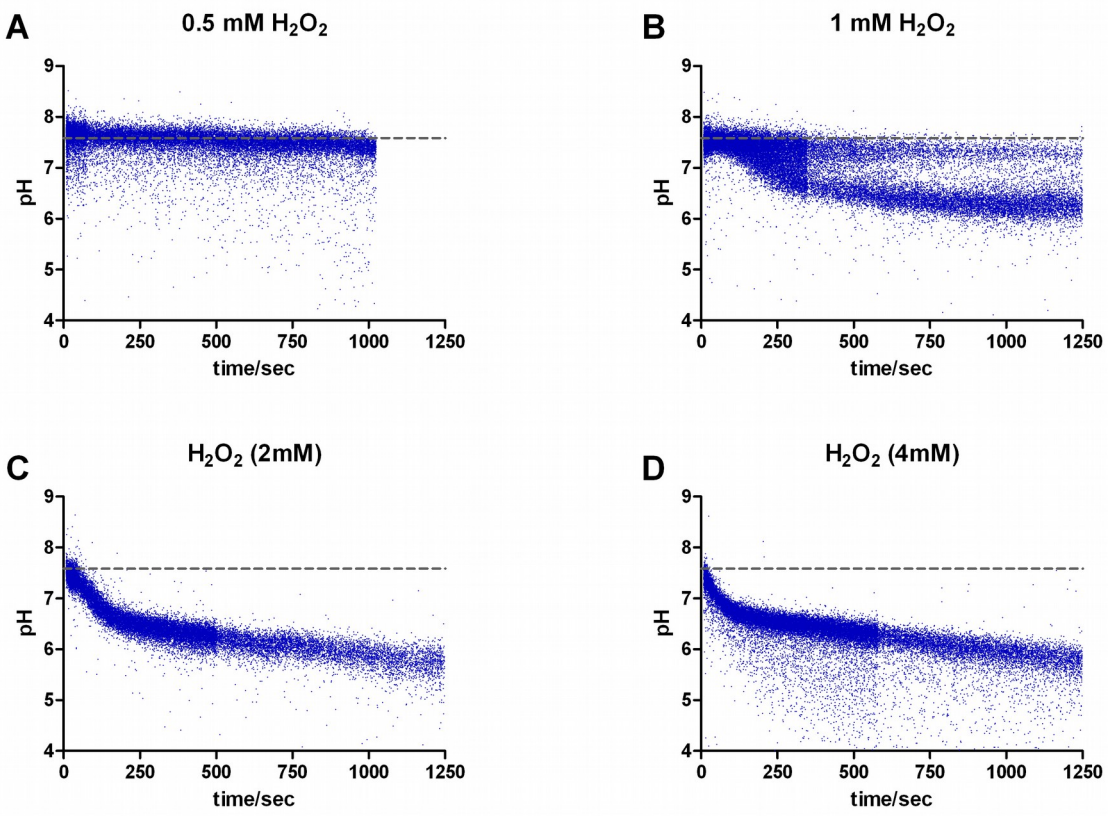

Fig.C76
Cytosolic pH changes by H_2O_2 are dependent on the concentration. Kinetics of pH changes after H_2O_2 addition to pHluorin-expressing WΣ-cells. At 1 mM H_2O_2 a population split can be observed, indicating a transition point.

However, the initial probe oxidation by peroxide still needs to be explained. In this regard it is interesting that the Glr1-knockout not only showed an increased oxidation in the glutathione reporter but also in the roGFP2-Orp1 reporter. This could mean two things: first, the glutathione-pool is directly connected to the hydrogen peroxide pool or second, the roGFP2-Grx1 probe itself is oxidized by H_2O_2-dependent processes and constantly reduced by glutathione (which is catalyzed by the Grx1-fusion). The first possibility would involve enzymes which convert peroxide to oxidized glutathione within seconds for example by glutathione peroxidases which give rise to GSSG levels that are then detected by the probe. In this case a knockout-screen for the rescue of the *Δglr1*-phenotype would be possible. The second case could be clarified in *in vitro* studies on the roGFP2. There is, however, the possibility that endogenous Orp1 (or another peroxidase), although not directly coupled, could act on the roGFP2-Grx1 probe and thus artificially create a signal on the wrong sensor. Measurements in a strain deleted for Orp1 and/or other peroxidase encoding genes could test this hypothesis.

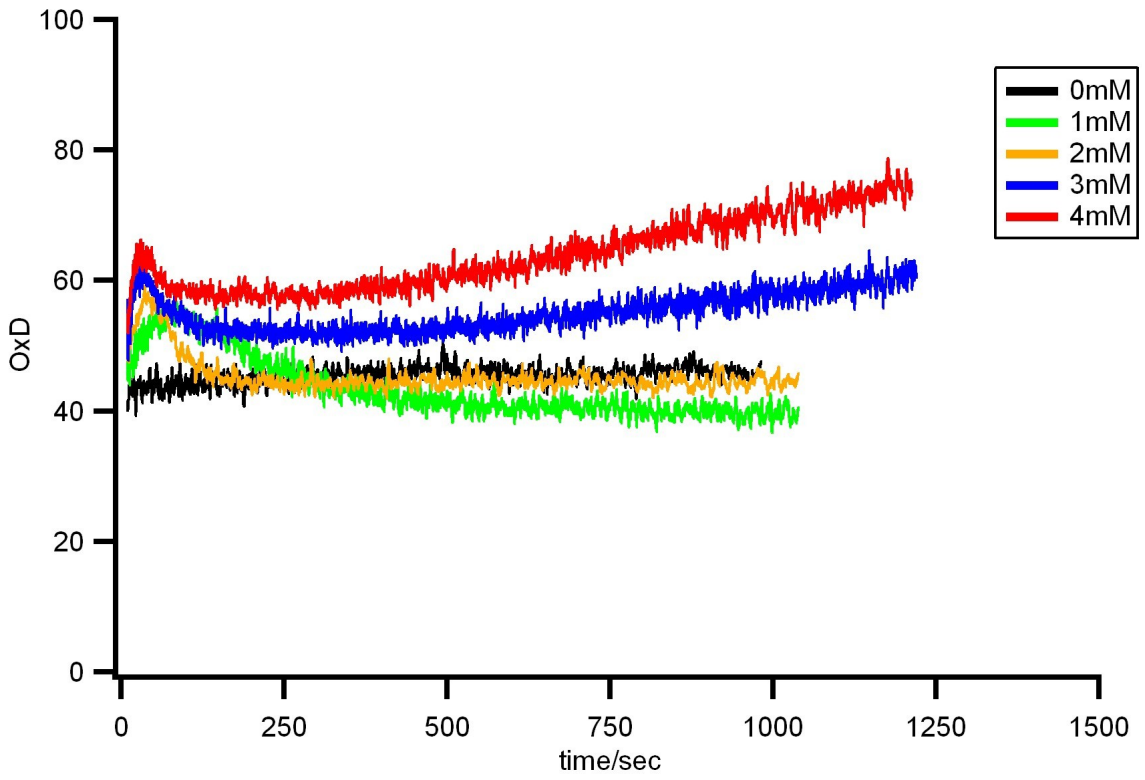

Fig.C77
Kinetics GSH/GSSG-oxidation of WΣ after H_2O_2 treatment measured by roGFP2-Grx1. Cells were shocked with different amounts of H_2O_2 and the data of the single cells were box-smoothened over 25 cells.

6.2.2 Dissection of the peroxide response kinetics (roGFP2-Orp1)

From the response of the roGFP2-Orp1 reporter after H_2O_2 addition [Fig.C31] one can conclude that peroxide buffering in old glucose-grown cells is up-regulated whereas glycerol-grown cells already have a stronger buffering from the beginning [Fig.C33a,b].

Although the differences in the buffering of oxidative insults between fermenting and respiring cells do not appear very large - for 2 mM H_2O_2 young cells in glucose showed about 90% oxidation whereas cells in glycerol only rose to about 70% - respiring cells survived 10 fold higher peroxide concentrations, demonstrated by a plating assay [Fig.C61]. From these observations one could conclude that the *Δglr1* background would be much more sensitive to H_2O_2 and die at much lower peroxide concentrations as compared to wild-type cells, whereas Ucc5179, which had a more reduced cytosol, would survive even higher concentrations. This experiment remains to be done.

In a direct comparison of yeast strains in glucose medium the plateaus (more precise – the value after 15 minutes peroxide treatment) of the roGFP2-Orp1 reporter are plotted against increasing amounts of hydrogen-peroxide [Fig.C78]. All strains reached a fist oxidation-maximum at 1 mM H_2O_2. At this concentration WΣ-Δ*glr1* showed 100% oxidation whereas Ucc5179 and BY4742 barely reached 70%. WΣ-wild-type with about 80% oxidation had an intermediate phenotype. At concentrations higher than 2 mM the 15 minute-exposure value rose again. A similar behavior was seen in the roGFP2-Grx1 probe where the pH breaks down and oxidation rises again at peroxide concentrations higher than 2 mM [Fig.C77].
This relates the roGFP2-Orp1 response to the roGFP2-Grx1 response. Assuming that all strains are identical in the cytosolic peroxide levels the only conclusion would be that the roGFP2-Orp1 reporter does not show the real situation. Here one has to recall that roGFP was originally designed for measuring the glutathione equilibrium, which is already possible without the Grx1-fusion. The fusion with the Orp1 protein brings the probe also in equilibrium with the hydrogen-peroxide pool but most likely does not abolish the roGFP's sensitivity to glutathione. Since both roGFP2-Grx1 and roGFP2-Orp1 were normalized with diamide and DTT in the same way, their oxidation status should also be comparable. If this were the case then the glutathione pool should determine the minimal oxidation state of the roGFP2-Orp1 reporter. Interestingly, steady-state oxidation of roGFP2-Orp1 is always lower than roGFP2-Grx1 in wild-type cells. Since disulfide formation is a reversible process, roGFP2 oxidation can also be passed back to the Orp1-protein. Orp1 itself needs to be reduced by other proteins, most likely the thioredoxin (Trx-) system. It was argued that about 90% Orp1 oxidation is necessary to oxidize 50% of roGFP2 (Meyer and Dick, 2010). At low peroxide levels, Orp1 will be efficiently kept at a low oxidation status by the thioredoxins and act as a kinetic drain for roGFP2 oxidation. But still the glutathione system may influence the roGFP2-Orp1 reporter when the differences are large enough. When the cells are flushed by peroxide, Orp1 would be 100% oxidized and able to oxidize roGFP2 to a higher level than the glutathione-pool. On the contrary the rate of reduction by glutathione would eventually limit further oxidation by Orp1 and roGFP will never reach 100%. This scenario would also explain the highly oxidized roGFP2-Orp1 phenotype in a Δ*glr1* strain. Because glutathione in this background is already highly oxidized, the Trx/Orp1-system would not be able to reduce roGFP below a certain level. Conversely, when peroxide is added, glutathione would not be able to counteract roGFP2 oxidation by Orp1 and the reporter would reach 100% oxidation. Strain differences in maximal roGFP2-Orp1 oxidation would then be attributed to a differentially regulated glutathione pool.

Seen in this light, the aging experiments done with roGFP2-Orp1 do not indicate an increase in peroxide resistance anymore but rather reflect the Glr1-mediated glutathione reduction under fermentative conditions, which limits the maximal probe oxidation by H_2O_2. However, the increased basal roGFP2-Orp1 oxidation in old cells would definitely indicate an increase in

peroxide production. Especially, because of the overlaid age-associated glutathione reduction, the peroxide levels would even be underestimated. The reason why no increase in H_2O_2 is detected in the Δ*glr1* background [Fig.C8c] may come from the small linear range of roGFP2-Orp1 under those conditions. If peroxide changes are lower than 100 µM a difference between old and young could be hidden by the uncertainty in the autofluorescence model.

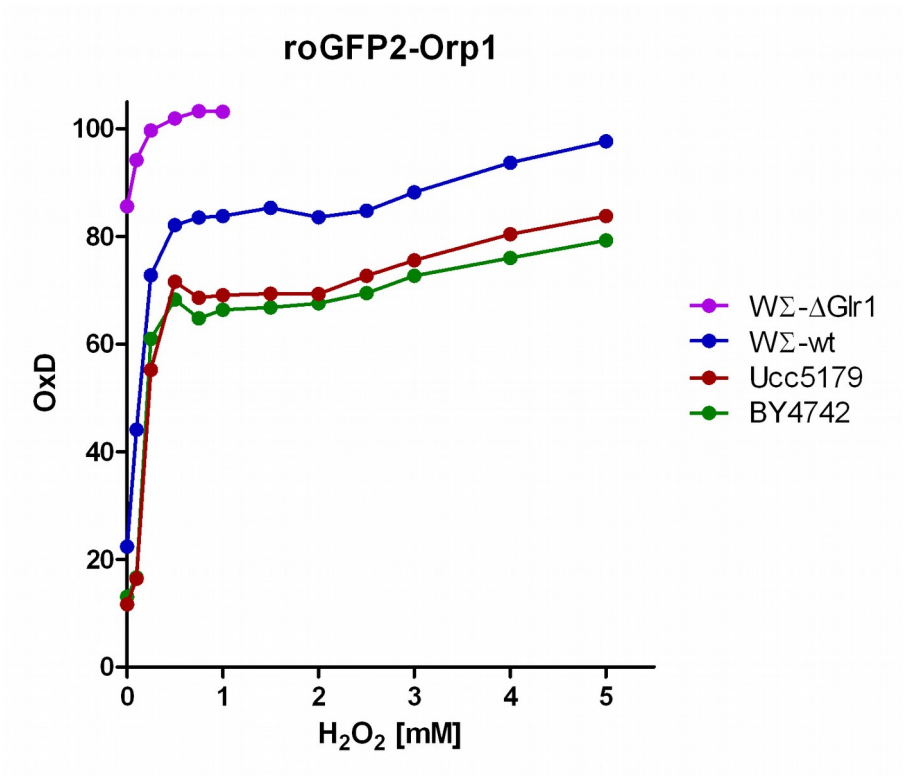

Fig.C78
Peroxide titration of the roGFP2-Orp1 reporter in different strain backgrounds. Cells were treated with H_2O_2 and probe oxidation was measured after 15 minutes exposure.

6.2.3 Cause of the H_2O_2-mediated pH-drop

Glucose withdrawal leads to a cytosolic acidification in yeast cells (Orij et al., 2011);(Dechant et al., 2010). The cellular energy production seems to play an essential role in this response. In yeast there are two major ATP driven proton-pumps, which regulate the cytosolic pH: the plasmamembrane ATPase Pma1 and the vacuolar ATPase Vma1. These ATPases can consume a substantial fraction of the total energy produced in the cell. Thus the pH is directly coupled to the energy supply of the cells. If glycolytic enzymes are preferentially impaired by H_2O_2, the acidification after a peroxide shock would be the result of ATP shortage, linking the glutathione-response to the energy metabolism.
From my data I can see that respiratory grown cells are extremely sensitive to the treatment with the protonophor DNP [Fig.C65]. The substance acts as a chemical uncoupler and equilibrates proton gradients across membranes. The mitochondrial function depends on a proton gradient for protein import and energy production. In respiring cells they are the main source of ATP and therefore more sensitive than fermenting cells to the uncoupler.

A hint, that the recorded kinetics after H_2O_2-shocks are indeed determined by the ATP levels can be found when 1 mM H_2O_2 is used. In some cases (maybe influenced by temperature or culture density) a population split could be seen in the pHluorin reporter ([Fig.C52] and [Fig.C76]). In a study from (Osorio et al., 2003) the authors determined the cellular adenosine-nucleotide concentration after H_2O_2 treatment. There seems to be a sharp decline in adenosine-nucleotide levels between 0.6 and 1 mM H_2O_2. The population split that I observed in the kinetics is most probably reflecting this transition where some cells still have enough ATP-production to maintain the pH and some cells which are just below this threshold and acidification wins. This would also have an inverse effect on the glutathione pool where cells with lower ATP would acidify, activate Glr1 and faster reduce the glutathione.

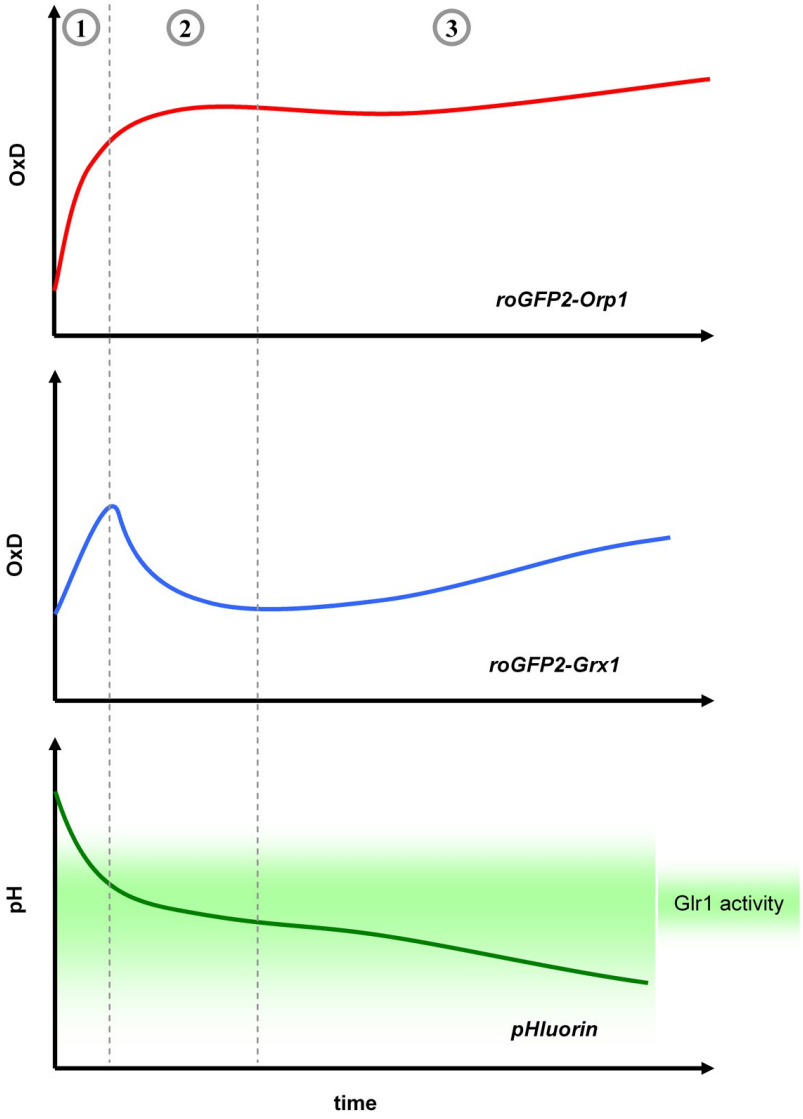

H2O2 addition > 2mM

1
- Diffusion of peroxide through aquaporins
- Glutathione oxidation
- Depletion of ATP levels and less efficient H^+ clearance (acidification)

2
- Equilibration of peroxide-pool
- pH mediated Glr1 activation reduces glutathione
- Maintenance of pH by basal energy production

3
- Breakdown of energy production, further acidification
- Drifting out of the pH optimum for Glr1 leads less GSSG clearance
- Slow response of peroxide reporter to the glutathione pool

Fig.C79
Synopsis of the reporter responses upon H_2O_2 treatment.

Taken together, the metabolic state, growth condition and energy production are closely linked to pH homeostasis which in turn influences the redox-systems directly by changing the electrochemical potential and indirectly by enzyme-mediated changes of the buffer-systems. A synopsis of the peroxide-mediated events and their interpretation is depicted in [Fig.C79].

6.2.4 Possible explanation of pH kinetics after acetic acid shock

Depending on the growth conditions, also the shocks with acetic acid showed a complex kinetics behavior. Whereas in glucose the recovery from 500 ppm acetic acid took more than 20 minutes [Fig.C50_young cells], the glycerol-grown cells showed a short acidification but then a fast recovery within 2 minutes [Fig.C53b]. This may be explained by an increased cytosolic buffering capacity of the glycerol-grown cells or an increased metabolism of the acetate during respiration. Another interpretation of this data, consistent with the previous hypothesis may be the following. Acetic acid is a weak organic acid with a pK_a of 4.75. Weak organic acids are thought to work as protonophores in acidic medium (Beales, 2004). The pH of my yeast synthetic medium is 3.93. At this pH acetate gets protonated, becomes neutral and is able to cross biological membranes. In the cytosol near neutral pH it becomes deprotonated again and leads to acidification. This raises the ATP consumption by the H^+-ATPases (Pma1 and Vma1). In glucose ATP becomes limiting and adaptation processes require gene or protein regulation, which takes time. However, in glycerol ATP is mostly generated by mitochondria and an increase in the proton-gradient over the inner mitochondrial membrane leads to a more effective ATP-production, which facilitates pH homeostasis. The fact that acetate does not induce the same effect as DNP (pK_a 4.09) could easily be explained considering that acetate is a natural metabolite and can feed into biological pathways like the Acetyl-CoA-synthases (Acs1 & Acs2) (Van den Berg and Steensma, 1995) as a substrate for the TCA-cycle. Mitochondria in this scenario would be shielded by the cytosol whereas the DNP-protonophor can diffuse through the cell and short-circuit the mitochondria already at low concentrations.

6.3 Metabolism and pH in aging cells – and some speculations

Depending on the individual pKa values of the amino-acid side-chains, protonation can influence the surface charge of a protein and therefore also affects protein folding. It was recently described that an acidic pH leads to clustering of metabolic enzymes to filaments during nutritional shortage and help cells to survive and recover from starvation (Petrovska et al., 2014). If this is also true for aged cells, this may explain their growth arrest and their long post replicative survival time. Another study by (Orij et al., 2012) could identify a lower cytosolic pH as a determinant for a lower growth rate.
When looking at the age dependent changes in fermenting cells it becomes apparent that their onset is always at around 45 h (and a bit later for roGFP2-Orp1 expressing cells). At this time the vitality parameters start to decline and further increase in budscars becomes minor. This strongly suggests that cells under fermenting conditions do not show a gradual decline until reaching a certain threshold but rather imminently enter a crisis and develop a senescent phenotype. This is supported by a study of (Fehrmann et al., 2013) where they show that S288C on average accomplishes only 5.4 more divisions after the division rate starts to decrease.

It is interesting that the fermenting cells start to produce peroxide when the culture accumulates post-replicative cells whereas the respiring cells cease to increase peroxide levels when the first post-replicative cells appear. A very speculative interpretation would be a scenario where

fermenting cells lose glucose repression when they get old and switch to respiration. Trace amounts of fermentable carbon sources may be present in the medium due to autolysis of some cells but may soon be used up and cells become post-replicative. In an aging glycerol culture when cell grow larger maybe also the amount of mitochondria rises, which would lead to a steadily increasing amount of peroxide until the cell-size only marginally increases and the first cells become stationary.
In most cases the replicative lifespan assays are performed on YPD plates consisting of autolytic yeast extract, trypsin digested proteins and glucose. However, the composition of yeast-extract is not defined and it is likely that it contains fermentable carbon sources like pyruvate and glycerol. In a microdissection assay where only single cells are kept in one spot on an YPD-agar plate, the residual fermentable carbon sources could still be sufficient to support growth when cells start to respire. The prediction would therefore be that cells grown on synthetic plates will live shorter. If this holds true, lifespan should be increased in my aging assay, when some glycerol or ethanol is added to the medium.

One can speculate, if the observed pH drop in old cells is also produced by energy shortage. This would suggest that glycolysis in old cells is insufficient or that the energy requirement is higher. Implying this, one would expect more stable pH conditions in cells grown in glycerol, which mainly depend on mitochondria for energy production. If especially the glycolytic pathway is prone to damage by oxidative stress or other aging factors, this would also explain the longevity phenotype I observed in respiring cells.
Forcing cells to respire could also have further beneficial effects. Mitochondria not only fulfill the purpose of energy production but also play an important role in redox-biology by synthesizing iron-sulfur-clusters (ISC) (Lill, 2009). These clusters mostly function as catalytic centers for many essential proteins ranging from mitochondrial electron transport (complex I – III) to enzymatic function (aconitase, biotin synthase) and genome integrity (Rad3 - helicase, Pol3) (Netz et al., 2012) . For those transport processes, a functional mitochondrial membrane potential ($\Delta\Psi$) is needed. Actively working mitochondria would better maintain their $\Delta\Psi$ and keep the ISC-synthesis at a high level. In the presence of glucose, oxidative phosphorylation is suppressed, and therefore also the proton transport from the mitochondrial matrix to the intermembrane space by the respiratory complexes is absent. In this case ATP is imported into the mitochondria via adenine-nucleotide-carrier and hydrolyzed by the (nuclear encoded) F_1 subunit of the ATP synthase to generate the proton gradient (Traba et al., 2008); (Clark-Walker, 2003). A cellular ATP shortage would then also affect the $\Delta\Psi$.
The key question here would be, whether $\Delta\Psi$ is stable in WΣ old cells or finally breaks down.

On the other hand, the pH of the intermembrane space is coupled to the cytosolic pH ([Fig.C66] and (Ayer et al., 2013)). Thus a drop of the cytosolic pH in ATP depleted cells would help to maintain the mitochondrial membrane potential, which in turn could facilitate mitochondrial protein import and may allow the mitochondria to fulfill their function at a low ATP-state. Since glucose starvation leads to a decrease in pH (Dechant et al., 2010) it would perfectly make sense to up-regulate mitochondrial function for switching to alternative carbon sources or generate more ISC-containing repair-enzymes. Additionally Dechant and coworkers report that the V_1-complex of the vacuolar ATPase Vma1 dissociates from the membrane bound V_0 subunit when glucose is depleted and the pH drops. Conversely when glucose is added, the pH rises (initially by the ATP-hydrolysis of Pma1), Vma1 assembles and becomes active. Vma1 seems also to be involved in the activation of the PKA/Ras-pathway by somehow stimulating

cAMP production. A low glycolytic flux would therefore lead to Vma1 disassembly and repression of the PKA pathway, which promotes longevity.

If the ATP-pool of glucose-grown cells is really lower or more sensitive than under respiration, it would also explain the age-associated acidification during fermentation and the longevity in respiration.
To test this entire hypothesis an experiment should be considered to rise the cellular ATP levels maybe by an artificial ATP-regeneration system e.g. creatin kinase (Canonaco et al., 2002). This system should extend lifespan of glucose-grown cells and make cells less sensitive to H_2O_2 mediated pH changes.

6.3.1 Conflicting reports

For cells grown in glucose it is reported that during replicative aging the mitochondrial morphology changes from an elongated network to fractured vesicles (Wang et al., 2014) and at relative early time-points mitochondrial membrane-potential breaks down (Hughes and Gottschling, 2012). In the study form Huges and Gottschling, mitochondrial fractioning comes along with a rise in vacuolar pH. A shortage in ATP would affect the vacuolar proton-pump (Vma1) and could explain the reduced acidity of the vacuole. Overexpression of Vma1, however, can postpone the mitochondrial fractioning and extends lifespan, which would argue against this hypothesis, because this would deplete the ATP even faster, except if there was a feedback regulation, which couples ATP-production to an acidic vacuole. The authors argue that the import of neutral amino acids into the vacuole (mediated amongst others by the V-ATPase-dependent transporter AVT1) gets impaired when the vacuolar pH increases, which somehow influences the mitochondrial energy metabolism and thus their membrane potential. A former study from the same group (Veatch et al., 2009) demonstrated that loss of ΔΨ leads to impaired iron metabolism and elevated levels of cytosolic iron. In concordance to impaired ISC biogenesis at low ΔΨ they observe severe genomic rearrangements, indicated by loss-of-heterozygosity studies of chromosomal markers. By artificially interfering with ISC biogenesis (downregulation of Nar1), similar frequencies of chromosomal rearrangements could be triggered. However, their study was mainly focused on ρ^0-petites, which do not play a role in WΣ.
Indeed petite cells seem to be a problem in the field of replicative aging. Similar to my observation that the S288C background turns into petites at high rates the study of (Fehrmann et al., 2013) addresses this question and directly contradicts the study of (Hughes and Gottschling, 2012). By flow-chamber measurements they could track the entire lifespan of yeast and monitor the division-rate of individual cells together with a ΔΨ-dependent mitochondrial marker (preCox4-mCherry). Fehrmann and colleagues showed that loss of ΔΨ is a stochastic event that occurs at a more or less constant rate over the aging process (about 3% per generation). By limited pedigree analysis in the flow chamber they could visualize the division speed of ΔΨ+ and ΔΨ- cells and their offspring. The slow division rate of aged ΔΨ- cells was inherited to 100% to daughter cells whereas ΔΨ+ offspring regained the high division rate of a young culture which means that ΔΨ- cells terminally turn petite. As a consequence their data shows that loss of ΔΨ is not a prerequisite for the onset of aging as cells, which maintained ΔΨ also entered senescence. In addition, the authors could show a significant increase in the preCox4-mCherry fluorescence in post senescent ΔΨ+ (grande) cells.

Considering that WΣ has negligible petite content it is most likely that mitochondrial ΔΨ is also maintained in this strain. This argues that a low ATP-state would still be sufficient to keep basal mitochondrial functionality in old cells. Genomic defects arising from impaired iron metabolism would then be unlikely in WΣ. This needs to be addressed in future experiments.

In a very recent follow-up study from the Gottschling lab (Henderson et al., 2014) the authors use localized ratiometric pHluorin to show mother-daughter asymmetry in aged cells by a microscopy based approach. For their assay they used a S288C derived mother enrichment strain. Contradictory to my results they demonstrate that pHluorin targeted to the cellular cortex indicates a rise in pH in old mother cells and a re-acidification in the budding daughter. Furthermore, they could show an accumulation of the Pma1 plasma-membrane ATPase in old mothers. They argue that this excess of Pma1 would compete with Vma1 for the free protons (only about 3000 in a yeast cell) and thereby deplete the vacuolar store.
To bring these results in concordance with my observation, it first has to be considered, that I could measure my cells directly from the medium whereas Henderson et al. had to enrich and prepare them first for microscopy. According to their protocol they grew the cells in YEPD purified them in biotin depleted YEPD over magnetic columns and then resuspended them in Verduyn low-fluorescence medium for imaging. Unfortunately, the pH of the Verduyn-medium was not supplied by the authors so it is not clear whether cells have experienced a pH shock during preparation. Microscopic signal quantification in living cells is always problematic because of the uncertainty in the fluorescent background. Localizing of fluorescent proteins to distinct foci is therefore a good way to reduce those artifacts. The problem of localizing pHluorin to the direct vicinity of Pma1 is that Pma1 could deplete protons in its local microdomain possibly masking a global change. Accumulation of Pma1 in old cells could well lead to an extended proton depletion zone around the plasma-membrane whereas in newly synthesized daughters with few Pma1 molecules one would expect a more equilibrated cortical pH. The cells used for imaging always had less then 20 budscars. A survival curve for the used strain was determined by the authors and the median lifespan was 38 divisions. Therefore the measured cells were not even close to senescence; in fact the survival curve indicates that about 90% of the cells are alive at this time. A limiting ATP concentration would not be expected for this stage. In my aging assay I determined the cytosolic pH of WΣ to be between 7.6 – 7.8. In the study by Henderson et al., the cortical pH for young cells was around 7.1 and increased to 7.4 already after 3 divisions when Pma1 becomes more abundant. Cells with 13 divisions had a cortical pH of 7.8, which slightly drops to 7.6 at 18 divisions. They next reasoned that reduction of Pma1 activity (by expression of the mutant pma1-105 allele) could increase vacuolar acidity and extend lifespan similar to overexpression of Vma1 in their previous study (Hughes and Gottschling, 2012). Indeed the median lifespan could be increased from 38 to 49 generations. As a final conclusion, the authors state that acidification in the buds re-acidifies the vacuole and rejuvenates the daughter cells. Since I did not do any pH measurements in the mother enrichment strain, I cannot rule out that I would observe a similar phenotype. In addition, I was always working with a haploid strain therefore conditions could be different in a diploid background.
Care should also be taken when using the pma1-105 allele as it was shown that this mutant would counter intuitively increase the cytosolic pH under certain conditions maybe by promoting the vacuolar proton transport system(Maresová et al., 2010).

It was shown previously that sporulation of old yeast cells is able to rejuvenate the four spores to full replicative capacity (Ünal et al., 2011). Rejuvenation even was possible when meiotic

divisions were blocked by inactivating the polo like kinase Cdc5 during sporulation and only a single spore was formed. In this context it would be interesting, if Pma1 levels during meiosis will also decrease in old cells and if overexpression of Pma1 would prevent vacuoles from re-acidification and spores from resetting their replicative clock. Regarding the relative low pH of young cells observed by Henderson et al. and the high pH I measured for WΣ, it would be necessary to check whether different wild-type strain backgrounds also show these large differences and if their initial pH is correlated with their respective lifespan. The absolute pH values could also be a matter of the detection method. Whereas a pH of 7.5 was determined by (Ayer et al., 2013) using flow cytometry, a low pH of 7.1 was measured by (Orij et al., 2012) using a micro-plate reader where cells devoid of plasmid could not be excluded.

Taken together the study by Henderson et al. demonstrates the importance of H^+-ATPases in the aging process and brings up an interesting concept of antagonizing proton pumps leading to compartment specific proton depletion. Whether this is a growth condition or strain specific feature or a general cause of cellular aging remains to be shown.

6.4 Other interpretations of age associated changes

An alternative or additional explanation for the aging phenotypes should also be discussed here. When cells age and gain budscars, their size increases. Fluorescent proteins produced from constitutive promoters ($P_{TEF1(Ashbya)}$ tested in glucose; $P_{TEF1(Asbbya)}$, P_{Act1} and P_{TDH3} tested in glycerol) accumulate in aging cells ([Fig.B10b] and [Fig.B16]). This can have several reasons. First, protein-expression is often regulated by feedback mechanisms to adapt concentrations to actual requirements. If a cell now has a larger volume, more proteins would be needed to reach the same concentration. Second, when cell division takes longer (for example when a cell needs to repair DNA or to clear misfolded proteins), some promoters will still continue to express genes and excess proteins have to be degraded to maintain stoichiometry or they accumulate leading to protein imbalance which may again lead to delay of division or growth of the cell. It is hard to tell how high the real protein-concentrations will be in an old cell, because not only the cell volume increases but also the volume of the organelles is dynamic. If for example the vacuole fills most of the volume of an old cell, then cytosolic protein-concentrations could very well be much higher, which could make aggregation more likely. It is reported that chromatin packaging declines when cells age due to loss of chromatin bound nucleosomes and that consequently overexpression of histones is able to extend lifespan (Feser et al., 2010). Reduced silencing could also lead to accumulation of proteins and thereby challenge the proteostasis network (Hu et al., 2014). This observation is not only constricted to yeast but also applies to higher organisms [reviewed in (Wood and Helfand, 2013).

The better H_2O_2 buffering in old cells (seen by the roGFP2-Orp1 reporter) might be the result of just accumulating more detoxifying enzymes like peroxidases or catalase (this may be checked by GFP-fusions and quantification).

If a yeast cell has accumulated damage, it can also enter apoptosis. It could well be that the acidification seen in my aging assays is the snapshot of cells currently undergoing apoptosis. Staining for apoptotic markers in low pH cells, although challenging for the small fraction of old cells and even more challenging not to introduce artifacts on the pH measurements, could provide evidence for this hypothesis.

Based on the observation that cells grown in glycerol are usually much smaller than the cells grown in glucose it was hypothesized that cell-size could play a role in aging. There was also a study, which correlates the smaller cell-size of different mutants with longevity and enlarged cells with shorter lifespan (Yang et al., 2011). On the other hand an increased cell size could just be the result of a delay in cell cycle and therefore amplified by defects occurring during aging. Cells in glycerol usually grow much slower than in glucose. Transferred to the natural environment of yeast, this situation resembles starvation which requuires resistance and durability. Glucose means that nutrients are available and fast propagation has priority.

6.5 The redox homeostasis in senescent cells

In contrast to replicative aging, cells in my senescent model did not show an obvious decrease in roGFP oxidation levels [Fig.C70] despite their acidification [Fig.C74]. There are several ways to explain these results. First, the model for autofluorescence in the senescent assay was insufficient masking subtle changes in the roGFP2-Grx1 reporter because of its unfavorable "signal to autofluorescence ratio". Second, Glr1 levels in senescent cells may be decreased which would compensate its activation at lower pH. Third, reduction equivalents might get limiting in senescent cells, which then would also limit the glutathione turnover by Glr1. Strikingly all the tested clones were already more reduced than wild-type from the beginning arguing for a general deregulation in the glutathione-homeostasis. Additionally no increase in H_2O_2 levels could be detected by the roGFP2-Orp1 reporter [Fig.C72] indicating that telomere induced senescence differs from replicative senescence which conversely also means that replicative senescence in WΣ is most likely not triggered by shortened telomeres.

6.6 Final model

In this work I could successfully monitor changes in the cytosolic glutathione equilibrium, hydrogen-peroxide abundance and pH in replicatively aged yeast cells. Surprisingly, the glutathione reporter was progressively more reduced in aging cells during fermentative growth whereas hydrogen-peroxide levels seem to rise at the same time. Simultaneously, the redox-pools became more resistant to oxidant treatment and the pH in old cells decreased. The reducing phenotype turned out to be dependent on the glutareductase Glr1. Using *in vivo* acidification measurements I could demonstrate that Glr1 is pH dependently regulated and could reproduce the glutathione-reduction phenotype in young yeast cells by lowering the cytosolic pH. Furthermore, similar pH changes occurred in a model system for senescence but no distinct changes in the redox reporters suggesting that redox homeostasis is differentially regulated in senescent cells.

Yeast cells grown under respiratory conditions have a lower cytosolic pH and a more reduced glutathione-pool, consistent with the Glr1 activation. During aging, oxidation of both the glutathione and peroxide-pools increased in this case. Unfortunately, pH measurements in old respiring cells could not be performed due to instrument problems.

Interestingly, respiring cells have an extended replicative lifespan even when Glr1 is deleted and their cytoplasm is highly oxidized. In fermenting cells Glr1 knockout also leads to a strong oxidation without affecting the replicative lifespan. This leads to the conclusion that homeostasis of the glutathione-pool is not limiting replicative lifespan in yeast.

Given that the cytosolic pH is actively maintained by H^+-ATPases, I speculate that the age-associated acidification may be the result of impaired ATP production. The final model for age related redox changes in the WΣ-strain is shown in [Fig.C80].

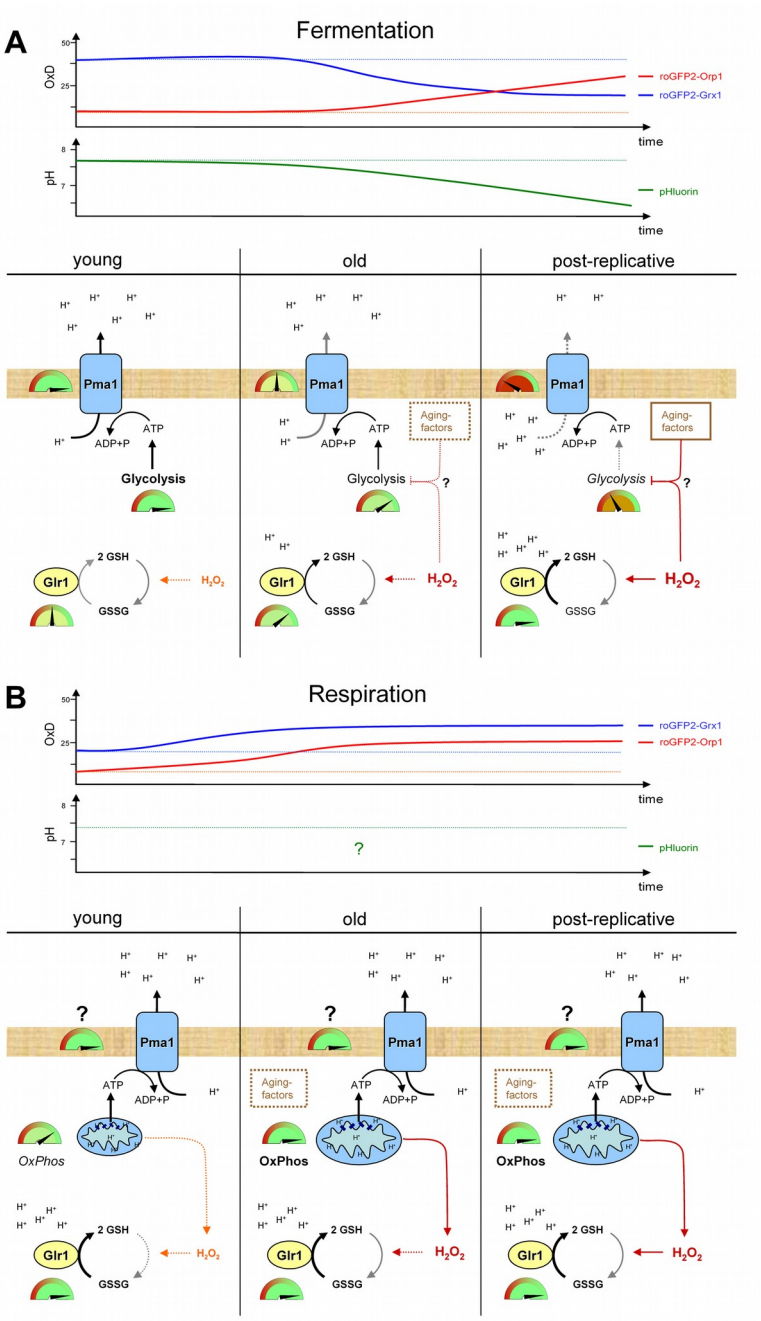

Fig.C80
Model of age related redox changes in WΣ
a.) Model for fermentative growth. In young cells the pH is slightly alkaline and Glr1 works under suboptimal conditions. When cells get older, glycolysis may get impaired by increased amounts of H_2O_2 or other age related factors and ATP level decline. A reduced proton clearance from the cytosol results in acidification and better conditions for Glr1 to reduce GSSG to GSH. In post-replicative cells the effects get more prominent and the acidic pH provides optimal conditions for Glr1.
b.) Model for respiratory growth. Respiring cells are already more acidic than fermenting cells and Glr1 works at optimal conditions. When cells get older, they become larger and most likely the mitochondria become more abundant. This probably raises the H_2O_2 production and glutathione oxidation. Since the pH was not measured yet in aging cells it is unclear whether ATP production is stable or not. Other aging factors may contribute to the phenotypes.

7 Supplements

7.1 The redox-response and lifespan of Ucc5179

In recent years the mother enrichment program became a popular model system to study age-associated changes. Since WΣ was always used as a haploid strain I also measured the redox reporters in the haploid mother enrichment strain Ucc5179. To allow the offspring of the old cells to rejuvenate, no estradiaol was added to the culture and therefore the daughter arresting system was not induced. There is also the diploid strain Ucc5185, which was generated from the mating of Ucc5179 and Ucc5181.
The genotypes for the strains are listed according to (Lindstrom and Gottschling, 2009) in [Table C2].

Table C 2 – Genotypes of the mother enrichment strains

Ucc5179	*MATα ade2::hisG his3 leu2 lys2 ura3Δ0 trp1Δ63 hoΔ::PSCW11-cre-EBD78-NATMX loxP-UBC9-loxP LEU2loxP-CDC20-Intron-loxP-HPHMX*
Ucc5181	*MAT⟨ ade2::hisG his3 leu2 trp1Δ63 ura3Δ0 met15Δ::ADE2 hoΔ::PSCW11-cre-EBD78-NATMX loxPUBC9-* *loxP-LEU2 loxP-CDC20-Intron-loxP-HPHMX*
Ucc5185	*MATα/MAT⟨ ade2::hisG/ade2::hisG his3/his3 leu2/leu2 LYS2/lys2 ura3Δ0/ura3Δ0 trp1Δ63/trp1Δ63 MET15/met15Δ::ADE2 hoΔ::PSCW11-cre-EBD78-NATMX/hoΔ::PSCW11-cre-EBD78-NATMX loxP-UBC9-loxP-LEU2/loxP-UBC9-loxP-LEU2 loxP-CDC20-Intron-loxPHPHMX/ loxP-CDC20-Intron-loxP-HPHMX*

Due to the deletion of the ade2 gene in Ucc5179 colonies turn red when external adenine supply is low. Deletion of this gene leads to accumulation of the metabolite P-ribosylaminoimidazole (also termed AIR), which is oxidized to a red pigment (ribosylamino amidazolecarboxylate) in a respiration dependent manner ((Kim et al., 2002) and literature cited therein). Petite cells, which are unable to respire, will remain white and can therefore easily be distinguished by their colony color. I took advantage of this feature to keep track on the petite content during the aging process.

7.1.1 Ucc5179 - Fermentation

An aging experiment was performed with the Ucc5179 strain under fermentative growth conditions. Based on the color of the colonies on YPD-agar plates [Supp.C01] the fraction of petite cells was quantified over the replicative lifespan [Supp.C02a]. The strain nearly quantitatively turned into petites during the monitored lifetime.

The roGFP2-Orp1 reporter was measured over time. No changes in probe oxidation could be detected and old cells behaved in the same way as young cells [Fig.C7b]. However, when shocked with 2 mM H_2O_2 [Supp.C03a], both young and old cells seem to become slightly more resistant. When treated with 1 mM diamide, a similar behavior could be observed [Supp.C03b].

With the roGFP2-Grx1 reporter a more reducing cytosol was observed in the older cells [Fig.C7a]. Shocks with 2 mM H_2O_2 only had little effects on the roGFP2-Grx1 probe and the shift in oxidation of old cells was more or less the same as for the young cells [Supp.C03c]. Treatment with 1 mM diamide led to a higher probe oxidation with stronger resistance in the old cells [Supp.C03d]. Again also the young cells seem to become slightly more resistant.

The lack of H_2O_2 production in old Ucc5179 cells can easily be explained by the respiratory deficiency of the accumulating petites.
The glutathione reduction phenotype in the Ucc5179 [Fig.C7a] strain however, showed a different progression as in WΣ [Fig.C6]. This could also be due to the accumulation of petites as it follows the same trend as the petite-quantification [Supp.C02a]. I have never determined the pH in the petite background, therefore it cannot be ruled out that the observed reduction is a result of Glr1 stimulation by a lower pH of petite cells rather than a general age dependent acidification.

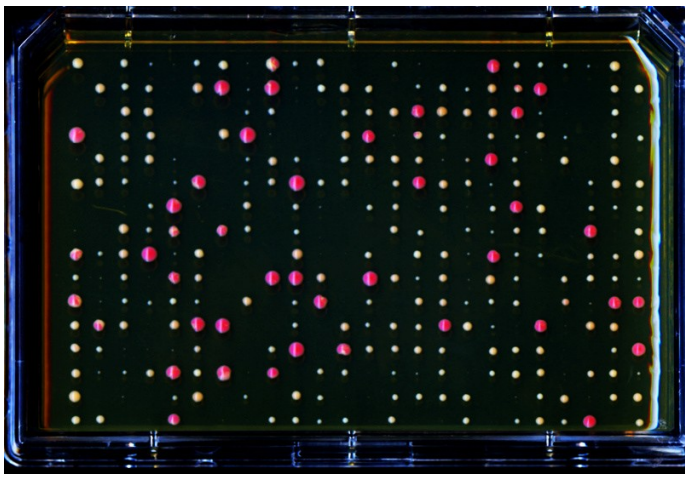

Supp.C1
Colony forming assay of a 26.9 h old Ucc5179 culture expressing roGFP2-Orp1. The red color indicates respiratory competent *grande* cells and the white colonies are respiratory deficient *petite* cells. The intermediate color may be attributed to the conversion of most progenies to *petite* cells after sorting a single *grande* cell.

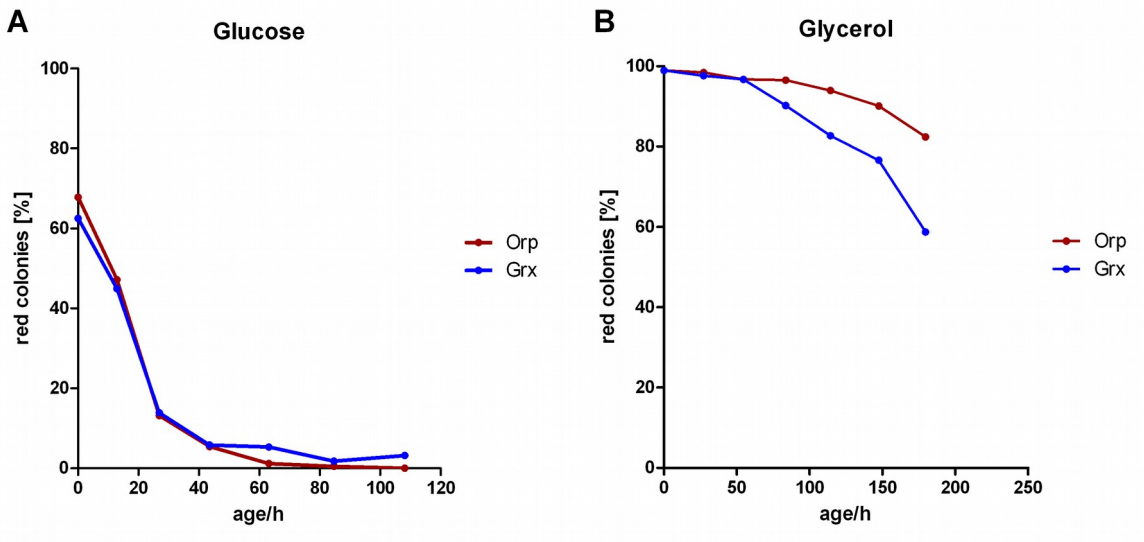

Supp.C2
Quantification of red colonies during replicative aging in Ucc5179 under fermentative conditions. The red color is an indicator for respiration competent cells. The cells were expressing either the roGFP2-Orp1 (red) or the roGFP2-Grx1 probe (blue).
a.) Aging experiment performed under fermenting conditions in glucose medium
b.) Aging experiment performed under respiring conditions in glycerol/ethanol medium

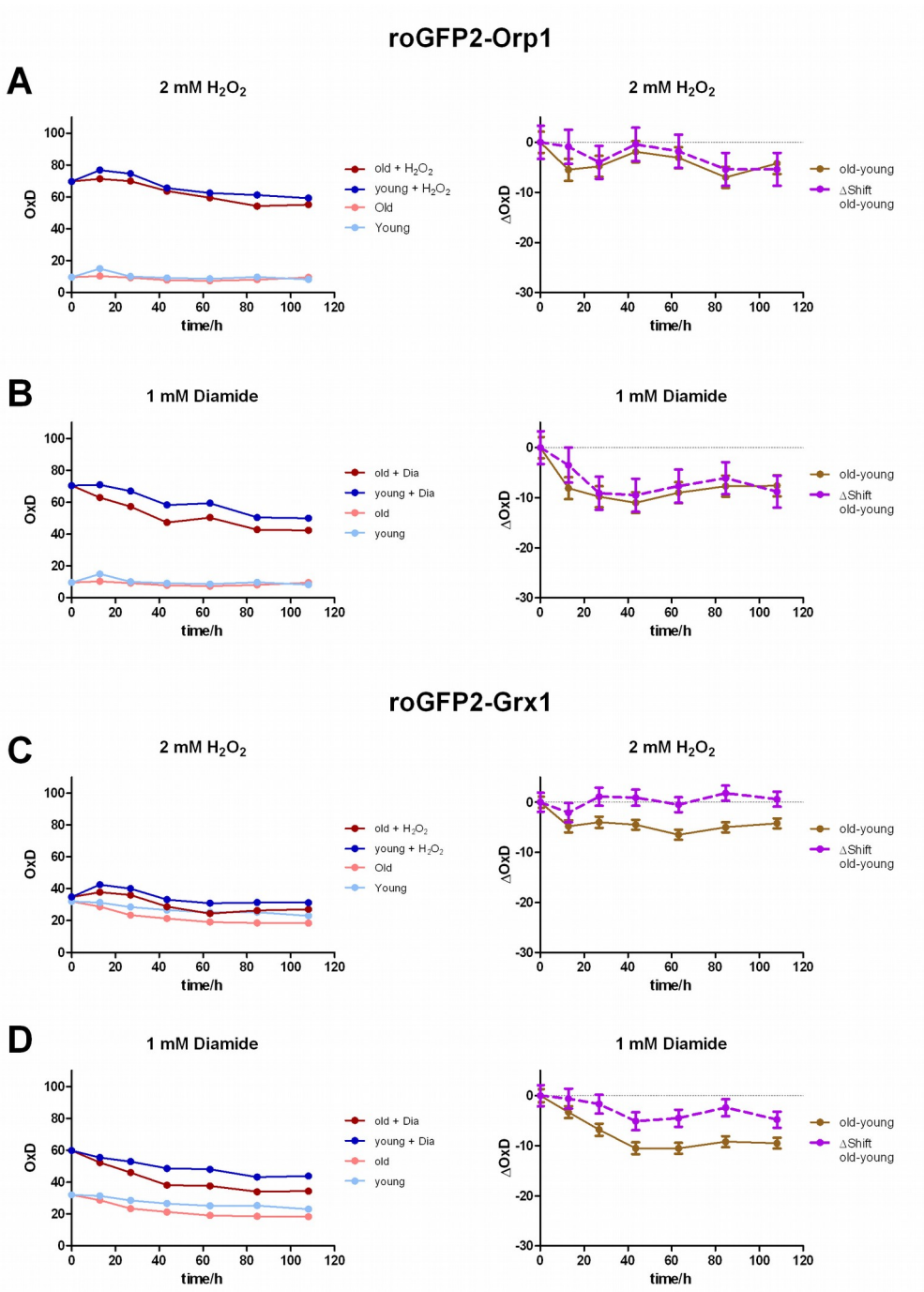

Supp.C3
Replicative aging in Ucc5179 under fermentative conditions after oxidant treatment. On the left side basal probe oxidation for young (light colors) and old cells (dark color) is shown. On the right side the difference of the maximal oxidation between old and young cells (light brown) or the differences in the oxidation shifts after peroxide treatment for old and young cells is plotted (dashed violet). Error bars represent the standard deviation of repeated probe calibration during the experiment.
a.) Ucc5179-cells expressing roGFP2-Orp1. Cells were treated with 2 mM H_2O_2.
b.) Ucc5179-cells expressing roGFP2-Orp1. Cells were treated with 1 mM diamide.
c.) Ucc5179-cells expressing roGFP2-Grx1. Cells were treated with 2 mM H_2O_2.
d.) Ucc5179-cells expressing roGFP2-Grx1. Cells were treated with 1 mM diamide.

7.1.2 Ucc5179 - Respiration

Under respiring conditions, the quantification of petite cells revealed that most of the measured cells are from the grande-phenotype [Supp.C02b]. In the presence of the roGFP2-Orp1 reporter the grande fraction was increased in old cells. It has to be mentioned that this representation could be misleading because only reporter-expressing cells were sorted on the plate. In glycerol/ethanol medium petite cells are not able to grow under those conditions and gradually lose reporter fluorescence. This should be reflected in the fraction of living cells. Unfortunately, this parameter could not be determined during this experiment. This was due to the weak expression of TagBFP in the parallel grown cell-line which prevented a clear separation of the dead cells from both strains.
Considering the high percentage of colony forming units (measured on YPD medium) [Fig.C20d] and the high fraction of grande cells compared to the growth in glucose, it is not clear why the replicative lifespan was reduced in glycerol/ethanol medium. Additionally, it is not intuitive why the roGFP2-Orp1 reporter increased the fraction of grande cells without increasing the lifespan.
However, assuming a constant (or increasing) petite frequency for each cell-division, the replicative oldest cells would have the highest probability of being petite. In this case the glycerol/ethanol medium would behave like a filter by eliminating the petites from the analysis. Cells with a slower growth rate would accomplish fewer divisions in the same time and are therefore more likely of still being grande. If the roGFP2-Orp1 expressing cells in glycerol divide slower than the roGFP2-Grx1 expressing cells (which is indicated by the raw data – not shown here), then the fraction of grande cells will stay larger for a longer time. In the final state, lifespan for Ucc5179 in glycerol/ethanol-medium would not be limited by aging but only by acquiring respiratory deficiency at an average budscar number of about 23. This would also explain why the roGFP2-Orp1 protein has no effect on the maximal replicative lifespan in this setup, because the medium would prevent the (petite) cells from reaching it.

Consistent with this assumption, no major changes could be detected by the redox reporters. In contrast to WΣ [Fig.C21], steady state level of peroxide is extremely low seen by the highly reduced state of the roGFP2-Orp1 reporter and only marginally increased in the old cells [Supp.C04a]. Both diamide and peroxide treatment oxidized young and old cells to the same level [Supp.C05a,b].
The glutathione pool measured by roGFP2-Grx1 did not show clear changes during the aging process under respiratory conditions in the mother enrichment strain [Supp.C04b]. Treatment with peroxide and diamide revealed no differences between old and young cells [Supp.C05c,d].

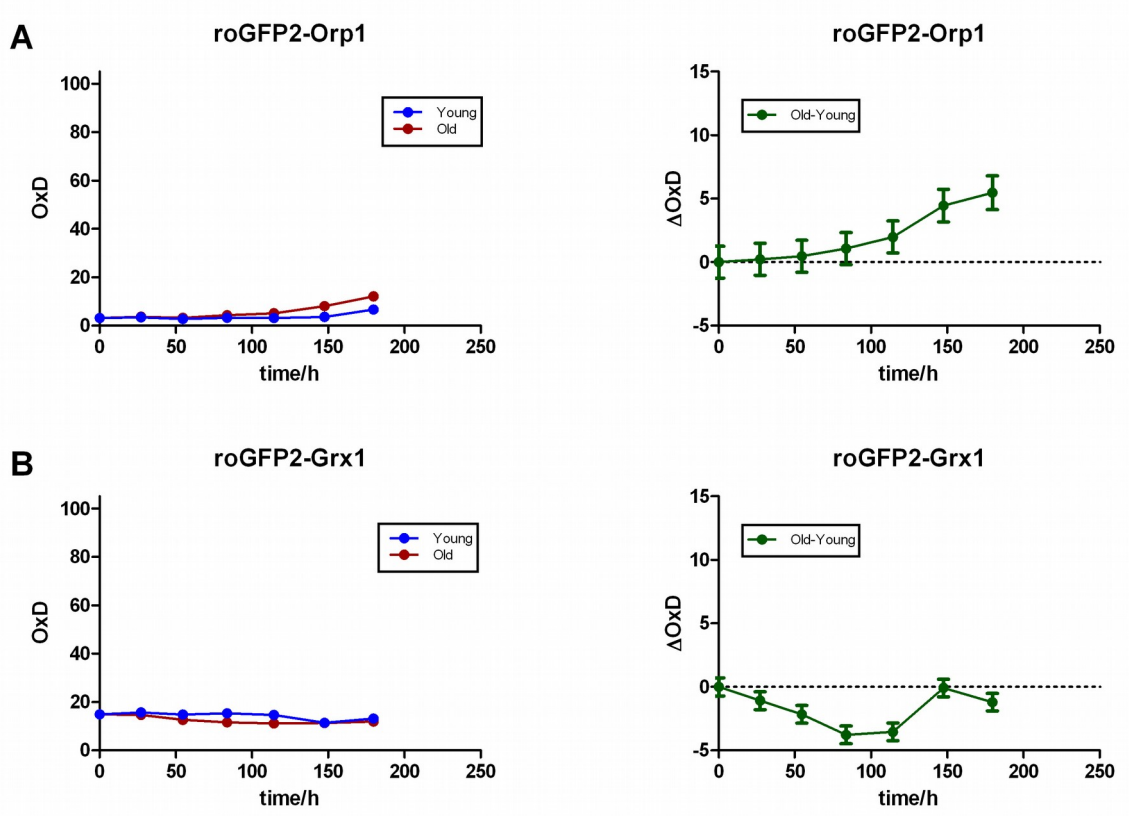

Supp.C4
Replicative aging in Ucc5179 under respiratory conditions. Average probe oxidation is shown for the old cells (red) and the internal young-cell control (blue). On the right the difference in probe oxidation between young and old cells is plotted (green). Error bars represent the standard error of repeated probe calibration during the experiment.
a.) Ucc5179-cells expressing roGFP2-Orp1
b.) Ucc5179-cells expressing roGFP2-Grx1

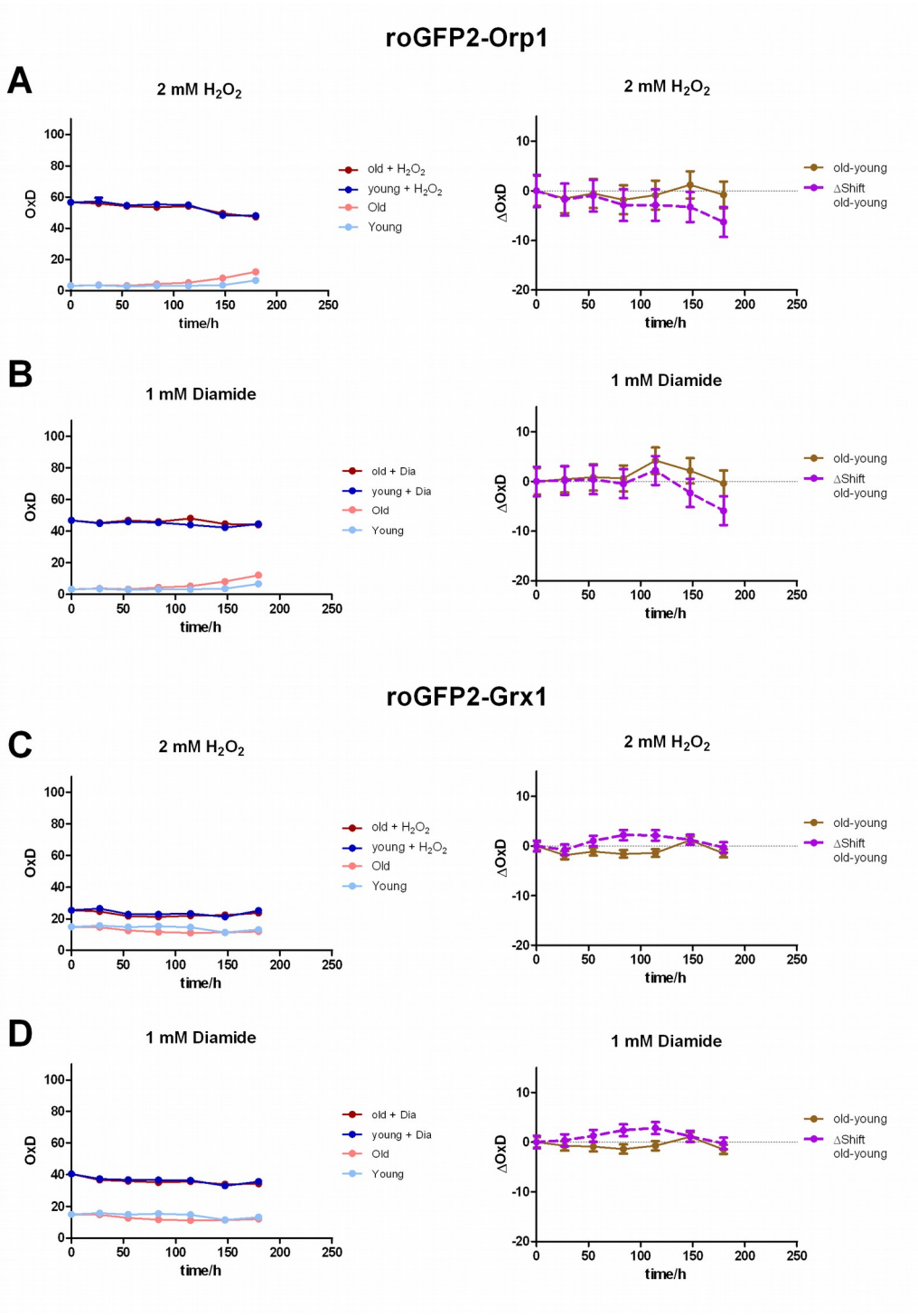

Supp.C5
Replicative aging in Ucc5179 under respiratory conditions after oxidant treatment. The layout is the same as in [Supp.C3].
a.) Ucc5179-cells expressing roGFP2-Orp1. Cells were treated with 2 mM H_2O_2
b.) Ucc5179-cells expressing roGFP2-Orp1. Cells were treated with 1 mM diamide
c.) Ucc5179-cells expressing roGFP2-Grx1. Cells were treated with 2 mM H_2O_2
d.) Ucc5179-cells expressing roGFP2-Grx1. Cells were treated with 1 mM diamide

7.1.3 Ucc5179 - Petites behave differently

Due to the high petite frequency of Ucc5179, an aging culture nearly quantitatively turns into petite cells during an aging experiment [Supp.C02a]. To test whether those cells would behave differently in the redox-reporters, eight petite and eight grande colonies were picked, cultured separately and then combined into a pure petite and pure grande culture. The cultures were then tested for colony formation and the amount of petite cells was determined. The petite cultures consisted to 100% of petite cells for both for roGFP2-Orp1 and roGFP-Grx1 expressing cells, whereas the grande cultures had a petite content of 5.7% for roGFP2 Orp1 and 6.5% for roGFP2-Grx1. For each of the cultures a growth curve and the doubling time was determined [Supp.C06]. The cultures were then tested for the response to diamide and peroxide treatment. Except for the peroxide response seen by the roGFP2-Grx1 reporter [Supp.C07d], all reporters indicate an increased resistance of petite cells to oxidative treatment [Supp.C07a-c]. Since the grande cultures still contained residual petites but the petite cultures were pure, the responses of a theoretical 100% grande culture could be calculated:

$$OxD_{Grande(100\%)} = (OxD_{Grande} - (Fraction_{petite} \bullet OxD_{petite}))/Fraction_{grande} \qquad \textit{Equation (C8)}$$

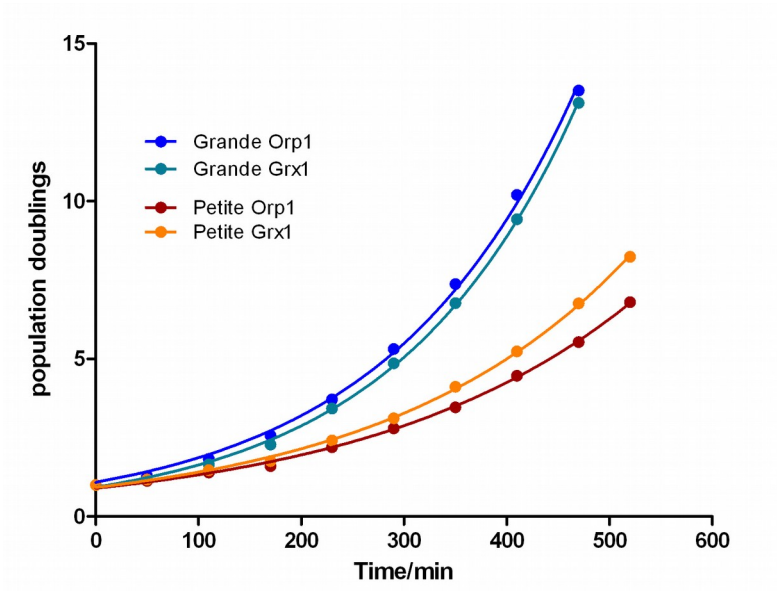

Supp.C6
Representative growth curves of roGFP2-Grx1/Orp1 expressing Ucc5179 in synthetic complete medium supplemented with glucose. For every growth curve eight individual *grande* or *petite* cells were picked and mixed to equal amounts. During the experiment the cells were not allowed to enter stationary phase. The data was fitted with a singe-exponential function.
The doubling times were: Grande Orp = 128.5 min; Grande Grx = 123.1 min;
Petite Orp = 178.6 min; Petite Grx = 164.5.

To see if the accumulation of petites could account for the observed changes in young cells in Ucc5179, the fraction of petites in the young culture from the aging experiment had to be estimated because the petites were only determined for the old cells by single cell spotting. To do this the petite content of the quantified old culture from the previous day was considered as a starting condition and by applying the determined individual growth rates the petite content was calculated for young cells on the actual day. De novo petite formation was neglected in this

model [Supp.C08a,b]. The response to oxidants from the 100% model cultures were then adapted to the calculated composition of the young cells from the aging experiment.
The calculated responses to diamide treatment match very well with the measured values of the young cells from the aging experiment [Supp.C08c,d], however, the response of the H_2O_2 treated cells could not be reconstructed for the early time-points [Supp.C08e,f]. By comparing the peroxide responses with the model cultures [Supp.C07b,d] it can be seen that the observed values from the aging experiment are much more oxidized than the pure grande culture could get. This could have several reasons. Addition of H_2O_2 changes the cellular pH, which influences reporter activity. Since no kinetics have been recorded for the model culture the signal may have not been saturated when measured for the model and oxidation could have been underestimated. Another explanation would be that the aging culture was measured under slightly different conditions (maybe the medium was stronger buffered because of the PBS from the enriched cells). This underlines again the importance of measuring old and young cells in parallel to avoid bias of experimental variations.

Taken together, caveats should be taken when working with a culture that contains substantial amounts of petite cells as they can behave significantly different as compared to grande cells. In the model cultures, the responses to diamide and peroxide treatment indicates that the glutathione and peroxide pools in petite cells are more effectively buffered than in grande cells.

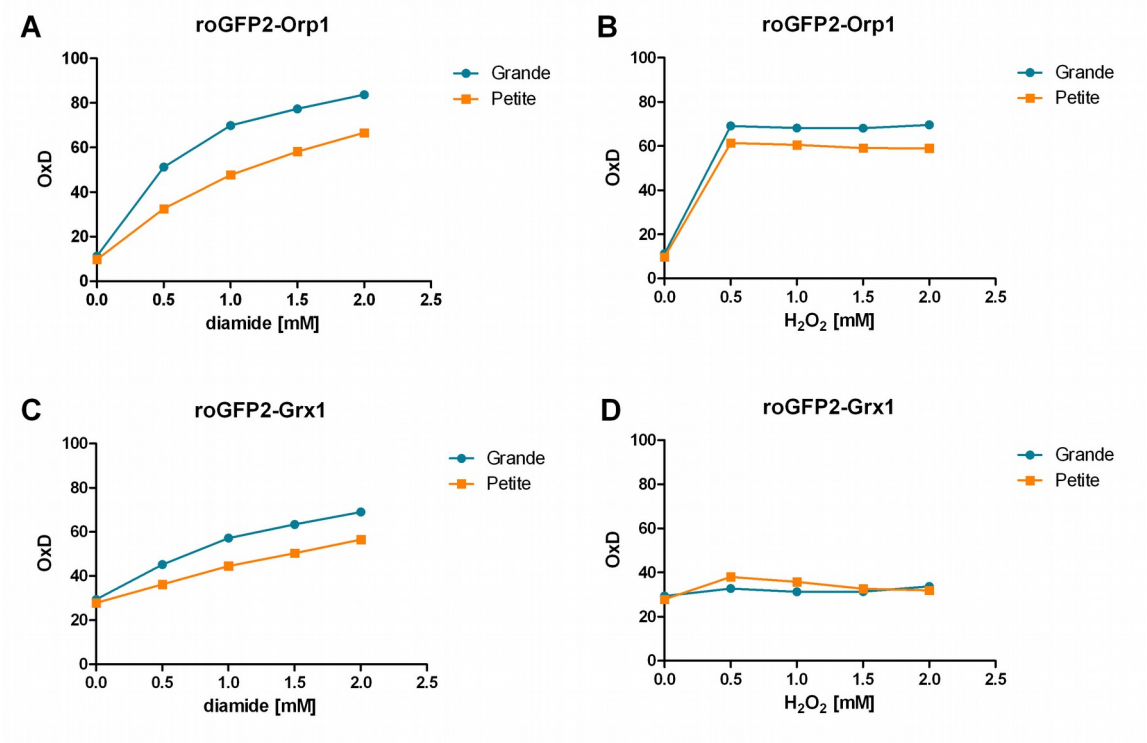

Supp.C7
Differences of *grande* and *petite*-cells after oxidant treatment in the Ucc5179 background under fermentative conditions. The cultures of *grande*- and *petite*-cells are the same as described in [Supp.C6]. Redox-reporters were measured about 15 minutes after oxidant treatment.
a.) Ucc5179-cells expressing roGFP2-Orp1 treated with diamide
b.) Ucc5179-cells expressing roGFP2-Orp1 treated with H_2O_2
c.) Ucc5179-cells expressing roGFP2-Grx1 treated with diamide
d.) Ucc5179-cells expressing roGFP2-Grx1 treated with H_2O_2

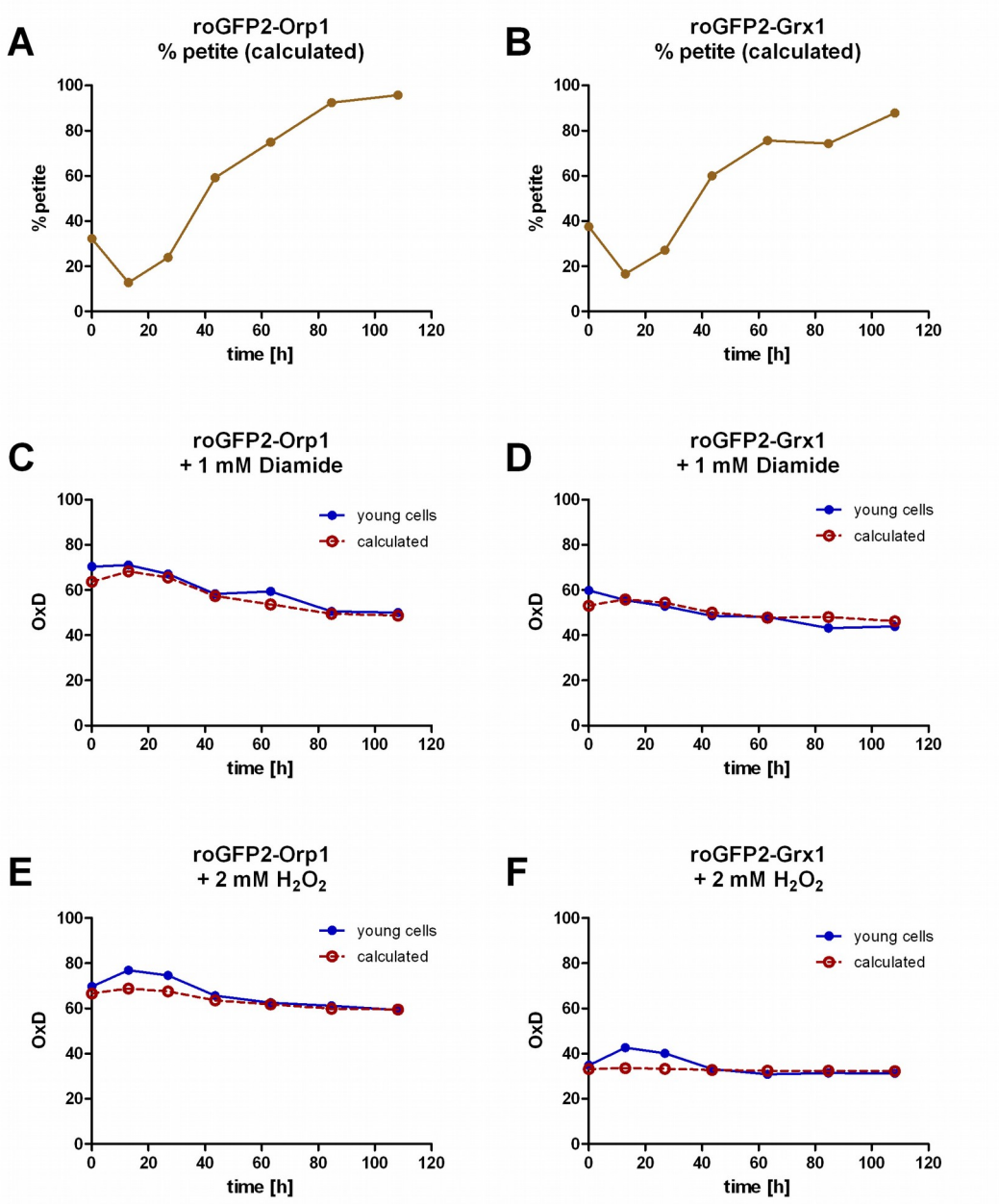

Supp.C8
Influence of the petite-content of Ucc5179 on the redox-response after oxidant treatment. Based on the amount of petite cells from the aging experiment [Supp.C2] and the growth-rate [Supp%_007], a theoretical petite content of the young culture was calculated and the redox-response, determined in [Supp.C7], was adapted to this composition. The measured young cells from the aging experiment is shown (solid-blue) and compared to a theoretical culture of equal petite content (dashed-red).
a.) Calculated petite-content of the young cells expressing roGFP2-Orp1
b.) Calculated petite-content of the young cells expressing roGFP2-Grx1
c.) roGFP2-Orp1 expressing cells treated with 1 mM diamide
d.) roGFP2-Grx1 expressing cells treated with 1 mM diamide
e.) roGFP2-Orp1 expressing cells treated with 2 mM H_2O_2
f.) roGFP2-Grx1 expressing cells treated with 2 mM H_2O_2

7.2 Influence of H_2O_2 on the pHluorin reporter

To rule out that cytosolic acidification seen after addition of H_2O_2 is due to oxidation of the pHluorin protein, the reporter was measured in the same way as pHluorin calibration was usually done but in the presence of peroxide in the buffer. The measurement was performed for three different buffers in WΣ wild type and the parallel grown Glr1-overexpressing strain [Supp.C09].
The results show that the pHluorin reporter is indeed influenced by the presence of peroxide at concentrations higher than 1 mM. However, the measured pH was increased by H2O2 and the effect was stronger at high pH.
This indicates that the cytosolic acidification upon peroxide addition is not mimicked by the oxidation of the pHluorin protein and even is underestimated at higher peroxide level.

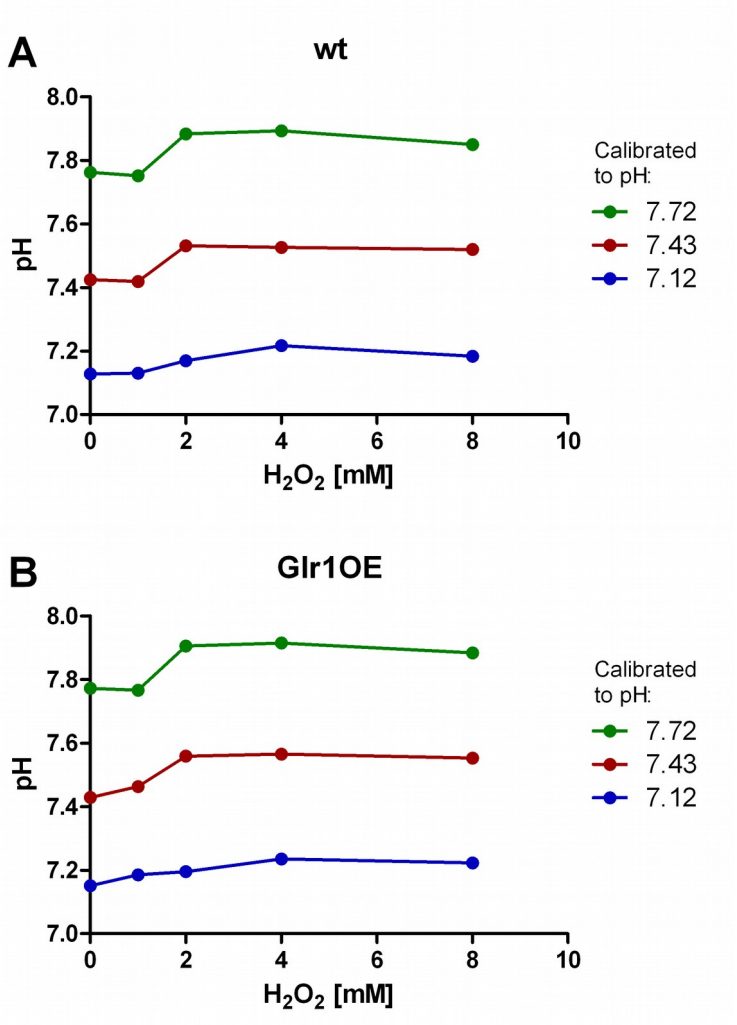

Supp.C9
Influence of H_2O_2 on the pHluorin reporter. WΣ-cells expressing the pHluorin reporter were permeabilized with digitonin in buffered solutions containing increasing amounts of H_2O_2. The calibration curve determined in the absence of peroxide was applied to the measurements.
a.) Readout of the pHluorin reporter in WΣ wild-type
b.) Readout of the pHluorin reporter in WΣ overexpressing Glr1

7.3 Reporter-measurements can be done in the presence of TagBFP

When properly compensated, measurements of the ratiometric reporters can be performed for two different cell-types in the same culture, if one of them also contains TagBFP as a marker-protein.
To demonstrate this, a mixed culture was set up and calibrated with pH-standard-solutions. Individually processed, both calibration curves – fitted with a sigmoidal function – match nearly perfectly [Supp.C10]. Parallel measurements of logarithmically growing mixed-cultures also give highly similar results.

Table C 3 – Parallel redox and pH measurements of differentially tagged strains

	Blank	TagBFP	Difference (Blank-TagBFP)
pH_measurement#1	7.582	7.582	0.000
pH_measurement#2	7.547	7.559	-0.012
pH_measurement#3	7.556	7.566	-0.010
roGFP2-Grx1	39.3%	39.6%	-0.30%
roGFP2-Orp1	14.4%	13.0%	1.40%

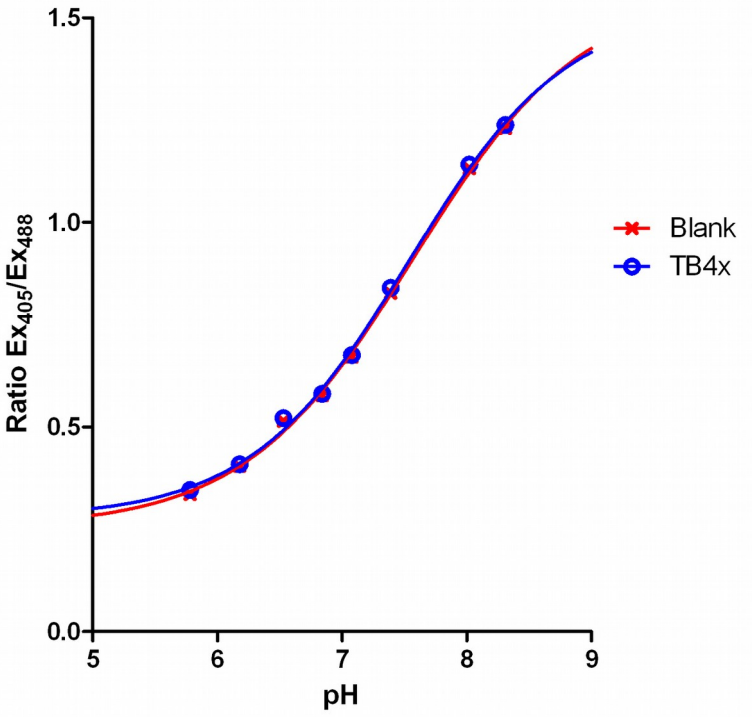

Supp.C10
Cytosolic pHluorin can be co-detected with TagBFP. An example pH-calibration-curve is depicted showing the ratio of the pHluorin-relevant channels while digitonin-permeabilized WΣ-cells were equilibrated in different pH-buffers. The cells were either expressing only pHluorin (blank) or coexpressing pRS304-P_{TEF1}-TagBFP4x (TB4x). Note that both cell-types were co-cultured and co-detected. The influence of TagBFP on the other fluorescent channels was eliminated by applying a compensation matrix.

7.4 Larger cells do not show an increased pH

In the model of (Henderson et al., 2014) it is stated that the pH gradually rises when cells are getting older. The alkalization process should already start after 3 divisions of the mother cell. When cells are getting older their size increases which can be detected by the forward-scatter parameter in the flow-cytometer (see *Part A*).
To investigate whether the cytosolic pH is correlated with the cell-size, I determined the pH in different strain backgrounds. Cells from the single-cell gate were chosen and the pH was plotted against the forward-scatter (area-parameter) [Supp.C11]. A linear fit was applied to the data to visualize the trend. The parameters are summarized in [Table C4].
It can clearly be seen that there is only a weak correlation between forward-scatter and pH. Cells with larger scatter seem to be slightly more acidic than cells with smaller scatter. There is definitely no alkalization visible in larger cells. Note that the ploidy of the strain is also reflected in the forward-scatter parameter.

Table C 4 – pH-measurements in different strain backgrounds

	Ploidy	pH (mean)	FSC-A (mean)	slope (fitting)	R^2 (fitting)
BY4741	haploid	7.88	3.48	-0.02147	0.005149
BY4743	diploid	7.90	6.06	-0.01876	0.003826
SEY6210	haploid	7.80	3.83	-0.05038	0.03188
Ucc5179	haploid	7.81	3.78	-0.01359	0.002525
Ucc5185	diploid	7.80	6.36	-0.01887	0.003197
W303aα	diploid	7.90	6.99	-0.02257	0.01121
WΣ (clone 1)	haploid	7.81	4.51	-0.01439	0.005311
WΣ (clone 2)	haploid	7.82	4.34	-0.01819	0.007486

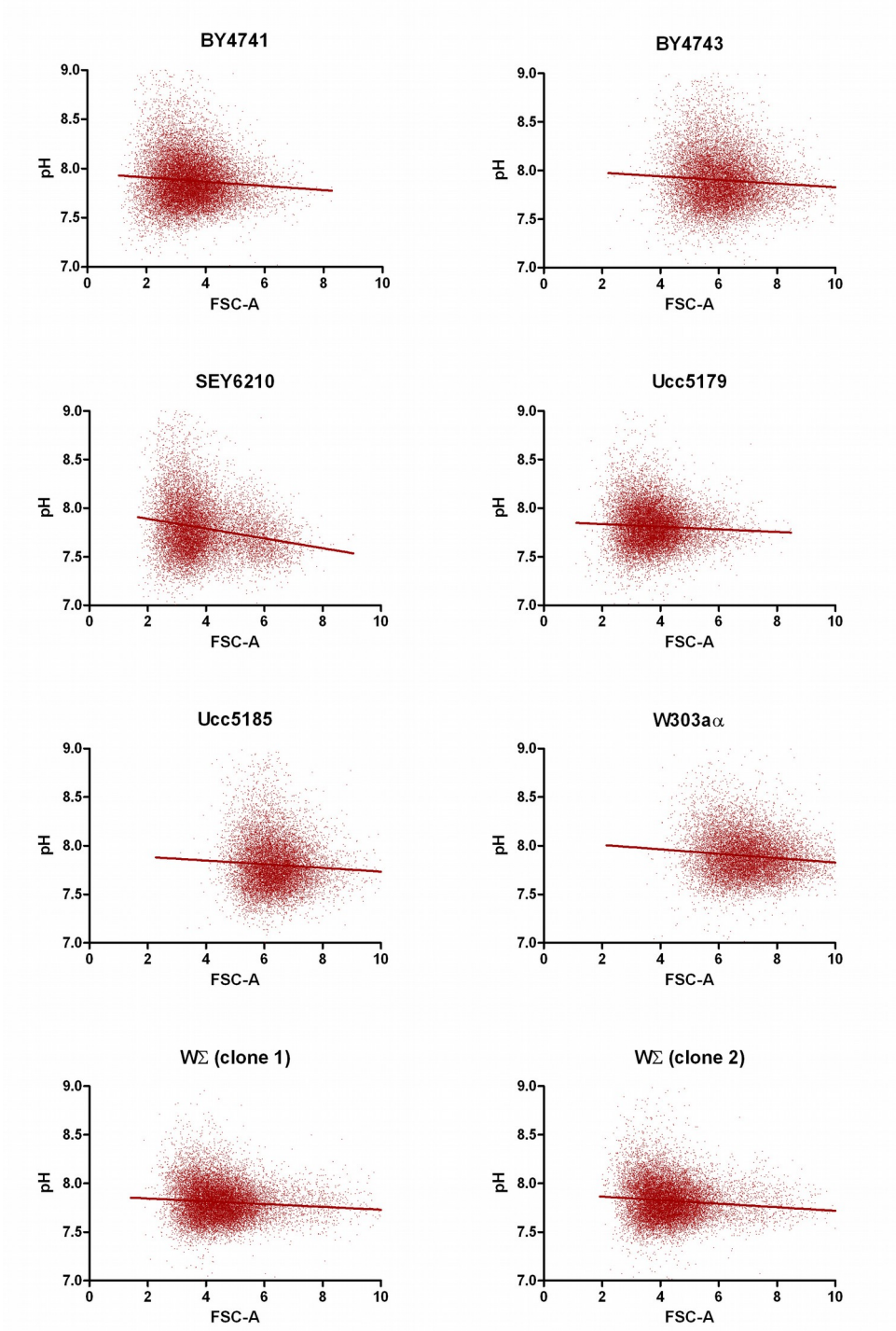

Supp.C11
Correlation between pH and forward-scatter in different strain backgrounds. The pH was determined independently for each strain and events from the single-cell gating were plotted against the normalized forward-scatter (area-parameter). To visualize the trend a straight line was fitted to the data-points. Haploid strains are: BY4741, SEY6210, Ucc5179 and WΣ. Diploid strains are: BY4743, Ucc5185 and W303aα.

Appendix

1 Materials and Methods

1.1 Growth medium

Yeast media were prepared as described by (Sherman, 2002).
Synthetic medium contained:

Table D 1- Composition of the yeast synthetic medium

YNB (Difco) w/o aminoacids and ammonium sulfate	1.7 g/l
Ammonium sulfate	5 g/l
Glucose (fermentative growth)	2%
Glycerol + Ethanol (non-fermentative growth)	3% + 2%
Amino acid/nucleobase mix	see below

Table D 2- Composition of the supplements for the synthetic complete medium

Amino acid/ nucleobase	mg/l
Ade-Sulfat	20
Ura	20
Trp	20
His-HCl	20
Arg-HCl	20
Met	20
Tyr	30
Leu	60
Ile	30
Lys-HCl	30
Phe	50
Glu	100
Asp	100
Val	150
Thr	200
Ser	400

Appropriate dropout mixes of the amino-acids above were created and when needed supplemented with remaining amino-acids from 100x stocks. Synthetic complete (SC) medium refers to glucose containing medium supplemented with all amino acids. The dropout for example SC(-His) contained all the amino-acids except histidine.

SG-medium (or SG3E2) refers to synthetic medium with all amino acids but containing 3% glycerol and 2% ethanol instead of glucose.

Selective plates were prepared with the same recipe as the dropout media but containing 1.5% agar.
For plasmid-shuffling 5-Fluoroorotic acid (f.c. 1mg/ml) was added from a 100x stock in DMSO.

1.2 Yeast transformation

Transformation of yeast cells was done by using the lithium acetate/single-stranded carrier DNA/polyethylene glycol method (Gietz and Woods, 2002).

1.3 SYTOX-Green staining

For the cell-cycle analysis the cells were stained with SYTOX-Green™ (*Invitrogen*). Cells were harvested (0.68 OD-units) in logarithmic phase and centrifuged at 3000 rpm for 5 minutes. The supernatant was discarded and cells were resuspended in 70% ethanol and incubated over night at 4°C. Samples were then spun down again, washed once with water and then resuspended in 0.5 ml 50mM Tris/HCl (pH=8.0). RNase A was added (f.c. 200µg/ml) and incubated for 3h at 37°C. Samples were then centrifuged at 3000 rpm for 5 minutes and resuspended in 0.5 ml 50mM Tris/HCl (pH=7.5). Proteinase K was added (f.c. 1mg/ml) and the samples were incubated at 50°C for 45 minutes. Samples were then centrifuged again at 3000 rpm for 5 minutes and resuspended in 0.5 ml 50mM Tris/HCl (pH=7.5). For the DNA staining, a 50mM Tris/HCl (pH=7.5) buffer containing 1µM SYTOX-Green™ was prepared and 50 µl of cells were transferred to 1 ml of the buffer. Prior to the measurement cells were sonicated. Finally, the samples were analyzed on the cytometer at the lowest possible flow-rate.

1.4 Instrument specifications & detection

The available lasers and the fluorescent detectors of the flow-cytometers used in this work is given in the following tables.

Table D 3- Instrument specifications of the FACS-Canto II

FACS Canto II		
Excitation	Detector	Spectral range (nm)
405 nm	405-A	502-535
	405-B	425-475
488 nm	488-A	750-810
	488-B	670-735
	488-D	564-606
	488-E	515-545
	SSC (488-F)	483-493
	FSC	483-493
633 nm	633-A	750-810
	633-C	650-670

Table D 4 - Instrument specifications of the FACS-Aria IIIu

FACS Aria IIIu		
Excitation	Detector	Spectral range (nm)
407 nm	407-A	600-620
	407-B	502-520
	407-C	430-470
488 nm	488-A	675-715
	488-B	515-545
	SSC (488-C)	483-493
	FSC	483-493
561 nm	561-A	750-810
	561-B	663-677
	561-C	600-620
	561-D	574.5-590.5
633 nm	633-A	750-810
	633-B	650-670

For every fluorescent marker an appropriate detector in the flow-cytometers was chosen.

Table D 5- Fluorophore detection in the flow-cytometers

Fluorophore	Detectors	
	FACS CantoII	FACS AriaIIIu
sfGFP	488-E	488-B
T-Sapphire	405-A	407-B
TagBFP	405-B	407-C
roGFP2 constructs	488-E/405-A	488-B/407-B
Alexa633	633-C	633-B
Propidium iodide	488-B	561-C
SYTOX Green	488-E	Not used

1.5 Data Processing

For the colony-forming assay living cells from the single-cell population were sorted in a 384-well format on YPD agar plates. Cells were defined as “living” when their reporter fluorescence was clearly separable from the autofluorescence. In addition, when working with the FACS-Aria IIIu and propidium iodide (PI) was added, cells also had to be PI-negative to be considered living.
The fraction of old, living cells was always done relative to the internal young-cell control, to account for cells that were damaged by sonication.
Agar-plates with sorted single-cells were grown at 30°C in a humidified incubator, until all colonies were clearly visible. The plates were scanned and colonies were counted manually. The number of sorted cells (in most cases 384) was set to 100%.

For most of the flow-cytometric experiments, in which a steady state reporter level was measured, it was sufficient to work with population averages of the compensated data. These values were directly calculated by the FACS-Diva 6.1.3 software (*BD Bioscience*). The data were then transferred to Microsoft Excel 2003 and the mean values of the selected gates and channels were used for the calculations.

From all values the autofluorescence was subtracted and when possible the data were normalized to the bright CST standard beads. For aging experiments were CST-beads were measured multiple times during an experiment day, interpolation of the CST-values were performed to match the acquisition-time of the cell-sample.

For experiments were single cell resolution was necessary, the gates were specified with FlowJo v10.07 software (*TreestarInc.*) and single cell data were then imported into Microsoft Excel for further calculations.

Nearly all graphs were created with Prism 5 software (*GraphPad*) and function fittings were performed mostly with the built-in formulas. For live-kinetic recordings a delay of 10 seconds between mixing and recording was anticipated and the previously acquired basal reporter activity was fixed as a fitting-constant at t=0.

Spline interpolation and box smoothening was done with Igor Pro v6.30 software (*WaveMetrics*). Shortly, spline interpolation was performed by using the "Interpolate" command with the "cubic spline" option. The fluorescence and event-time of the Rainbow beads were used as source waves and the event-time of the cells as x-destination. The data were pre-averaged over 9-14 nodes and the end-nodes were chosen by extrapolation. The data were transferred back to excel and the last interpolated Rainbow-bead data-point was set to 100% and the parameter was defined as "Laser intensity". This parameter was then used to scale the CST measurement, which was acquired immediately after the kinetic to the time-points of the single-cell events. Then the individual cellular events were normalized by the extrapolated CST-values. Finally, normalized autofluorescence was subtracted and redox calculations were performed.

The data for the budscars were fitted with a Gompertz function:

$$Y(x)=a\cdot\exp(-b\cdot\exp(-c\cdot x)) \qquad \textit{Equation (D1)}$$

where "a" defines the saturation, "b" the displacement and "c" the rate.

Sigmoidal fittings were done with the following formula:

$$Y(x)=Y_{\min}+\frac{(Y_{\max}-Y_{\min})}{(1+10^{\hat{}}((a-x)\cdot b))} \qquad \textit{Equation (D2)}$$

2 Chemicals and Reagents

Table D 6 – List of chemicals

	Manufacturer	Catalog number
Alexa633-Succinimidyl-ester	Invitrogen	A20005
Alpha-factor (WHWLQLKPGQPMY)	Peptide Specialty Laboratories GmbH (Heidelberg)	special order
Ammoniumsulfate	Merck	1211
ConcanavalinA	Sigma-Aldrich	C2010
Cycloheximide	Sigma-Aldrich	C7698
Diamide	Sigma-Aldrich	D3648
Digitonin	Sigma-Aldrich	D141
N,N-Dimethylformamide (DMF)	Sigma-Aldrich	227056
Dimethylsulfoxid (DMSO)	Grüssing (Filsum)	10281
2,4-Dinitrophenol (DNP)	Sigma-Aldrich	D198501
Desoxycorticosterone (21-Hydroxyprogesterone) (DOC)	Sigma-Aldrich	D6875
Dithiothreitol (DTT)	ROTH	6908.4
EDTA	AppliChem	A3553
Ethanol	Sigma-Aldrich	32205
17β-Estradiol	Sigma-Aldrich	E8875
5-Fluoroorotic Acid (5-FOA) 100 mg/ml	Zymo Research	F9003
Glucose (D(+)-Glucose monohydrate)	Merck	1.08342
Glycerol	Sigma-Aldrich	15523
Geneticindisulfat (G418)	ROTH	0239.4
H_2O_2	Merck	1.07209
HEPES	ROTH	9105.4
HygromycinB	Invivogen	ant-hm-5
Lithium acetate dihydrate	Sigma-Aldrich	L6883
2-(N-Morpholino) ethanesulfonic acid hydrate (MES)	Sigma-Aldrich	M5287
$NaHCO_3$	FERAK (Berlin-West)	01141
Nourseothricin (ClonNAT)	Werner BioAgents	#
Polyethylene glycol (PEG4000)	SERVA	33136
Propidium iodide (PI)	Merck	537059
ProteinaseK	ROTH	7528.2
RNaseA	ROTH	7156.2
Salmon Sperm DNA	Invitrogen	15632-011
Solophenylflavin (Direct yellow96)	Bruno Ludewig – Farbstoffe (48486 Emsbüren)	MU12447
Sorbitol	Merck	1.07758
SYTOX®-Green	Life-Technologies	S7020
Tris-(hydroxymethyl)-aminomethan (Tris)	ROTH	4855.2
Yeast nitrogen base (Difco) w/o aminoacids and ammonium sulfate	Becton, Dickinson	233520
Zeocin®	Invitrogen	R25001

BD™ Cytometer Setup & Tracking Beads", (BD-Bioscience Cat.no. 641319)
Sphero™ Rainbow Calibration Particles", (Spherotech Cat no. RCP-30-5A (8 peaks)

3 References

Abreu, I., and Cabelli, D. (2010). Superoxide dismutases—a review of the metal-associated mechanistic variations. Biochim. Biophys. Acta (BBA)-Proteins … *1804*, 263–274.

Åkerfelt, M., Morimoto, R., and Sistonen, L. (2010). Heat shock factors: integrators of cell stress, development and lifespan. Nat. Rev. Mol. Cell … *11*, 545–555.

Ayer, A., Fellermeier, S., Fife, C., Li, S., and Smits, G. (2012). A genome-wide screen in yeast identifies specific oxidative stress genes required for the maintenance of sub-cellular redox homeostasis. PLoS One *7*, e44278.

Ayer, A., Sanwald, J., Pillay, B., and Meyer, A. (2013). Distinct redox regulation in sub-cellular compartments in response to various stress conditions in Saccharomyces cerevisiae. PLoS One *8*, e65240.

Bardwell, L. (2005). A walk-through of the yeast mating pheromone response pathway. Peptides *25*, 1465–1476.

Barros, M., and Bandy, B. (2004). Higher respiratory activity decreases mitochondrial reactive oxygen release and increases life span in Saccharomyces cerevisiae. J. Biol. … *279*, 49883–49888.

Baruffini, E., Lodi, T., Dallabona, C., and Foury, F. (2007). A single nucleotide polymorphism in the DNA polymerase gamma gene of Saccharomyces cerevisiae laboratory strains is responsible for increased mitochondrial. Genetics *177*, 1227–1231.

Baruffini, E., Ferrero, I., and Foury, F. (2010). In vivo analysis of mtDNA replication defects in yeast. Methods *51*, 426–436.

Beales, N. (2004). Adaptation of Microorganisms to Cold Temperatures, Weak Acid Preservatives, Low pH, and Osmotic Stress: A Review. Compr. Rev. Food Sci. Food Saf. *3*, 1–20.

Van den Berg, M.A., and Steensma, H.Y. (1995). ACS2, a Saccharomyces cerevisiae gene encoding acetyl-coenzyme A synthetase, essential for growth on glucose. Eur. J. Biochem. *231*, 704–713.

Billinton, N., and Knight, a W. (2001). Seeing the wood through the trees: a review of techniques for distinguishing green fluorescent protein from endogenous autofluorescence. Anal. Biochem. *291*, 175–197.

Calderwood, S., Murshid, A., and Prince, T. (2009). The shock of aging: molecular chaperones and the heat shock response in longevity and aging–a mini-review. Gerontology *55*, 550–558.

Canonaco, F., Schlattner, U., Pruett, P., Wallimann, T., and Sauer, U. (2002). Functional expression of phosphagen kinase systems confers resistance to transient stresses in Saccharomyces cerevisiae by buffering the ATP pool. J. Biol. … *277*, 31303–31309.

Chen, C., Dewaele, S., Braeckman, B., Desmyter, L., Verstraelen, J., Borgonie, G., Vanfleteren, J., and Contreras, R. (2003). A high-throughput screening system for genes extending life-span. Exp. Gerontol. *38*, 1051–1063.

Clark-Walker, G. (2003). Kinetic properties of F 1-ATPase influence the ability of yeasts to grow in anoxia or absence of mtDNA. Mitochondrion *2*, 257–265.

Conomos, D., Pickett, H., and Reddel, R. (2013). Alternative lengthening of telomeres: remodeling the telomere architecture. Front. Oncol. *3*, 27.

Dechant, R., Binda, M., Lee, S., Pelet, S., Winderickx, J., and Peter, M. (2010). Cytosolic pH is a second messenger for glucose and regulates the PKA pathway through V-ATPase. EMBO … *5*, 4–8.

Defossez, P.A., Prusty, R., Kaeberlein, M., Lin, S.J., Ferrigno, P., Silver, P.A., Keil, R.L., and Guarente, L. (1999). Elimination of replication block protein Fob1 extends the life span of yeast mother cells. Mol. Cell *3*, 447–455.

Delaney, J.R., Chou, A., Olsen, B., Carr, D., Murakami, C., Ahmed, U., Sim, S., An, E.H., Castanza, A.S., Fletcher, M., et al. (2013). End-of-life cell cycle arrest contributes to stochasticity of yeast replicative aging. FEMS Yeast Res. *13*, 267–276.

Delaunay, A., Pflieger, D., Barrault, M.B., Vinh, J., and Toledano, M.B. (2002). A thiol peroxidase is an H2O2 receptor and redox-transducer in gene activation. Cell *111*, 471–481.

Diakov, T.T., Tarsio, M., and Kane, P.M. (2013). Measurement of vacuolar and cytosolic pH in vivo in yeast cell suspensions. J. Vis. Exp. 1–7.

Dimitrov, L.N., Brem, R.B., Kruglyak, L., and Gottschling, D.E. (2009). Polymorphisms in multiple genes contribute to the spontaneous mitochondrial genome instability of Saccharomyces cerevisiae S288C strains. Genetics *183*, 365–383.

Dooley, C.T., Dore, T.M., Hanson, G.T., Jackson, W.C., Remington, S.J., and Tsien, R.Y. (2004). Imaging dynamic redox changes in mammalian cells with green fluorescent protein indicators. J. Biol. Chem. *279*, 22284–22293.

Dowell, R.D., Ryan, O., Jansen, A., Cheung, D., Agarwala, S., Danford, T., Bernstein, D.A., Rolfe, P.A., Heisler, L.E., Chin, B., et al. (2010). Genotype to phenotype: a complex problem. Science *328*, 469.

Ephrussi, B., de Margerie-Hottinguer, H., and Roman, H. (1955). SUPPRESSIVENESS: A NEW FACTOR IN THE GENETIC DETERMINISM OF THE SYNTHESIS OF RESPIRATORY ENZYMES IN YEAST. Proc. Natl. Acad. Sci. U. S. A. *41*, 1065–1071.

Fehrmann, S., Paoletti, C., Goulev, Y., Ungureanu, A., Aguilaniu, H., and Charvin, G. (2013). Aging yeast cells undergo a sharp entry into senescence unrelated to the loss of mitochondrial membrane potential. Cell Rep. *5*, 1589–1599.

Feser, J., Truong, D., Das, C., Carson, J.J., Kieft, J., Harkness, T., and Tyler, J.K. (2010). Elevated histone expression promotes life span extension. Mol. Cell *39*, 724–735.

Fontana, L., Partridge, L., and Longo, V.D. (2010). Extending healthy life span--from yeast to humans. Science *328*, 321–326.

Gaisne, M., Bécam, a. M., Verdière, J., and Herbert, C.J. (1999). A "natural" mutation in Saccharomyces cerevisiae strains derived from S288c affects the complex regulatory gene HAP1 (CYP1). Curr. Genet. *36*, 195–200.

Ghaemmaghami, S., Huh, W.-K., Bower, K., Howson, R.W., Belle, A., Dephoure, N., O'Shea, E.K., and Weissman, J.S. (2003). Global analysis of protein expression in yeast. Nature *425*, 737–741.

Gietz, R.D., and Woods, R.A. (2002). Transformation of yeast by lithium acetate/single-stranded carrier DNA/polyethylene glycol method. Methods Enzymol. *350*, 87–96.

Goldstein, A.L., and McCusker, J.H. (1999). Three new dominant drug resistance cassettes for gene disruption in Saccharomyces cerevisiae. Yeast *15*, 1541–1553.

Grad, I., and Picard, D. (2007). The glucocorticoid responses are shaped by molecular chaperones. Mol. Cell. Endocrinol. *275*, 2–12.

Grimminger, V., Richter, K., Imhof, A., Buchner, J., and Walter, S. (2004). The Prion Curing Agent Guanidinium Chloride Specifically Inhibits ATP Hydrolysis by Hsp104. J. Biol. Chem. *279*, 7378–7383.

Gueldener, U., Heinisch, J., Koehler, G.J., Voss, D., and Hegemann, J.H. (2002). A second set of loxP marker cassettes for Cre-mediated multiple gene knockouts in budding yeast. Nucleic Acids Res. *30*, e23.

Gutscher, M., Pauleau, A.-L., Marty, L., Brach, T., Wabnitz, G.H., Samstag, Y., Meyer, A.J., and Dick, T.P. (2008). Real-time imaging of the intracellular glutathione redox potential. Nat. Methods *5*, 553–559.

Gutscher, M., Sobotta, M.C., Wabnitz, G.H., Ballikaya, S., Meyer, A.J., Samstag, Y., and Dick, T.P. (2009). Proximity-based protein thiol oxidation by H2O2-scavenging peroxidases. J. Biol. Chem. *284*, 31532–31540.

Harman, D. (1956). Aging: a theory based on free radical and radiation chemistry. J. Gerontol. *11*, 298–300.

Henderson, K.A., Hughes, A.L., and Gottschling, D.E. (2014). Mother-daughter asymmetry of pH underlies aging and rejuvenation in yeast. Elife *3*.

Hon, T., Hee, C.L., Hu, Z., Iyer, V.R., and Zhang, L. (2005). The heme activator protein Hap1 represses transcription by a heme-independent mechanism in Saccharomyces cerevisiae. Genetics *169*, 1343–1352.

Hu, Z., Chen, K., Xia, Z., Chavez, M., Pal, S., Seol, J.H., Chen, C.C., Li, W., and Tyler, J.K. (2014). Nucleosome loss leads to global transcriptional up-regulation and genomic instability during yeast aging. Genes Dev. *28*, 396–408.

Hughes, A.L., and Gottschling, D.E. (2012). An early age increase in vacuolar pH limits mitochondrial function and lifespan in yeast. Nature *492*, 261–265.

Kaeberlein, M., McVey, M., and Guarente, L. (1999). The SIR2/3/4 complex and SIR2 alone promote longevity in Saccharomyces cerevisiae by two different mechanisms. Genes Dev. *13*, 2570–2580.

Kaeberlein, M., Steffen, K.K., Hu, D., Dang, N., Kerr, E.O., Tsuchiya, M., Fields, S., and Kennedy, B.K. (2006). Comment on "HST2 mediates SIR2-independent life-span extension by calorie restriction". Science *312*, 1312; author reply 1312.

Kim, G., Sikder, H., and Singh, K.K. (2002). A colony color method identifies the vulnerability of mitochondria to oxidative damage. Mutagenesis *17*, 375–381.

Kirchman, P. a., and Botta, G. (2007). Copper supplementation increases yeast life span under conditions requiring respiratory metabolism. Mech. Ageing Dev. *128*, 187–195.

Kirschke, E., Goswami, D., Southworth, D., Griffin, P.R., and Agard, D. a. (2014). Glucocorticoid receptor function regulated by coordinated action of the Hsp90 and Hsp70 chaperone cycles. Cell *157*, 1685–1697.

Kuge, S., Arita, M., Murayama, A., Maeta, K., Izawa, S., Inoue, Y., and Nomoto, A. (2001). Regulation of the yeast Yap1p nuclear export signal is mediated by redox signal-induced reversible disulfide bond formation. Mol. Cell. Biol. *21*, 6139–6150.

Kupiec, M. (2014). Biology of telomeres: lessons from budding yeast. FEMS Microbiol. Rev. *38*, 144–171.

Kwan, E.X., Foss, E.J., Tsuchiyama, S., Alvino, G.M., Kruglyak, L., Kaeberlein, M., Raghuraman, M.K., Brewer, B.J., Kennedy, B.K., and Bedalov, A. (2013). A Natural Polymorphism in rDNA Replication Origins Links Origin Activation with Calorie Restriction and Lifespan. PLoS Genet. *9*, e1003329.

Lam, Y.T., Aung-Htut, M.T., Lim, Y.L., Yang, H., and Dawes, I.W. (2011). Changes in reactive oxygen species begin early during replicative aging of Saccharomyces cerevisiae cells. Free Radic. Biol. Med. *50*, 963–970.

Lamming, D.W., Latorre-Esteves, M., Medvedik, O., Wong, S.N., Tsang, F.A., Wang, C., Lin, S.-J., and Sinclair, D.A. (2006). Response to Comment on "HST2 Mediates SIR2-Independent Life-Span Extension by Calorie Restriction."Science (80-.). *312*, 1312–1312.

Lan, C., Lee, H.C., Tang, S., and Zhang, L. (2004). A novel mode of chaperone action: Heme activation of Hap1 by enhanced association of Hsp90 with the repressed Hsp70-Hap1 complex. J. Biol. Chem. *279*, 27607–27612.

Laun, P., Pichova, A., Madeo, F., Fuchs, J., Ellinger, A., Kohlwein, S., Dawes, I., Fröhlich, K.U., and Breitenbach, M. (2001). Aged mother cells of Saccharomyces cerevisiae show markers of oxidative stress and apoptosis. Mol. Microbiol. *39*, 1166–1173.

Lee, S.S., Vizcarra, I. a., Huberts, D.H.E.W., Lee, L.P., and Heinemann, M. (2012). Whole lifespan microscopic observation of budding yeast aging through a microfluidic dissection platform. Proc. Natl. Acad. Sci. *109*, 4916–4920.

Li, J., and Buchner, J. (2012). Structure, function and regulation of the hsp90 machinery. Biomed. J. *36*, 106–117.

Lill, R. (2009). Function and biogenesis of iron-sulphur proteins. Nature *460*, 831–838.

Lindquist, S., and Kim, G. (1996). Heat-shock protein 104 expression is sufficient for thermotolerance in yeast. Proc. Natl. Acad. Sci. U. S. A. *93*, 5301–5306.

Lindstrom, D.L., and Gottschling, D.E. (2009). The mother enrichment program: A genetic system for facile replicative life span analysis in Saccharomyces cerevisiae. Genetics *183*, 413–422.

Lundblad, V., and Blackburn, E.H. (1993). An alternative pathway for yeast telomere maintenance rescues est1- senescence. Cell *73*, 347–360.

Maresová, L., Hosková, B., Urbánková, E., Chaloupka, R., and Sychrová, H. (2010). New applications of pHluorin--measuring intracellular pH of prototrophic yeasts and determining changes in the buffering capacity of strains with affected potassium homeostasis. Yeast *27*, 317–325.

Martínez-Ruiz, A., Villanueva, L., González de Orduña, C., López-Ferrer, D., Higueras, M.A., Tarín, C., Rodríguez-Crespo, I., Vázquez, J., and Lamas, S. (2005). S-nitrosylation of Hsp90 promotes the inhibition of its ATPase and endothelial nitric oxide synthase regulatory activities. Proc. Natl. Acad. Sci. U. S. A. *102*, 8525–8530.

Medvedik, O., Lamming, D.W., Kim, K.D., and Sinclair, D. a. (2007). MSN2 and MSN4 link calorie restriction and TOR to sirtuin-mediated lifespan extension in Saccharomyces cerevisiae. PLoS Biol. *5*, 2330–2341.

Mense, S.M., and Zhang, L. (2006). Heme: a versatile signaling molecule controlling the activities of diverse regulators ranging from transcription factors to MAP kinases. Cell Res. *16*, 681–692.

Meyer, A.J., and Dick, T.P. (2010). Fluorescent protein-based redox probes. Antioxid. Redox Signal. *13*, 621–650.

Miceli, M. V., Jiang, J.C., Tiwari, A., Rodriguez-Quiñones, J.F., and Jazwinski, S.M. (2012). Loss of mitochondrial membrane potential triggers the retrograde response extending yeast replicative lifespan. Front. Genet. *2*, 102.

Miesenböck, G., De Angelis, D.A., and Rothman, J.E. (1998). Visualizing secretion and synaptic transmission with pH-sensitive green fluorescent proteins. Nature *394*, 192–195.

Molin, M., Yang, J., Hanzén, S., Toledano, M.B., Labarre, J., and Nyström, T. (2011). Life Span Extension and H2O2 Resistance Elicited by Caloric Restriction Require the Peroxiredoxin Tsa1 in Saccharomyces cerevisiae. Mol. Cell *43*, 823–833.

Morano, K. a., and Thiele, D.J. (1999). The Sch9 protein kinase regulates Hsp90 chaperone complex signal transduction activity in vivo. EMBO J. *18*, 5953–5962.

Morano, K. a., Grant, C.M., and Moye-Rowley, W.S. (2012). The Response to Heat Shock and Oxidative Stress in Saccharomyces cerevisiae. Genetics *190*, 1157–1195.

Morgan, B., Ezeriņa, D., Amoako, T.N.E., Riemer, J., Seedorf, M., and Dick, T.P. (2013). Multiple glutathione disulfide removal pathways mediate cytosolic redox homeostasis. Nat. Chem. Biol. *9*, 119–125.

Mortimer, R.K., and Johnston, J.R. (1959). Life span of individual yeast cells. Nature *183*, 1751–1752.

Netz, D.J.A., Stith, C.M., Stümpfig, M., Köpf, G., Vogel, D., Genau, H.M., Stodola, J.L., Lill, R., Burgers, P.M.J., and Pierik, A.J. (2012). Eukaryotic DNA polymerases require an iron-sulfur cluster for the formation of active complexes. Nat. Chem. Biol. *8*, 125–132.

Nieto-Sotelo, J., Wiederrecht, G., Okuda, A., and Parker, C.S. (1990). The yeast heat shock transcription factor contains a transcriptional activation domain whose activity is repressed under nonshock conditions. Cell *62*, 807–817.

Nordeen, S.K., Suh, B.J., Kühnel, B., and Hutchison, C.A. (1990). Structural determinants of a glucocorticoid receptor recognition element. Mol. Endocrinol. *4*, 1866–1873.

Orij, R., Postmus, J., Beek, A. Ter, Brul, S., and Smits, G.J. (2009). In vivo measurement of cytosolic and mitochondrial pH using a pH-sensitive GFP derivative in Saccharomyces cerevisiae reveals a relation between intracellular pH and growth. Microbiology *155*, 268–278.

Orij, R., Brul, S., and Smits, G.J. (2011). Intracellular pH is a tightly controlled signal in yeast. Biochim. Biophys. Acta *1810*, 933–944.

Orij, R., Urbanus, M.L., Vizeacoumar, F.J., Giaever, G., Boone, C., Nislow, C., Brul, S., and Smits, G.J. (2012). Genome-wide analysis of intracellular pH reveals quantitative control of cell division rate by pH(c) in Saccharomyces cerevisiae. Genome Biol. *13*, R80.

Osorio, H., Carvalho, E., del Valle, M., Günther Sillero, M. a., Moradas-Ferreira, P., and Sillero, A. (2003). H2O2, but not menadione, provokes a decrease in the ATP and an increase in the inosine levels in Saccharomyces cerevisiae. An experimental and theoretical approach. Eur. J. Biochem. *270*, 1578–1589.

Outten, C.E., and Culotta, V.C. (2004). Alternative start sites in the Saccharomyces cerevisiae GLR1 gene are responsible for mitochondrial and cytosolic isoforms of glutathione reductase. J. Biol. Chem. *279*, 7785–7791.

Pereira, C., and Saraiva, L. (2013). Interference of aging media on the assessment of yeast chronological life span by propidium iodide staining. Folia Microbiol. (Praha). *58*, 81–84.

Petrovska, I., Nüske, E., Munder, M.C., Kulasegaran, G., Malinovska, L., Kroschwald, S., Richter, D., Fahmy, K., Gibson, K., Verbavatz, J.M., et al. (2014). Filament formation by metabolic enzymes is a specific adaptation to an advanced state of cellular starvation. Elife *2014*, 1–19.

Picard, D. (2002). Heat-shock protein 90, a chaperone for folding and regulation. Cell. Mol. Life Sci. *59*, 1640–1648.

Picard, D., Khursheed, B., Garabedian, M.J., Fortin, M.G., Lindquist, S., and Yamamoto, K.R. (1990). Reduced levels of hsp90 compromise steroid receptor action in vivo. Nature *348*, 166–168.

Pratt, W.B., Morishima, Y., and Osawa, Y. (2008). The Hsp90 chaperone machinery regulates signaling by modulating ligand binding clefts. J. Biol. Chem. *283*, 22885–22889.

Ralser, M., Kuhl, H., Ralser, M., Werber, M., Lehrach, H., Breitenbach, M., and Timmermann, B. (2012). The Saccharomyces cerevisiae W303-K6001 cross-platform genome sequence: insights into ancestry and physiology of a laboratory mutt. Open Biol. *2*, 120093.

Ringvoll, J., Uldal, L., and Roed, M. (2007). Mutations in the RAD27 and SGS1 genes differentially affect the chronological and replicative lifespan of yeast cells growing on glucose and glycerol. FEMS Yeast … *7*, 848–859.

Rinnerthaler, M., Büttner, S., Laun, P., Heeren, G., Felder, T.K., Klinger, H., Weinberger, M., Stolze, K., Grousl, T., Hasek, J., et al. (2012). Yno1p/Aim14p, a NADPH-oxidase ortholog, controls extramitochondrial reactive oxygen species generation, apoptosis, and actin cable formation in yeast. Proc. Natl. Acad. Sci. U. S. A. *109*, 8658–8663.

Ristow, M., and Schmeisser, K. (2014). Mitohormesis: Promoting Health and Lifespan by Increased Levels of Reactive Oxygen Species (ROS). Dose. Response. *12*, 288–341.

Roth, L., and Polotsky, A. (2012). Can we live longer by eating less? A review of caloric restriction and longevity. Maturitas *71*, 315–319.

Scroggins, B.T., Robzyk, K., Wang, D., Marcu, M.G., Tsutsumi, S., Beebe, K., Cotter, R.J., Felts, S., Toft, D., Karnitz, L., et al. (2007). An acetylation site in the middle domain of Hsp90 regulates chaperone function. Mol. Cell *25*, 151–159.

Sharma, P., Agrawal, V., and Roy, N. (2011). Mitochondria-mediated hormetic response in life span extension of calorie-restricted Saccharomyces cerevisiae. Age (Omaha). *33*, 143–154.

Sherman, F. (2002). Getting Started with Yeast • Contents •. Methods Enzymol. *350*, 3–41.

Sikorski, R.S., and Hieter, P. (1989). A system of shuttle vectors and yeast host strains designed for efficient manipulation of DNA in Saccharomyces cerevisiae. Genetics *122*, 19–27.

Smeal, T., Claus, J., Kennedy, B., Cole, F., and Guarente, L. (1996). Loss of transcriptional silencing causes sterility in old mother cells of S. cerevisiae. Cell *84*, 633–642.

Sorger, P.K., Lewis, M.J., and Pelham, H.R. (1987). Heat shock factor is regulated differently in yeast and HeLa cells. Nature *329*, 81–84.

Sreedhar, A.S., Kalmár, E., Csermely, P., and Shen, Y.-F. (2004). Hsp90 isoforms: functions, expression and clinical importance. FEBS Lett. *562*, 11–15.

Stankiewicz, M., and Mayer, M.P. (2012). The universe of Hsp90. Biomol. Concepts *3*, 4–22.

Steinkraus, K. a, Kaeberlein, M., & Kennedy, B. K. (2008). Replicative aging in yeast: the means to the end. *Annual Review of Cell and Developmental Biology*, *24*(June), 29–54. doi:10.1146/annurev.cellbio.23.090506.123509

Tachibana, T., Okazaki, S., Murayama, A., Naganuma, A., Nomoto, A., and Kuge, S. (2009). A major peroxiredoxin-induced activation of yap 1 transcription factor is mediated by reduction-sensitive disulfide bonds and reveals a low level of transcriptional activation. J. Biol. Chem. *284*, 4464–4472.

Taipale, M., Jarosz, D.F., and Lindquist, S. (2010). HSP90 at the hub of protein homeostasis: emerging mechanistic insights. Nat. Rev. Mol. Cell Biol. *11*, 515–528.

Tanaka, T., Izawa, S., and Inoue, Y. (2005). GPX2, encoding a phospholipid hydroperoxide glutathione peroxidase homologue, codes for an atypical 2-Cys peroxiredoxin in Saccharomyces cerevisiae. J. Biol. Chem. *280*, 42078–42087.

Timmermann, B., Jarolim, S., Russmayer, H., Kerick, M., Michel, S., Krüger, A., Bluemlein, K., Laun, P., Grillari, J., Lehrach, H., et al. (2010). A new dominant peroxiredoxin allele identified by whole-genome re-sequencing of random mutagenized yeast causes oxidant-resistance and premature aging. Aging (Albany. NY). *2*, 475–486.

Traba, J., Froschauer, E.M., Wiesenberger, G., Satrústegui, J., and Del Arco, A. (2008). Yeast mitochondria import ATP through the calcium-dependent ATP-Mg/Pi carrier Sal1p, and are ATP consumers during aerobic growth in glucose. Mol. Microbiol. *69*, 570–585.

Trotter, E.W., Rand, J.D., Vickerstaff, J., and Grant, C.M. (2008). The yeast Tsa1 peroxiredoxin is a ribosome-associated antioxidant. Biochem. J. *412*, 73–80.

Tsutsumi, S. (2012). Charged linker sequence modulates eukaryotic heat shock protein 90 (Hsp90) chaperone activity. Proc. … *109*, 2937–2942.

Ünal, E., Kinde, B., and Amon, A. (2011). Gametogenesis eliminates age-induced cellular damage and resets life span in yeast. Science (80-.). *332*, 1554–1557.

Veal, E. a., Ross, S.J., Malakasi, P., Peacock, E., and Morgan, B. a. (2003). Ybp1 is required for the hydrogen peroxide-induced oxidation of the Yap1 transcription factor. J. Biol. Chem. *278*, 30896–30904.

Veatch, J.R., McMurray, M. a, Nelson, Z.W., and Gottschling, D.E. (2009). Mitochondrial dysfunction leads to nuclear genome instability via an iron-sulphur cluster defect. Cell *137*, 1247–1258.

Veine, D.M., Arscott, L.D., and Williams, C.H. (1998). Redox potentials for yeast, Escherichia coli and human glutathione reductase relative to the NAD+/NADH redox couple: enzyme forms active in catalysis. Biochemistry *37*, 15575–15582.

Wandinger, S.K., Suhre, M.H., Wegele, H., and Buchner, J. (2006). The phosphatase Ppt1 is a dedicated regulator of the molecular chaperone Hsp90. EMBO J. *25*, 367–376.

Wang, I.-H., Chen, H.-Y., Wang, Y.-H., Chang, K.-W., Chen, Y.-C., and Chang, C.-R. (2014). Resveratrol modulates mitochondria dynamics in replicative senescent yeast cells. PLoS One *9*, e104345.

Wang, Y., Gibney, P. a., West, J.D., and Morano, K. a. (2012). The yeast Hsp70 Ssa1 is a sensor for activation of the heat shock response by thiol-reactive compounds. Mol. Biol. Cell *23*, 3290–3298.

Whitesell, L., and Lindquist, S. (2009). Inhibiting the transcription factor HSF1 as an anticancer strategy. Expert Opin. Ther. Targets *13*, 469–478.

Wider, D., Péli-Gulli, M.-P., Briand, P.-A., Tatu, U., and Picard, D. (2009). The complementation of yeast with human or Plasmodium falciparum Hsp90 confers differential inhibitor sensitivities. Mol. Biochem. Parasitol. *164*, 147–152.

Woo, D.K., and Poyton, R.O. (2009). The absence of a mitochondrial genome in rho0 yeast cells extends lifespan independently of retrograde regulation. Exp. Gerontol. *44*, 390–397.

Wood, J.G., and Helfand, S.L. (2013). Chromatin structure and transposable elements in organismal aging. Front. Genet. *4*, 274.

Xie, Z., Zhang, Y., Zou, K., Brandman, O., Luo, C., Ouyang, Q., and Li, H. (2012). Molecular phenotyping of aging in single yeast cells using a novel microfluidic device. Aging Cell *11*, 599–606.

Yang, J., Dungrawala, H., Hua, H., Manukyan, A., Abraham, L., Lane, W., Mead, H., Wright, J., and Schneider, B.L. (2011). Cell size and growth rate are major determinants of replicative lifespan. Cell Cycle *10*, 144–155.

Young, M.J., and Court, D. a. (2008). Effects of the S288c genetic background and common auxotrophic markers on mitochondrial DNA function in Saccharomyces cerevisiae. Yeast *25*, 903–912.

Zadrag, R., Bartosz, G., and Bilinski, T. (2008). Is the yeast a relevant model for aging of multicellular organisms? An insight from the total lifespan of Saccharomyces cerevisiae. Curr. Aging Sci. *1*, 159–165.

Zamocky, M., Furtmüller, P.G., and Obinger, C. (2008). Evolution of catalases from bacteria to humans. Antioxid. Redox Signal. *10*, 1527–1548.

Zapata-Hommer, O., and Griesbeck, O. (2003). Efficiently folding and circularly permuted variants of the Sapphire mutant of GFP. BMC Biotechnol. *3*, 5.

Zhang, L., and Hach, A. (1999). Molecular mechanism of heme signaling in yeast: the transcriptional activator Hap1 serves as the key mediator. Cell. Mol. Life Sci. *56*, 415–426.

Zhang, Y., Luo, C., Zou, K., Xie, Z., and Brandman, O. (2012). Single cell analysis of yeast replicative aging using a new generation of microfluidic device. PLoS One *7*, e48275.